Propagation of Surface Acoustic Waves in a Finite Elastic Plate Covered with Periodic Electrodes

Jinghui Wu

Scuola di Dottorato
Department of Mechanical and Aerospace Engineering
Politecnico di Torino

Supervisors:
Prof. Erasmo Carrera
Prof. Ji Wang
Prof. Riccardo Augello

July 2023

Declaration

I hereby declare that, the contents and organization of this dissertation constitute my own original work and does not compromise in any way the rights of third parties, including those relating to the security of personal data.

Jinghui Wu
July 2023

Acknowledgements

First, I would like to extend my deepest gratitude to my supervisors, Prof. Erasmo Carrera, Prof. Ji Wang and Prof. Riccardo Augello, for their continuous guidance and timely supervision during my Ph.D. program.

Since my master's degree, I have been studying with Professor Wang Ji, and I have made progress little by little, and now I am about to complete my PhD. I would like to thank you for your dedication in the daily discussions, the revision and finalisation of my thesis, for giving me the opportunity to see the world during my doctoral studies, and for your supervision of my studies, which has allowed me to make continuous progress. Your rigorous attitude and love for governance and research will benefit me for the rest of my life.

Prof. Erasmo Carrera's priceless insights into mechanics and his passion and dedication to his work have inspired my research activities. During the period of my studies at the Politecnico di Torino, Dr. Riccardo Augello provided me with continuous assistance at every step of my activities and encouraged me with his dedication to research.

I am also deeply greateful to Prof. Alfonso Pagani, Prof. Marco Petrolo, Prof. Matteo Filippi and Prof. Enrico Zappino for their constant and kind support. And I want express my thanks to Piezoelectric Device Laboratory, MUL2 group and all all my fellow students. It is my honor to have been a member of these vibrant and creative teams.

Thanks to China Scholarship Council (CSC) for providing me the opportunity to this exchange study.

Finally, in these last words, I would like to thank my mom for her patience and generous support.

Grazie a tutti

Jinghui Wu

Abstract

The propagation properties of surface acoustic waves (SAWs) in laminated structures have important applications for research in areas such as SAW devices, civil engineering and geological exploration. For more complex layered structures, which generally need to be solved by numerical analysis, this paper combines the Rayleigh-Ritz method and the transfer matrix method to analyse the propagation characteristics of low-order SAWs in a two-dimensional finite elastic structure. Since the finite element method (FEM) is one of the most commonly used numerical calculation tools in the design and analysis of device structures, with its advantages of simplicity and ease of operation, this paper uses the Carrera Unified Formulation (CUF) framework combined with viscous-spring artificial boundaries to analyse the propagation properties of low-order SAWs in finite three-dimensional layered structures. The compact stiffness matrix form constructed using the CUF can effectively reduce the computational cost of finite elements while ensuring computational reliability. This paper presents a more systematic study of several fundamental wave problems in layered structures, to provide valuable theoretical references for the application and design of SAWs devices. Both methods can be used to characterise the propagation of SAW in finite elastic plates covered with periodic electrodes, with the Rayleigh-Ritz method being more applicable to models with relatively simple structures, and finite element calculations can be performed using CUF for models with more complex cover shapes. The main contents and results of this paper are as follows:

(1) The propagation characteristics of SAWs in an isotropic elastic plate are investigated by the Rayleigh-Ritz method and by using a combination of the Legendre polynomial and a trigonometric form as a displacement function. The boundary conditions of the structure are taken into account in the trial function and the corresponding characteristic equations are obtained by substituting Lagrangian functions. The effects of boundary conditions and plate thickness on the dispersion characteristics, modes, and corresponding stress distributions of the low-order SAWs in the structure are investigated by numerical calculations. The study shows that the propagation characteristics of the low-order SAWs in the plate are related to the plate thickness; in the present

model, the boundary condition on the bottom surface of the plate has little effect on the wave velocity of the low-order SAWs in the structure, but has a certain degree of influence on the modes and the corresponding stress distributions.

(2) The effects of cover layer material, layer thickness, and each boundary condition on the dispersion characteristics of low-order SAWs in a finite elastic structure with a cover layer are discussed, taking into account the boundary conditions at the intersection. The results show that the cladding material has a significant effect on the wave velocities of the low-order SAWs in the structure; the cladding thickness within a certain range affects the wave velocities of the low-order SAWs in the structure; the stress boundary conditions at the intersection have a significant effect on the modes and the corresponding stress distributions of the low-order SAWs.

(3) Combining the Rayleigh-Ritz method and the transfer matrix, the effects of the cover material, layer thickness, and each boundary condition on the dispersion characteristics of low-order SAWs in a finite elastic structure with a cover layer that does not completely cover the substrate layer are discussed. The results show that the free boundary conditions on both sides of the cover layer perpendicular to the wave propagation direction need to be considered in the calculation of this model, otherwise, numerical results consistent with the case where the cover layer is of equal width with the substrate layer are obtained; compared with the above-calculated model, the number of low-order SAW velocities in this calculated model varies in the same range of cover layer thicknesses.

(4) The effect of the number of electrodes and materials on the dispersion characteristics of low-order SAWs in a finite elastic plate covered with periodic electrodes with a fixed bottom edge of the substrate is discussed. The results show that the number of electrodes has almost no effect on the wave velocities of the low-order SAWs in the adopted model with the same structure, dimensions, and materials, but that different combinations of cover materials have a significant effect on the dispersion characteristics of the low-order SAWs in the structure.

(5) A compact stiffness matrix was constructed from the one-dimensional beam model of CUF and a viscous-spring artificial boundary was established at the model boundary to analyse the propagation characteristics of low-order SAWs in a finite three-dimensional layered structure. The results show that the size of the cover layer has a certain influence on the wave velocities of the low-order SAWs in the structure; in this computational model, the thickness of the cover layer has a relatively large influence on the wave

velocities of the low-order SAWs in the structure, while the length of the cover layer has an extremely small influence on the wave velocities of the low-order SAWs in the structure.

Keywords-laminated structure, low-order SAWs, Rayleigh-Ritz method, the transfer matrix, CUF, viscous-spring artificial boundary

Table of contents

List of figures

List of tables

Chapter 1

Introduction

1.1 Foreword

SAW was discovered by Lord Rayleigh (John William Strutt) during his research into seismic waves and did not receive much attention until R. M. White and F. W. Voltmer discovered that metal interdigital transducer (IDT) could excite surface waves in piezoelectric materials, and a variety of SAW devices began to emerge. Because the velocity of SAW is generally five magnitudes slower than that of electromagnetic waves, and has the advantages of stable propagation and easy to sample and process, SAW devices have a wide range of applications in industry, communications and other fields.

SAWs are generally referred to as elastic waves that are generated near the surface of an elastic solid and propagate along the surface or interface, and in this paper we are focusing on Rayleigh waves. As a type of SAW, Rayleigh waves are influenced by longitudinal and vertical shear components in their travel, and their particles exhibit an elliptical trajectory, and their energy decays exponentially with increasing distance to the elastic object surface, generally concentrated in a wavelength range near the elastic solid surface.

Unlike Love and Lamb waves, Rayleigh waves are not bulk waves, but because of their longitudinal and vertical motion properties, when a medium is attached to the surface of an elastic structure, the medium has an effect on the mode and velocity of the Rayleigh waves in the structure, and this is the mechanism by which the SAW sensor works.

For decades, a large number of studies have been carried out on SAWs in semi-infinite space. For relatively simple models, the propagation characteristics of SAWs under the corresponding models can be analysed by analytical methods, based on the wave equation and taking into account the relevant boundary conditions. However, for more complex boundary conditions, it is often impossible to obtain an analytical solution, and although the FEM method is an effective tool for analysing such problems, it requires a high level of computer CPU and memory when the structure is complex. In this paper, it is argued that by simplifying the model and extracting the unitary structure and setting reasonable boundary conditions, the Rayleigh-Ritz method is used to study the unitary structure.

In this paper, the propagation characteristics of low-order SAWs in a structure under the influence of an overlying thin layer are considered, taking an isotropic structure as the object of study. The paper adopted the Rayleigh-Ritz method by setting a reasonable form of displacement function and considering the boundary conditions corresponding to each part of the structure, and then obtaining the transfer matrix according to the boundary conditions among the parts of the structure, through which the sections of the structure are combined into a whole for consideration, so as to analyse the influence of the material and thickness of the attached layer on the wave velocity and mode of the SAWs in the structure. In addition, the influence of the various boundary conditions in the structure on the calculation results is analysed systematically. In addition to analysing the SAWs propagation characteristics in a two-dimensional structure with a covering layer by the Rayleigh-Ritz method, a three-dimensional model of the structure covered with a thin metal layer is constructed using the one-dimensional beam model of the CUF, and a viscous-spring artificial boundary is established to enable the structure to analyse the SAWs propagation. The effect of the thin layer on the propagation characteristics of the SAWs in the structure is analysed by finite element calculations in a three-dimensional geometry model.

1.2 Background

In recently years, with the rapid development of numerical computation techniques, FEM plays an increasingly important role in the analysis of mechanical phenomena in complex structures, for example, in the design and performance analysis of SAWs devices, where FEM is one of the most popular tools on the market today [2–19]. However, during finite element calculations, the three-dimensional computational model often requires a large amount of computer RAM and CPU. In order to reduce computational costs, the structure is often simplified to a two-dimensional model when designing devices and conducting studies on the wave propagation characteristics in the device, and the analysis is generally performed only through the structure of intercepted units [9, 20–27]. For relatively simple structural models, the propagation properties of SAWs in structures can generally be studied by analytical, semi-analytical, and numerical analysis methods. Enzevaee and Shodja considered the effects of the surface and the intersection between layers, and used the Wentzel-Kramers- Brillouin singular uptake theory to analyze the dispersion relations of shear wave in structures covered with ultrathin functional gradient piezoelectric layers on a transversely isotropic semi-infinite space [28]; Wu and Dzenis analyzed the dispersion relations of antiplanar SAWs propagating in an elastic half-space coated with anisotropic layers by means of the Stroh formula [29]; Ezzin et al. analysed the propagation characteristics of Rayleigh waves in a structure covered with a piezoelectric layer on a piezomagnetic material based on the Stroh formula, taking into account the continuity of each physical quantity at the layer-layer interface [30]; Salah et al. investigated the propagation characteristics of Rayleigh waves in a structure covered with a layer of a functional gradient piezoelectric material on a semi-infinite homogeneous medium by means of the stiffness matrix method and the ordinary differential equation [31].

In geographical studies, one of the main tools for geological exploration is through the analysis of the propagation properties of SAWs (generally referred to as: elastic waves) in multi-layered structures [32–40]. In contrast to SAW devices, ground is often modelled in semi-infinite space and is also mainly studied using analytical, semi-analytical and numerical analysis methods. Leong and Aung proposed a new forward modelling method, the weighted average forward modelling method, to obtain Rayleigh waves in multilayered soils [36]; Adler used the matrix method to analyse SAWs in multilayered structures [41, 42]; Haskell used a matrix form proposed by Thomson to obtain the phase velocity dispersion equation in multilayered media [43]; Smeulders proposed an exact stiffness formulation to analyse transient and steady-state wave propagation properties in multilayered dry, saturated/unsaturated isotropic poroelastic media [44]; Chai et al. used the thin-layer method to analyse saturated SAWs propagation properties in a multi-layered porous semi-infinite space [45]; Kuznetsov used the Weiskopf model to analyse the dispersion properties of Rayleigh-Lamb waves in a structure with a sand layer over an isotropic substrate [46]; Philippacopoulos proposed to calculate Rayleigh waves in partially saturated layered semi-infinite space based on Biot theory [47]; The problem of SAWs propagation in multilayered elastic structures is analysed mainly by linking the layers to each other through boundary conditions at each intersection so that they form a whole [48].

In this paper, the propagation properties of SAWs in finite layered structures in two and three dimensions are analysed by the Rayleigh-Ritz method with a transfer matrix and the CUF with a viscous-spring artificial boundary, respectively [49–64]. Stoklasová et al. showed that the Rayleigh-Ritz method can be applied to calculate the velocity of SAWs propagating in the general direction of an arbitrarily symmetric anisotropic medium, and that a reasonable setting of the displacement function can transform the problem of solving the velocity of SAWs can be transformed into a simple linear characteristic equation [65]. In FEM calculations, mechanical phenomena in a wide range of 3D geometries can be calculated analytically by constructing stiffness matrices from the CUF, a hierarchical formulation that provides a framework and a fine-grained structural theory through a variable kinematic description [66–77].Petrolo et al. studied the wave propagation properties in a higher-order 1D model structure that model was obtained based on the beam model construction of the CUF, and the control equations were obtained based on the principle of virtual work and the FEM to analyse the wave propagation properties in laminated beam and layered annular cylindrical structures [78].

In the FEM analysis, a finite structure can be converted into a semi-infinite/infinite space by setting reasonable boundary conditions. Among them, the Perfect Matching Layer (PML) absorption boundary and the viscous-spring artificial boundary are both more widely used, especially in the studies of wave propagation [79–90]. The PML is a virtual anisotropic medium introduced near the boundary set up so that waves entering the region are gradually consumed and cannot be reflected back into the computational space [81, 91]; the viscous-spring artificial boundary is a system of springs and dampers set up at the unit nodes of the boundary, also with the aim of consuming waves released from the computational body by springs and damping to avoid their reflection back into the computational body [87, 92].

In this paper, the propagation characteristics of elastic waves in finite isotropic structures (an elastic thick plate, a finite structure covered with a thin layer, a finite laminated structure with the width of the cover layer smaller than the bottom plate, a finite structure with T-shaped cover layer) are investigated.

1.3 Current status and applications of domestic and international research

Since Rayleigh's discovery of SAWs propagating on elastic solid surfaces, the propagation properties of SAWs in semi-infinite space with various boundary conditions and different media materials have been studied since then [93–101]; Sharma analysed the propagation properties of Rayleigh waves in a viscoelastic medium [96]; Pillarisetti et al. first analyzed the effect of Mindlin boundary conditions on Rayleigh wave propagation in a semi-infinite elastic space by analytical methods, and then used COMSOL to numerically simulate the change of waves in the structure after adding Mindlin boundaries to different regions of the free surface, with a view to controlling low-frequency surface waves by establishing relevant boundary conditions [102]; Tian et al. used the Stroh method, combined with boundary conditions, to transform the fluctuation problem in a piezoelectric semiconductor elastic plate into a linear eigenvalue problem, and numerically analysed the effects of boundary conditions, plate thickness, etc. on the elastic waves in the plate [103].

The propagation properties of SAWs in multilayer structures have been of continuous interest in studies on SAWs in fields, such as: SAW devices and geophysical exploration, mainly for semi-infinite layered models [33, 38, 41, 43, 45, 101, 104, 105]. Based on the properties of the SAWs inherent in it, it has a wide range of applications in SAW devices, such as filters, resonators, and sensors [12, 15, 18, 106]. The main study on SAW devices is the propagation characteristics of SAWs in a unitary structure with a piezoelectric material as a substrate and various conductive materials as electrodes [107–111]. The study of SAWs propagation properties in multilayer structures has also been carried out by experimental, analytical, semi-analytical and numerical methods. The analytical and semi-analytical methods are mostly used for simpler structures [43, 47, 104, 110, 112], while the experimental and numerical methods are more general for relatively complex structures. For device design, the covering layer, i.e. the electrode layer, is generally discontinuous, and this structure is more complex than the semi-infinite layered spatial structure, making it difficult to obtain a direct analytical solution, thus many scholars studied the unitary or complete SAW device structure by means of FEM [4, 15], coupling-of-modes (COM) [105], etc. Wang and Tang simulated the three-dimensional propagation of Rayleigh waves in a medium with directional cracks by the staggered-grid finite difference method [113]; Tiwary et al. analyzed and designed a SAW device by finite element software and simplified the model to two dimensions for calculation [11]; Endoh et al. developed a simplified two-dimensional SAW device model and used the FEM and frequency domain analysis to analyze the SAWs propagation and excitation in a metal fence structure of finite thickness [3]; Goto et al. used a combination of finite element and COM methods to design the structure of TC-SAW devices [114]; Buchner et al. considered the structure of a SAW device as an infinite structure along the wave propagation direction and used the FEM to analyse the propagation and excitation of SAW devices through periodic boundary conditions to calculate parameters such as eigenfrequencies and wave velocities in one of the periodic structures [115]. To the best of the authors' knowledge, there has been no systematic study of the propagation properties of low-order SAWs in finite periodic elastic structures covered with a metal layer by the Rayleigh-Ritz method.

As an energy method, the Rayleigh-Ritz method can not only analyse the vibration of individual structures, it can also be applied to the vibration analysis of multi-unit assemblies, multilayers and other structures [116–124]. The eigenfrequencies of multi-layered/multi-body structures are analysed by the Rayleigh-Ritz method, which generally uses two ways to obtain the characteristic equations of the whole structure, firstly by setting up/getting a displacement function that satisfies the boundary conditions/continuity conditions at the intersection interfaces: Jin et al. set up a displacement function for a sandwich-type beam based on Reddy's higher-order shear deformation theory, and by means of a displacement continuity on the contact surfaces between the layers, and the displacement function of the middle layer was constructed on the basis of the displacements of the top and bottom layers, and then the corresponding energy integral was obtained by using the relationship between the spring boundary and the structure, and the characteristic equations of the whole structure could be obtained after finishing according to the Rayleigh-Ritz method [125]; Zhao et al. used the Ritz method to calculate the propagation characteristics of bulk waves in a structure with a thin piezoelectric layer overlying the middle region of a rectangular silicon layer, where the displacement of the upper and lower contact surfaces was also considered continuously [126]; Zhao et al. proposed a quantitative spectral prediction method and used it to study the coupled vibration behavior of piezoelectric multilayers at ultra-high frequencies by setting up a reasonable displacement function model [127]; D'Ottavio et al. proposed the Sublaminate Generalized Unified Formulation (SGUF) to construct the generalized displacements of the layers in a composite plate containing piezoelectric layers, and then analyzed the free vibration of the structure by the Ritz method [128]; Li and Fu introduced the Heaviside step function in the displacement function, and considered the displacement continuous and simply-supported in the establishment of the displacement function boundary conditions, by which the buckling control equations of the piezoelectric layered cylindrical shell structure were obtained [129]. Another is to obtain the transfer matrix by organising the boundary conditions and using the transfer matrix to relate the various parts to obtain the characteristic equations of the whole structure, such as: Woodcock proposed an advanced general modelling method for multilayer composites with arbitrary boundary conditions based on the Rayleigh-Ritz method, combining the first shear deformation theory of a single layer and the multilayer method, by which the shear stress at the intersection between layers and the The transfer matrix was obtained through the shear stress and displacement continuity between the plies, which can be applied to analyse the eigenfrequencies of multilayer composites with arbitrary boundary conditions [130]; Zhou et al. analysed the eigenfrequencies of a toroidal plate structure fixed by a rigid medium through the Ritz method, and obtained the conversion relationship between the unknown coefficients through the displacement continuity between the two parts to obtain the transfer matrix, which was used to integrate the two independent parts into The transfer matrix was used to integrate the two independent parts into a whole, thus obtaining the characteristic equations of the whole structure [131].

The transfer matrix has a wide range of applications in problems such as vibrations of continuous systems, where it is mainly used to establish the sequential relationships between the various parts of the system by means of boundary conditions in the structure, thus organising them to obtain a transfer matrix [3, 132, 133]. Initially, the transfer matrix method was mainly used to analyse vibrations in one-dimensional linear elastic structures [134], but with the development of computer technology, the Myklestad method evolved into the traditional transfer matrix method and was further developed for the analysis of structures composed of multiple mechanical elements [135]; Rui et al. proposed a linear transfer matrix for multi-body systems based on the traditional transfer matrix method to analyse the mechanical properties of complex linear multi-mechanical component systems [136]; Subrahmanyam and Garg analysed the stresses in beams under various possible boundary conditions (shear deformation, rotational inertia, spring support, discontinuities in mass and stiffness distribution, etc.) by means of transfer matrices [137]; Zhan et al. investigated the reflection, transmission and absorption properties of single, double and multilayer graphene by means of transfer matrices, optical properties such as transmission and absorption by means of transfer matrices [138]; Lee and Lee used the transfer matrix method in the calculation of the bending vibration properties of Bernoulli-Euler beams with different taper ratios [139]; Attar used the transfer matrix method in the study of the vibration problems of stepped beams with an arbitrary number of transverse cracks and general form boundary conditions by means of the analytical method to obtain the crack The general form of the characteristic equation of the beam is obtained by means of the transfer matrix as a function of information on frequency, crack characteristics (size and location), boundary conditions, etc. [140]; Chen et al. analyzed wave propagation in magneto-electro-elastic multilayers using the global transfer matrix [141]; Gao et al. investigated the propagation characteristics of SAWs in a ZnO/Si-Bi layer structure using the transfer matrix method [142]; Xu and Datta related the layers by means of a transfer matrix to obtain the characteristic equations of the overall structure to analyze the SAWs dispersion properties in a three-layer plate [143]; Vinh et al. proposed a transfer matrix that can be used to calculate the orthogonal layers in a simpler form than the conventional transfer matrix, and this matrix will be useful to calculate the wave propagation in an elastic half-space covered by an arbitrary number of different homogeneous orthogonal layers [144]; Liu and Fan used the transfer matrix method to analyse the propagation of Rayleigh waves in a layered semi-infinite space [38]. The transmission matrix method is generally able to reduce the physical degrees of freedom of the system, which is advantageous for reducing the computational cost. The method constructs the matrix of the whole system by matrix multiplication, which may lead to an increase in the accumulation of computational errors as the number of divisions in the system increases [135].

The FEM has been used quite extensively in the study of wave propagation related problems [80, 145]. In order to analyse wave propagation problems in infinite/semi-infinite space, it is necessary to simplify the model by setting reasonable boundaries to avoid the false reflections on the boundary of the finite element model [4, 85]. Liu and Jerry proposed to introduce progressive damping (an exponentially increasing function) into a part of the cell in front of the finite boundary of the finite element model to reduce wave reflections, a scheme validated by Abaqus/Standard software calculations [146]; Huang et al. set up PMLs at the ends and bottom of the finite element model to 'absorb' waves at the boundary, and analysed the dispersion properties of surface waves at discontinuities between periodic gratings using traveling wave excitation and hierarchical cascading techniques [147]; Harari and Hughes showed that the Galerkin/least squares method with DtN boundary conditions was designed to show superiority in SAW problems, providing accurate solutions at relatively low grid resolution and allowing numerical damping of unresolved waves [148]; Wang and Zhang used a high-precision staggered-grid finite-difference numerical method to simulate Rayleigh wave propagation in an elastic medium with discrete subsurface fractures, and used PML to implement absorption boundary conditions in the simulation interval [149]; Hu et al. applied the Nearly Perfect Matching Layer (NPML) as the absorption boundary for SAW models in three dimensions, and the NPML formulation deviates from the standard PML by inaccurate changes in variables, but this change does not actually affect the wave propagation in the desired region, which reduces the computational cost compared to using the PML [150]; Song and Li used the viscous-spring artificial boundary to numerically simulate the explosion process of a concentrated charge in a mass of soil and found that the equivalent viscous-spring boundary can effectively reduce the boundary effects and has a high performance in soil [86]; Liu et al. applied artificial viscous-spring boundary conditions to the analysis of wave propagation in a three-dimensional land structure, where the boundary can act directly on the nodes of the finite elements and "absorb" the waves on the boundary by setting a reasonable viscous-spring coefficient to reduce the interference caused by false reflections at the boundary [89].

Through recent developments, it is easy to observe that new frameworks can be constructed using CUF, enabling finite element calculations of metals and multilayer composites under mechanical, thermal, electrical and magnetic loads in one-, two- and three-dimensional models [151, 68, 70, 71, 149, 152–155]. Carrera et al. used a one-dimensional high-order beam model combined with the Lagrangian multiplier method to perform a global/local analysis of variable kinematic models for unilateral simply-supported square beam structures, cylindrical thin-walled structures and bridge-type structures [74]; Li et al. introduced a Node-Dependent Kinematics (NDK) shell finite element formulation for steady-state thermodynamic analysis of laminar structures based on the CUF framework to study multilayer shell structures under coupled thermodynamic FE models [156]. Carrera et al. successfully analysed the non-linear strain-displacement relationship of the structure using CUF by implementing higher order one-dimensional finite units distributed along the thickness direction of a two-dimensional thin-walled beam structure [69]; Zappino et al. used equivalent single-layer (ESL) and multilayer (Layer-Wise, LW) models and analysed the kinematic model of multilayer plates by means of a two-dimensional model in the CUF framework, and the continuity of transverse stresses between the interfaces of the layers was satisfied when an LW model with a sufficient number of expansion terms was used [155]; Wu et al. used CUF to implement a refined and layered model to study interlayer stresses in composite flexible structures [157]; Carrera et al. constructed a non-linear model through the CUF framework to study the variation of natural frequencies and associated modalities of composite beam structures under large displacements/rotations [158]; Petrolo et al. analysed the wave propagation properties of laminated beams and layered toroidal cylindrical structures based on the 1D beam model of the CUF by using an implicit algorithm based on the Newmark method and a dissipative explicit algorithm based on the Tchamwa-Wielgosz method to obtain direct time integrals of the equations of motion [78]; Entezari et al. applied refined finite units based on the Lord-Shulman generalized theory of thermoelasticity in a three-dimensional model in the CUF framework to analyse the problem of thermoelastic wave propagation in discs made of functionally graded materials [159]. The viscous-spring artificial boundary is well integrated with the FEM, and since it acts directly on the nodes of the finite element and corresponds to the nodes of the CUF element, it can be introduced into the CUF to study the propagation of low-order SAWs in finite structures.

1.4 Purpose and content of the study

1.4.1 Purpose of the study

In this paper, we study the propagation of low-order SAWs in finite isotropic elastic structures based on the extended Rayleigh-Ritz method and the CUF framework with a viscous-spring artificial boundary. The effects of boundary conditions, layer thickness and cover material on the dispersion characteristics of low-order SAWs in structures with less than the substrate are also discussed.

1.4.2 The content of the study

Chapters 2 to 5 of this paper mainly adopt the Rayleigh-Ritz method, and in Chapter 6 the FEM in the CUF framework is used to investigate the propagation characteristics of low-order SAWs in the finite elastic structures, as shown in Fig 1.1, and the main contents of the each chapter are:

Chapter 1 Introduction, provides a brief overview of the relevant theories used in this paper and their applications, introduces the background to the research, and presents the purpose and content of the research.

Chapter 2 The propagation characteristics of low-order Rayleigh waves in finite elastic plates, this chapter uses a combination of Legendre polynomials and trigonometric functions as displacement functions, and the boundary conditions of the structure are considered in the trial functions. The effects of boundary conditions, plate thickness on the dispersion characteristics, displacement modes and stress distribution of low-order SAWs in the structure are analysed numerically by the Rayleigh-Ritz method.

Chapter 3 The propagation characteristics of low-order SAWs in finite structures covered with thin layers on an isotropic substrate are considered, considering that the structure consists of two parts, a transfer matrix is obtained based on the boundary conditions at the intersection to analyse the effect of each boundary condition, the thickness of the cover and the material on the dispersion characteristics, the displacement modes and the corresponding stress distribution of the low-order Rayleigh waves in the structure.

Chapter 4 The propagation characteristics of SAWs in a periodic isotropic structure with a finite layer, considering that the width of the cover layer is smaller than that of the substrate layer, the structure is divided into four parts, several sets of boundary conditions are considered and the corresponding transfer matrices are obtained to construct the characteristic equations of the whole structure..

Chapter 5 The propagation of low-order SAWs in a finite elastic plate covered with periodic electrodes. On the basis of the previous two chapters, the influence of the number of electrodes and material combinations on the dispersion characteristics of low-order sound surface waves in the structure is numerically analysed using a computational model with the bottom edge of the substrate fixed and considering the stress boundary conditions on the free surface of the cover layer and the stress continuum at the interface between the upper and lower layers.

Chapter 6 Analysis of the propagation properties of sound surface waves in finite structures by CUF, using a one-dimensional beam model in the CUF framework, a compact stiffness matrix form is constructed and a viscoelastic artificial boundary is placed on the boundary to allow the analysis of the propagation properties of SAWs in the finite structures. The wave velocities and corresponding displacement modes of low-order SAWs in a three-dimensional finite laminar structure are obtained at a low computational cost.

Chapter 7 Summary of the full text and outlook for future work.

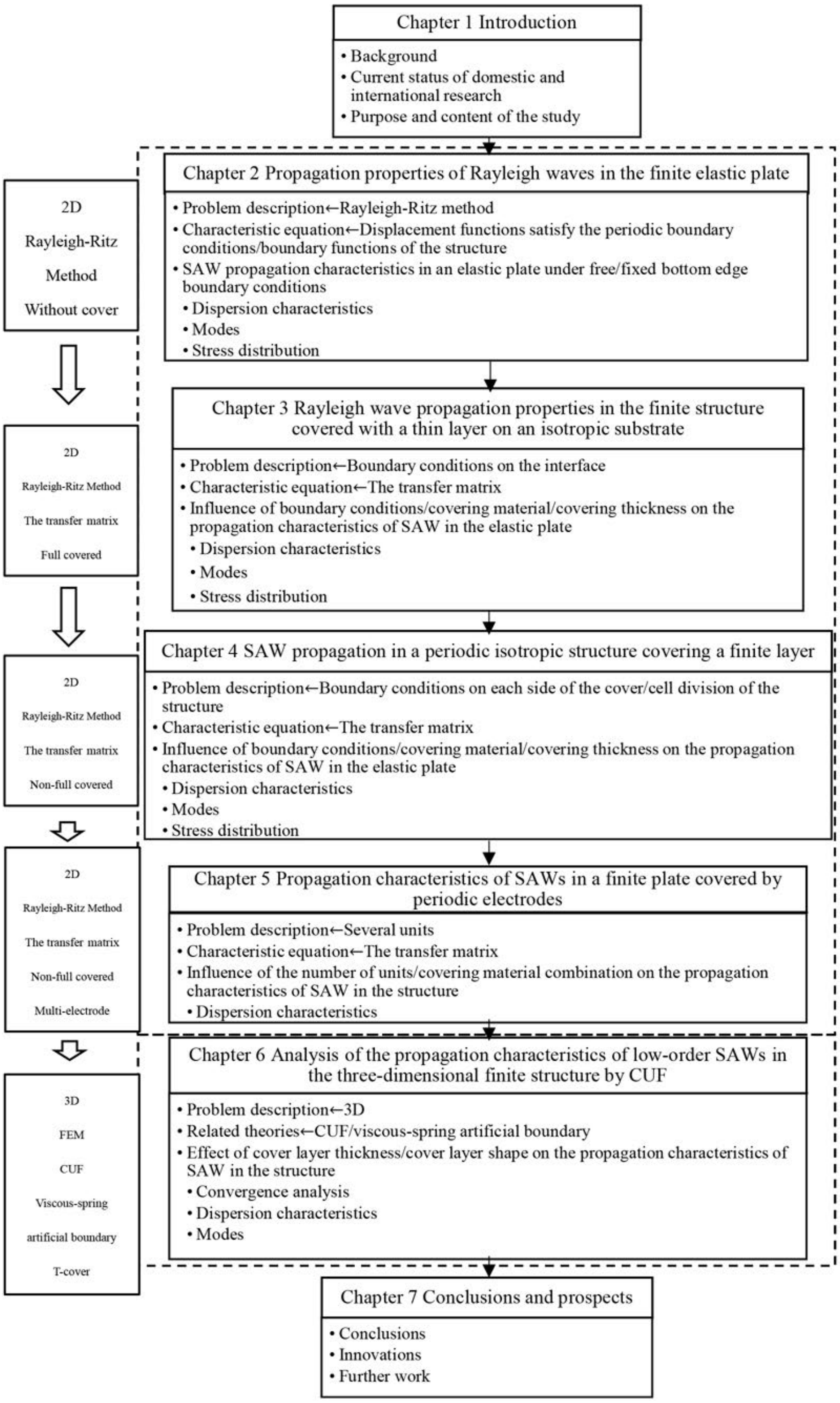

Fig. 1.1 The research framework

Chapter 2

Propagation properties of SAWs in the finite elastic plate

Rayleigh waves are a type of SAWs formed by coupling waves of compression (P-waves) and shear (S-waves), which propagate mainly at the surface and interface of a medium and whose energy decays rapidly with increasing depth. Since Rayleigh's discovery of Rayleigh waves during his studies of seismic waves, research on the geographical aspects of Rayleigh waves has gradually begun to emerge. Rayleigh waves are often generated at low frequencies in earthquakes, and although their speed is less than that of a P-wave or an S-wave, their amplitude is often greater than either, so they can cause more damage to the surface. Similarly, scholars can use its propagation stability to analyse land structure, explore for oil and other research activities. In an isotropic homogeneous medium, the wave velocity of Rayleigh waves is basically determined by the material, but with the development of material preparation technology, the research results on the characteristics of Rayleigh wave propagation in different media are becoming more and more abundant; as Rayleigh waves have the characteristics of stability and easy access in signal transmission, they also have a wide range of applications in communication, industrial testing and other fields.

For the propagation characteristics of Rayleigh waves, in a semi-infinite isotropic medium space, the analysis can be based on the classical Rayleigh wave equation; and to study the propagation characteristics of Rayleigh waves in a plate, the Rayleigh-Lamb frequency equation is generally used for analysis. When the thickness of the plate is small, the analysis is usually obtained as a Lamb wave; when the plate thickness is large, i.e. when the influence of the two free surfaces on each other is small or tends to zero, then it can be considered that a Rayleigh wave appears in the plate. In a single homogeneous elastic half-space, Rayleigh waves generally do not disperse, whereas Lamb waves have dispersion properties, i.e. the velocity of the Lamb wave changes with frequency when the thickness of the plate is a certain amount.

In general, when Rayleigh and Lamb waves occur in a plate, the stress on the free surface of the plate should be zero; the energy of Rayleigh waves is mainly concentrated near the surface, and the maximum amplitude usually occurs near the surface, while Lamb waves do not, so the Rayleigh and Lamb waves can be distinguished according to the displacement mode.

This chapter investigates the propagation properties of SAWs in an isotropic plate by means of the Rayleigh-Ritz method, focusing on the dispersion curves, displacement modes and corresponding stress distributions of the waves in the structure in a Cartesian coordinate system. In the paper, a displacement function in the form of a combination of Legendre polynomials and trigonometric functions are used, in which the boundary functions are also considered (in this chapter, the cases when the bottom edge of the plate is a free boundary and a fixed boundary are considered respectively), and the Rayleigh-Ritz method is used to convert the wave propagation problem into a characteristic equation, and then the eigenvalues and eigenvectors are used to obtain the phase velocity, generalised displacement and stress distribution of the wave, respectively. The effects of boundary conditions and plate thickness on the propagation characteristics of SAWs in structures are investigated numerically.

The dispersion curves showed that, in this case, if the upper and lower plate surfaces are all free boundaries and the plate thickness is greater than three wavelengths, it is generally assumed that Rayleigh waves are present in the structure; however, if the plate thickness is small, e.g. only one wavelength, the low-order SAWs present in the structure are usually assumed to be Lamb waves.

2.1 Problem description

Consider an elastic plate of thickness, h, with a width, a, along the direction of wave propagation, as shown in Fig. 2.1.

The constitutive relation of the elastic solid can be expressed as:

$$\sigma_{ij} = c_{ijkl}\gamma_{kl} \tag{2.1}$$

Since the two-dimensional model is constructed in this chapter, $i, j, k, l = 1, 3$, and c_{ijkl} are elastic constants, where the subscripts of the fourth-order elastic constants can be converted to second-order, as shown in Tab. 2.1.

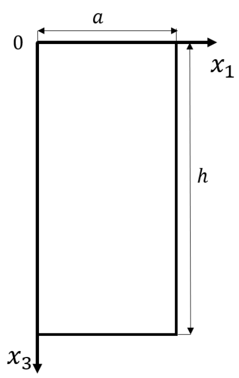

Fig. 2.1 The model of the elastic plate in 2D

Table 2.1 The relationships among the subscripts

i,k \ j,l	1	2	3
1	1	6	5
2	6	2	4
3	5	4	3

The strain can be expressed as:

$$\gamma_{ij} = \frac{1}{2}\left(u_{i,j} + u_{j,i}\right) \tag{2.2}$$

The differential equation of motion for any point in an elastic material, without regard to physical force, is:

$$\sigma_{ij,j} = \rho \ddot{u}_i \tag{2.3}$$

Therefore, the following variational equation can be obtained:

$$\int_V \delta u_i \left(\sigma_{ij,j} - \rho \ddot{u}_i\right) dV = 0 \tag{2.4}$$

To study the propagation characteristics of waves in a thick plate, we need to consider the following two boundary conditions on the upper and lower surfaces of the plate. The first is the stress boundary condition. Assuming that the upper and lower surfaces of the plate are free edges, so the stress on the upper and lower surfaces is zero, i.e:

$$\sigma_{3j}\left(x_3 = 0\right) = 0, \sigma_{3j}\left(x_3 = h\right) = 0, j = 1,2 \tag{2.5}$$

When the bottom of the thick plate ($x_3 = h$) is a fixed boundary, the displacement of the lower surface should be:

$$u_i\,(x_3 = h) = 0 \tag{2.6}$$

For different boundary conditions, the boundary functions take the following form:

(1) Free boundary condition

$$f(x_3) = 1 \tag{2.7}$$

(2) Fixed boundary condition

$$f(x_3) = 1 - \frac{x_3}{h} \tag{2.8}$$

2.2 Characteristic equation

To allow the finite elastic plate to satisfy periodic boundary conditions, the displacement function used in this section takes the form of:

$$\begin{aligned} u_i &= f\,(x_3)\,U e^{j\omega t} \\ &= f\,(x_3)\left[\sum_{n=0}^{N} A_{in} P_n\left(\frac{2x_3}{h} - 1\right)\sin\left(\frac{kx_1}{a}\right) + \sum_{n=0}^{N} B_{in} P_n\left(\frac{2x_3}{h} - 1\right)\cos\left(\frac{kx_1}{a}\right)\right] e^{j\omega t} \end{aligned} \tag{2.9}$$

Here $f(x_3)$ is the boundary function, $P_n(x)$ is the Legendre polynomial, and $j = \sqrt{-1}$, in this case, $N = 15$.

Substituting the displacement function into Eq. 2.4 yields:

$$\begin{aligned} &\int_V \left(c_{11}\frac{\partial u_1}{\partial x_1}\frac{\partial u_1}{\partial x_1} + c_{15}\frac{\partial u_1}{\partial x_1}\frac{\partial u_1}{\partial x_3} + c_{51}\frac{\partial u_1}{\partial x_3}\frac{\partial u_1}{\partial x_1} + c_{55}\frac{\partial u_1}{\partial x_3}\frac{\partial u_1}{\partial x_3}\right) \\ &+ \left(c_{55}\frac{\partial u_3}{\partial x_1}\frac{\partial u_3}{\partial x_1} + c_{53}\frac{\partial u_3}{\partial x_1}\frac{\partial u_3}{\partial x_3} + c_{35}\frac{\partial u_3}{\partial x_3}\frac{\partial u_3}{\partial x_1} + c_{33}\frac{\partial u_3}{\partial x_3}\frac{\partial u_3}{\partial x_3}\right) \\ &+ \left(c_{15}\frac{\partial u_1}{\partial x_1}\frac{\partial u_3}{\partial x_1} + c_{13}\frac{\partial u_1}{\partial x_1}\frac{\partial u_3}{\partial x_3} + c_{55}\frac{\partial u_1}{\partial x_3}\frac{\partial u_3}{\partial x_1} + c_{53}\frac{\partial u_1}{\partial x_3}\frac{\partial u_3}{\partial x_3}\right) \\ &+ \left(c_{51}\frac{\partial u_3}{\partial x_1}\frac{\partial u_1}{\partial x_1} + c_{55}\frac{\partial u_3}{\partial x_1}\frac{\partial u_1}{\partial x_3} + c_{31}\frac{\partial u_3}{\partial x_3}\frac{\partial u_1}{\partial x_1} + c_{35}\frac{\partial u_3}{\partial x_3}\frac{\partial u_1}{\partial x_3}\right) \\ &- \rho\omega^2\left(u_1^2 + u_3^2\right) dV = 0 \end{aligned} \tag{2.10}$$

Table 2.2 Boundary functions for different boundary conditions

Poisson's ratio	Young's modulus(GPa)	Density(kg/m^3)
0.17	72.66	2203

Here ω is the angular frequency, ρ is the density of the medium material, and the characteristic equation can be obtained:

$$\begin{bmatrix} [K_{u_1u_1}] & [K_{u_1u_3}] \\ [K_{u_3u_1}] & [K_{u_3u_3}] \end{bmatrix} \begin{Bmatrix} \{A\} \\ \{B\} \end{Bmatrix} - \omega^2 \begin{bmatrix} [M_{u_1u_1}] & [0] \\ [0] & [M_{u_3u_3}] \end{bmatrix} \begin{Bmatrix} \{A\} \\ \{B\} \end{Bmatrix} = \begin{Bmatrix} \{0\} \\ \{0\} \end{Bmatrix} \tag{2.11}$$

where $\left[K_{u_iu_j}\right]$ and $\left[M_{u_iu_j}\right]$ $(i,j=1,3)$ denote the stiffness matrix and the mass matrix respectively, the specific forms of which are given in the appendix of this chapter; $\{A\}$ and $\{B\}$ are column vectors consisting of unknown coefficients A_{in} and B_{in}, according to $v_R = \frac{\omega}{k}$, v_R is the speed of the SAW, ω is the angular velocity and k is the wave number. When the material is each isoelastic: $c_{11} = c_{22} = c_{33} = E\nu/[(1+\nu)(1-\nu)] + 2E/[2(1+\nu)]$; $c_{44} = c_{55} = c_{66} = E/[2(1+\nu)]$; $c_{12} = c_{13} = c_{23} = E\nu/[(1+\nu)(1-\nu)]$, where E denotes Young's modulus and ν denotes Poisson's ratio.

2.3 Numerical results and discussions

In this section we used fussed glass as the dielectric material to develop the calculations. The material parameters for fussed glass were given in Tab. 2.2. The normalized wave velocity v_R/v_T was used in the calculations in this section, where $v_T = \sqrt{\frac{\mu}{\rho}}$, the normalized structure thickness is $\frac{h}{\lambda}$ and the normalized structure width is $\frac{a}{\lambda}$, where λ is the wavelength (when not otherwise described in the text, the wavelength corresponding to the first order Rayleigh wave mode in fused glass/fused silica is generally used).

2.3.1 Propagation characteristics of SAWs at free boundary conditions

When using the Rayleigh wave formula to solve for Rayleigh waves in two-dimensional space, considered that the space is a semi-infinite space, and because the energy of Rayleigh waves is concentrated near the free surface, its energy decays rapidly as the distance to the free surface increases, so in solving for the SAWs in a finite thick plate need to set a reasonable plate thickness to get the ideal Rayleigh waves. According to Fig. 2.2, there are stable Rayleigh waves in the structure when the thickness of the plate reaches more than three wavelengths, which is consistent with the conclusion that the energy of the Rayleigh waves is mainly focused in the range of about one wavelength near the free surface for the analytical solution.

Thus, when a plate thickness is six wavelengths, the displacement modes of the SAWs are shown in Fig. 2.3 and the corresponding stress distribution is shown in Fig. 2.4, provided that the upper and lower surfaces of the finite plate are free. When the plate thickness is small, e.g. one tenth of a wavelength, the displacement modes corresponding to the lower order wave velocities in the plate are shown in Fig. 2.5 and the corresponding stress distributions are shown in Fig. 2.6. On the free surface of an elastic solid, the SAW generally exhibits both symmetrical and anti-symmetrical modes, so in a thick plate structure where both the upper and lower surfaces are free, a single SAW velocity may correspond to multiple order modes. The solid line in the figure shows the distribution of displacement/shear stress ($\sigma_{x_3x_1}$) for u_3 and the dashed line shows the distribution of displacement/normative stress ($\sigma_{x_3x_3}$) for u_1, where the normalised amplitude is: $u_i/\max(u_i)$, where $i = 1,3$.

According to Figs. 2.3 and 2.4 it can be observed that the results are almost identical to those of Fig. 2.2. When the thickness of the plate is greater than a certain value (three wavelengths), a stable Rayleigh wave is generated in the finite plate, and as shown in Fig. 2.4, the corresponding stress distribution in the plate at this time conforms to the stress boundary conditions corresponding to the free boundary conditions.

A comparison of Figs. 2.3, 2.5 and 2.7 showed that the maximum amplitude of the Rayleigh waves was mainly near the two surfaces of the plate, while the amplitude of the Lamb waves did not change significantly in attenuation, but according to Figs. 2.4, 2.6 and 2.8, the method used in this chapter satisfied the free boundary conditions of the model, regardless of the thickness of the plate.

2.3.2 SAWs propagation characteristics in a plate with a fixed boundary condition on the bottom surface

When a fixed boundary is used for the bottom surface of the thick plate ($x_3 = h$), the number of modes of the SAWs obtained in the structure changes as the free surface is reduced, but there is no effect on the magnitude of the SAW velocity in the structure. By comparing the results with those obtained with the free boundary condition, as in Fig. 2.9, it can be found that the wave velocity of Rayleigh waves appears in the structure when the bottom surface is fixed and the thickness of the plate is at λ.

When a plate thickness of six wavelengths is used, the displacement mode corresponding to the first order Rayleigh wave velocity is shown in Fig. 2.10 and the stress distribution is shown in Fig. 2.11 for a fixed bottom surface; when a plate thickness of one wavelength

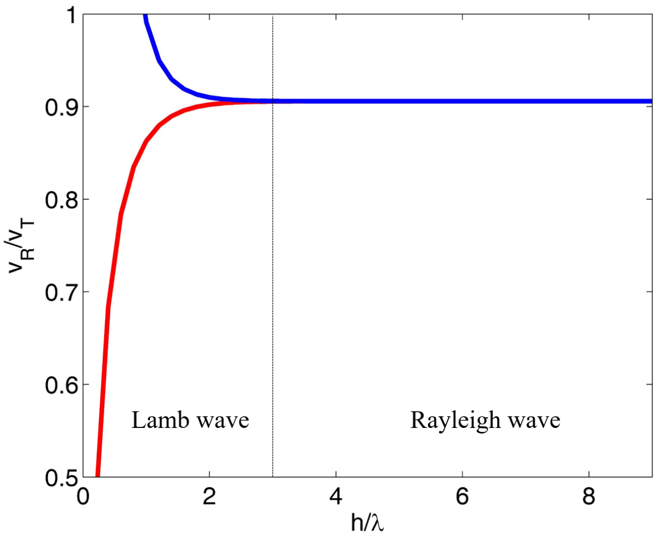

Fig. 2.2 The relationship between the thickness of the plate and the normalized wave velocity

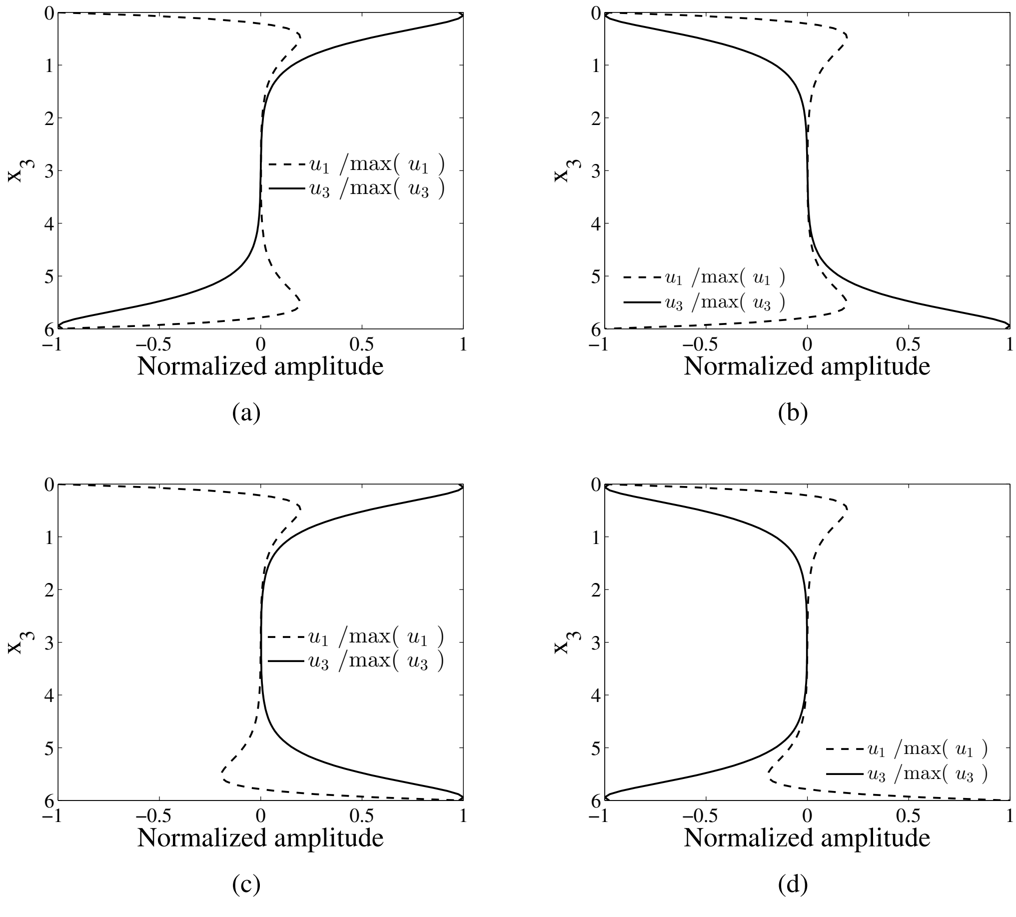

Fig. 2.3 First four Rayleigh wave modes for a plate thickness of 6λ with free boundary conditions: (a) the 1st mode; (b) the 2nd mode; (c) the 3rd mode; (d) the 4th mode

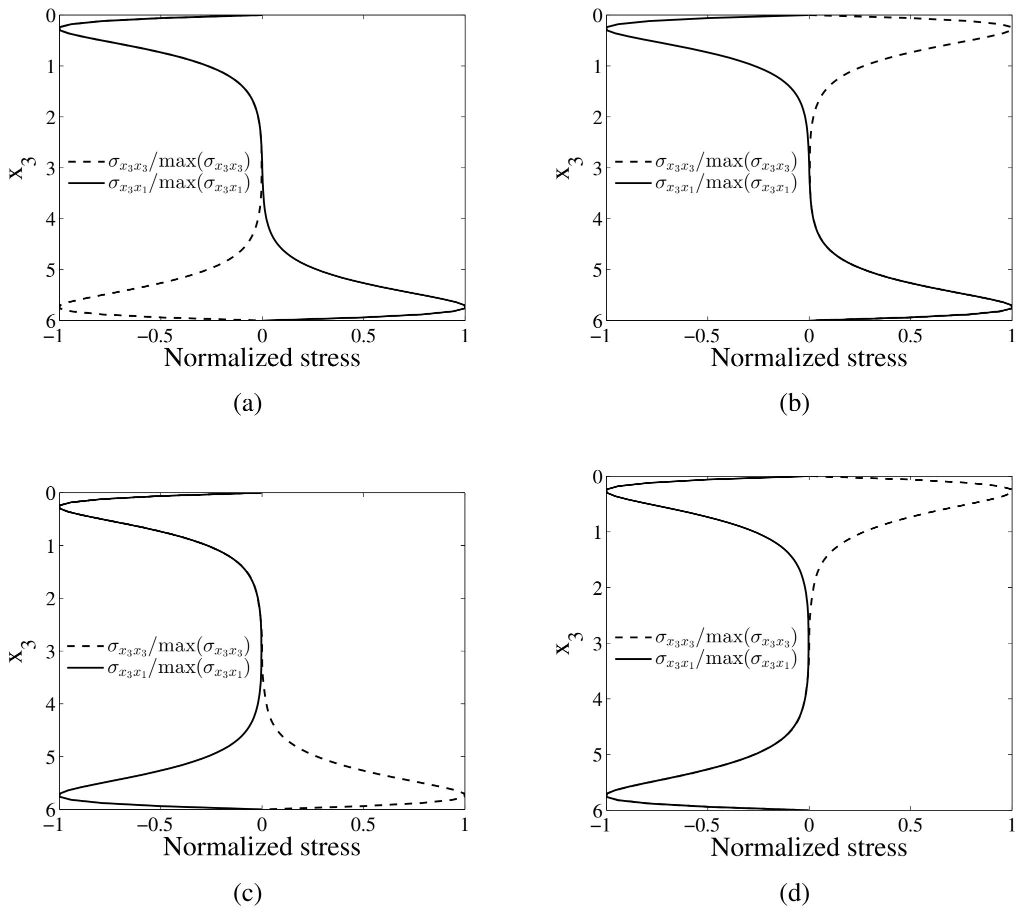

Fig. 2.4 First four stress distributions of Rayleigh waves for a plate thickness of 6λ with free boundary conditions: the stress distribution of (a) the 1st mode; (b) the 2nd mode; (c) the 3rd mode; (d) the 4th mode

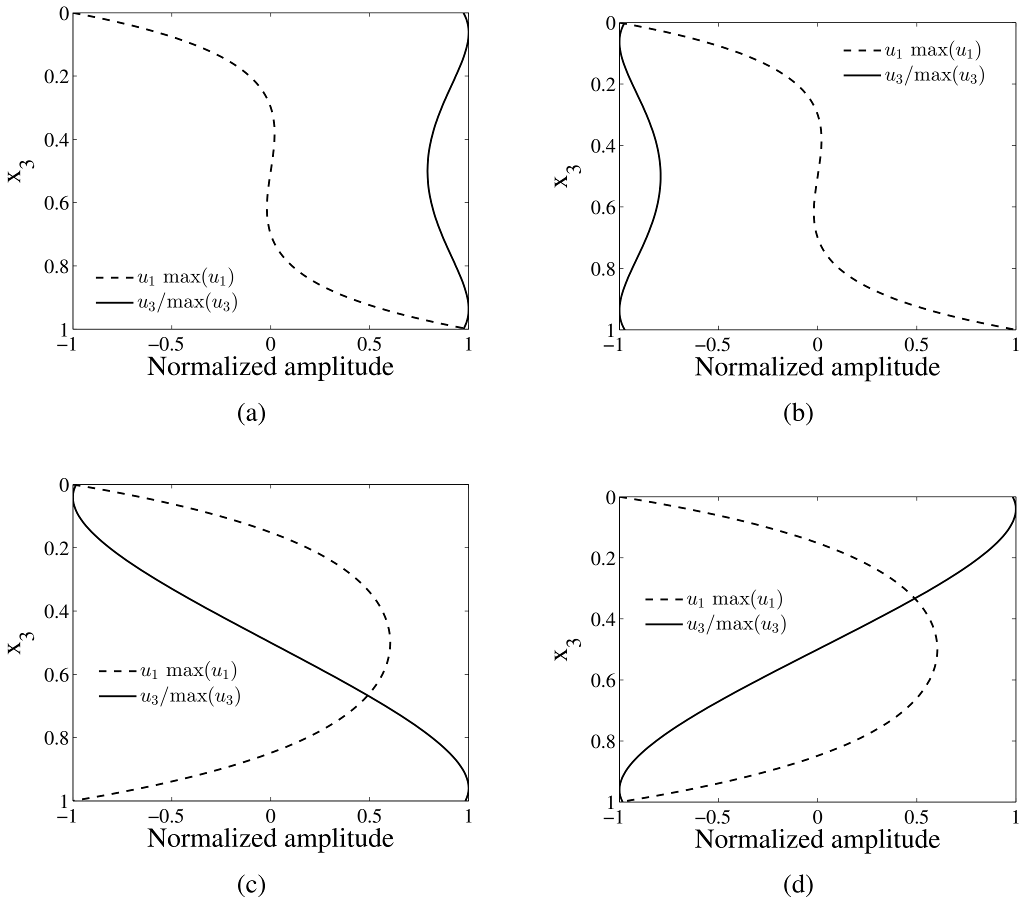

Fig. 2.5 First four Rayleigh wave modes for a plate thickness of λ with free boundary conditions: (a) the 1st mode; (b) the 2nd mode; (c) the 3rd mode; (d) the 4th mode

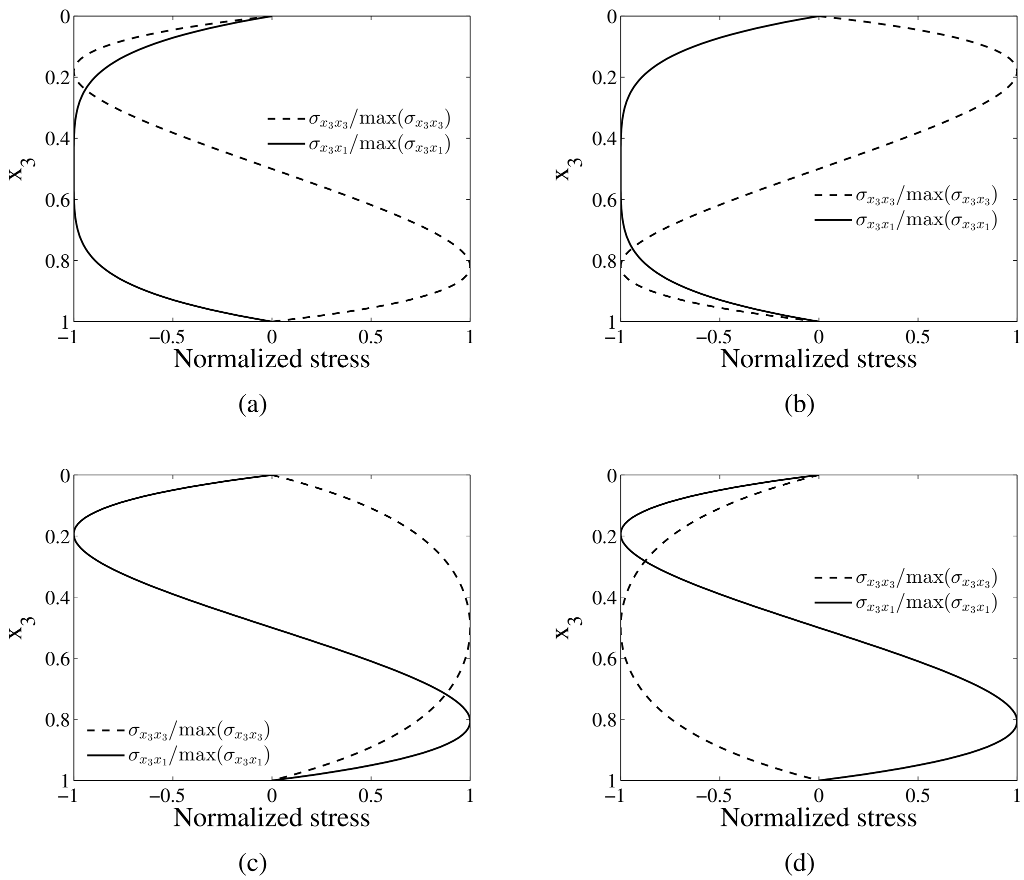

Fig. 2.6 First four stress distributions of Rayleigh waves for a plate thickness of λ with free boundary conditions: the stress distribution of (a) the 1st mode; (b) the 2nd mode; (c) the 3rd mode; (d) the 4th mode

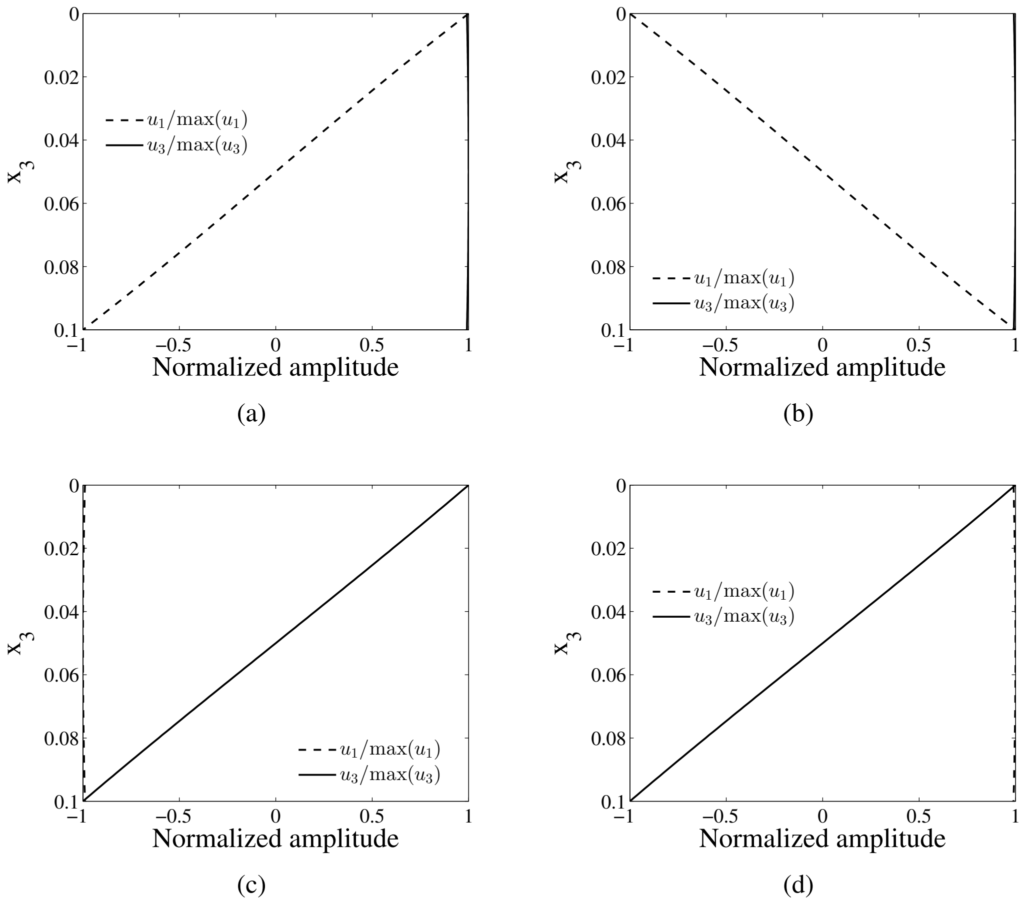

Fig. 2.7 First four Rayleigh wave modes for a plate thickness of 0.1λ with free boundary conditions: (a) the 1st mode; (b) the 2nd mode; (c) the 3rd mode; (d) the 4th mode

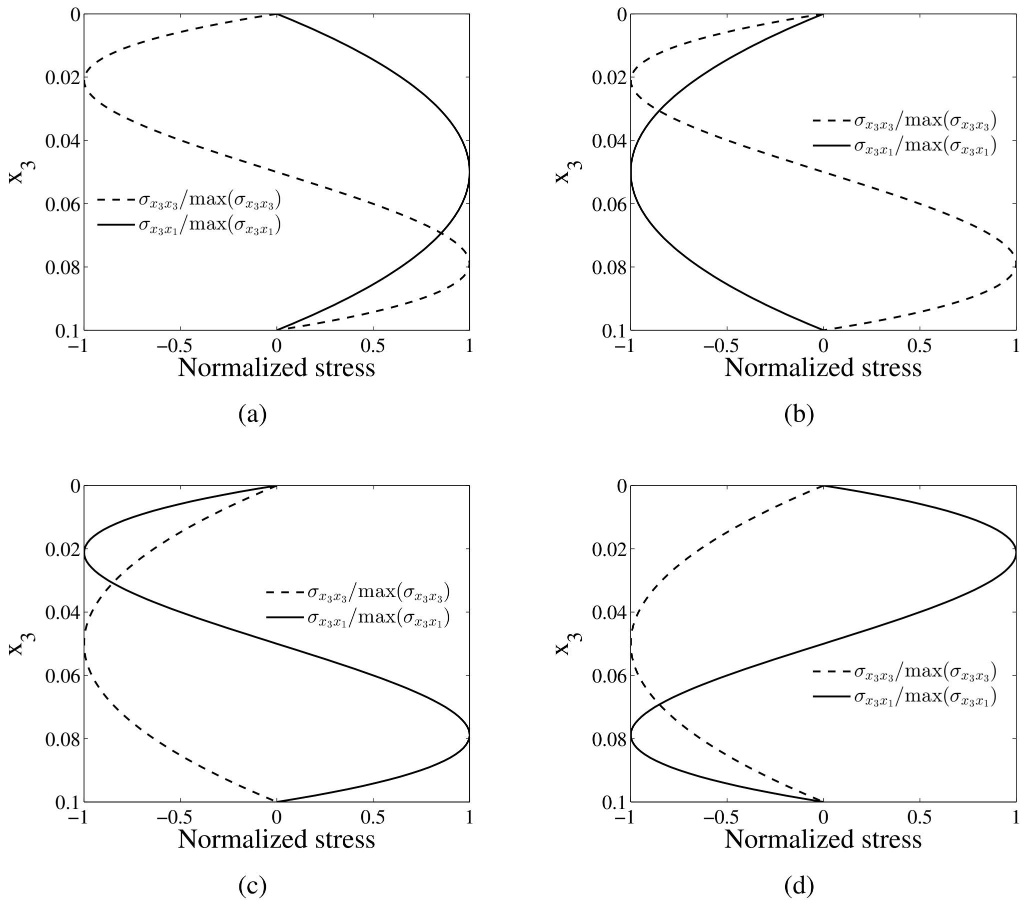

Fig. 2.8 First four stress distributions of Rayleigh waves for a plate thickness of 0.1λ with free boundary conditions: the stress distribution of (a) the 1st mode; (b) the 2nd mode; (c) the 3rd mode; (d) the 4th mode

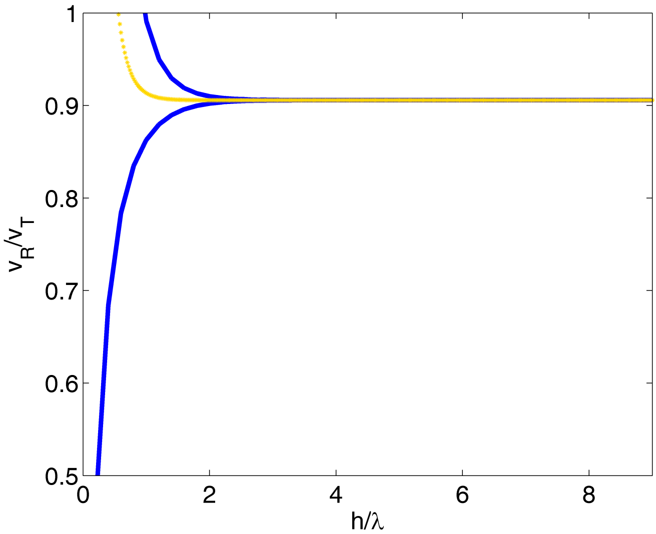

Fig. 2.9 The relationship between the thickness of the plate and the normalized wave velocity under different boundary conditions

is used, the displacement mode corresponding to the first order Rayleigh wave velocity is shown in Fig. 2.12 and the stress distribution is shown in Fig. 2.13; when a plate thickness of one tenth of a wavelength is used, the displacement mode corresponding to the first order Rayleigh wave velocity is shown in Fig. 2.14 and the stress distribution is shown in Fig. 2.15. The displacement mode corresponding to the first order Rayleigh wave velocity is shown in Fig. 2.14 and the stress distribution is shown in Fig. 2.15.

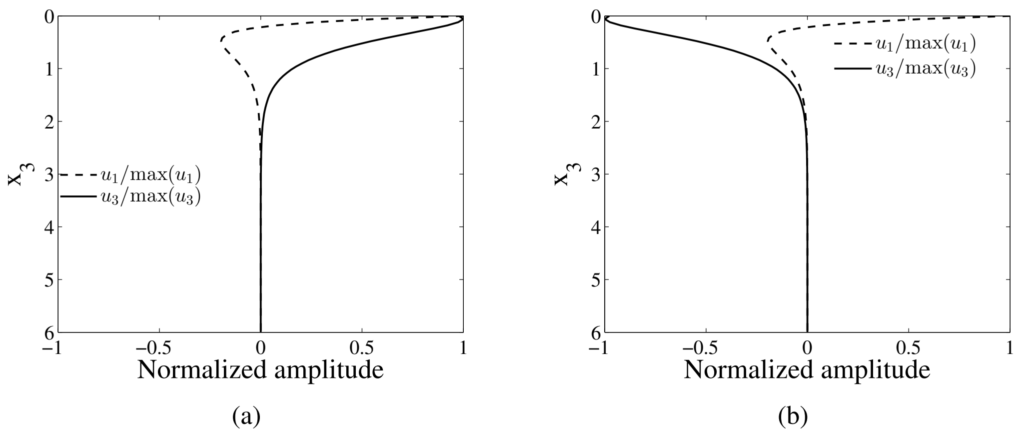

Fig. 2.10 First two Rayleigh wave modes for a plate thickness of 6λ with fixed boundary conditions on the bottom surface: (a) the 1st mode; (b) the 2nd mode

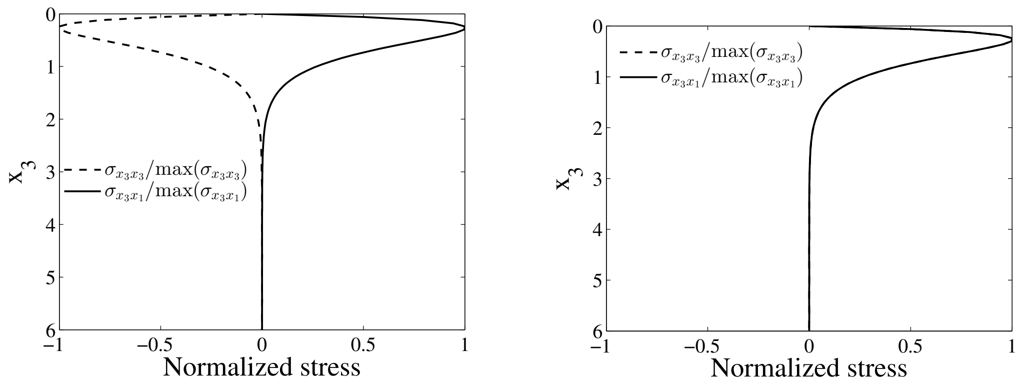

(a) (b)

Fig. 2.11 First two stress distributions of Rayleigh waves for a plate thickness of 6λ with fixed boundary conditions on the bottom surface: the stress distribution of (a) the 1st displacement mode; (b) the 2nd displacement mode

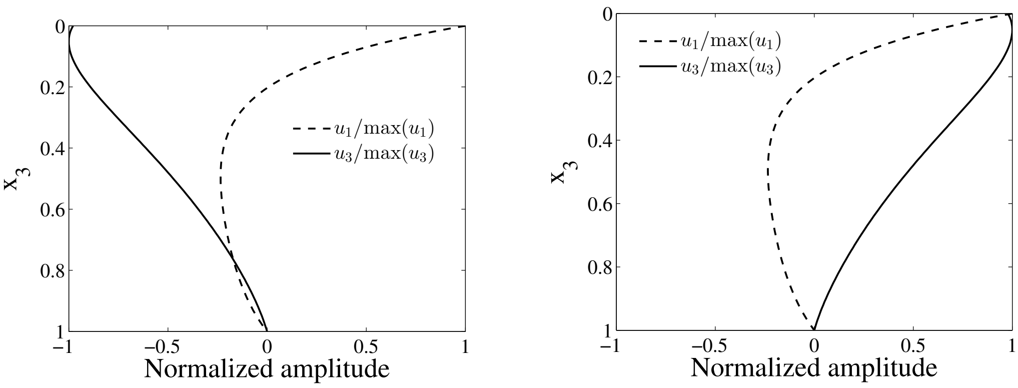

(a) (b)

Fig. 2.12 First two Rayleigh wave modes for a plate thickness of λ with fixed boundary conditions on the bottom surface: (a) the 1st mode; (b) the 2nd mode

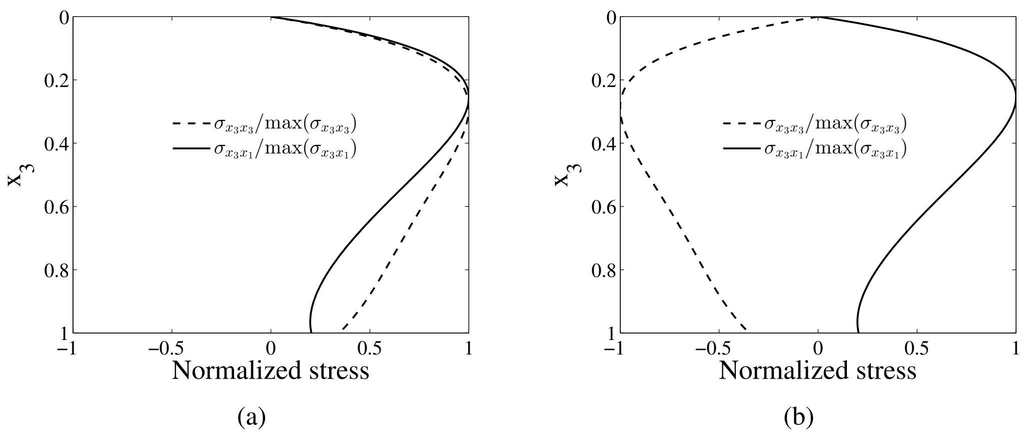

Fig. 2.13 First two stress distributions of Rayleigh waves for a plate thickness of λ with fixed boundary conditions on the bottom surface: the stress distribution of (a) the 1st displacement mode; (b) the 2nd displacement mode

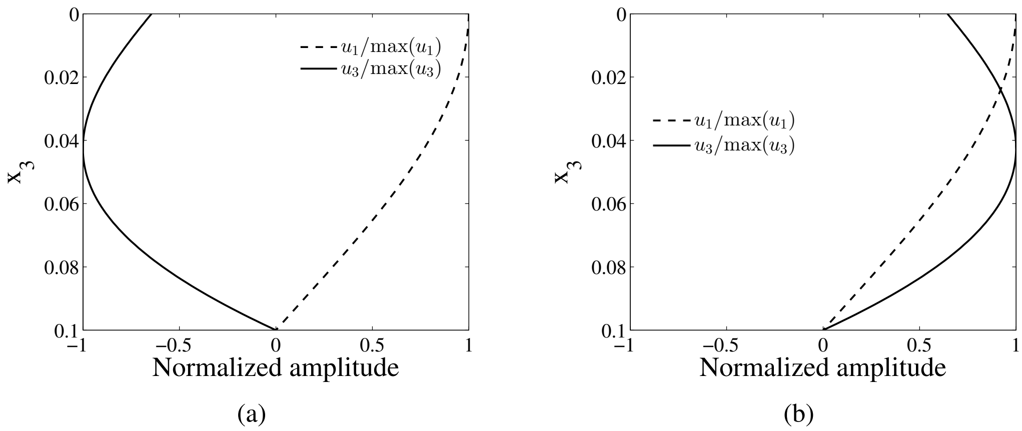

Fig. 2.14 First two Rayleigh wave modes for a plate thickness of 0.1λ with fixed boundary conditions on the bottom surface: (a) the 1st mode; (b) the 2nd mode

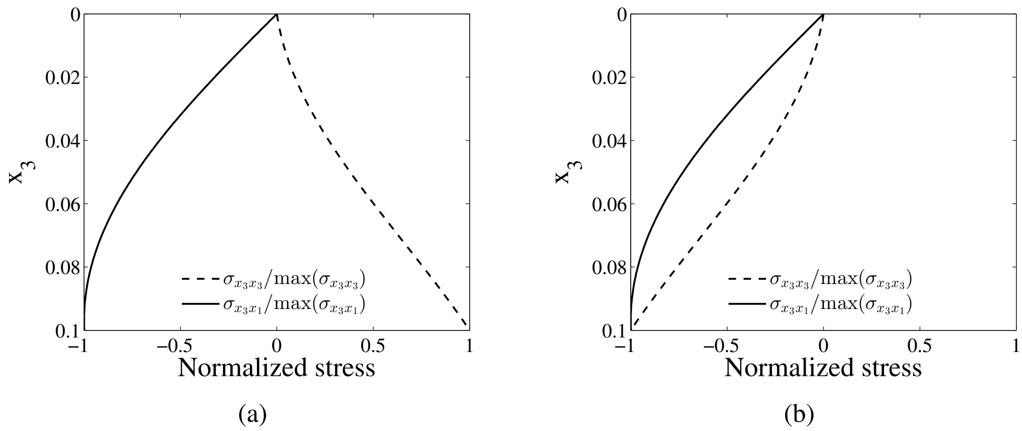

Fig. 2.15 First two stress distributions of Rayleigh waves for a plate thickness of 0.1λ with fixed boundary conditions on the bottom surface: the stress distribution of (a) the 1st displacement mode; (b) the 2nd displacement mode

2.4 Summary

In this chapter, the characteristic equations for an elastic plate of finite size obtained by the Rayleigh-Ritz method for different boundary conditions are derived, and the SAWs in an isotropic elastic thick plate are obtained using a reasonable form of the displacement function. The influence of the plate thickness and each boundary condition on the SAWs in the structure is discussed numerically. The numerical results show that:

(1) When the bottom edge of a thick plate is fixed, the thickness of the plate where the low-order Rayleigh waves occur is slightly thinner than if both sides of the plate were free. Again, however, the number of displacement modes in the lower order Rayleigh waves is reduced due to the reduction in the number of free surfaces.

(2) The trial function form used in this chapter allows the stress distribution corresponding to the low-order SAWs velocities in the structure to be made to conform to the corresponding boundary conditions for different plate thickness conditions.

Appendix

Stiffness matrix:

$$
\begin{aligned}
\left[K_{u_iu_j}\right]_{m_1n_1} &= c_{i1k1}E^{1,1}_{U_ipU_k\bar{p}}F_1^{0,0} + c_{i1k2}E^{1,0}_{U_ipU_k\bar{p}}F_1^{0,1} + c_{i1k3}E^{1,0}_{U_ipU_k\bar{p}}F_1^{0,0} \\
&\quad + c_{i2k1}E^{0,1}_{U_ipU_k\bar{p}}F_1^{1,0} + c_{i2k2}E^{0,0}_{U_ipU_k\bar{p}}F_1^{1,1} + c_{i2k3}E^{0,0}_{U_ipU_k\bar{p}}F_1^{1,0} \\
&\quad + c_{i3k1}E^{0,1}_{U_ipU_k\bar{p}}F_1^{0,0} + c_{i3k2}E^{0,0}_{U_ipU_k\bar{p}}F_1^{0,1} + c_{i3k3}E^{0,0}_{U_ipU_k\bar{p}}F_1^{0,0} \\
\left[K_{u_iu_j}\right]_{m_2n_1} &= c_{i1k1}E^{1,1}_{U_ipU_k\bar{p}}F_2^{0,0} + c_{i1k2}E^{1,0}_{U_ipU_k\bar{p}}F_2^{0,1} + c_{i1k3}E^{1,0}_{U_ipU_k\bar{p}}F_2^{0,0} \\
&\quad + c_{i2k1}E^{0,1}_{U_ipU_k\bar{p}}F_2^{1,0} + c_{i2k2}E^{0,0}_{U_ipU_k\bar{p}}F_2^{1,1} + c_{i2k3}E^{0,0}_{U_ipU_k\bar{p}}F_2^{1,0} \\
&\quad + c_{i3k1}E^{0,1}_{U_ipU_k\bar{p}}F_2^{0,0} + c_{i3k2}E^{0,0}_{U_ipU_k\bar{p}}F_2^{0,1} + c_{i3k3}E^{0,0}_{U_ipU_k\bar{p}}F_2^{0,0} \\
\left[K_{u_iu_j}\right]_{m_1n_2} &= c_{i1k1}E^{1,1}_{U_ipU_k\bar{p}}F_3^{0,0} + c_{i1k2}E^{1,0}_{U_ipU_k\bar{p}}F_3^{0,1} + c_{i1k3}E^{1,0}_{U_ipU_k\bar{p}}F_3^{0,0} \\
&\quad + c_{i2k1}E^{0,1}_{U_ipU_k\bar{p}}F_3^{1,0} + c_{i2k2}E^{0,0}_{U_ipU_k\bar{p}}F_3^{1,1} + c_{i2k3}E^{0,0}_{U_ipU_k\bar{p}}F_3^{1,0} \\
&\quad + c_{i3k1}E^{0,1}_{U_ipU_k\bar{p}}F_3^{0,0} + c_{i3k2}E^{0,0}_{U_ipU_k\bar{p}}F_3^{0,1} + c_{i3k3}E^{0,0}_{U_ipU_k\bar{p}}F_3^{0,0} \\
\left[K_{u_iu_j}\right]_{m_2n_2} &= c_{i1k1}E^{1,1}_{U_ipU_k\bar{p}}F_4^{0,0} + c_{i1k2}E^{1,0}_{U_ipU_k\bar{p}}F_4^{0,1} + c_{i1k3}E^{1,0}_{U_ipU_k\bar{p}}F_4^{0,0} \\
&\quad + c_{i2k1}E^{0,1}_{U_ipU_k\bar{p}}F_4^{1,0} + c_{i2k2}E^{0,0}_{U_ipU_k\bar{p}}F_4^{1,1} + c_{i2k3}E^{0,0}_{U_ipU_k\bar{p}}F_4^{1,0} \\
&\quad + c_{i3k1}E^{0,1}_{U_ipU_k\bar{p}}F_4^{0,0} + c_{i3k2}E^{0,0}_{U_ipU_k\bar{p}}F_4^{0,1} + c_{i3k3}E^{0,0}_{U_ipU_k\bar{p}}F_4^{0,0}
\end{aligned}
\tag{2.12}
$$

Mass matrix is:

$$
\begin{aligned}
\left[M_{u_iu_j}\right]_{m_1n_1} &= \rho E^{0,0}_{U_ipU_k\bar{p}}F_1^{0,0} \\
\left[M_{u_iu_j}\right]_{m_2n_1} &= \rho E^{0,0}_{U_ipU_k\bar{p}}F_2^{0,0} \\
\left[M_{u_iu_j}\right]_{m_1n_2} &= \rho E^{0,0}_{U_ipU_k\bar{p}}F_3^{0,0} \\
\left[M_{u_iu_j}\right]_{m_2n_2} &= \rho E^{0,0}_{U_ipU_k\bar{p}}F_4^{0,0}
\end{aligned}
\tag{2.13}
$$

where,

$$E_{U_i p U_k \bar{p}}^{\alpha,\beta} = \int_0^h \frac{d^\alpha P_p\left(\frac{2x_3}{h}-1\right)}{dx_3^\alpha} \frac{d^\beta P_{\bar{p}}\left(\frac{2x_3}{h}-1\right)}{dx_3^\beta} dx_3 \tag{2.14}$$

$$\begin{aligned}
F_1^{\alpha,\beta} &= \int_0^a \frac{d^\alpha \sin(kx_1)}{dx_1^\alpha} \frac{d^\beta \sin(kx_1)}{dx_1^\beta} dx_1 \\
F_2^{\alpha,\beta} &= \int_0^a \frac{d^\alpha \cos(kx_1)}{dx_1^\alpha} \frac{d^\beta \cos(kx_1)}{dx_1^\beta} dx_1 \\
F_3^{\alpha,\beta} &= \int_0^a \frac{d^\alpha \cos(kx_1)}{dx_1^\alpha} \frac{d^\beta \sin(kx_1)}{dx_1^\beta} dx_1 \\
F_4^{\alpha,\beta} &= \int_0^a \frac{d^\alpha \cos(kx_1)}{dx_1^\alpha} \frac{d^\beta \cos(kx_1)}{dx_1^\beta} dx_1
\end{aligned} \tag{2.15}$$

where α and β are the orders of the partial divisions; p and $\bar{p}$ are the orders of the polynomials; $i,k = 1,2,3$. The elements in the stiffness matrix, $\mathbf{K}$, and the mass matrix, $\mathbf{M}$, can be expressed as follows: $\left[K_{u_i u_j}\right]_{m_1 n_1}, \left[K_{u_i u_j}\right]_{m_2 n_1}, \left[K_{u_i u_j}\right]_{m_1 n_2}, \left[K_{u_i u_j}\right]_{m_2 n_2}$ and $\left[M_{u_i u_j}\right]_{m_1 n_1}, \left[M_{u_i u_j}\right]_{m_1 n_2}, \left[M_{u_i u_j}\right]_{m_2 n_1}, \left[M_{u_i u_j}\right]_{m_2 n_2}$ of the form and $m_1 = 2p+1, n_1 = 2\bar{p}+1, m_2 = 2(p+1), n_2 = 2(\bar{p}+1)$.

Chapter 3

Propagation properties of low-order SAWs in a finite structure covered by a thin layer

The motion of Rayleigh waves is elliptical under the influence of P and S waves. Therefore, when other materials are attached to the medium to form a layered structure, the vibration modes and wave velocities of the Rayleigh waves in the original medium are affected definitely. In general, Rayleigh waves in a layered half-space structure have dispersive properties. This property is also used in geographical research to detect and analyse subsurface structures and to conduct shallow surface exploration studies.

In the field of geological exploration, scholars have been studying the propagation characteristics of Rayleigh waves in a simplified semi-infinite stratified space model based on actual geological conditions, and have been developing techniques to extract SAWs of various orders more accurately, to improve the accuracy and safety of geological exploration, by combining actual exploration data. The matrix method has been used to analyse the propagation properties of SAWs in semi-infinite stratified space, the fluctuation equation combined with boundary conditions to analyse the propagation properties of SAWs in structures, and the Boundary Element Method (BEM).

Since the discovery by R. M. White and F. W. Voltmer in the 1970s that metal IDTs could excite SAWs in piezoelectric materials, SAW devices have been developing rapidly. At that time, when computer technology was not yet developed, experimental, analytical and semi-analytical methods were the main methods to study the propagation characteristics of SAWs.

Since there are typically hundreds of pairs of IDTs in an SAW device, the size of the device in the direction of wave propagation is very large in relation to a single unit and can often be approximated to be infinitely long. Therefore, in a large number of studies of SAW devices, it is common to take a unit from the structure, set reasonable boundary conditions (periodic or absorption boundaries) and use it instead of the whole structure as the object of study in order to reduce computational costs. With the development of technology and the innovation of computer technology, the FEM has been widely used in the study of SAW propagation due to its flexibility and versatility. However, the FEM generally requires high computer performance and has the disadvantages of long computation time and inability to guarantee the continuity of physical quantities (e.g. stress and strain) over the whole area.

There have been numerous studies on the propagation of SAWs in multilayer structures, but the effects of boundary conditions, the covering material and thickness on wave velocities, modes and stress distributions have not been systematically investigated. In this chapter, the propagation characteristics of SAWs in periodic structures covered with thin plates on an isotropic substrate are investigated. Using the Rayleigh-Ritz method, the SAW problem is transformed into a linear eigenvalue problem, and then the transfer matrix is obtained by combining the boundary conditions (the number of unknown coefficients is reasonably reduced by selecting the boundary conditions that must be considered in order to reduce the matrix operations), and the SAW velocities and displacement modes are then expressed in terms of eigenvalues and eigenvectors. In this chapter, fused silica is used as the base material and Au and Al_2O_3 as the covering material. The effect of the boundary conditions and the thickness of the covering layer on the propagation characteristics of Rayleigh waves in the structure is studied numerically.

3.1 Problem description

Consider an isotropic substrate plate of thickness h covered by an isotropic metal layer of thickness $\bar{h}$ where the direction of SAW propagation is x_1 and the thickness direction of the plate is x_3, as shown in Fig. 3.1.

By setting the boundary at $x_1 = 0$ and $x_1 = a$ (generally a is taken to be one wavelength) as a periodic boundary and setting $h = 6\lambda$, the calculation of a semi-infinite space is transformed into an analysis of a finite computational model.

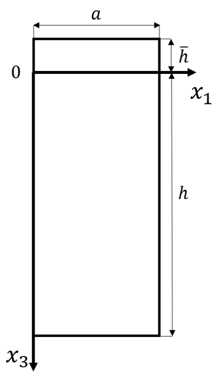

Fig. 3.1 A finite solid covered by a thin plate

To satisfy the periodic boundary conditions for the structure, it is useful to set the displacement function of the covering layer in the form as:

$$\begin{aligned}\bar{u}_i &= \bar{f}(x_3)\bar{U}e^{j\omega t} \\ &= \bar{f}(x_3)\left[\sum_{n=0}^{N}\bar{A}_{in}P_n\left(\frac{2x_3}{\bar{h}}+1\right)\sin\left(\frac{kx_1}{a}\right)+\sum_{n=0}^{N}\bar{B}_{in}P_n\left(\frac{2x_3}{\bar{h}}+1\right)\cos\left(\frac{kx_1}{a}\right)\right]e^{j\omega t}\end{aligned} \tag{3.1}$$

The displacement function of the substrate in the form as:

$$\begin{aligned}u_i &= f(x_3)Ue^{j\omega t} \\ &= f(x_3)\left[\sum_{n=0}^{N}A_{in}P_n\left(\frac{2x_3}{h}-1\right)\sin\left(\frac{kx_1}{a}\right)+\sum_{n=0}^{N}B_{in}P_n\left(\frac{2x_3}{h}-1\right)\cos\left(\frac{kx_1}{a}\right)\right]e^{j\omega t}\end{aligned} \tag{3.2}$$

where $i = 1, 3$, $f(x)$ and $\bar{f}(x)$ are boundary functions which, if not otherwise stated in this paper, are both used to describe the boundary conditions on $x_3 = h$ and $x_3 = -\bar{h}$ in the structure, see Tab. 3.1 for the specific functional form, and $P_n(x)$ remains a Legendre polynomial.

The following boundary conditions generally need to be considered for calculating the model:

(1) Continuous displacement at the interface

$$u_i(x_3 = 0) = \bar{u}_i(x_3 = 0) \tag{3.3}$$

Table 3.1 Boundary functions for different boundary conditions

Boundary condition	$f(x_3)$	$\bar{f}(x_3)$
Fixed boundary condition	$1-\frac{x_3}{h}$	/
Free boundary condition	1	1

(2) Continuous stress at the interface

$$\sigma_{3i}(x_3=0)=\bar{\sigma}_{3i}(x_3=0) \tag{3.4}$$

(3) Free boundary condition

$$\bar{\sigma}_{3i}\left(x_3=-\bar{h}\right)=0 \tag{3.5}$$

(4) Fixed boundary condition at the bottom of the substrate

$$u_i(x_3=h)=0 \tag{3.6a}$$

Free boundary condition at the bottom of the substrate

$$\sigma_{3i}(x_3=h)=0 \tag{3.6b}$$

3.2 Equation derivation

According to the Rayleigh-Ritz method, the kinetic energy of the substrate is:

$$T_S=\frac{1}{2}\rho\int_0^h\int_0^a \dot{u}^2 dx_1 dx_3 \tag{3.7}$$

where ρ refers to the density of the substrate material.

The strain energy of the substrate is:

$$V_S=\frac{1}{2}c_{ijkl}\int_0^h\int_0^a u_{i,k}u_{j,l}dx_1 dx_3 \tag{3.8}$$

where c_{ijkl} represents the elastic constant of the substrate material.

Similarly the kinetic and strain energies of the cover can be obtained:

$$T_C=\frac{1}{2}\bar{\rho}\int_{\bar{h}}^0\int_0^a \dot{\bar{u}}^2 dx_1 dx_3 \tag{3.9}$$

$$V_C = \frac{1}{2}\bar{c}_{ijkl}\int_{\bar{h}}^{0}\int_{0}^{a}\bar{u}_{i,k}\bar{u}_{j,l}dx_1dx_3 \tag{3.10}$$

where $\bar{\rho}$ and $\bar{c}_{ijkl}$ represent the material density and elastic constants of the covering layer respectively.

Combining the above equations yields the kinetic and potential energies of the entire structure, i.e.:

$$T = T_S + T_C \tag{3.11}$$

$$V = V_S + V_C \tag{3.12}$$

From the Lagrangian equation:

$$\Lambda = T - V \tag{3.13}$$

and the principle of minimum energy, obtain:

$$\frac{\partial\Lambda}{\partial A_{i,n}} = 0, \frac{\partial\Lambda}{\partial B_{i,n}} = 0, \frac{\partial\Lambda}{\partial \bar{A}_{i,n}} = 0, \frac{\partial\Lambda}{\partial \bar{B}_{i,n}} = 0 \tag{3.14}$$

Then the characteristic equation can be obtained as:

$$\left(\mathbf{K} - \omega^2\mathbf{M}\right)\alpha = 0 \tag{3.15}$$

where α is the column vector consisting of the unknown coefficients A_{in},B_{in},$\bar{A}_{in}$ and $\bar{B}_{in}$, while **K** and **M** represent the stiffness and mass matrices respectively, shown as:

$$[K] = \begin{bmatrix} [K^S] & [0] \\ [0] & [K^C] \end{bmatrix}, [M] = \begin{bmatrix} [M^S] & [0] \\ [0] & [M^C] \end{bmatrix}, \{\alpha\} = \begin{Bmatrix} \{\alpha^S\} \\ \{\alpha^C\} \end{Bmatrix} \tag{3.16}$$

where the superscripts S and C represent the substrate and the overlay respectively, and the elements in the matrix are referred to in the Appendix section of Chapter 2 for their exact form.

3.3 Numerical results and discussions

In this section we studied the propagation characteristics of Rayleigh waves in a periodic structure covered by a thin layer. We mainly analysed the effect of each boundary condition on the propagation characteristics of low-order Rayleigh waves in the structure; the effect of the covering layer material on the dispersion curve of low-order Rayleigh waves in the structure; and the effect of the covering layer thickness on the dispersion curve of low-order Rayleigh waves in the structure. In the model, x_1 is the direction of wave propagation and x_3

Table 3.2 The material properties used in this section [1]

Material	ν	E(GPa)	ρ(kg/m^3)
Fused quartz	0.17	72.66	2203
Au condition	0.416	78.75	19300
Al_2O_3	0.267	413.00	3978

is the direction of substrate thickness, and fused silica is used as the material for the substrate in the model in this chapter. The relevant physical parameters of the materials involved in the calculation cases are given in Tab. 3.2. In this section, the normalised wave velocity is v_R/v_T, where v_R is the SAW velocity in the structure and v_T is the shear wave velocity of the substrate material.

3.3.1 Influence of boundary conditions on the propagation characteristics of low-order Rayleigh waves in the structure

In this subsection, Au is used as the covering material, $\bar{h} = 0.1\lambda$, $h = 6\lambda$, and λ denotes the wavelength if not otherwise stated in this section. The wave velocities of the SAWs obtained for different boundary conditions are given in Tab. 3.3; Figs. 3.2 to 3.5 show the first six orders of Rayleigh wave modes for different boundary conditions, where the normalised amplitude used here is: $\mathbf{u}$/max($\mathbf{u}$), where $\mathbf{u} = (u_i, \bar{u}_i)^T$, $i = 1,3$. Figs 3.2 and 3.4 show the displacement on the contact surface considered only for continuous. Figs. 3.3 and 3.5 show the displacement modes obtained when the displacement and stress continuity on the contact surface are considered, and the amplitude near the intersection is larger due to the influence of the covering layer on the substrate after the stress boundary condition is considered, so the lower left corner of the displacement diagram The displacement mode when the normalised amplitude is: $u_i/\max(u_i)$ is also shown; Figs. 3.6 to 3.9 show the stress distribution corresponding to the first six orders of the displacement mode of Rayleigh waves under different boundary conditions, where the normalised stress is: $\sigma/\max(\sigma)$, where $\sigma = (\sigma_{x_ix_j}, \bar{\sigma}_{x_ix_j})^T$.

From Tab. 3.3, the stress boundary conditions involved in the structure have very little effect on the low-order SAW velocities in this model, and because of the relatively large thickness of the substrate used in this case the substrate thickness is six wavelengths. In addition to the continuity of the upper and lower layer displacements, further consideration of the continuity of the stresses at the interface between the upper and lower layers in the transfer matrix does not affect the calculation of the low-order SAW velocities.

Table 3.3 The first six normalized SAW velocities under different boundary conditions

Boundary condition	v_R/v_T					
	1	2	3	4	5	6
Substrate bottom surface is free, displacement is continuous	0.4887	0.4887	0.7109	0.7109	0.9058	0.9058
Substrate bottom surface is free, displacement and stress are continuous	0.4887	0.4887	0.7109	0.7109	0.9058	0.9058
Substrate bottom surface is fixed, displacement is continuous	0.4887	0.4887	0.7109	0.7109	0.9058	0.9058
Substrate bottom surface is fixed, displacement and stress are continuous	0.4887	0.4887	0.7109	0.7109	0.9058	0.9058

However, from Figs. 3.2 to 3.3, it is easy to see that the stress continuity conditions on the interface have an influence on the modes of the lower order SAWs. When only the displacement continuum at the upper and lower interfaces is considered in the transfer matrix, the maximum amplitude in the substrate is essentially near the upper and lower interfaces, and the fixed boundary conditions at the base of the substrate have relatively little effect on the displacement modes at $x_3 = 0$. However, when the stress continuity condition at the upper/lower layer interface is also considered in the transfer matrix, the maximum amplitude may no longer occur near the upper/lower layer interface but may be shifted up to the upper/lower part of the cover layer.

In contrast to Figs. 3.2 and 3.3, Figs. 3.4 and 3.5 show the first six orders of modal diagrams for a fixed bottom edge of the base, with only displacement continuity at the upper and lower intersections and with displacement and stress continuity at the upper and lower intersections, respectively. The first four orders of the modal diagrams in Figs. 3.2 and 3.4 are not distinguishable, while the fifth and sixth orders of the modal diagrams in Fig. 3.4 are mainly constrained by the fixed boundary at the bottom edge of the footing, where the displacement at the bottom edge is zero. In contrast to Fig. 3.3, the first six orders of the mode in Fig. 3.5 are constrained by a fixed boundary condition at the bottom edge of the base, and the displacement at the bottom edge is zero.

As can be seen from Figs. 3.6 to 3.9, the stress continuity boundary at the interface between the upper and lower layers is considered in the transfer matrix to have a significant effect on the stress distribution in the structure. The discontinuity may occur at the intersection. However, when only the displacements at the intersection between the upper and lower layers are considered in the transfer matrix, the stress distribution and the maximum values of the modes corresponding to the first six orders of SAW in the structure are basically concentrated near the free surface, and the displacements and stresses at the intersection basically satisfy the continuity condition, and the boundary condition of zero stress on the free surface is satisfied.

Therefore, it is considered that in the analysis of the propagation properties of low-order SAWs in this model, it is generally only necessary to consider the displacement continuity condition at the intersection in the transfer matrix.

3.3.2 Effect of the material of the covering layer on the propagation velocity of low-order Rayleigh waves in the structure

Tiersten [109] indicated that dispersion phenomena can be divided into two types based on the shear wave velocity ratio of the covering material to the substrate material:

(1) Loading dispersion

$$\frac{\bar{v}_T}{v_T} < \frac{1}{\sqrt{2}} \tag{3.17}$$

(2) Stiffening dispersion

$$\frac{\bar{v}_T}{v_T} > \sqrt{2} \tag{3.18}$$

where $\bar{v}_T$ is the shear wave velocity of the thin layer and v_T is the shear wave velocity of the substrate. When the shear wave velocity of the thin layer is less than the shear wave velocity of the substrate, the phase velocity of the Rayleigh mode decreases with frequency and the thin layer is known as a " loading " substrate. On the other hand, when the shear wave velocity of the thin layer is greater than the shear wave velocity of the substrate, the phase velocity increases, causing the substrate to stiffen, i.e. the first SAW velocity present in the structure is greater than the first SAW velocity of the substrate material. The substrate material adopted in this paper is fused silica with $v_T = 3754$m/s and the covering material is either Au or Al_2O_3 with $\bar{v}_T = 1200$m/s for Au and $\bar{v}_T = 6401$m/s for Al_2O_3. Therefore, the loading dispersion curve appears when Au is used as the covering material, while the stiffening dispersion appears when Al_2O_3 is used as the covering material. The results shown in Fig. 3.10 were obtained by considering the boundary conditions where the bottom surface is free and the displacement is continuous at the interface.

The dispersion curves obtained with Al_2O_3 as a covering material are significantly different from those obtained with Au as a covering material for the same range of layer thicknesses. The latter showed a clear decaying trend with increasing layer thickness, while

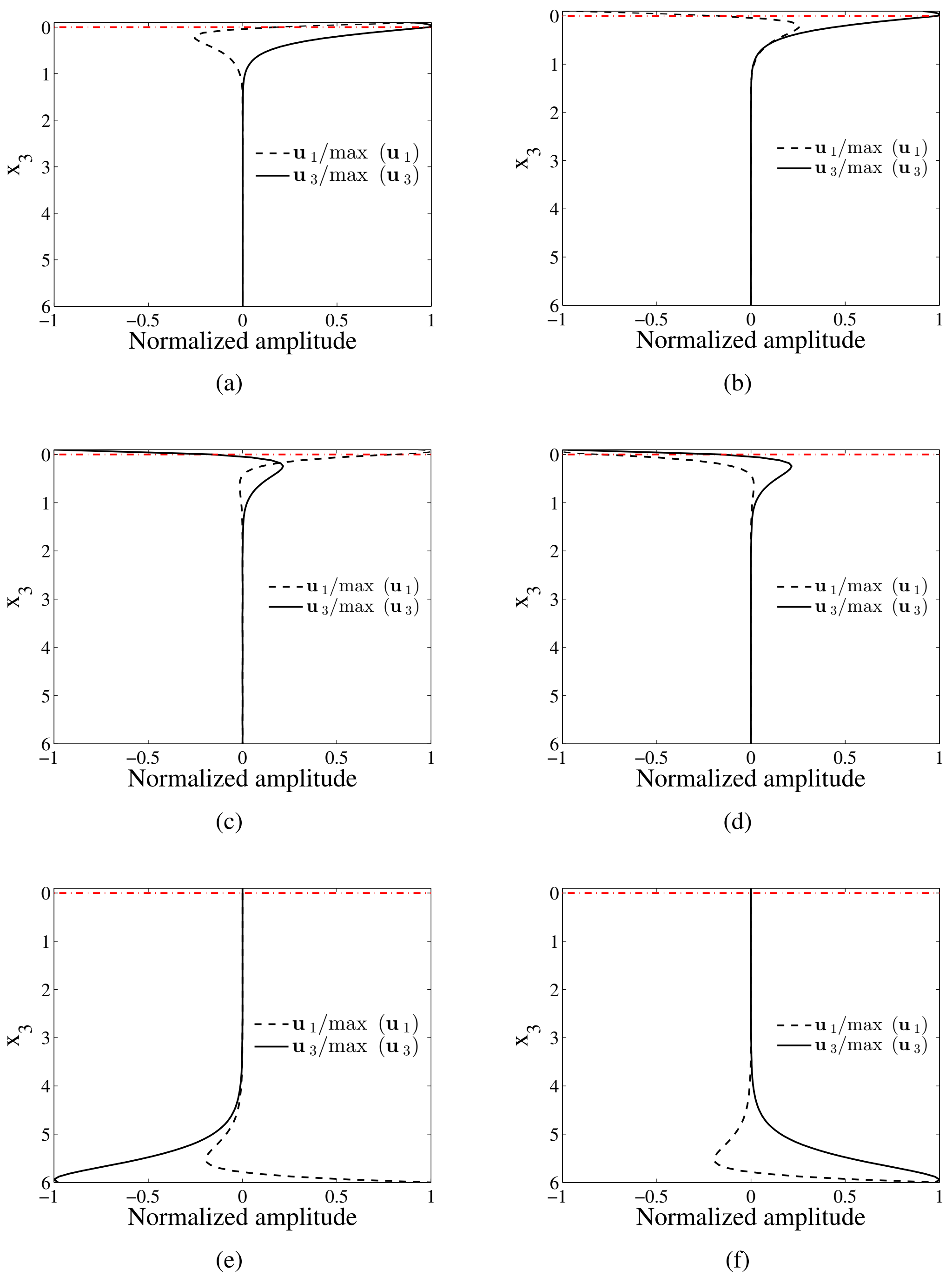

Fig. 3.2 First six SAW modes with displacement continuity at the interface under free boundary conditions on the bottom surface of the substrate: (a) the 1st mode; (b) the 2nd mode; (c) the 3rd mode; (d) the 4th mode;(e) the 5th mode;(f) the 6th mode

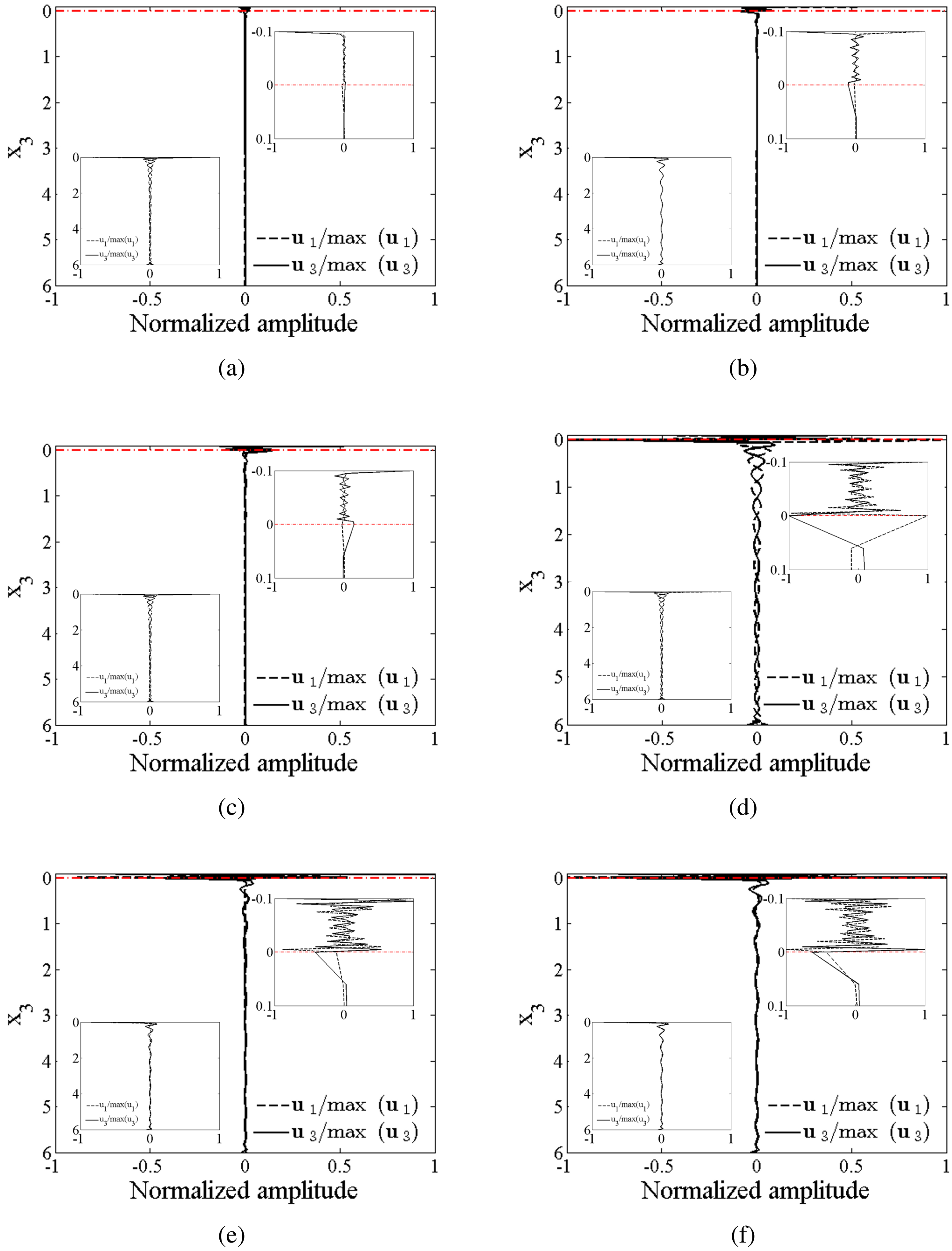

Fig. 3.3 First six SAW modes with displacement and stress continuity at the interface under free boundary conditions on the bottom surface of the substrate: (a) the 1st mode; (b) the 2nd mode; (c) the 3rd mode; (d) the 4th mode;(e) the 5th mode;(f) the 6th mode

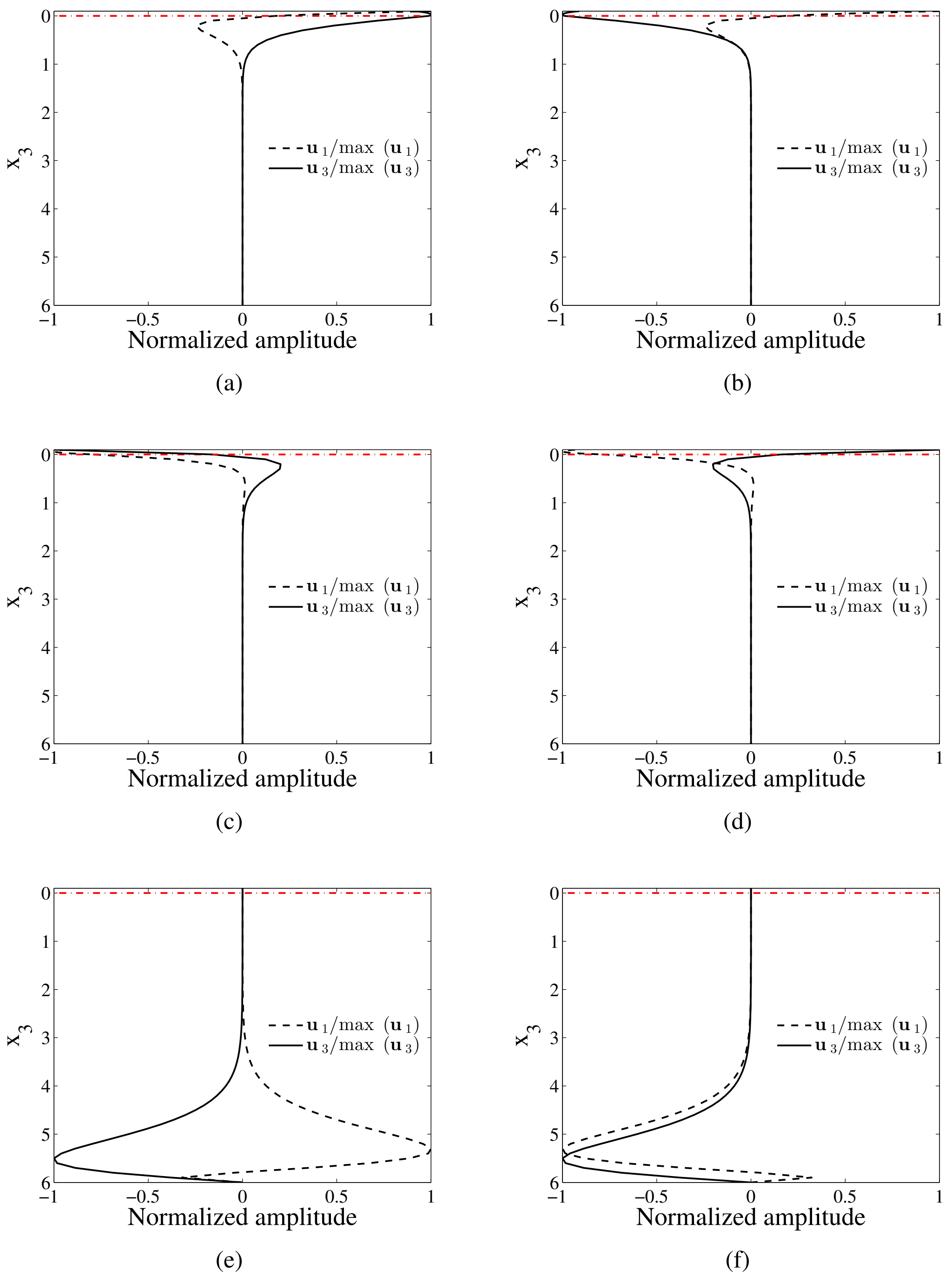

Fig. 3.4 First six SAW modes with displacement continuity at the interface under fixed boundary conditions on the bottom surface of the substrate: (a) the 1st mode; (b) the 2nd mode; (c) the 3rd mode; (d) the 4th mode;(e) the 5th mode;(f) the 6th mode

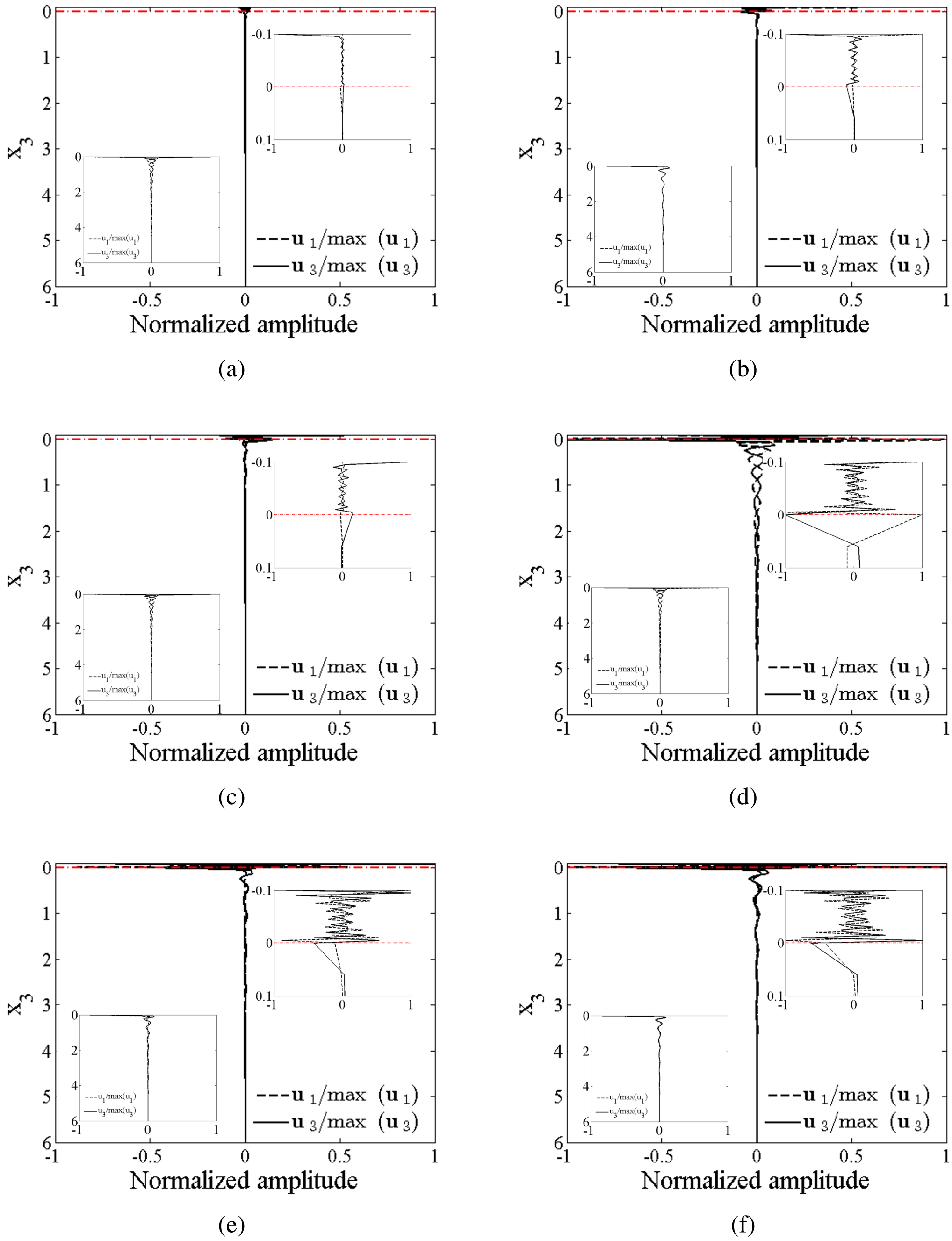

Fig. 3.5 First six SAW modes with displacement and stress continuity at the interface under fixed boundary conditions on the bottom surface of the substrate: (a) the 1st mode; (b) the 2nd mode; (c) the 3rd mode; (d) the 4th mode;(e) the 5th mode;(f) the 6th mode

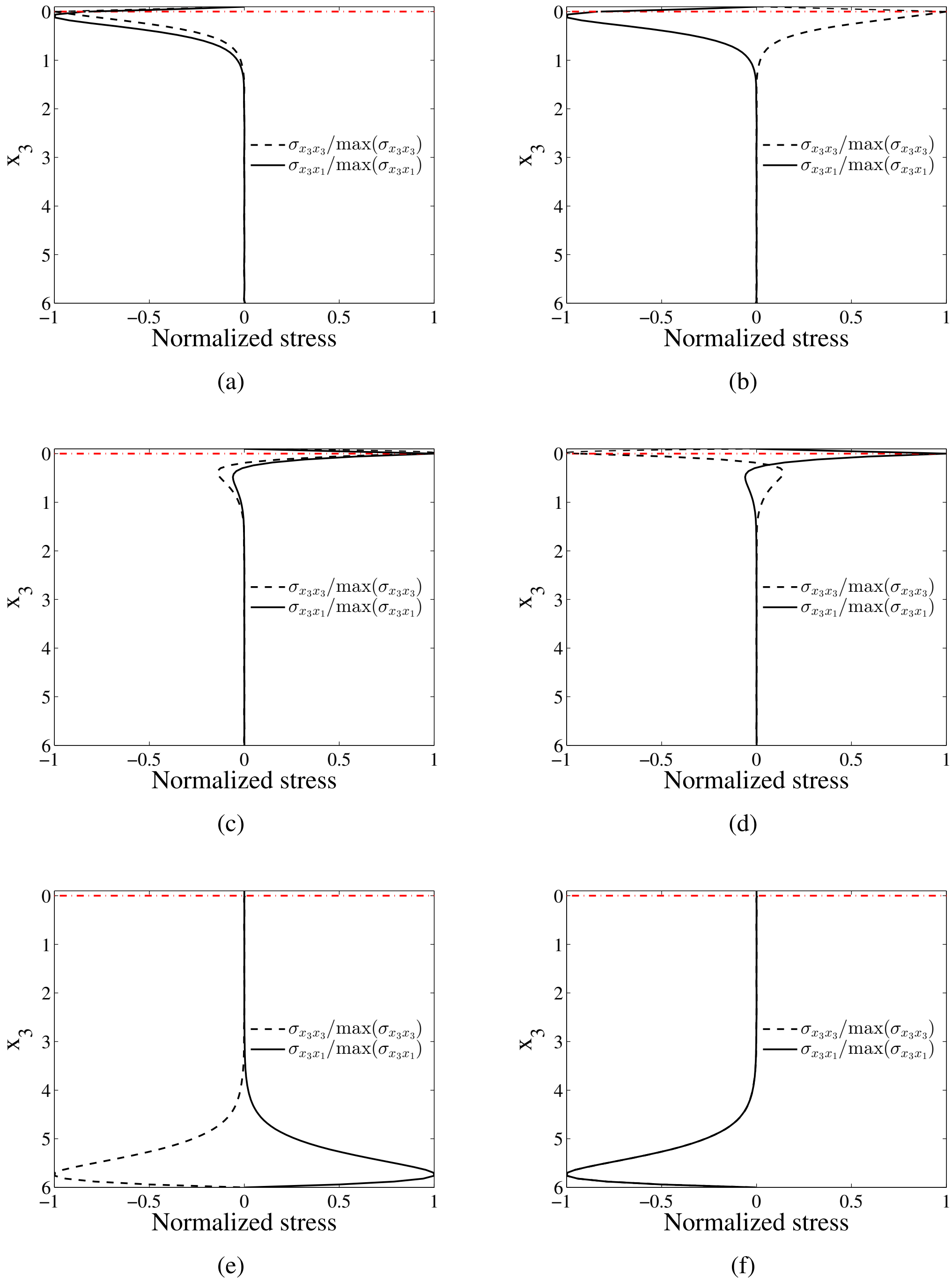

Fig. 3.6 First six stress distributions of Rayleigh waves with displacement continuity at the interface under free boundary conditions on the bottom surface of the substrate: the stress distribution of (a) the 1st mode; (b) the 2nd mode; (c) the 3rd mode; (d) the 4th mode;(e) the 5th mode;(f) the 6th mode

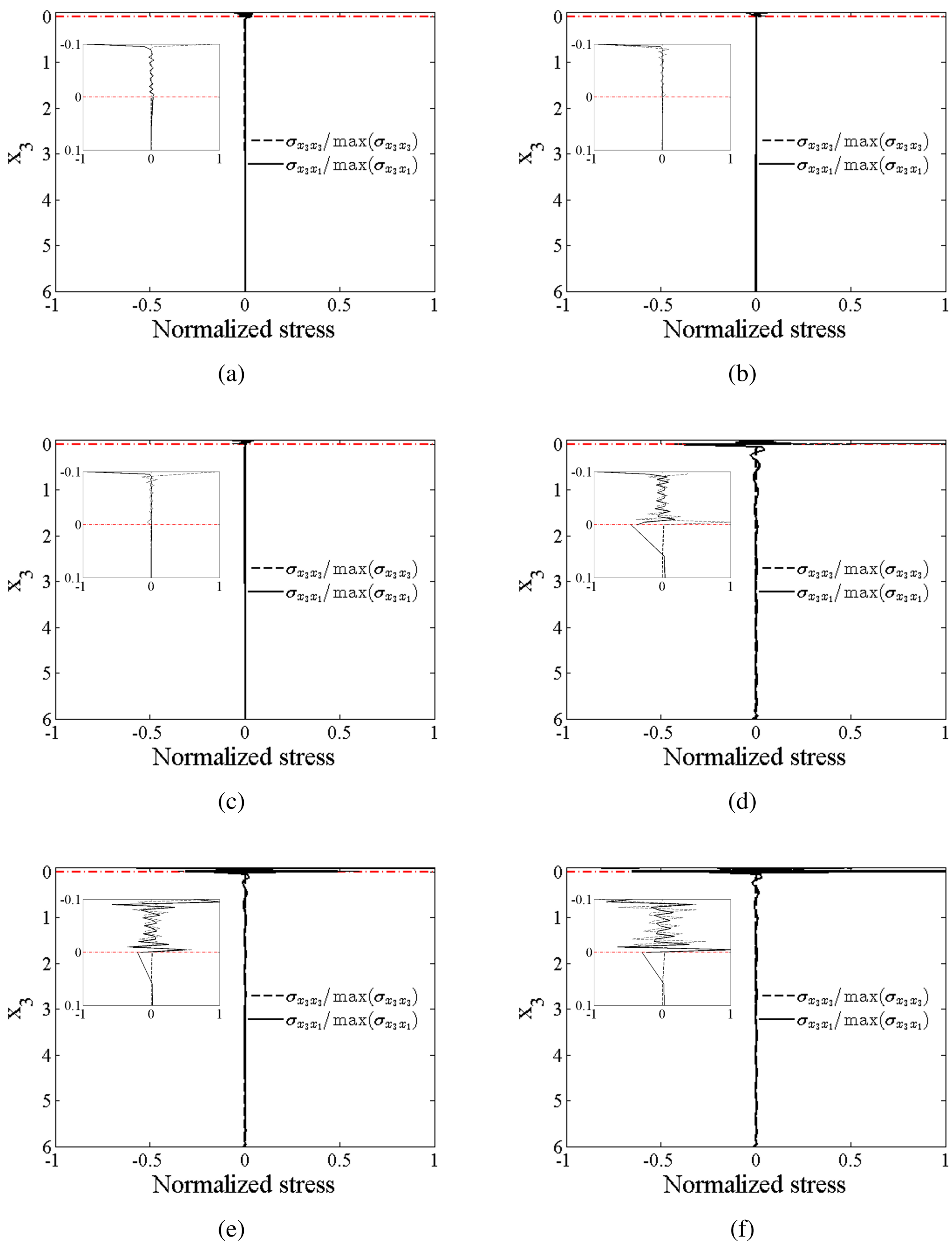

Fig. 3.7 First six stress distributions of SAWs with displacement and stress continuity at the interface under free boundary conditions on the bottom surface of the substrate: the stress distribution of (a) the 1st mode; (b) the 2nd mode; (c) the 3rd mode; (d) the 4th mode;(e) the 5th mode;(f) the 6th mode

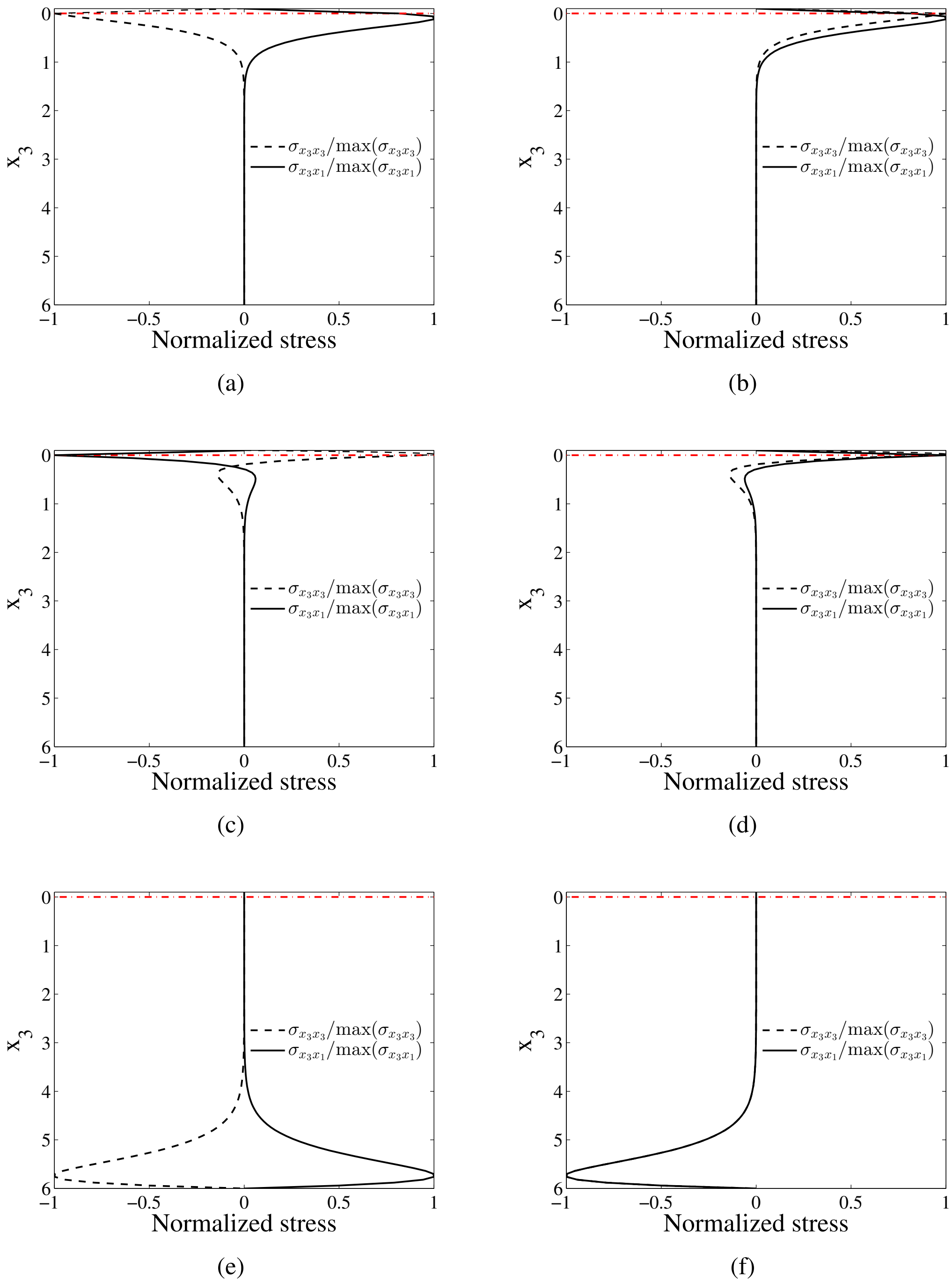

Fig. 3.8 First six stress distributions of SAWs with displacement continuity at the interface under fixed boundary conditions on the bottom surface of the substrate: the stress distribution of (a) the 1st mode; (b) the 2nd mode; (c) the 3rd mode; (d) the 4th mode;(e) the 5th mode;(f) the 6th mode

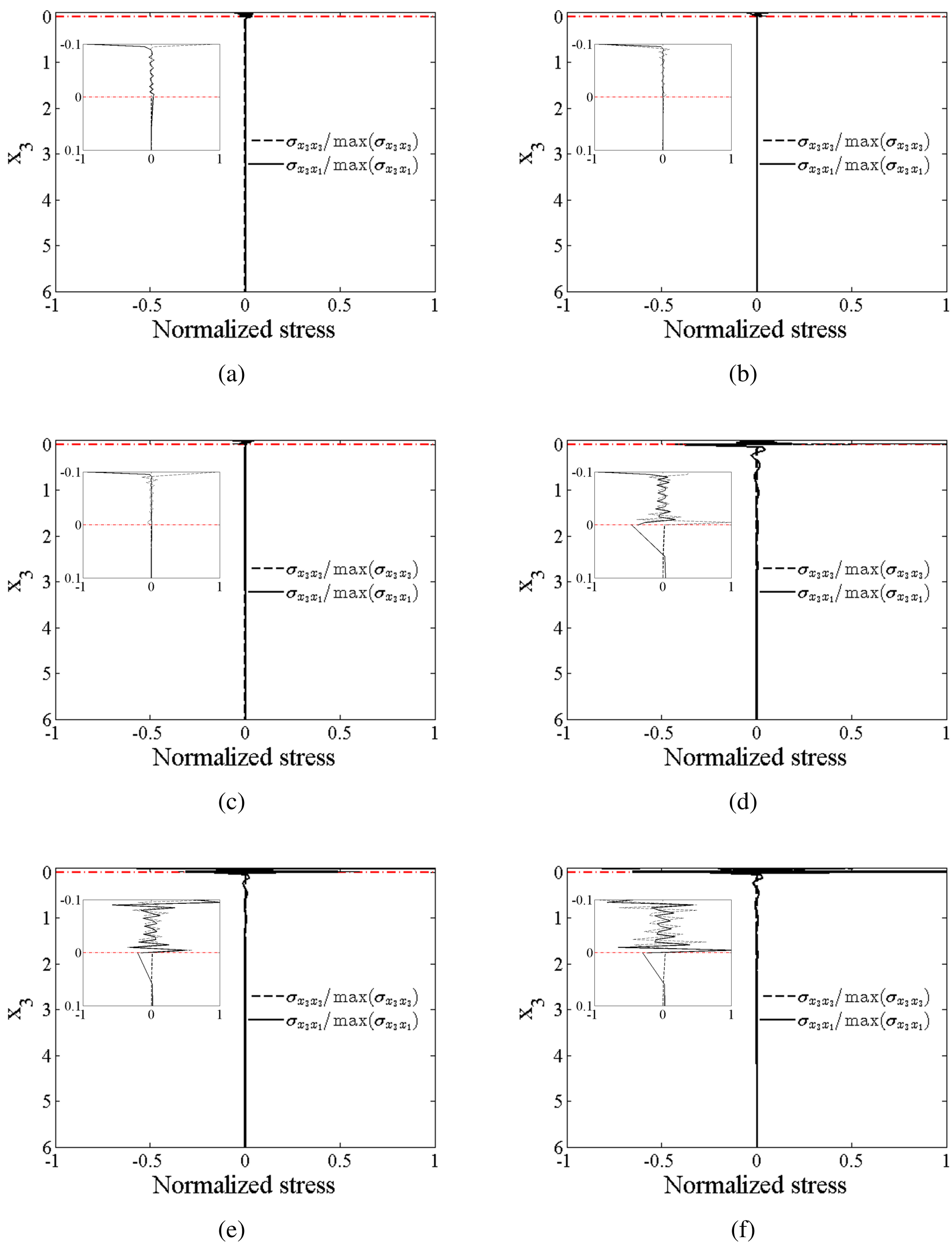

Fig. 3.9 First six stress distributions of SAWs with displacement and stress continuity at the interface under fixed boundary conditions on the bottom surface of the substrate: the stress distribution of (a) the 1st mode; (b) the 2nd mode; (c) the 3rd mode; (d) the 4th mode; (e) the 5th mode; (f) the 6th mode

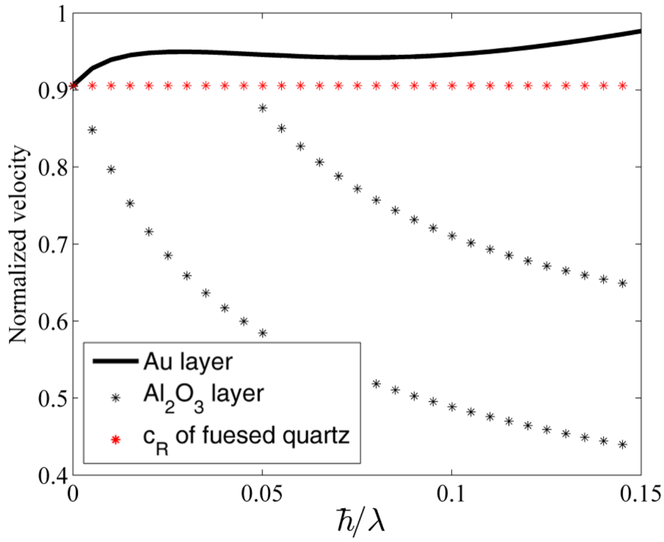

Fig. 3.10 Dispersion curves of Rayleigh waves with different covering materials

the former showed an overall increasing trend, but with a gentler curve trend in the range of $\bar{h}/\lambda \in [0.025, 0.08]$, with a decreasing and then increasing change.

Taking Al_2O_3 as the thin layer material, the displacement modes in the structure as shown in Figs. 3.11 and 3.12 and the corresponding stress distributions as shown in Figs. 3.13 and 3.14 for a thin layer thickness of one tenth of a wavelength. Compared to the displacement mode and corresponding stress distribution when Au was the thin layer material, considering only the displacement continuum condition on the contact surface, it is easy to see that the former decays slightly slower with depth than the latter. The number of low-order SAWs in the structure with Al_2O_3 as the covering material is less than the number of low-order SAWs in the structure with Au as the covering material for the same covering layer thickness and around the first SAW velocity of the substrate material.

3.3.3 Effect of covering thickness on the propagation of low-order Rayleigh waves in the structure

In this subsection, Au was adopted as the covering layer material with a substrate thickness of six wavelengths. Based on the conclusions of the previous section, Fig. 3.15 shows the effect of the cover layer thickness on the low-order Rayleigh wave velocity in the structure under different boundary conditions. According to the results in the figure, the effect of the stress boundary conditions on the low-order Rayleigh wave velocity in the structure is essentially ignorable in the present structure.

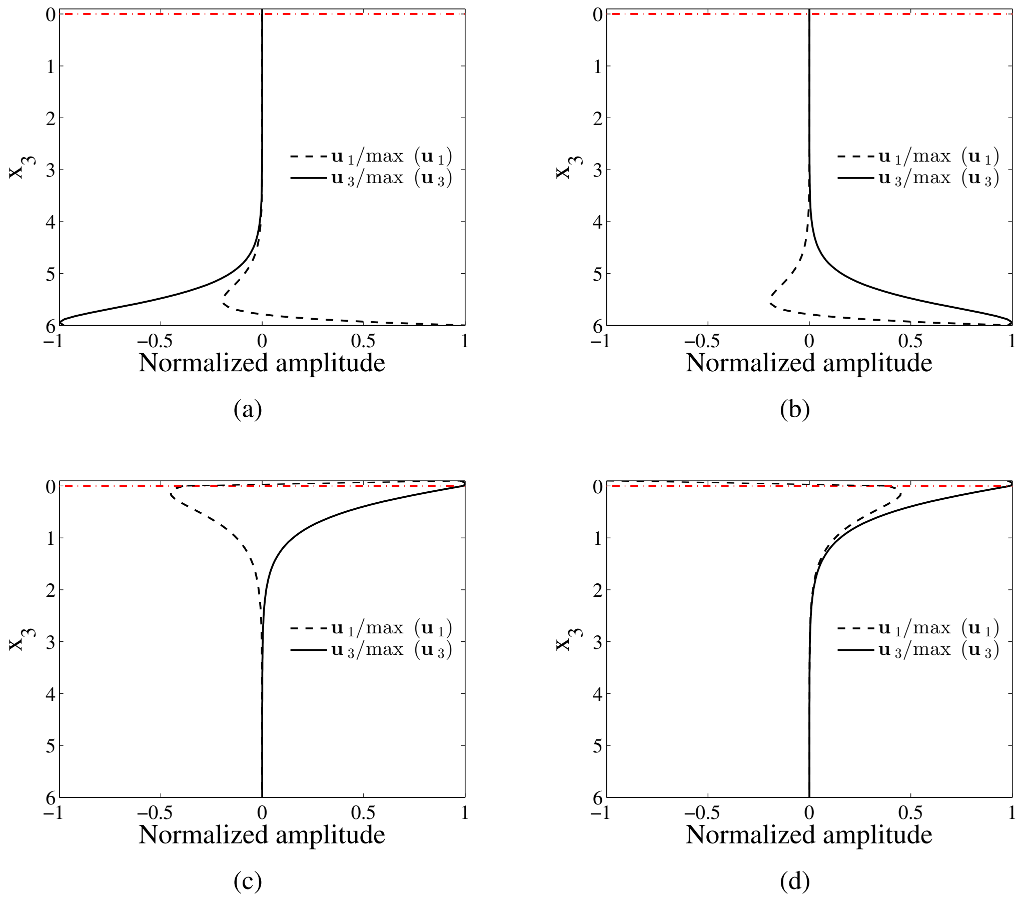

Fig. 3.11 First four SAW modes with displacement continuity at the interface under free boundary conditions on the bottom surface of the substrate: (a) the 1st mode; (b) the 2nd mode; (c) the 3rd mode; (d) the 4th mode

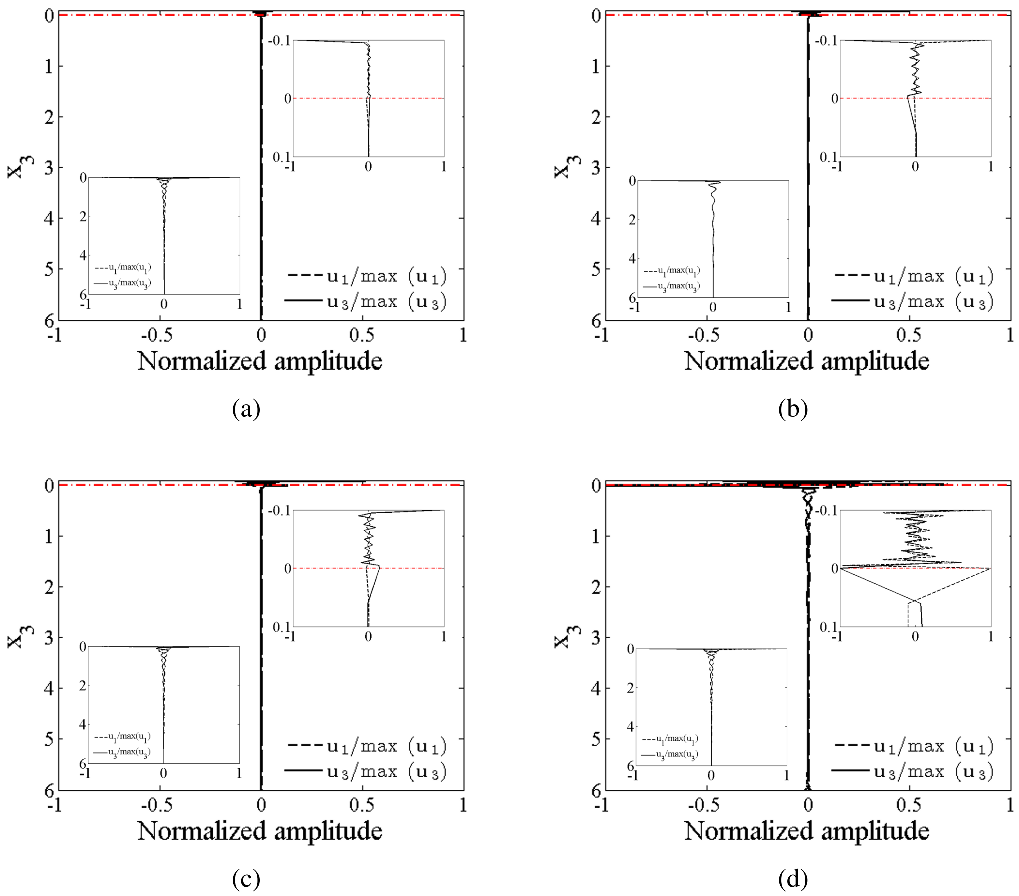

Fig. 3.12 First four SAW modes with displacement and stress continuity at the interface under free boundary conditions on the bottom surface of the substrate: (a) the 1st mode; (b) the 2nd mode; (c) the 3rd mode; (d) the 4th mode

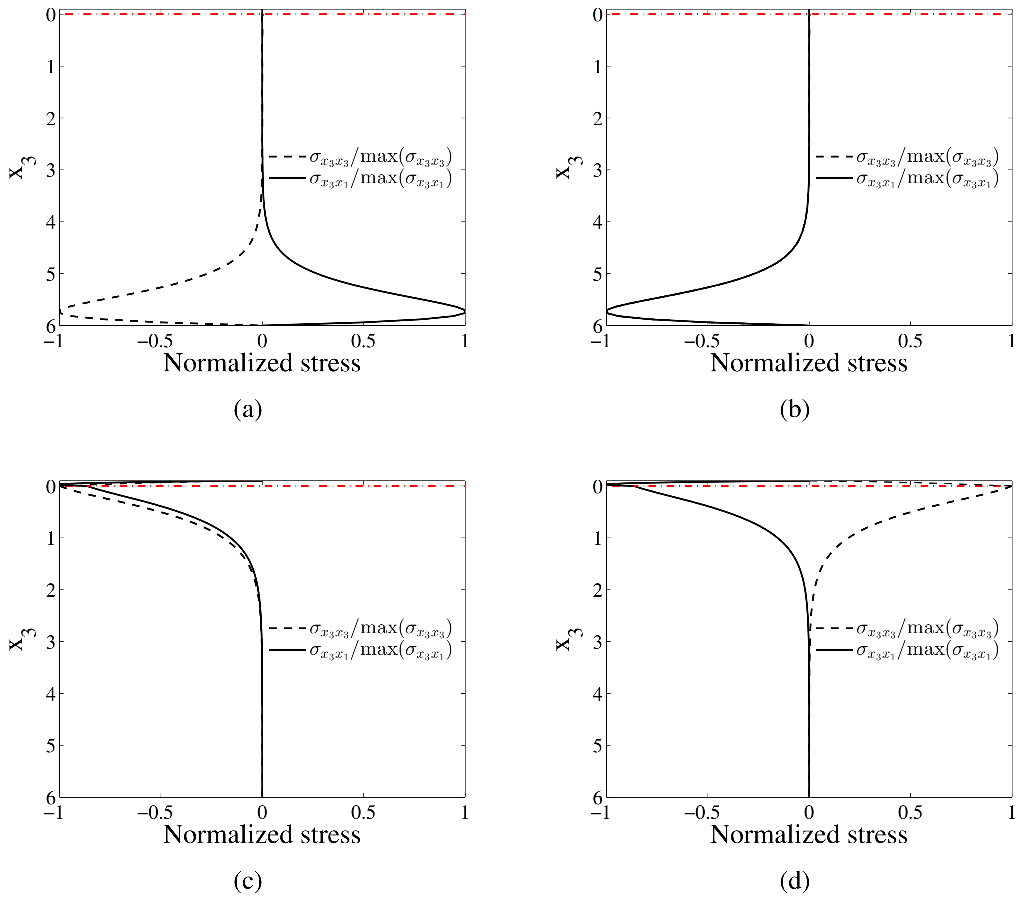

Fig. 3.13 First four stress distributions of SAWs with displacement continuity at the interface under free boundary conditions on the bottom surface of the substrate: the stress distribution of (a) the 1st mode; (b) the 2nd mode; (c) the 3rd mode; (d) the 4th mode

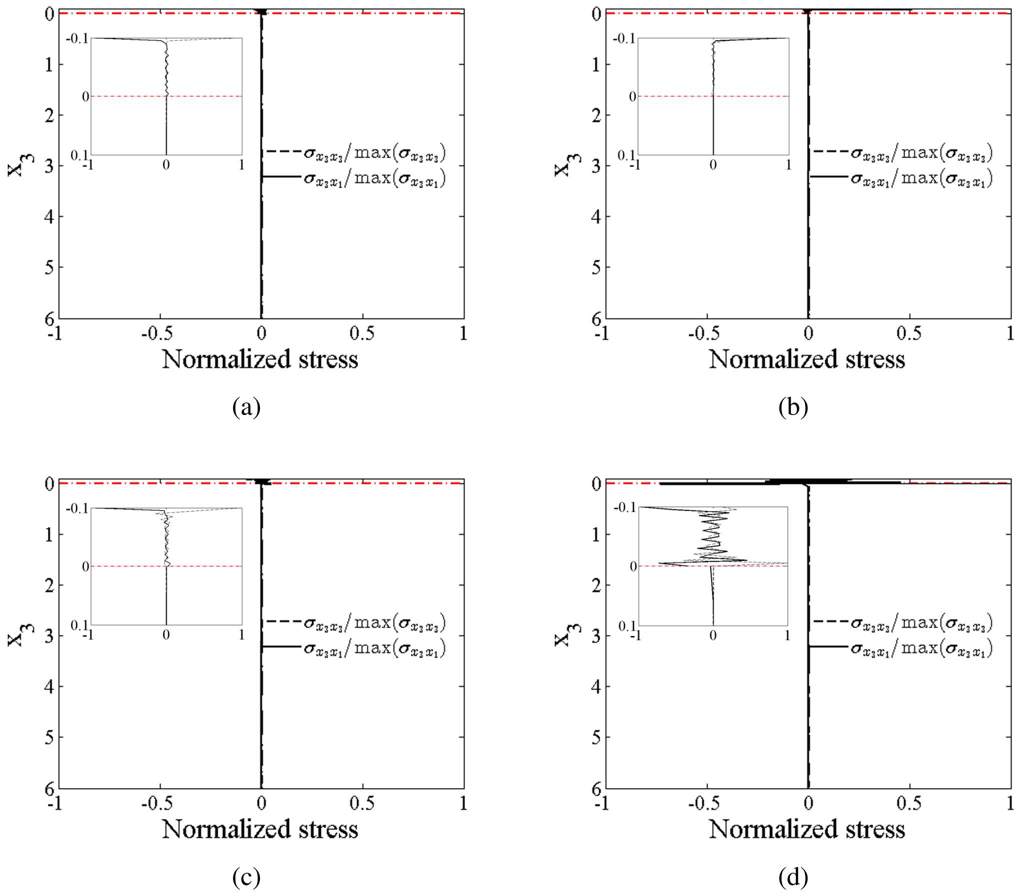

Fig. 3.14 First four stress distributions of SAWs with displacement and stress continuity at the interface under free boundary conditions on the bottom surface of the substrate: the stress distribution of (a) the 1st mode; (b) the 2nd mode; (c) the 3rd mode; (d) the 4th mode

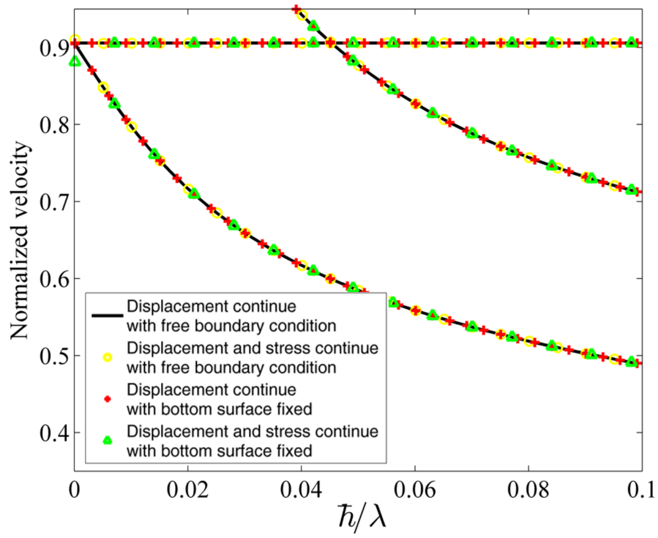

Fig. 3.15 The relationship between the thickness of the Au layer and low velocities of the SAWs under different boundary conditions

Fig. 3.16 highlights that as the thickness increases the lower order wave velocity decreased and gradually tended to cover the Rayleigh wave velocity of the material and the number of lower order Rayleigh wave modes increases. The results obtained by considering each boundary were used at this point and the results were compared with those already available in the thesis and it can be seen that the two are in good agreement.

3.4 Summary

In this chapter, the characteristic equations for the finite elastic structure covered with a thin layer are derived by the Rayleigh-Ritz method and the transfer matrices are used to investigate the effect of different boundary conditions, cover materials and cover thickness on the dispersion characteristics of low-order SAWs in the structure.

(1) In the calculation model in the chapter, whether or not stress continuity boundary conditions are considered at the layer-to-layer interface would not affect the wave velocities of the low-order SAWs in the structure, but would have some effect on its mode and corresponding stress distribution; whereas, when the substrate has a large thickness ($h > 3\lambda$), the use of free or fixed boundary conditions at the bottom edge would generally have no effect on the wave velocities of the low-order SAWs in the structure; when only displacement continuity conditions are considered at the interface

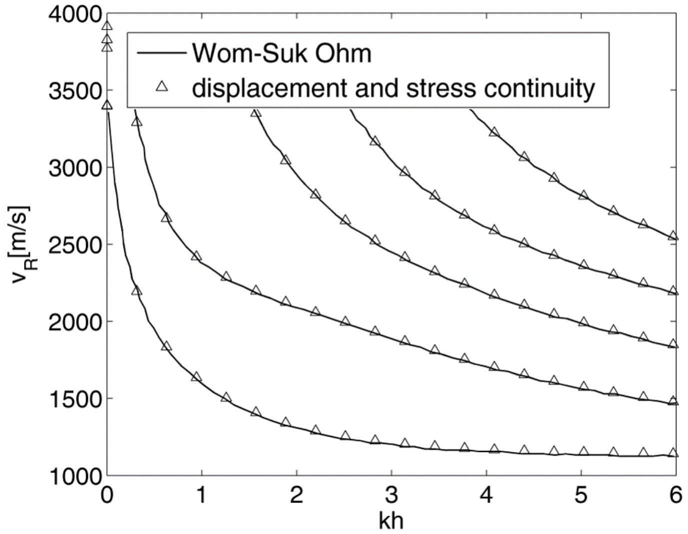

Fig. 3.16 The relationship between the Au layer thickness and the SAW velocities

between the upper and lower layers, the material of the covering layer would have some effect on the range of energy concentration of the low-order SAWs in the structure.

(2) When both the covering and the substrate are composed of isotropic materials, the ratio of the shear wave velocity of the covering material to the shear wave velocity of the substrate material allows an analysis of whether loaded or hardened dispersion occurs in the structure. The influence of the two types of material produces a significant difference in the low-order SAW velocities and the number of modes in the structure. The low-order SAW velocities in the loading structure is generally less than or equal to the SAW velocity in the substrate material and may take the form of multi-order modes. The stiffened covering material exhibits the opposite result.

(3) Under the influence of the stiffening-type material Al_2O_3 applied in this chapter, this wave velocity showed an overall tendency to increase with increasing thickness of the covering layer, but during this time there was a more gentle period of decline in the low-order SAW velocities. This characteristic is significantly different from the effect of the loading-type material Au on the low-order SAW velocities in the structure used in this chapter.

3.5 Appendix

3.5.1 Stiffness and mass matrices in this chapter

The expression for the stiffness matrix in this chapter is:

$$[K] = \begin{bmatrix} [K_{11}^S] & [K_{13}^S] & [0] & [0] \\ [K_{31}^S] & [K_{33}^S] & [0] & [0] \\ [0] & [0] & [K_{11}^C] & [K_{13}^C] \\ [0] & [0] & [K_{31}^C] & [K_{33}^C] \end{bmatrix} \tag{3.19}$$

where the expressions for the elements in the stiffness matrix are:

$$\begin{aligned} \left[K^S\right]_{m_1n_1} &= c_{i1k1}E^{1,1}_{U_ipU_k\bar{p}}F_1^{0,0} + c_{i1k2}E^{1,0}_{U_ipU_k\bar{p}}F_1^{0,1} + c_{i1k3}E^{1,0}_{U_ipU_k\bar{p}}F_1^{0,0} \\ &+ c_{i2k1}E^{0,1}_{U_ipU_k\bar{p}}F_1^{1,0} + c_{i2k2}E^{0,0}_{U_ipU_k\bar{p}}F_1^{1,1} + c_{i2k3}E^{0,0}_{U_ipU_k\bar{p}}F_1^{1,0} \\ &+ c_{i3k1}E^{0,1}_{U_ipU_k\bar{p}}F_1^{0,0} + c_{i3k2}E^{0,0}_{U_ipU_k\bar{p}}F_1^{0,1} + c_{i3k3}E^{0,0}_{U_ipU_k\bar{p}}F_1^{0,0} \end{aligned}$$

$$\begin{aligned} \left[K^S\right]_{m_2n_1} &= c_{i1k1}E^{1,1}_{U_ipU_k\bar{p}}F_2^{0,0} + c_{i1k2}E^{1,0}_{U_ipU_k\bar{p}}F_2^{0,1} + c_{i1k3}E^{1,0}_{U_ipU_k\bar{p}}F_2^{0,0} \\ &+ c_{i2k1}E^{0,1}_{U_ipU_k\bar{p}}F_2^{1,0} + c_{i2k2}E^{0,0}_{U_ipU_k\bar{p}}F_2^{1,1} + c_{i2k3}E^{0,0}_{U_ipU_k\bar{p}}F_2^{1,0} \\ &+ c_{i3k1}E^{0,1}_{U_ipU_k\bar{p}}F_2^{0,0} + c_{i3k2}E^{0,0}_{U_ipU_k\bar{p}}F_2^{0,1} + c_{i3k3}E^{0,0}_{U_ipU_k\bar{p}}F_2^{0,0} \end{aligned}$$

$$\begin{aligned} \left[K^S\right]_{m_1n_2} &= c_{i1k1}E^{1,1}_{U_ipU_k\bar{p}}F_3^{0,0} + c_{i1k2}E^{1,0}_{U_ipU_k\bar{p}}F_3^{0,1} + c_{i1k3}E^{1,0}_{U_ipU_k\bar{p}}F_3^{0,0} \\ &+ c_{i2k1}E^{0,1}_{U_ipU_k\bar{p}}F_3^{1,0} + c_{i2k2}E^{0,0}_{U_ipU_k\bar{p}}F_3^{1,1} + c_{i2k3}E^{0,0}_{U_ipU_k\bar{p}}F_3^{1,0} \\ &+ c_{i3k1}E^{0,1}_{U_ipU_k\bar{p}}F_3^{0,0} + c_{i3k2}E^{0,0}_{U_ipU_k\bar{p}}F_3^{0,1} + c_{i3k3}E^{0,0}_{U_ipU_k\bar{p}}F_3^{0,0} \end{aligned}$$

$$\begin{aligned} \left[K^S\right]_{m_2n_2} &= c_{i1k1}E^{1,1}_{U_ipU_k\bar{p}}F_4^{0,0} + c_{i1k2}E^{1,0}_{U_ipU_k\bar{p}}F_4^{0,1} + c_{i1k3}E^{1,0}_{U_ipU_k\bar{p}}F_4^{0,0} \\ &+ c_{i2k1}E^{0,1}_{U_ipU_k\bar{p}}F_4^{1,0} + c_{i2k2}E^{0,0}_{U_ipU_k\bar{p}}F_4^{1,1} + c_{i2k3}E^{0,0}_{U_ipU_k\bar{p}}F_4^{1,0} \\ &+ c_{i3k1}E^{0,1}_{U_ipU_k\bar{p}}F_4^{0,0} + c_{i3k2}E^{0,0}_{U_ipU_k\bar{p}}F_4^{0,1} + c_{i3k3}E^{0,0}_{U_ipU_k\bar{p}}F_4^{0,0} \end{aligned}$$

$$\begin{aligned} \left[K^C\right]_{m_1n_1} &= \bar{c}_{i1k1}\bar{E}^{1,1}_{U_ipU_k\bar{p}}F_1^{0,0} + \bar{c}_{i1k2}\bar{E}^{1,0}_{U_ipU_k\bar{p}}F_1^{0,1} + \bar{c}_{i1k3}\bar{E}^{1,0}_{U_ipU_k\bar{p}}F_1^{0,0} \\ &+ \bar{c}_{i2k1}\bar{E}^{0,1}_{U_ipU_k\bar{p}}F_1^{1,0} + \bar{c}_{i2k2}\bar{E}^{0,0}_{U_ipU_k\bar{p}}F_1^{1,1} + \bar{c}_{i2k3}\bar{E}^{0,0}_{U_ipU_k\bar{p}}F_1^{1,0} \end{aligned}$$

$$
\begin{aligned}
&+\bar{c}_{i3k1}\bar{E}^{0,1}_{U_ipU_k\bar{p}}F_1^{0,0}+\bar{c}_{i3k2}\bar{E}^{0,0}_{U_ipU_k\bar{p}}F_1^{0,1}+\bar{c}_{i3k3}\bar{E}^{0,0}_{U_ipU_k\bar{p}}F_1^{0,0}\\
\left[K^C\right]_{m_2n_1} &= \bar{c}_{i1k1}\bar{E}^{1,1}_{U_ipU_k\bar{p}}F_2^{0,0}+\bar{c}_{i1k2}\bar{E}^{1,0}_{U_ipU_k\bar{p}}F_2^{0,1}+\bar{c}_{i1k3}\bar{E}^{1,0}_{U_ipU_k\bar{p}}F_2^{0,0}\\
&+\bar{c}_{i2k1}\bar{E}^{0,1}_{U_ipU_k\bar{p}}F_2^{1,0}+\bar{c}_{i2k2}\bar{E}^{0,0}_{U_ipU_k\bar{p}}F_2^{1,1}+\bar{c}_{i2k3}\bar{E}^{0,0}_{U_ipU_k\bar{p}}F_2^{1,0}\\
&+\bar{c}_{i3k1}\bar{E}^{0,1}_{U_ipU_k\bar{p}}F_2^{0,0}+\bar{c}_{i3k2}\bar{E}^{0,0}_{U_ipU_k\bar{p}}F_2^{0,1}+\bar{c}_{i3k3}\bar{E}^{0,0}_{U_ipU_k\bar{p}}F_2^{0,0}\\
\left[K^C\right]_{m_1n_2} &= \bar{c}_{i1k1}\bar{E}^{1,1}_{U_ipU_k\bar{p}}F_3^{0,0}+\bar{c}_{i1k2}\bar{E}^{1,0}_{U_ipU_k\bar{p}}F_3^{0,1}+\bar{c}_{i1k3}\bar{E}^{1,0}_{U_ipU_k\bar{p}}F_3^{0,0}\\
&+\bar{c}_{i2k1}\bar{E}^{0,1}_{U_ipU_k\bar{p}}F_3^{1,0}+\bar{c}_{i2k2}\bar{E}^{0,0}_{U_ipU_k\bar{p}}F_3^{1,1}+\bar{c}_{i2k3}\bar{E}^{0,0}_{U_ipU_k\bar{p}}F_3^{1,0}\\
&+\bar{c}_{i3k1}\bar{E}^{0,1}_{U_ipU_k\bar{p}}F_3^{0,0}+\bar{c}_{i3k2}\bar{E}^{0,0}_{U_ipU_k\bar{p}}F_3^{0,1}+\bar{c}_{i3k3}\bar{E}^{0,0}_{U_ipU_k\bar{p}}F_3^{0,0}\\
\left[K^C\right]_{m_2n_2} &= \bar{c}_{i1k1}\bar{E}^{1,1}_{U_ipU_k\bar{p}}F_4^{0,0}+\bar{c}_{i1k2}\bar{E}^{1,0}_{U_ipU_k\bar{p}}F_4^{0,1}+\bar{c}_{i1k3}\bar{E}^{1,0}_{U_ipU_k\bar{p}}F_4^{0,0}\\
&+\bar{c}_{i2k1}\bar{E}^{0,1}_{U_ipU_k\bar{p}}F_4^{1,0}+\bar{c}_{i2k2}\bar{E}^{0,0}_{U_ipU_k\bar{p}}F_4^{1,1}+\bar{c}_{i2k3}\bar{E}^{0,0}_{U_ipU_k\bar{p}}F_4^{1,0}\\
&+\bar{c}_{i3k1}\bar{E}^{0,1}_{U_ipU_k\bar{p}}F_4^{0,0}+\bar{c}_{i3k2}\bar{E}^{0,0}_{U_ipU_k\bar{p}}F_4^{0,1}+\bar{c}_{i3k3}\bar{E}^{0,0}_{U_ipU_k\bar{p}}F_4^{0,0}
\end{aligned}
\tag{3.20}
$$

The mass matrix is:

$$
[M]=\begin{bmatrix}
\left[M^S_{11}\right] & [0] & [0] & [0]\\
[0] & \left[M^S_{33}\right] & [0] & [0]\\
[0] & [0] & \left[M^C_{11}\right] & [0]\\
[0] & [0] & [0] & \left[M^C_{33}\right]
\end{bmatrix}
\tag{3.21}
$$

The individual elements of the mass matrix were expressed as:

$$
\begin{aligned}
\left[M^S\right]_{m_1n_1} &= \rho E^{0,0}_{U_ipU_k\bar{p}}F_1^{0,0}\\
\left[M^S\right]_{m_2n_1} &= \rho E^{0,0}_{U_ipU_k\bar{p}}F_2^{0,0}\\
\left[M^S\right]_{m_1n_2} &= \rho E^{0,0}_{U_ipU_k\bar{p}}F_3^{0,0}\\
\left[M^S\right]_{m_2n_2} &= \rho E^{0,0}_{U_ipU_k\bar{p}}F_4^{0,0}\\
\left[M^C\right]_{m_1n_1} &= \rho \bar{E}^{0,0}_{U_ipU_k\bar{p}}F_1^{0,0}\\
\left[M^C\right]_{m_2n_1} &= \rho E^{\ 0,0}_{\ U_ipU_k\bar{p}}F_2^{0,0}
\end{aligned}
\tag{3.22}
$$

$$\left[M^C\right]_{m_1n_2} = \rho \bar{E}^{0,0}_{U_ipU_k\bar{p}} F^{0,0}_3$$
$$\left[M^C\right]_{m_2n_2} = \rho \bar{E}^{0,0}_{U_ipU_k\bar{p}} F^{0,0}_4$$

where,

$$E^{\eta,\xi}_{U_ipU_k\bar{p}} = \int_0^h \frac{d^\eta f(x_3)P_p\left(\frac{2x_3}{h}-1\right)}{dx_3^\eta}\frac{d^\xi f(x_3)P_{\bar{p}}\left(\frac{2x_3}{h}-1\right)}{dx_3^\xi}dx_3,$$
$$\bar{E}^{\eta,\xi}_{\bar{U}_ip\bar{U}_k\bar{p}} = \int_{-\bar{h}}^0 \frac{d^\eta \bar{f}(x_3)P_p\left(\frac{2x_3}{\bar{h}}+1\right)}{dx_3^\eta}\frac{d^\xi \bar{f}(x_3)P_{\bar{p}}\left(\frac{2x_3}{\bar{h}}+1\right)}{dx_3^\xi}dx_3 \tag{3.23}$$

3.5.2 The derivation process for each element of the transfer matrix

Since the Legendre polynomials are characterized by $P_n(1) = 1$, $P_n(-1) = (-1)^{(n-1)}$ and orthogonality, when considering only the continuity of the displacement function, substituting Eqs. 3.1 and 3.2 into Eq. 3.3 leads to the following equations:

$$\begin{aligned}
A_{11} - A_{12} + A_{13} + \ldots + (-1)^{n-1} A_{1n} &= \bar{A}_{11} + \bar{A}_{12} + \bar{A}_{13} + \ldots + \bar{A}_{1n},\\
B_{11} - B_{12} + B_{13} + \ldots + (-1)^{n-1} B_{1n} &= \bar{B}_{11} + \bar{B}_{12} + \bar{B}_{13} + \ldots + \bar{B}_{1n},\\
A_{31} - A_{32} + A_{33} + \ldots + (-1)^{n-1} A_{3n} &= \bar{A}_{31} + \bar{A}_{32} + \bar{A}_{33} + \ldots + \bar{A}_{3n},\\
B_{31} - B_{32} + B_{33} + \ldots + (-1)^{n-1} B_{3n} &= \bar{B}_{31} + \bar{B}_{32} + \bar{B}_{33} + \ldots + \bar{B}_{3n}.
\end{aligned} \tag{3.24}$$

In this case only the first term remains on the left-hand side of the equation in Eq. 3.24, and the other terms on the left-hand side are moved to the right-hand side of the equation to give four unknown quantities:

$$\begin{aligned}
A_{11} &= \bar{A}_{11} + \bar{A}_{12} + \bar{A}_{13} + \ldots + \bar{A}_{1n} + A_{12} - A_{13} + \ldots + (-1)^n A_{1n},\\
B_{11} &= \bar{B}_{11} + \bar{B}_{12} + \bar{B}_{13} + \ldots + \bar{B}_{1n} + B_{12} - B_{13} + \ldots + (-1)^n B_{1n},\\
A_{31} &= \bar{A}_{31} + \bar{A}_{32} + \bar{A}_{33} + \ldots + \bar{A}_{3n} + A_{32} - A_{33} + \ldots + (-1)^n A_{3n},\\
B_{31} &= \bar{B}_{31} + \bar{B}_{32} + \bar{B}_{33} + \ldots + \bar{B}_{3n} + B_{32} - B_{33} + \ldots + (-1)^n B_{3n}.
\end{aligned} \tag{3.25}$$

Expanding Eq. 3.4, it can be written as:

$$\begin{cases}
c_{33}\frac{\partial u_3}{\partial z} + c_{31}\frac{\partial u_1}{\partial x} = \bar{c}_{33}\frac{\partial \bar{u}_3}{\partial z} + \bar{c}_{31}\frac{\partial \bar{u}_1}{\partial x}\\
c_{55}\left(\frac{\partial u_3}{\partial x} + \frac{\partial u_1}{\partial z}\right) = \bar{c}_{55}\left(\frac{\partial \bar{u}_3}{\partial x} + \frac{\partial \bar{u}_1}{\partial z}\right)
\end{cases} \tag{3.26}$$

Substituting Eqs. 3.1 and 3.2 into Eq. 3.26 yields:

$$\begin{aligned}
&\frac{c_{33}}{kh}\left[2A_{32}-6A_{33}+12A_{34}-\ldots+(-1)^{n}n(n-1)A_{3n}\right]\\
&-c_{31}\left[B_{11}-B_{12}+B_{13}+\ldots+(-1)^{n}B_{1n}\right]\\
&=\frac{\bar{c}_{33}}{k\bar{h}}\left[2\bar{A}_{32}+6\bar{A}_{33}+12\bar{A}_{34}+\ldots+n(n-1)\bar{A}_{3n}\right]\\
&-\bar{c}_{31}\left[\bar{B}_{11}+\bar{B}_{12}+\bar{B}_{13}+\ldots+\bar{B}_{1l}\right]\\
&\frac{c_{33}}{kh}\left[2B_{32}-6B_{33}+12B_{34}-\ldots+(-1)^{n}n(n-1)B_{3n}\right]\\
&+c_{31}2\left[A_{11}-A_{12}+A_{13}+\ldots+(-1)^{n}A_{1n}\right]\\
&=\frac{\bar{c}_{33}}{k\bar{h}}\left[2\bar{B}_{32}+6\bar{B}_{33}+12\bar{B}_{34}+\ldots+n(n-1)\bar{B}_{3n}\right]\\
&+\bar{c}_{31}2\left[\bar{A}_{11}+\bar{A}_{12}+\bar{A}_{13}+\ldots+\bar{A}_{1l}\right]
\end{aligned} \tag{3.27}$$

$$\begin{aligned}
&c_{55}\left\{2\left[A_{31}-A_{32}+\ldots+(-1)^{n-1}A_{3n}\right]\right.\\
&\left.+\frac{1}{kh}\left[2B_{12}-6B_{13}+12B_{14}+\ldots+(-1)^{n}n(n-1)B_{1n}\right]\right\}\\
&=\bar{c}_{55}\left\{2\left[\bar{A}_{31}+\bar{A}_{32}+\ldots+\bar{A}_{3n}\right]\right.\\
&\left.+\frac{1}{kh}\left[2\bar{B}_{12}+6\bar{B}_{13}+12\bar{B}_{14}+\ldots+n(n-1)\bar{B}_{1n}\right]\right\}
\end{aligned}$$

$$\begin{aligned}
&c_{55}\left\{2\left[B_{31}-B_{32}+\ldots+(-1)^{n-1}B_{3n}\right]\right.\\
&\left.+\frac{1}{kh}\left[2A_{12}-6A_{13}+12A_{14}+\ldots+(-1)^{n}n(n-1)A_{1n}\right]\right\}\\
&=\bar{c}_{55}\left\{2\left[\bar{B}_{31}+\bar{B}_{32}+\ldots+\bar{B}_{3n}\right]\right.\\
&\left.+\frac{1}{kh}\left[2\bar{A}_{12}+6\bar{A}_{13}+12\bar{A}_{14}+\ldots+n(n-1)\bar{A}_{1n}\right]\right\}
\end{aligned}$$

This leads to the solution of four new unknown coefficients:

$$
\begin{aligned}
A_{12} &= 3A_{13} - 6A_{14} + \ldots + (-1)^{n-1}\frac{n(n-1)}{2}A_{1n} \\
&+ \frac{\bar{c}_{55}h}{c_{55}\bar{h}}\left[\bar{A}_{12} + 3\bar{A}_{13} + \ldots + \frac{n(n-1)}{2}\bar{A}_{1n}\right] \\
&+ \left(\frac{\bar{c}_{55}hk}{c_{55}} - hk\right)(\bar{B}_{31} + \bar{B}_{32} + \ldots + \bar{B}_{3n}) \\
\\
A_{32} &= 3A_{33} - 6A_{34} + \ldots + (-1)^{n-1}\frac{n(n-1)}{2}A_{3n} \\
&+ \frac{\bar{c}_{33}h}{c_{33}\bar{h}}\left[\bar{A}_{32} + 3\bar{A}_{33} + \ldots + \frac{n(n-1)}{2}\bar{A}_{3n}\right] \\
&+ \frac{(\bar{c}_{31} - c_{31})hk}{c_{33}}(\bar{B}_{11} + \bar{B}_{12} + \ldots + \bar{B}_{1n}) \\
\\
B_{12} &= 3B_{13} - 6B_{14} + \ldots + (-1)^{n-1}\frac{n(n-1)}{2}B_{1n} \\
&+ \frac{\bar{c}_{55}h}{c_{55}\bar{h}}\left[\bar{B}_{12} + 3\bar{B}_{13} + \ldots + \frac{n(n-1)}{2}\bar{B}_{1n}\right] \\
&+ hk\left(\frac{\bar{c}_{55}}{c_{55}} - 1\right)\left(\bar{A}_{31} + \bar{A}_{32} + \ldots + \bar{A}_{3n}\right) \\
\\
B_{32} &= 3B_{33} - 6B_{34} + \ldots + (-1)^{n-1}\frac{n(n-1)}{2}B_{3n} \\
&+ \frac{\bar{c}_{33}h}{c_{33}\bar{h}}\left[\bar{B}_{32} + 3\bar{B}_{33} + \ldots + \frac{n(n-1)}{2}\bar{B}_{3n}\right] \\
&+ \frac{(\bar{c}_{31} - c_{31})hk}{c_{33}}\left[\bar{A}_{11} + \bar{A}_{12} + \ldots + \bar{A}_{1n}\right]
\end{aligned}
\tag{3.28}
$$

Substituting Eq. 3.28 back into Eq. 3.25, obtain:

$$
\begin{aligned}
A_{11} &= 2A_{13} - 5A_{15} + \ldots + (-1)^{n-1}\left[\frac{n(n-1)}{2} - 1\right]A_{1n} \\
&+ \left\{\bar{A}_{11} + \left(1 + \frac{\bar{c}_{55}h}{c_{55}\bar{h}}\right)\bar{A}_{12} + \ldots + \left[1 + \frac{n(n-1)}{2}\right]\frac{\bar{c}_{55}h}{c_{55}\bar{h}}\bar{A}_{1n}\right\} \\
&- hk\left[\left(1 - \frac{\bar{c}_{55}}{c_{55}}\right)\bar{B}_{31} + \left(1 - \frac{\bar{c}_{55}}{c_{55}}\right)\bar{B}_{32} + \ldots + \left(1 - \frac{\bar{c}_{55}}{c_{55}}\right)\bar{B}_{3n}\right] \\
A_{12} &= 3A_{13} - 6A_{15} + \ldots + (-1)^{n-1}\frac{n(n-1)}{2}A_{1n} \\
&+ \left[\frac{\bar{c}_{55}h}{c_{55}\bar{h}}\bar{A}_{12} +_{55}\bar{A}_{13} + \ldots + \frac{n(n-1)}{2}\frac{\bar{c}_{55}h}{c_{55}\bar{h}}\bar{A}_{1n}\right] \\
&- hk\left[\left(1 - \frac{\bar{c}_{55}}{c_{55}}\right)\bar{B}_{31} + \left(1 - \frac{\bar{c}_{55}}{c_{55}}\right)\bar{B}_{32} + \ldots + \left(1 - \frac{\bar{c}_{55}}{c_{55}}\right)\bar{B}_{3n}\right] \\
B_{11} &= 2B_{13} - 5B_{15} + \ldots + (-1)^{n-1}\left[\frac{n(n-1)}{2} - 1\right]B_{1n} \\
&+ \left\{\bar{B}_{11} + \left(1 + \frac{\bar{c}_{55}h}{c_{55}\bar{h}}\right)\bar{B}_{12} + \ldots + \left[1 + \frac{n(n-1)}{2}\right]\frac{\bar{c}_{55}h}{c_{55}\bar{h}}\bar{B}_{1n}\right\} \\
&+ hk\left[\left(1 - \frac{\bar{c}_{55}}{c_{55}}\right)\bar{A}_{31} + \left(1 - \frac{\bar{c}_{55}}{c_{55}}\right)\bar{A}_{32} + \ldots + \left(1 - \frac{\bar{c}_{55}}{c_{55}}\right)\bar{A}_{3n}\right] \qquad (3.29) \\
B_{12} &= 3B_{13} - 6B_{15} + \ldots + (-1)^{n-1}\frac{n(n-1)}{2}B_{1n} \\
&+ \left[\frac{\bar{c}_{55}h}{c_{55}\bar{h}}\bar{B}_{12} + \frac{3\bar{c}_{55}h}{c_{55}\bar{h}}\bar{B}_{13} + \ldots + \frac{n(n-1)}{2}\frac{\bar{c}_{55}h}{c_{55}\bar{h}}\bar{B}_{1n}\right] \\
&+ hk\left[\left(1 - \frac{\bar{c}_{55}}{c_{55}}\right)\bar{A}_{31} + \left(1 - \frac{\bar{c}_{55}}{c_{55}}\right)\bar{A}_{32} + \ldots + \left(1 - \frac{\bar{c}_{55}}{c_{55}}\right)\bar{A}_{3n}\right] \\
A_{31} &= 2A_{33} - 5A_{35} + \ldots + (-1)^{n-1}\left[\frac{n(n-1)}{2} - 1\right]A_{3n} \\
&+ \left\{\bar{A}_{31} + \left(1 + \frac{\bar{c}_{33}h}{c_{33}\bar{h}}\right)\bar{A}_{32} + \ldots + \left[1 + \frac{n(n-1)}{2}\right]\frac{\bar{c}_{33}h}{c_{33}\bar{h}}\bar{A}_{3n}\right\} \\
&+ hk\left[\frac{(c_{31} - \bar{c}_{31})}{c_{33}}\bar{B}_{11} + \frac{(c_{31} - \bar{c}_{31})}{c_{33}}\bar{B}_{12} + \ldots + \frac{(c_{31} - \bar{c}_{31})}{c_{33}}\bar{B}_{1n}\right] \\
A_{32} &= 3A_{33} - 6A_{35} + \ldots + (-1)^{n-1}\frac{n(n-1)}{2}A_{3n} \\
&+ \left[\frac{\bar{c}_{33}h}{c_{33}\bar{h}}\bar{A}_{32} + \frac{3\bar{c}_{33}h}{c_{33}\bar{h}}\bar{A}_{33} + \ldots + \frac{n(n-1)}{2}\frac{\bar{c}_{33}h}{c_{33}\bar{h}}\bar{A}_{3n}\right]
\end{aligned}
$$

$$+hk\left[\frac{(c_{31}-\bar{c}_{31})}{c_{33}}\bar{B}_{11}+\frac{(c_{31}-\bar{c}_{31})}{c_{33}}\bar{B}_{12}+\ldots+\frac{(c_{31}-\bar{c}_{31})}{c_{33}}\bar{B}_{1n}\right]$$

$$\begin{aligned}B_{31}&=2B_{33}-5B_{35}+\ldots+(-1)^{n-1}\left[\frac{n(n-1)}{2}-1\right]B_{3n}\\&+\left\{\bar{B}_{31}+\left(1+\frac{\bar{c}_{33}h}{c_{33}\bar{h}}\right)\bar{B}_{32}+\ldots+\left[1+\frac{n(n-1)}{2}\right]\frac{\bar{c}_{33}h}{c_{33}\bar{h}}\bar{B}_{3n}\right\}\\&-hk\left[\frac{(c_{31}-\bar{c}_{31})}{c_{33}}\bar{A}_{11}+\frac{(c_{31}-\bar{c}_{31})}{c_{33}}\bar{A}_{12}+\ldots+\frac{(c_{31}-\bar{c}_{31})}{c_{33}}\bar{A}_{1n}\right]\end{aligned}\tag{3.29}$$

$$\begin{aligned}B_{32}&=3B_{33}-6B_{35}+\ldots+(-1)^{n-1}\frac{n(n-1)}{2}B_{3n}\\&+\left[\frac{\bar{c}_{33}h}{c_{33}\bar{h}}\bar{B}_{32}+\frac{3\bar{c}_{33}h}{c_{33}\bar{h}}\bar{B}_{33}+\ldots+\frac{n(n-1)}{2}\frac{\bar{c}_{33}h}{c_{33}\bar{h}}\bar{B}_{3n}\right]\\&-hk\left[\frac{(c_{31}-\bar{c}_{31})}{c_{33}}\bar{A}_{11}+\frac{(c_{31}-\bar{c}_{31})}{c_{33}}\bar{A}_{12}+\ldots+\frac{(c_{31}-\bar{c}_{31})}{c_{33}}\bar{A}_{1n}\right]\end{aligned}$$

Rectifying the equations, the independent unknown quantities exhibited in the right-hand side of Eq. 3.28 can be set to the new unknown vector $\bar{\alpha}$:

$$\begin{aligned}\{\alpha\}&=[S_1]\{\bar{\alpha}\}\\\{\alpha\}&=\left\{[A_1]\quad[B_1]\quad[A_3]\quad[B_3]\quad[\bar{A}_1]\quad[\bar{B}_1]\quad[\bar{A}_3]\quad[\bar{B}_3]\right\}^T\\\{\bar{\alpha}\}&=\left\{[\tilde{A}_1]\quad[\tilde{B}_1]\quad[\tilde{A}_3]\quad[\tilde{B}_3]\quad[\bar{A}_1]\quad[\bar{B}_1]\quad[\bar{A}_3]\quad[\bar{B}_3]\right\}^T\end{aligned}\tag{3.29}$$

where,

$$\begin{aligned}\{A_1\}&=\begin{bmatrix}A_{11}&A_{12}&\ldots&A_{1n}\end{bmatrix}^T\\\{B_1\}&=\begin{bmatrix}B_{11}&B_{12}&\ldots&B_{1n}\end{bmatrix}^T\\\{A_3\}&=\begin{bmatrix}A_{31}&A_{32}&\ldots&A_{3n}\end{bmatrix}^T\\\{B_3\}&=\begin{bmatrix}B_{31}&B_{32}&\ldots&B_{3n}\end{bmatrix}^T\\\{\bar{A}_1\}&=\begin{bmatrix}\bar{A}_{11}&\bar{A}_{12}&\ldots&\bar{A}_{1n}\end{bmatrix}^T\\\{\bar{B}_1\}&=\begin{bmatrix}\bar{B}_{11}&\bar{B}_{12}&\ldots&\bar{B}_{1n}\end{bmatrix}^T\end{aligned}$$

$$\begin{aligned}
\{\bar{A}_3\} &= \begin{bmatrix}\bar{A}_{31} & \bar{A}_{32} & \dots & \bar{A}_{3n}\end{bmatrix}^T \\
\{\bar{B}_3\} &= \begin{bmatrix}\bar{B}_{31} & \bar{B}_{32} & \dots & \bar{B}_{3n}\end{bmatrix}^T \\
\{\tilde{A}_1\} &= \begin{bmatrix}A_{13} & A_{14} & \dots & A_{1n}\end{bmatrix}^T \\
\{\tilde{B}_1\} &= \begin{bmatrix}B_{13} & B_{14} & \dots & B_{1n}\end{bmatrix}^T \\
\{\tilde{A}_3\} &= \begin{bmatrix}A_{33} & A_{34} & \dots & A_{3n}\end{bmatrix}^T \\
\{\tilde{B}_3\} &= \begin{bmatrix}B_{33} & B_{34} & \dots & B_{3n}\end{bmatrix}^T
\end{aligned} \tag{3.30}$$

The $[S_1]$ in Eq. 3.30 is the key to the conversion of the old unknown coefficients to the new unknown coefficients, which is achieved by Eq. 3.27.

In this section the substrate bottom surface ($x_3 = h$) is fixed and the top surface of the covering layer ($x_3 = -\bar{h}$) is free, so the specific forms of the displacement functions shown in following:

$$\bar{u}_i = \left[\sum_{n=0}^{N} \bar{A}_{in} P_n\left(\frac{2x_3}{\bar{h}}+1\right)\sin\left(\frac{kx_1}{a}\right) + \sum_{n=0}^{N} \bar{B}_{in} P_n\left(\frac{2x_3}{\bar{h}}+1\right)\cos\left(\frac{kx_1}{a}\right)\right] e^{j\omega t} \tag{3.31}$$

$$u_i = \left(1-\frac{x_3}{h}\right)\left[\sum_{n=0}^{N} A_{in} P_n\left(\frac{2x_3}{h}-1\right)\sin\left(\frac{kx_1}{a}\right) + \sum_{n=0}^{N} B_{in} P_n\left(\frac{2x_3}{h}-1\right)\cos\left(\frac{kx_1}{a}\right)\right] e^{j\omega t} \tag{3.32}$$

Since $f(x_3) = 1$ at $x_3 = 0$, the unknown coefficient relationship obtained under the displacement continuity condition is consistent with the result for the bottom surface being free, i.e. Eqs. 3.31 and 3.32 substituted into Eq. 3.3, still yields to Eq. 3.24.

Substituting Eqs. 3.31 and 3.31 into Eq. 3.26, obtain:

$$\begin{aligned}
& -\frac{c_{33}}{kh}\{A_{31} - 3A_{32} + 7A_{33} - \dots + (-1)^n [n(n-1)+1] A_{3n}\} \\
& - c_{31}[B_{11} - B_{12} + B_{13} - \dots + (-1)^n B_{1n}] \\
& = \frac{\bar{c}_{33}}{k\bar{h}}\left[2\bar{A}_{32} + 6\bar{A}_{33} + 12\bar{A}_{34} + \dots + n(n-1)\bar{A}_{3n}\right] \\
& + \bar{c}_{31}[\bar{B}_{11} + \bar{B}_{12} + \bar{B}_{13} + \dots + \bar{B}_{1l}]
\end{aligned}$$

$$
\begin{aligned}
&-\frac{c_{33}}{kh}\left\{B_{31}-3B_{32}+7B_{34}-\ldots+(-1)^n\left[n(n-1)+1\right]B_{3n}\right\}\\
&+c_{31}\left[A_{11}-A_{12}+A_{13}-\ldots+(-1)^n A_{1n}\right]\\
&=\frac{\bar{c}_{33}}{k\bar{h}}\left[2\bar{B}_{32}+6\bar{B}_{33}+12\bar{B}_{34}+\ldots+n(n-1)\bar{B}_{3n}\right]\\
&+\bar{c}_{31}\left[\bar{A}_{11}+\bar{A}_{12}+\bar{A}_{13}+\ldots+\bar{A}_{1l}\right]\\
&c_{55}\left\{2\left[A_{31}-A_{32}+\ldots+(-1)^{n-1}A_{3n}\right]\right.\\
&\left.+\frac{a}{kh}\left[-B_{11}+3B_{12}-7B_{13}+\ldots+(-1)^n\left[n(n-1)+1\right]B_{1n}\right]\right\}\\
&=\bar{c}_{55}\left\{2\left[\bar{A}_{31}+\bar{A}_{32}+\ldots+\bar{A}_{3n}\right]\right.\\
&\left.+\frac{a}{kh}\left[2\bar{B}_{12}+6\bar{B}_{13}+12\bar{B}_{14}+\ldots+n(n-1)\bar{B}_{1n}\right]\right\}\\
&c_{55}\left\{2\left[B_{31}-B_{32}+\ldots+(-1)^{n-1}B_{3n}\right]\right.\\
&\left.+\frac{1}{kh}\left[-A_{11}+3A_{12}-7A_{13}+\ldots+(-1)^n\left[n(n-1)+1\right]A_{1n}\right]\right\}\\
&=\bar{c}_{55}\left\{2\left[\bar{B}_{31}+\bar{B}_{32}+\ldots+\bar{B}_{3n}\right]\right.\\
&\left.+\frac{1}{kh}\left[2\bar{A}_{12}+6\bar{A}_{13}+12\bar{A}_{14}+\ldots+n(n-1)\bar{A}_{1n}\right]\right\}
\end{aligned}
\tag{3.33}
$$

These can be solved for as follows:

$$
\begin{aligned}
A_{12}&=3A_{13}-6A_{14}+\ldots+(-1)^{n-1}\frac{n(n-1)}{2}A_{1n}\\
&+\left\{\left(\frac{1}{2}+\frac{\bar{c}_{55}h}{c_{55}\bar{h}}\right)\bar{A}_{11}+\left(\frac{1}{2}+\frac{3\bar{c}_{55}h}{c_{55}\bar{h}}\right)\bar{A}_{12}+\ldots+\left[\frac{1}{2}+\frac{n(n-1)}{2}\frac{\bar{c}_{55}h}{c_{55}\bar{h}}\right]\bar{A}_{1n}\right\}\\
&+hk\left(\frac{\bar{c}_{55}}{c_{55}}-1\right)\left(\bar{B}_{31}+\bar{B}_{32}+\ldots+\bar{B}_{3n}\right)\\
A_{32}&=3A_{33}-6A_{34}+\ldots+(-1)^{n-1}\frac{n(n-1)}{2}A_{3n}
\end{aligned}
$$

$$
\begin{aligned}
&+\left\{\left(\frac{1}{2}+\frac{\bar{c}_{33}h}{c_{33}\bar{h}}\right)\bar{A}_{11}+\left(\frac{1}{2}+\frac{3\bar{c}_{33}h}{c_{33}\bar{h}}\right)\bar{A}_{12}+\ldots+\left[\frac{1}{2}+\frac{n(n-1)}{2}\frac{\bar{c}_{33}h}{c_{33}\bar{h}}\right]\bar{A}_{1n}\right\}\\
&+hk\left(\frac{\bar{c}_{31}-c_{31}}{c_{33}}\right)(\bar{B}_{31}+\bar{B}_{32}+\ldots+\bar{B}_{3n})\\
B_{12}&=3B_{13}-6B_{14}+\ldots+(-1)^{n-1}\frac{n(n-1)}{2}B_{1n}\\
&+\left\{\left(\frac{1}{2}+\frac{\bar{c}_{55}h}{c_{55}\bar{h}}\right)\bar{A}_{11}+\left(\frac{1}{2}+\frac{3\bar{c}_{55}h}{c_{55}\bar{h}}\right)\bar{A}_{12}+\ldots+\left[\frac{1}{2}+\frac{n(n-1)}{2}\frac{\bar{c}_{55}h}{c_{55}\bar{h}}\right]\bar{A}_{1n}\right\}\\
&+hk\left(1-\frac{\bar{c}_{55}}{c_{55}}\right)(\bar{B}_{31}+\bar{B}_{32}+\ldots+\bar{B}_{3n})\\
B_{32}&=3B_{33}-6B_{34}+\ldots+(-1)^{n-1}\frac{n(n-1)}{2}B_{3n}\\
&+\left\{\left(\frac{1}{2}+\frac{\bar{c}_{33}h}{c_{33}\bar{h}}\right)\bar{A}_{11}+\left(\frac{1}{2}+\frac{3\bar{c}_{33}h}{c_{33}\bar{h}}\right)\bar{A}_{12}+\ldots+\left[\frac{1}{2}+\frac{n(n-1)}{2}\frac{\bar{c}_{33}h}{c_{33}\bar{h}}\right]\bar{A}_{1n}\right\}\\
&-hk\left(\frac{\bar{c}_{31}-c_{31}}{c_{33}}\right)(\bar{B}_{31}+\bar{B}_{32}+\ldots+\bar{B}_{3n})
\end{aligned}
\tag{3.34}
$$

Substituting Eq. 3.34 back into Eq. 3.25, obtain:

$$
\begin{aligned}
A_{11}&=2A_{13}-5A_{14}+\ldots+(-1)^{n-1}\left[\frac{n(n-1)}{2}-1\right]A_{1n}\\
&+\left\{\left(\frac{3}{2}+\frac{\bar{c}_{55}h}{c_{55}\bar{h}}\right)\bar{A}_{11}+\left(\frac{3}{2}+\frac{3\bar{c}_{55}h}{c_{55}\bar{h}}\right)\bar{A}_{12}+\ldots+\left[\frac{3}{2}+\frac{n(n-1)}{2}\frac{\bar{c}_{55}h}{c_{55}\bar{h}}\right]\bar{A}_{1n}\right\}\\
&+hk\left(\frac{\bar{c}_{55}}{c_{55}}-1\right)(\bar{B}_{31}+\bar{B}_{32}+\ldots+\bar{B}_{3n})A_{12}\\
&=3A_{13}-6A_{14}+\ldots+(-1)^{n-1}\frac{n(n-1)}{2}A_{1n}\\
&+\left\{\left(\frac{1}{2}+\frac{\bar{c}_{55}h}{c_{55}\bar{h}}\right)\bar{A}_{11}+\left(\frac{1}{2}+\frac{3\bar{c}_{55}h}{c_{55}\bar{h}}\right)\bar{A}_{12}+\ldots+\left[\frac{1}{2}+\frac{n(n-1)}{2}\frac{\bar{c}_{55}h}{c_{55}\bar{h}}\right]\bar{A}_{1n}\right\}\\
&+hk\left(\frac{\bar{c}_{55}}{c_{55}}-1\right)(\bar{B}_{31}+\bar{B}_{32}+\ldots+\bar{B}_{3n})\\
A_{31}&=2A_{33}-5A_{34}+\ldots+(-1)^{n-1}\left[\frac{n(n-1)}{2}-1\right]A_{3n}
\end{aligned}
$$

$$
\begin{aligned}
&+\left\{\left(\frac{3}{2}+\frac{\bar{c}_{33}h}{c_{33}\bar{h}}\right)\bar{A}_{11}+\left(\frac{3}{2}+\frac{3\bar{c}_{33}h}{c_{33}\bar{h}}\right)\bar{A}_{12}+\ldots+\left[\frac{3}{2}+\frac{n(n-1)}{2}\frac{\bar{c}_{33}h}{c_{33}\bar{h}}\right]\bar{A}_{1n}\right\}\\
&+hk\left(\frac{\bar{c}_{31}-c_{31}}{c_{33}}\right)(\bar{B}_{31}+\bar{B}_{32}+\ldots+\bar{B}_{3n})\\
A_{32}&=3A_{33}-6A_{34}+\ldots+(-1)^{n-1}\frac{n(n-1)}{2}A_{3n}\\
&+\left\{\left(\frac{1}{2}+\frac{\bar{c}_{33}h}{c_{33}\bar{h}}\right)\bar{A}_{11}+\left(\frac{1}{2}+\frac{3\bar{c}_{33}h}{c_{33}\bar{h}}\right)\bar{A}_{12}+\ldots+\left[\frac{1}{2}+\frac{n(n-1)}{2}\frac{\bar{c}_{33}h}{c_{33}\bar{h}}\right]\bar{A}_{1n}\right\}\\
&+hk\left(\frac{\bar{c}_{31}-c_{31}}{c_{33}}\right)(\bar{B}_{31}+\bar{B}_{32}+\ldots+\bar{B}_{3n})\\
B_{12}&=3B_{13}-6B_{14}+\ldots+(-1)^{n-1}\frac{n(n-1)}{2}B_{1n}\\
&+\left\{\left(\frac{1}{2}+\frac{\bar{c}_{55}h}{c_{55}\bar{h}}\right)\bar{A}_{11}+\left(\frac{1}{2}+\frac{3\bar{c}_{33}h}{c_{33}\bar{h}}\right)\bar{A}_{12}+\ldots+\left[\frac{1}{2}+\frac{n(n-1)}{2}\frac{\bar{c}_{55}h}{c_{55}\bar{h}}\right]\bar{A}_{1n}\right\}\\
&+hk\left(1-\frac{\bar{c}_{55}}{c_{55}}\right)(\bar{B}_{31}+\bar{B}_{32}+\ldots+\bar{B}_{3n})\\
B_{31}&=2B_{33}-5B_{34}+\ldots+(-1)^{n-1}\left[\frac{n(n-1)}{2}-1\right]B_{3n}\\
&+\left\{\left(\frac{3}{2}+\frac{\bar{c}_{33}h}{c_{33}\bar{h}}\right)\bar{A}_{11}+\left(\frac{3}{2}+\frac{3\bar{c}_{33}h}{c_{33}\bar{h}}\right)\bar{A}_{12}+\ldots+\left[\frac{3}{2}+\frac{n(n-1)}{2}\frac{\bar{c}_{33}h}{c_{33}\bar{h}}\right]\bar{A}_{1n}\right\}\\
&+hk\left(\frac{\bar{c}_{31}-c_{31}}{c_{33}}\right)(\bar{B}_{31}+\bar{B}_{32}+\ldots+\bar{B}_{3n})\\
B_{32}&=3B_{33}-6B_{34}+\ldots+(-1)^{n-1}\frac{n(n-1)}{2}B_{3n}\\
&+\left\{\left(\frac{1}{2}+\frac{\bar{c}_{33}h}{c_{33}\bar{h}}\right)\bar{A}_{11}+\left(\frac{1}{2}+\frac{3\bar{c}_{33}h}{c_{33}\bar{h}}\right)\bar{A}_{12}+\ldots+\left[\frac{1}{2}+\frac{n(n-1)}{2}\frac{\bar{c}_{33}h}{c_{33}\bar{h}}\right]\bar{A}_{1n}\right\}\\
&-hk\left(\frac{\bar{c}_{31}-c_{31}}{c_{33}}\right)(\bar{B}_{31}+\bar{B}_{32}+\ldots+\bar{B}_{3n})
\end{aligned}
\tag{3.35}
$$

According to Eq. 3.35, the transformation matrix $[S_1]$ can be acquired for a fixed condition of the substrate bottom surface.

Chapter 4

Propagation properties of low-order SAWs in a periodic isotropic structure covering a finite layer

There have been a lot of achievements in the research on the propagation characteristics of SAWs in semi-infinite layered spaces. Scholars have analyzed the propagation characteristics of SAWs in layered structures of different dielectric materials through analytical methods, semi-analytical methods, numerical methods, and experimental methods. Propagation properties of SAWs. However, when the widths of the upper attachment and the base layer are different, more boundary conditions need to be considered than the above cases, so it is often difficult to obtain an accurate solution by analytical method. This structure is common in SAW devices, that is, the finite adhesion layer is regarded as the electrode, and the underlying medium is regarded as the structural model of the substrate.

Studies on the structure of SAW devices are often based on two-dimensional models, in which the electrodes are generally discontinuous. In view of the large computational effort required to analyse the entire structure of a SAW device, which would be computationally expensive if the FEM were used directly, numerical simulations are often carried out by intercepting a unit of the structure. By setting reasonable boundary conditions, such as periodic boundary conditions on both sides of the substrate vertical to the direction of wave propagation, and by applying a PML to the bottom surface of the substrate to reduce the effect of wave reflection on the bottom surface of the substrate, it is possible to analyse the propagation characteristics of surface waves by means of a finite structural model. However, according to the working principle of finite element, the accuracy of its calculation results is closely related to the mesh division in the structure.

The Rayleigh-Ritz method has a wide range of applications in the vibration analysis of structures as an energy method as well. It is based on the Hamiltonian principle and the principle of energy minimisation, and is used to obtain the minimum (optimum) eigenfrequency and the corresponding eigenvector of a structure in order to analyse the various mechanical phenomena. To analyse the vibration of a structure by means of the Rayleigh-Ritz method, a reasonable trial function is set up and an appropriate amount of displacement function expansion term is used to obtain a more accurate numerical solution. In general, the test function contains information about the shape characteristics and boundary conditions of the structure and is approximated by algebraic polynomials to improve the accuracy of the calculation. If the Rayleigh-Ritz method is to be used to analyse the vibration of a multi-unit body, the transfer matrix can be used to relate the various parts of the structure to obtain the stiffness and mass matrices of the whole structure, thus finding the eigenfrequencies of the structure as a whole.

In general, compared with the finite element method, the Rayleigh-Ritz method has lower requirements on the computer (the parameters of the calculator used for the calculations in this article are: Intel(R) Core(TM) i5 8250U CPU @ 1.60 GHz 1.80 GHz R AM 8.00 GB), and the calculation cost is relatively lower. In the last chapter, we mainly discussed the propagation characteristics of low-order SAWs in structures covered with thin layers on finite large isotropic substrates considering various boundary conditions. This chapter studies the propagation characteristics of low-order SAWs in a periodic structure covered with a finite-sized thin layer on an isotropic substrate. The influence of low-order SAWs propagation characteristics. First, by setting a reasonable displacement function, the stiffness matrix and mass matrix of each part of the structure are obtained, and then the transfer matrix is obtained according to the boundary conditions, and the stiffness matrix and mass matrix of each part are integrated into a new stiffness matrix and mass matrix, thus obtaining The characteristic equation of the whole structure uses the relationship between angular frequency and wave velocity to obtain corresponding results.

4.1 Problem description

This structure mainly adds a finite layered structure on the upper surface of the isotropic substrate. At this time, the structure can be divided into four parts, as shown in Fig. 4.1.

By setting the boundary at $x_1 = \frac{-a}{2}$ and $x_1 = \frac{a}{2}$ (generally a is taken to be one wavelength) as periodic boundaries with $h = 6\lambda$, the calculation of a semi-infinite space is transformed into a finite computational model.

Part one displacement functions can be expressed as:

$$
\begin{aligned}
u_i^{(1)} = f^{(1)}(x_3) \Bigg\{ & A_{il}^{(1)} P_l \left(\frac{2x_3}{h} - 1 \right) \sin \left[\frac{2k}{a - a_1} \left(x_1 + \frac{a_1 + a}{4} \right) \right] \\
& + B_{il}^{(1)} P_l \left(\frac{2x_3}{h} - 1 \right) \cos \left[\frac{2k}{a - a_1} \left(x_1 + \frac{a_1 + a}{4} \right) \right] \Bigg\} e^{j\omega t}
\end{aligned} \tag{4.1}
$$

Part two displacement functions:

$$
u_i^{(2)} = f^{(2)}(x_3) \left[A_{il}^{(2)} P_l \left(\frac{2x_3}{h} - 1 \right) \sin \left(\frac{kx_1}{a_1} \right) + B_{il}^{(2)} P_l \left(\frac{2x_3}{h} - 1 \right) \cos \left(\frac{kx_1}{a_1} \right) \right] e^{j\omega t} \tag{4.2}
$$

Part three displacement functions:

$$
u_i^{(3)} = f^{(3)}(x_3) \left[A_{il}^{(3)} P_l \left(\frac{2x_3}{\bar{h}} + 1 \right) \sin \left(\frac{kx_1}{a_1} \right) + B_{il}^{(3)} P_l \left(\frac{2x_3}{\bar{h}} + 1 \right) \cos \left(\frac{kx_1}{a_1} \right) \right] e^{j\omega t} \tag{4.3}
$$

Part four displacement functions:

$$
\begin{aligned}
u_i^{(4)} = f^{(4)}(x_3) \Bigg\{ & A_{il}^{(4)} P_l \left(\frac{2x_3}{h} - 1 \right) \sin \left[\frac{2k}{a - a_1} \left(x_1 - \frac{a + a_1}{4} \right) \right] \\
& + B_{il}^{(4)} P_l \left(\frac{2x_3}{h} - 1 \right) \cos \left[\frac{2k}{a - a_1} \left(x_1 - \frac{a + a_1}{4} \right) \right] \Bigg\} e^{j\omega t}
\end{aligned} \tag{4.4}
$$

where $i = 1, 3$ and $f^{(r)}(x_3)$ is the boundary function of the Part r with respect to the direction of x_3 , refer to Tab. 3.1 for the expression form, $r = 1, 2, 3, 4$ and $P_n(x)$ is the Legendre polynomial.

The calculation of this model needs to consider the following boundary conditions:

(1) Continuous displacement at the interface

$$
u_i^{(2)}(x_3 = 0) = u_i^{(3)}(x_3 = 0), \quad x_1 \in \left[-\frac{a_1}{2}, \frac{a_1}{2} \right] \tag{4.5a}
$$

$$
u_i^{(3)} \left(x_1 = -\frac{a_1}{2} \right) = u_i^{(2)} \left(x_1 = -\frac{a_1}{2} \right), \quad x_3 \in [0, h] \tag{4.5b}
$$

$$
u_i^{(2)} \left(x_1 = \frac{a_1}{2} \right) = u_i^{(4)} \left(x_1 = \frac{a_1}{2} \right), \quad x_3 \in [0, h] \tag{4.5c}
$$

(2) Continuous stress at the interface

$$
\sigma_{3i}^{(2)}(x_3 = 0) = \sigma_{3i}^{(3)}(x_3 = 0), \quad x_1 \in \left[-\frac{a_1}{2}, \frac{a_1}{2} \right] \tag{4.6}
$$

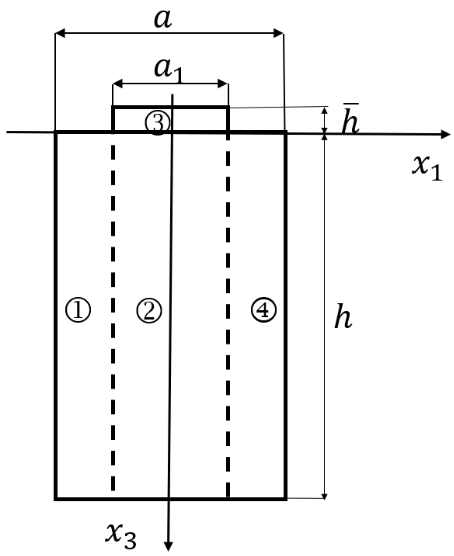

Fig. 4.1 A periodic solid covered by a finite layer

(3) Free boundary conditions

$$\sigma_{3i}^{(3)}\left(x_3=-\bar{h}\right)=0, x_1\in\left[-\frac{a_1}{2},\frac{a_1}{2}\right] \tag{4.7a}$$

$$\sigma_{3i}^{(3)}\left(x_3=0\right)=0, x_1\in\left[-\frac{a}{2},-\frac{a_1}{2}\right]\cup\left[\frac{a_1}{2},\frac{a}{2}\right] \tag{4.7b}$$

$$\sigma_{1i}^{(3)}\left(x_1=-\frac{a_1}{2}\right)=\sigma_{1i}^{(3)}\left(x_1=\frac{a_1}{2}\right)=0, x_3\in\left[-\bar{h},0\right] \tag{4.7c}$$

(4) Fixed boundary condition at the bottom of the substrate

$$u_i^{(r)}\left(x_3=h\right)=0,\ \ x_1\in\left[-\frac{a}{2},\frac{a}{2}\right], r=1,2,4 \tag{4.8a}$$

Free boundary condition at the bottom of the substrate

$$\sigma_{3i}^{(r)}\left(x_3=h\right)=0,\ \ x_1\in\left[-\frac{a}{2},\frac{a}{2}\right], r=1,2,4 \tag{4.8b}$$

4.2 Equation derivation

According to the model, the structure is divided into four parts for calculation, so according to the previous chapter, the kinetic and potential energies of this structure can be expressed as:

$$T = T^{(1)} + T^{(2)} + T^{(3)} + T^{(4)} \tag{4.9}$$

$$V = V^{(1)} + V^{(2)} + V^{(3)} + V^{(4)} \tag{4.10}$$

The steps are the same as in the previous chapter, obtaining the same form of the characteristic equation 3.15, with the stiffness matrix and mass matrix shown as:

$$[K] = \begin{bmatrix} \left[K^{(1)}\right] & [0] & [0] & [0] \\ [0] & \left[K^{(2)}\right] & [0] & [0] \\ [0] & [0] & \left[K^{(3)}\right] & [0] \\ [0] & [0] & [0] & \left[K^{(4)}\right] \end{bmatrix}$$

$$[M] = \begin{bmatrix} \left[M^{(1)}\right] & [0] & [0] & [0] \\ [0] & \left[M^{(2)}\right] & [0] & [0] \\ [0] & [0] & \left[M^{(3)}\right] & [0] \\ [0] & [0] & [0] & \left[M^{(4)}\right] \end{bmatrix} \tag{4.11}$$

$$\{\alpha\} = \begin{Bmatrix} \left\{\alpha^{(1)}\right\} \\ \left\{\alpha^{(2)}\right\} \\ \left\{\alpha^{(3)}\right\} \\ \left\{\alpha^{(4)}\right\} \end{Bmatrix}$$

The superscripts here represent the individual parts of the structure, where $\left\{\alpha^{(r)}\right\}$,$(r = 1,2,3,4)$ is a column vector consisting of the unknown coefficients $A_{in}^{(r)}$ and $B_{in}^{(r)}$, and the elements in the matrix are referred to the Appendix section of Chapter 2 for their exact form.

According to the previous chapter, the boundary conditions can be used to obtain the relationship between the corresponding unknown coefficients of each part, so that a transfer matrix, $[S]$, can be extracted. Therefore, the transfer matrix can be used to link the stiffness matrix and mass matrix of each part to obtain the mass matrix, $\left[\tilde{M}\right]$, and stiffness matrix, $\left[\tilde{K}\right]$:

$$\left[\tilde{K}\right] = [S]^T [K] [S], \left[\tilde{M}\right] = [S]^T [M] [S], \{\tilde{\alpha}\} = [S]^T \{\alpha\} [S] \tag{4.12}$$

Then, Eq. 3.15 can be rewritten as:

$$\left([\tilde{K}] - \omega^2 [\tilde{M}]\right) \{\tilde{\alpha}\} = 0 \tag{4.13}$$

By solving Eq. 4.13 for $v_R = \frac{\omega}{k}$, the wave velocities of the SAWs in the structure can be obtained for a given boundary condition.

4.3 Numerical results and discussion

This section mainly discusses the effects of different boundary conditions, finite cover plate thickness, and materials on the propagation characteristics of low-order SAWs in structures. Here, the size of the cover layer is: $a_1 = \frac{\lambda}{2}$, and the substrate is still six wavelengths thick. The material parameters used refer to Tab. 3.2.

4.3.1 The influence of boundary conditions on the propagation characteristics of SAWs

In this section we consider the wave velocities of low-order SAWs in a model structure with a covering layer thickness of one tenth of a wavelength for different combinations of boundary conditions, as shown in Tab. 4.1. Based on the results of the low-order SAW velocities in the structure for each boundary condition shown in Tab. 4.1, the results obtained when considering only the displacement continuity at the junction of each part and the stress continuity at the intersection of the substrate and the cover layer on top of that are consistent with those obtained in the previous chapter when considering the upper and lower layer displacement continuity/displacement and stress continuity. The calculated results are basically the same and do not reflect well the actual situation in this model where the overburden is not of the same width as the substrate. According to the comparison of the longitudinal data in Tab. 4.1 it can be found that the boundary conditions on each face of the upper cover layer can have some influence on the low-order SAWs velocities in the structure. Figs. 4.2 to 4.5 show the first five modes and corresponding stress distributions for free and fixed substrate bottom boundary conditions, respectively, after considering Eqs. 4.5, 4.6 and 4.7, with Au as the covering material and a thickness of one-tenth of a wavelength.

4.3.2 Effect of the covering layer thickness on the wave velocity of low-order SAWs

In this section we focus on the effect of the thickness of the covering layer on the dispersion curves of the SAWs in the structure in the present computational model. From the previous

Table 4.1 The velocities of the SAWs in the structure under different kinds of boundary conditions

Boundary conditions		Normalized velocity	Time (s)	Boundary conditions		Normalized velocity	Time (s)
Eq. 4.8a	Only Eq. 4.5	0.4887 0.7109 0.9058	0.506	Eq. 4.8b	Only Eq. 4.5	0.4887 0.7109 0.9058	0.633
	Eqs. 4.5 and 4.6	0.4887 0.6769 0.7111 0.9058	0.635		Eqs. 4.5 and 4.6	0.4887 0.6769 0.7111 0.9058	0.584
	Eqs. 4.5 and 4.7c	0.4935 0.5164 0.7334 0.8555 0.9058	1.126		Eqs. 4.5 and 4.6	0.4935 0.5164 0.7334 0.8555 0.9058	1.053
	Eqs. 4.5 and 4.7	0.4938 0.5195 0.7281 0.8180 0.9058	1.187		Eqs. 4.5 and 4.7	0.4938 0.5195 0.7281 0.8180 0.9058	1.258
	Eqs. 4.5, 4.6 and 4.7	0.4936 0.5164 0.7336 0.8561 0.9058	1.047		Eqs. 4.5, 4.6 and 4.7	0.4936 0.5164 0.7336 0.8561 0.9058	1.483

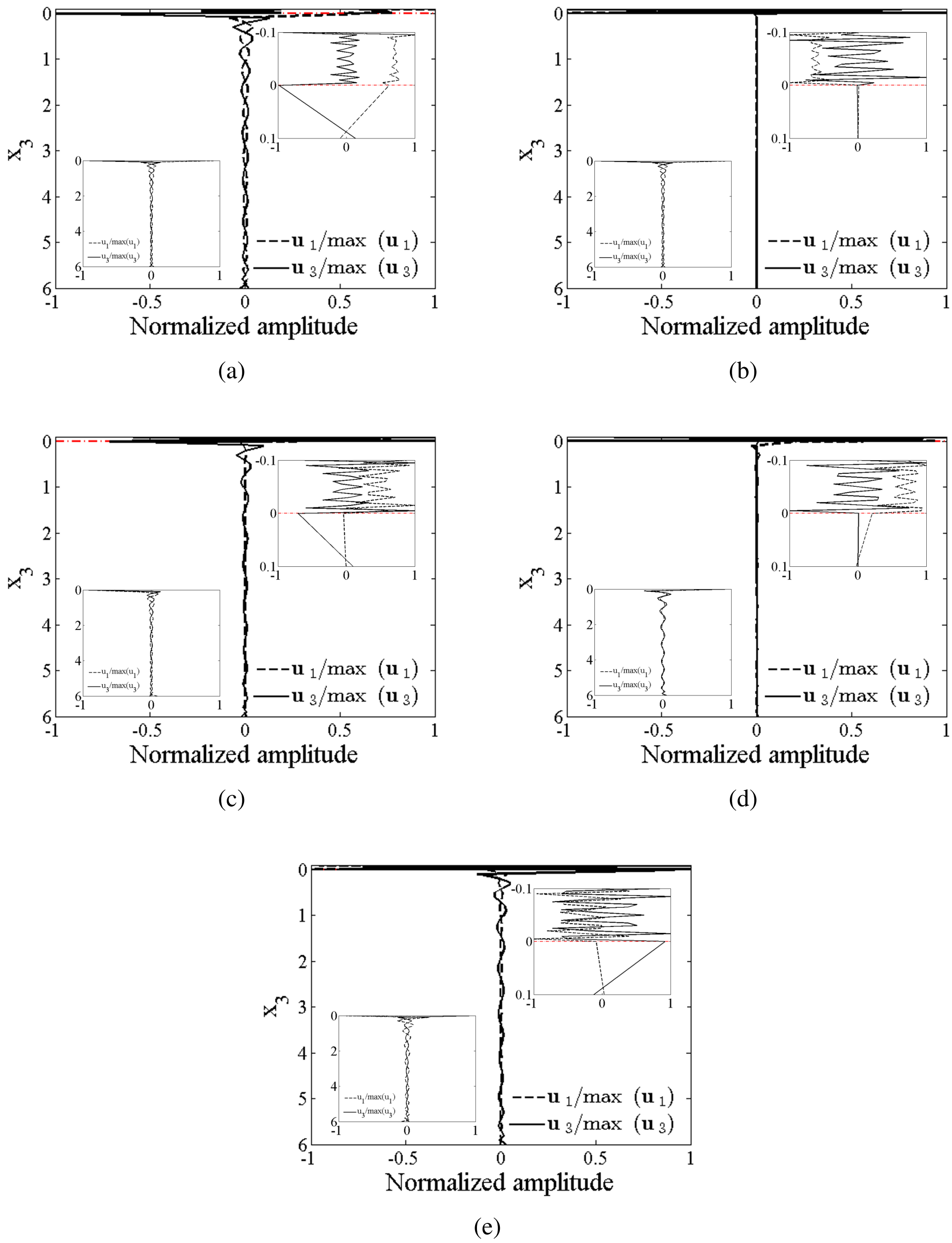

Fig. 4.2 First five SAW modes with free boundary conditions on the bottom surface of the substrate: (a) the 1st mode; (b) the 2nd mode; (c) the 3rd mode; (d) the 4th mode; (e) the 5th mode

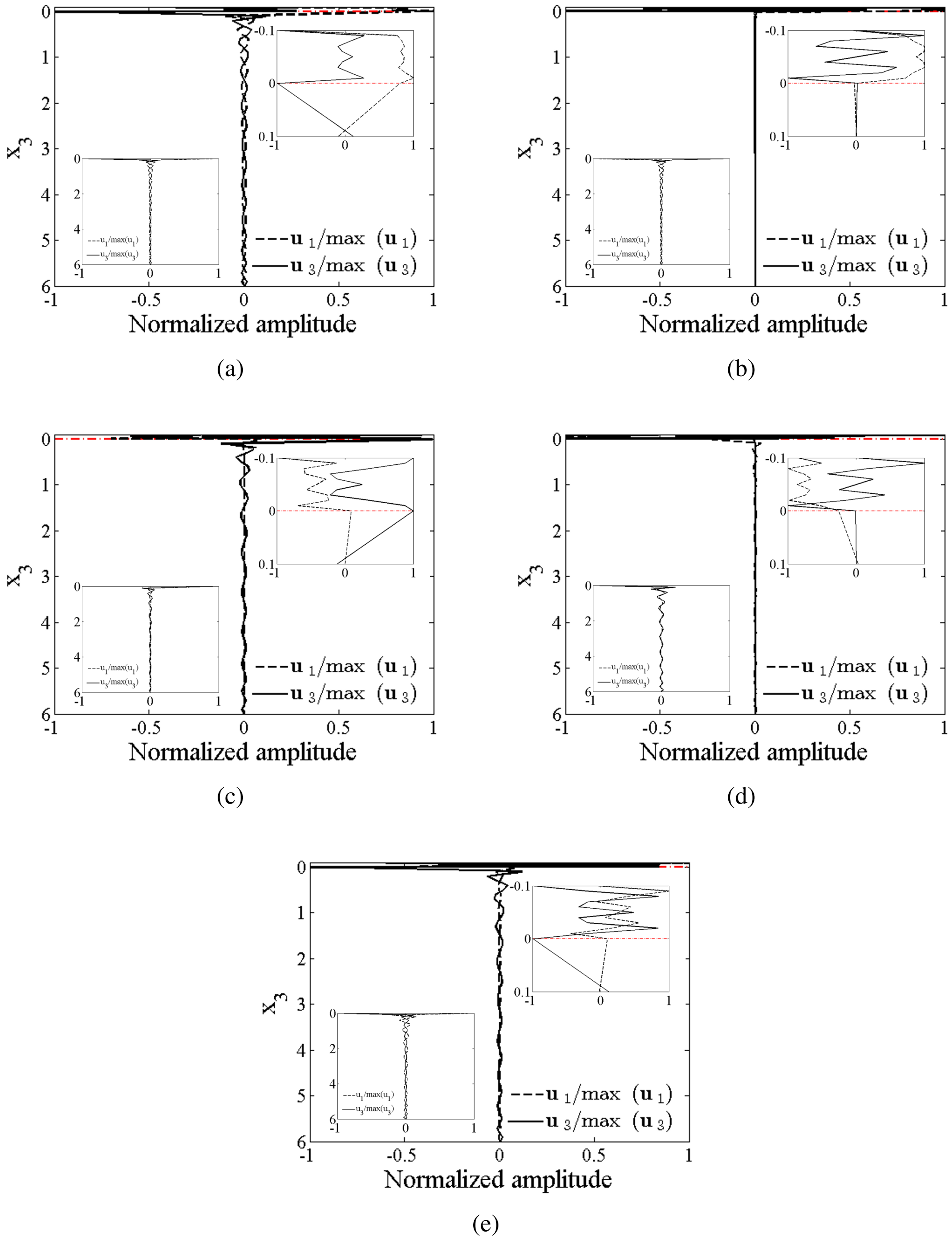

Fig. 4.3 First five SAW modes with fixed boundary conditions on the bottom surface of the substrate: (a) the 1st mode; (b) the 2nd mode; (c) the 3rd mode; (d) the 4th mode; (e) the 5th mode

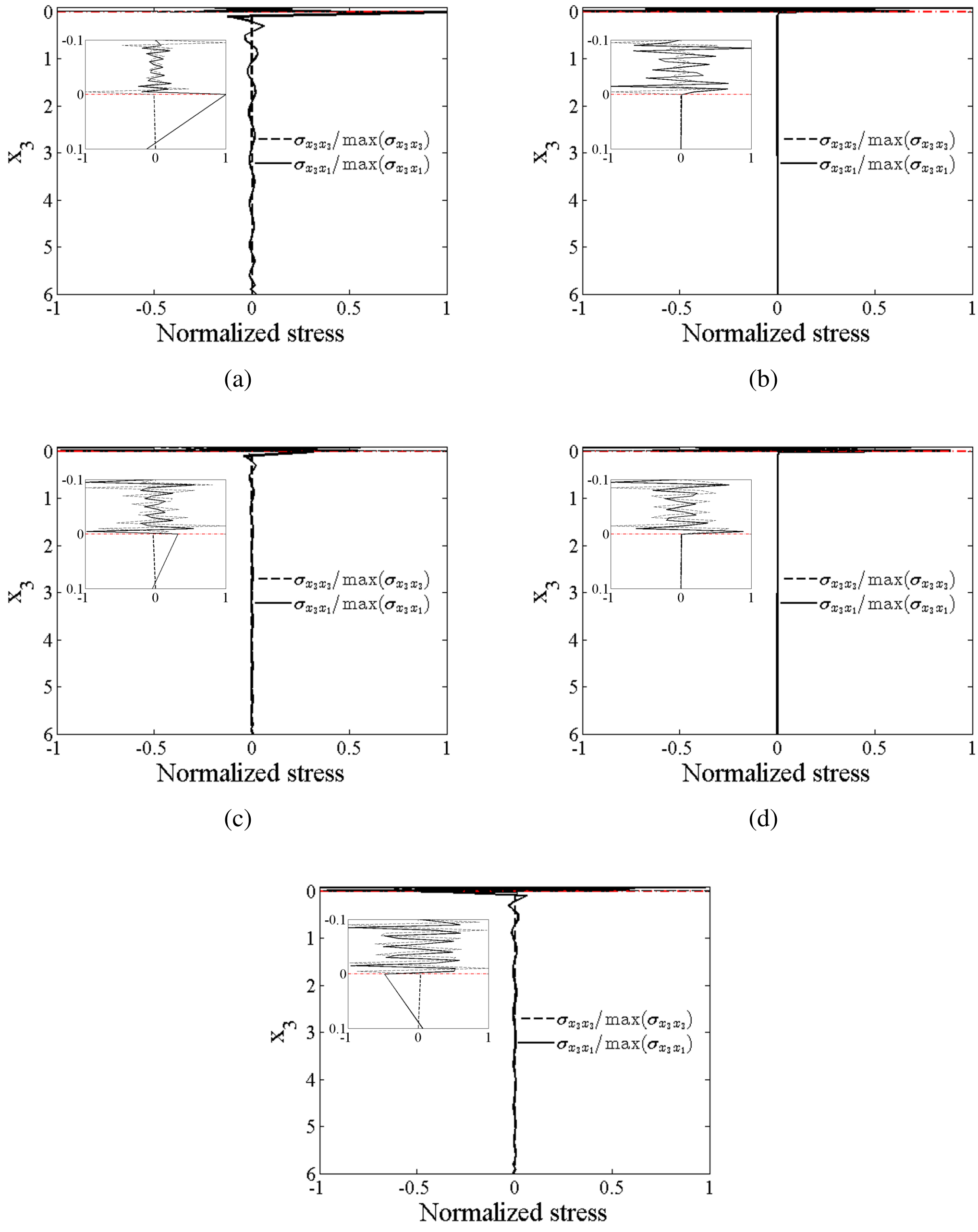

(e)

Fig. 4.4 First five stress distributions of SAWs with free boundary conditions on the bottom surface of the substrate: the stress distribution of (a) the 1st mode; (b) the 2nd mode; (c) the 3rd mode; (d) the 4th mode; (e) the 5th mode

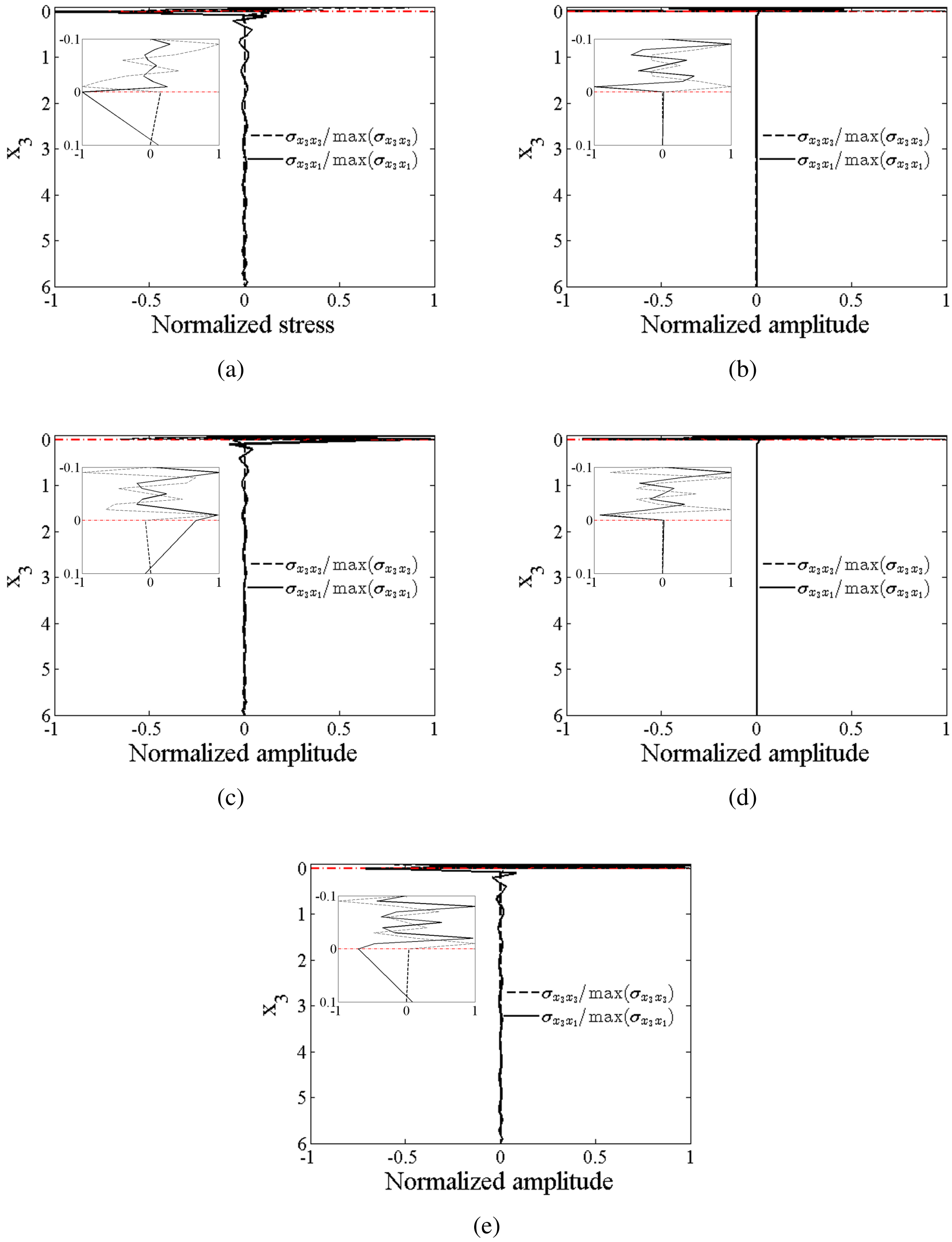

Fig. 4.5 First five stress distributions of SAWs with fixed boundary conditions on the bottom surface of the substrate: the stress distribution of (a) the 1st mode; (b) the 2nd mode; (c) the 3rd mode; (d) the 4th mode; (e) the 5th mode

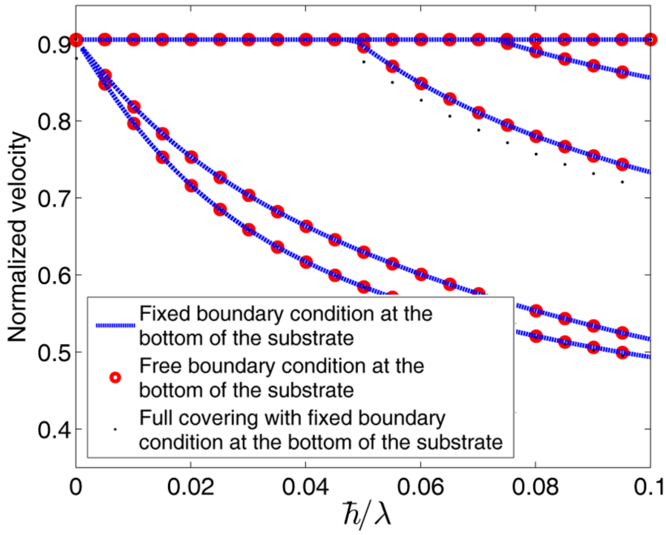

Fig. 4.6 Dispersion curves with different boundary conditions at the bottom of the substrate

chapter we already know that the thickness of the covering layer has a significant effect on the dispersion characteristics of the SAWs in the structure. In this chapter, the results of the previous chapter are used to analyse the effect of the thickness of the cover layer on the dispersion curves of the SAWs in each model. In consideration of the previous conclusions, the boundary conditions described in Eqs. 3.3 to 3.6a and Eqs. 4.7 to 4.8 are considered in this section, and Au is still used as the material for the overburden. Fig. 4.6 shows that for the same range of thickness variations, the wave velocity in this case decreases as the thickness of the covering layer increases, a trend that is generally consistent with the previous chapter, but the number of wave velocities less than the Rayleigh waves in the substrate is significantly greater in this computational model than the results obtained in the model with a thin full covering layer in the previous chapter.

4.3.3 Effect of the covering layer material on the propagation characteristics of low-order SAWs

In this section, the first analysis is that under the condition that the bottom surface of the substrate is a free boundary condition, the corresponding dispersion curves are calculated by using different covering materials, and the results are shown in Fig. 4.7.

As shown in Figs. 4.7 and 4.8, when Al_2O_3 is used as the covering layer material, $x_3 \in [0, 0.1\lambda]$, the trend of the wave velocity variation is basically the same as in the full-coverage condition. However, based on the results obtained in this section when compared with Fig. 4.6, it can be seen that there is also a difference in the displacement modes of the

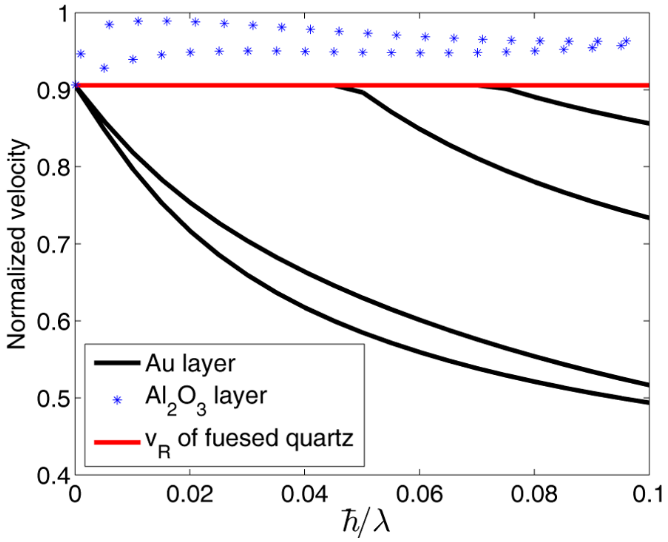

Fig. 4.7 Dispersion curves with different covering materials with a free boundary condition at the bottom of the substrate

SAWs in the structure for the covering layer material with $\frac{\bar{v}_T}{v_T} > \sqrt{2}$ and for the covering layer material with $\frac{\bar{v}_T}{v_T} < \sqrt{2}$ for the same boundary conditions. Compared to the previous chapter where the covering is the same width as the substrate, the number of dispersion curves has increased for the same normalised wave speed range. Figs. 4.9 and 4.10 show the first four order modes and corresponding stress distributions for a covering material of Al_2O_3 and a thickness of one tenth of a wavelength. As with the results of the previous section, regardless of whether the shear wave velocity of the overburden material is " loading" or " stiffening" with respect to the substrate, the energy is mainly concentrated near the intersection after taking into account the stress continuum between the upper covering layer and the substrate interface.

4.4 Summary

This chapter studies the propagation characteristics of Rayleigh waves in a structure covered by a finite thin layer, and discusses in detail the influence of various boundary conditions on the velocity of low-order SAWs, the corresponding displacement modes and stress distribution, mainly Including various boundary conditions, the thickness of the covering plate, and the influence of the material of the covering layer on the wave velocities. The specific conclusions are as follows:

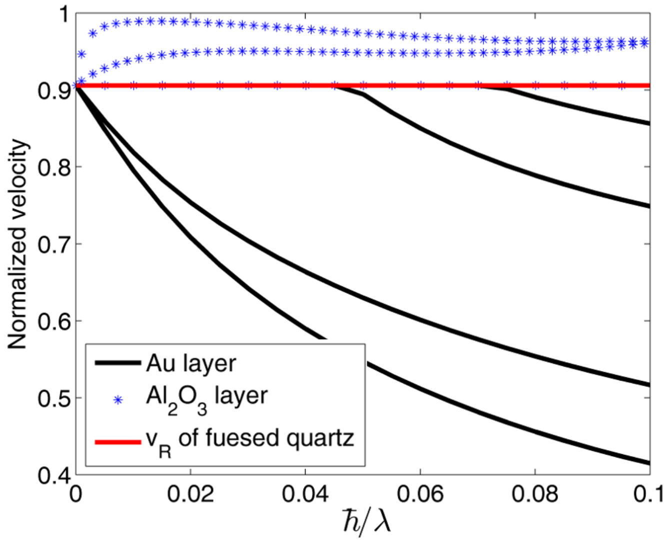

Fig. 4.8 Dispersion curves with different covering materials with a fixed boundary condition at the bottom of the substrate

(1) In the case of a finite covering layer, it is necessary to consider the boundary conditions corresponding to each surface of the upper covering layer to meet the actual situation. Among them, the side parallel to the x_3-axis has a greater influence on the low-order wave velocity in the structure, and on this basis, the boundary conditions corresponding to the free surface and the contact surface parallel to the x_1-axis also need to be considered. In addition, the obvious difference from the previous chapter is that, on the basis of considering the free boundary and displacement continuation conditions, the stress continuum boundary at the interface between the upper and lower layers needs to be further considered. As in the previous chapter, the boundary of the bottom surface will not have a significant impact on the velocity of low-order SAWs in the structure.

(2) Same as the previous chapter, for the covering material with $\frac{\bar{v}_T}{v_T} < \frac{1}{\sqrt{2}}$, within the calculation range of covering thickness in this chapter, the velocities of low-order SAWs in the structure decreases with increasing thickness of the cover layer, and the number of low-order SAWs will change with the increase of the thickness of the covering layer. But it is not the case for covering materials with $\frac{\bar{v}_T}{v_T} > \sqrt{2}$. When the covering thickness is extremely small ($\bar{h} < 0.01\lambda$), the low-order wave velocities in the structure increase rapidly with the thickness of the covering layer, and change in the velocities of the low-order SAWs in this computational model tends to stabilise when the thickness continues to increase.

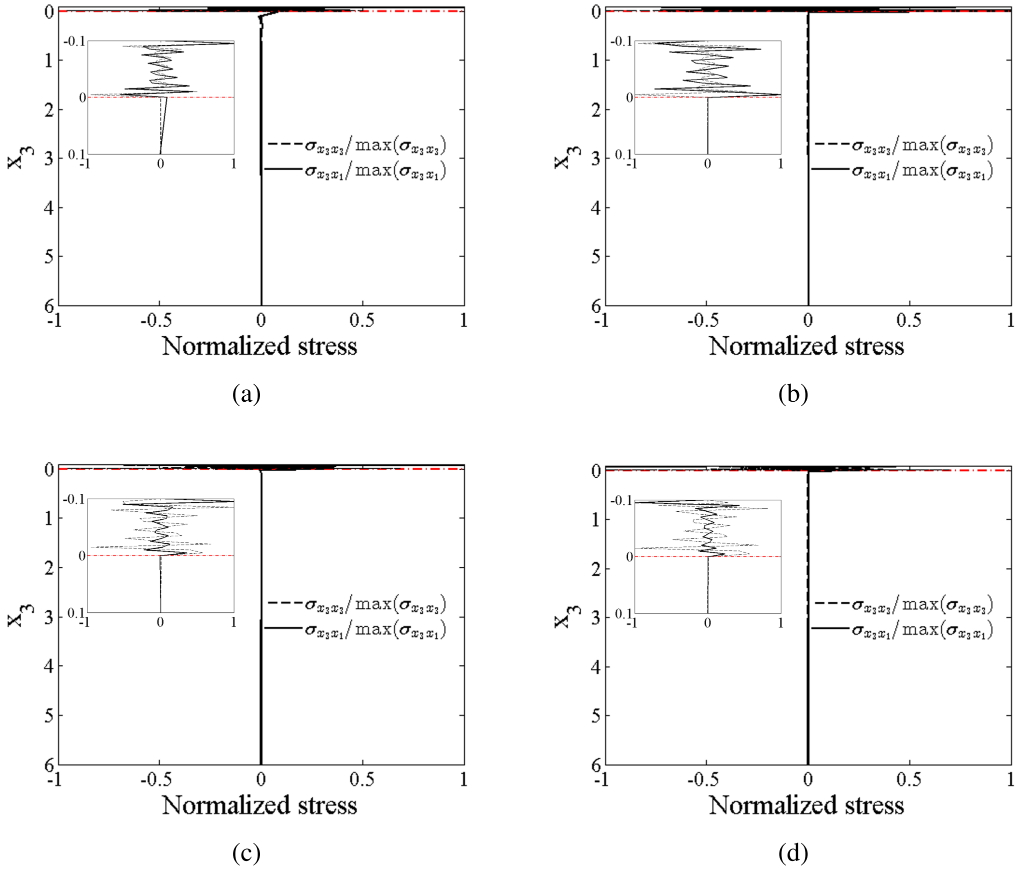

Fig. 4.9 First four SAW modes with free boundary conditions on the bottom surface of the substrate: (a) the 1st mode; (b) the 2nd mode; (c) the 3rd mode; (d) the 4th mode

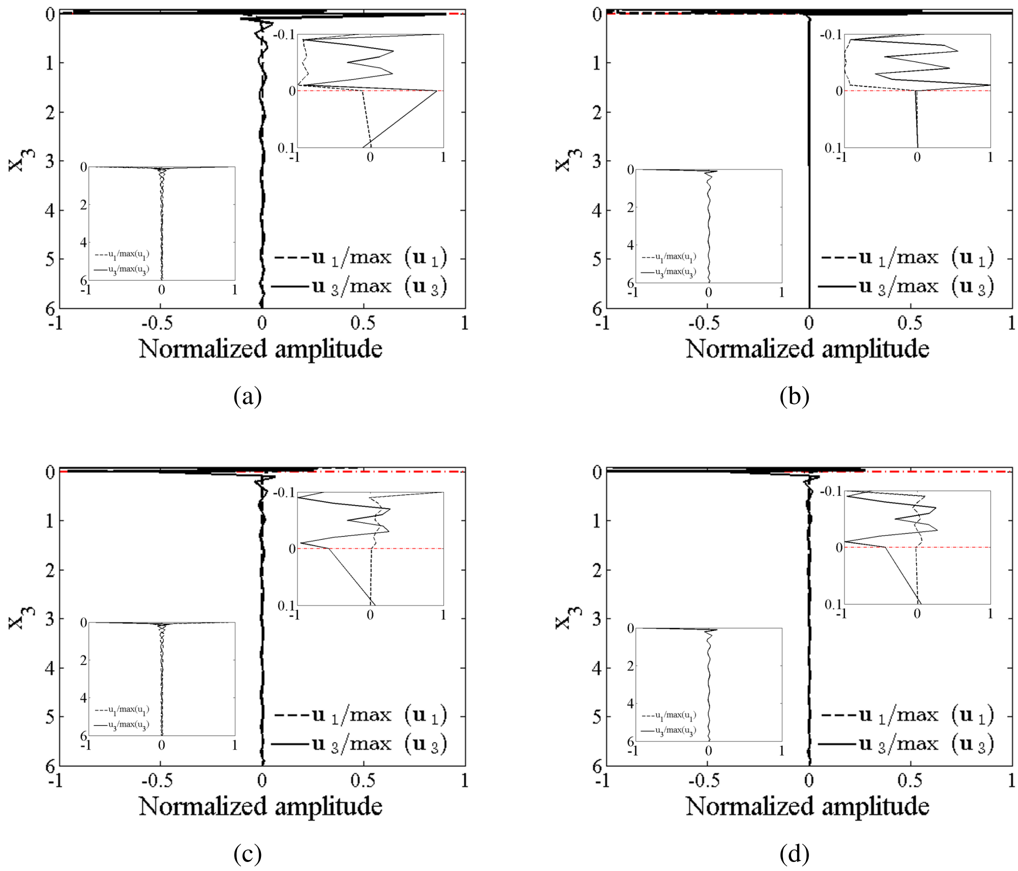

Fig. 4.10 First four SAW modes with fixed boundary conditions on the bottom surface of the substrate: (a) the 1st mode; (b) the 2nd mode; (c) the 3rd mode; (d) the 4th mode

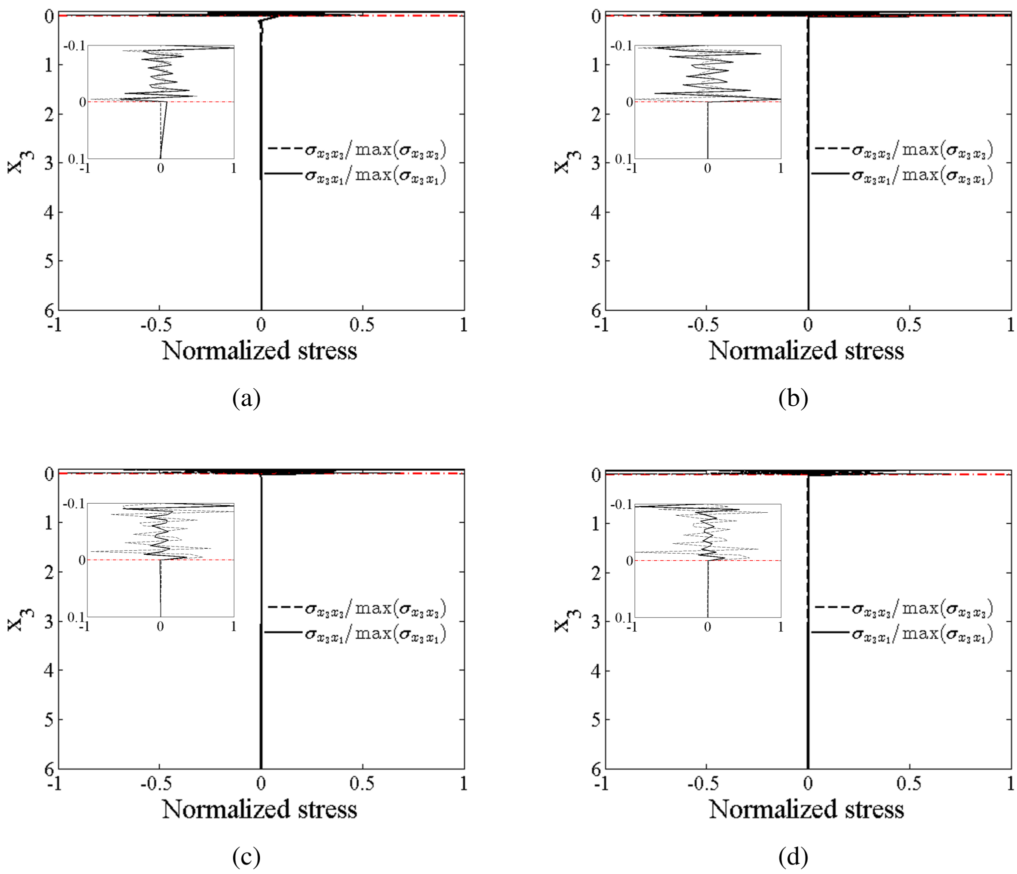

Fig. 4.11 First four stress distributions of SAWs with free boundary conditions on the bottom surface of the substrate: the stress distribution of (a) the 1st mode; (b) the 2nd mode; (c) the 3rd mode; (d) the 4th mode

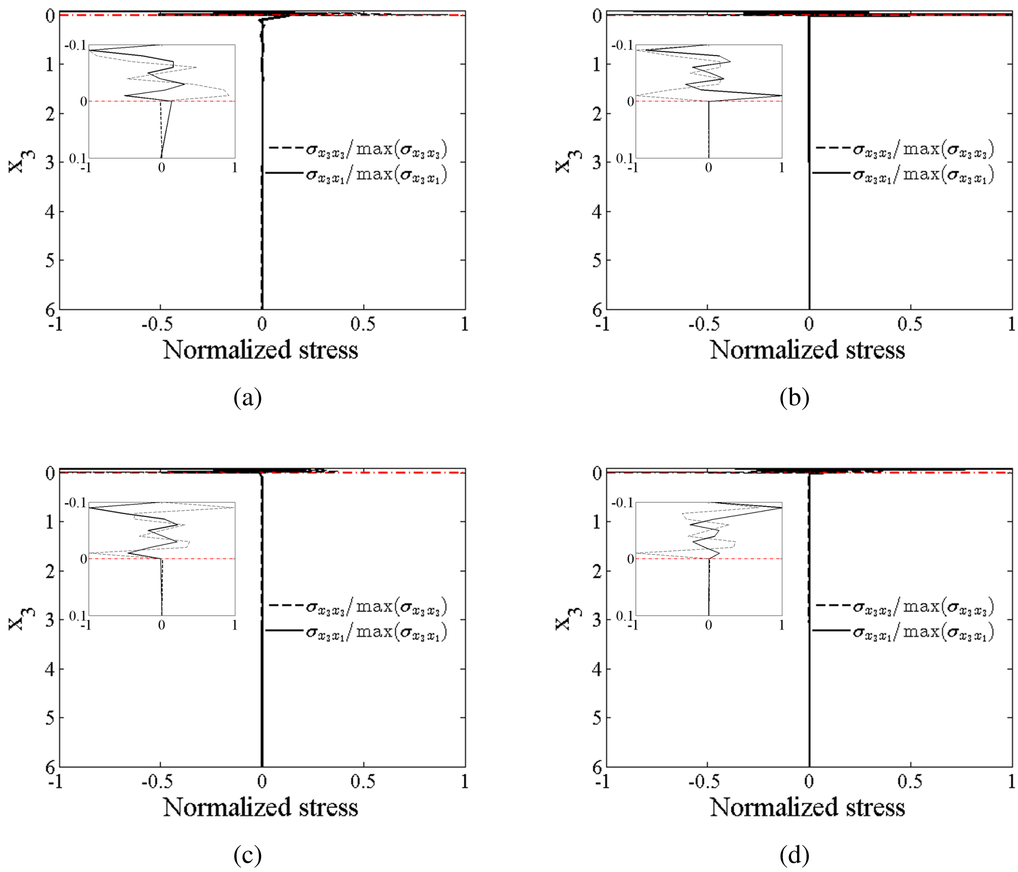

Fig. 4.12 First four stress distributions of SAWs with fixed boundary conditions on the bottom surface of the substrate: the stress distribution of (a) the 1st mode; (b) the 2nd mode; (c) the 3rd mode; (d) the 4th mode

4.5 Appendix

When the bottom surface of the substrate is free, $f^{(r)}(x_3) = 1$, and $r = 1,2,3,4$, if only the displacement continuity between the parts is considered, i.e., substituting the displacement functions Eqs. 4.1 to 4.4 into 4.5a, yields:

$$
\begin{aligned}
A_{11}^{(1)} &= -A_{12}^{(1)} - A_{13}^{(1)} - \ldots - A_{1n}^{(1)} - A_{11}^{(2)} - A_{12}^{(2)} - \ldots - A_{1n}^{(2)} \\
B_{11}^{(1)} &= -B_{12}^{(1)} - B_{13}^{(1)} - \ldots - B_{1n}^{(1)} + B_{11}^{(2)} + B_{12}^{(2)} + \ldots + B_{1n}^{(2)} \\
A_{31}^{(1)} &= -A_{32}^{(1)} - A_{33}^{(1)} - \ldots - A_{3n}^{(1)} - A_{31}^{(2)} - A_{32}^{(2)} - \ldots - A_{3n}^{(2)} \\
B_{31}^{(1)} &= -B_{32}^{(1)} - B_{33}^{(1)} - \ldots - B_{3n}^{(1)} + B_{31}^{(2)} + B_{32}^{(2)} + \ldots + B_{3n}^{(2)} \\
A_{11}^{(3)} &= -A_{12}^{(3)} - A_{13}^{(3)} - \ldots - A_{1n}^{(3)} + A_{11}^{(2)} - A_{12}^{(2)} + \ldots + (-1)^{n-1} A_{1n}^{(2)} \\
B_{11}^{(3)} &= -B_{12}^{(3)} - B_{13}^{(3)} - \ldots - B_{1n}^{(3)} + B_{11}^{(2)} - B_{12}^{(2)} + \ldots + (-1)^{n-1} B_{1n}^{(2)} \\
A_{31}^{(3)} &= -A_{32}^{(3)} - A_{33}^{(3)} - \ldots - A_{3n}^{(3)} + A_{31}^{(2)} - A_{32}^{(2)} + \ldots + (-1)^{n-1} A_{3n}^{(2)} \\
B_{31}^{(3)} &= -B_{32}^{(3)} - B_{33}^{(3)} - \ldots - B_{3n}^{(3)} + B_{31}^{(2)} - B_{32}^{(2)} + \ldots + (-1)^{n-1} B_{3n}^{(2)} \\
A_{11}^{(4)} &= -A_{12}^{(4)} - A_{13}^{(4)} - \ldots - A_{1n}^{(4)} - A_{11}^{(2)} - A_{12}^{(2)} - \ldots - A_{1n}^{(2)} \\
B_{11}^{(4)} &= -B_{12}^{(4)} - B_{13}^{(4)} - \ldots - B_{1n}^{(4)} + B_{11}^{(2)} + B_{12}^{(2)} + \ldots + B_{1n}^{(2)} \\
A_{31}^{(4)} &= -A_{32}^{(4)} - A_{33}^{(4)} - \ldots - A_{3n}^{(4)} - A_{31}^{(2)} - A_{32}^{(2)} - \ldots - A_{3n}^{(2)} \\
B_{31}^{(4)} &= -B_{32}^{(4)} - B_{33}^{(4)} - \ldots - B_{3n}^{(4)} + B_{31}^{(2)} + B_{32}^{(2)} + \ldots + B_{3n}^{(2)}
\end{aligned}
\tag{4.14}
$$

On the basis of the displacement continuum, if only Eq. 4.6 is considered, i.e:

$$
\begin{cases}
c_{33}\dfrac{\partial u_3^{(2)}}{\partial x_3} + c_{31}\dfrac{\partial u_1^{(2)}}{\partial x_1} = \bar{c}_{33}\dfrac{\partial u_3^{(3)}}{\partial x_3} + \bar{c}_{31}\dfrac{\partial u_1^{(3)}}{\partial x_1} \\
c_{55}\left(\dfrac{\partial u_3^{(2)}}{\partial x_1} + \dfrac{\partial u_1^{(2)}}{\partial x_3}\right) = \bar{c}_{55}\left(\dfrac{\partial u_3^{(3)}}{\partial x_1} + \dfrac{\partial u_1^{(3)}}{\partial x_3}\right)
\end{cases}
\tag{4.15}
$$

Substituting the displacement function into Eq. 4.15 to obtain:

$$
\begin{aligned}
A_{11}^{(1)} &= -A_{12}^{(1)} - A_{13}^{(1)} - \ldots - A_{1n}^{(1)} - A_{11}^{(2)} - A_{12}^{(2)} - \ldots - A_{1n}^{(2)} \\
B_{11}^{(1)} &= -B_{12}^{(1)} - B_{13}^{(1)} - \ldots - B_{1n}^{(1)} + B_{11}^{(2)} + B_{12}^{(2)} + \ldots + B_{1n}^{(2)}
\end{aligned}
$$

$$
\begin{aligned}
A_{31}^{(1)} &= -A_{32}^{(1)} - A_{33}^{(1)} - \ldots - A_{3n}^{(1)} - A_{31}^{(2)} - A_{32}^{(2)} - \ldots - A_{3n}^{(2)} \\
B_{31}^{(1)} &= -B_{32}^{(1)} - B_{33}^{(1)} - \ldots - B_{3n}^{(1)} + B_{31}^{(2)} + B_{32}^{(2)} + \ldots + B_{3n}^{(2)} \\
A_{11}^{(3)} &= \left\{ A_{11}^{(2)} - 2A_{13}^{(2)} + 5A_{15}^{(2)} + \ldots + (-1)^n \left[\frac{n(n-1)}{2} - 1 \right] A_{1n}^{(2)} \right\} \\
&\quad - \left\{ \left(1 + \frac{\bar{c}_{55} h}{c_{55} \bar{h}} \right) A_{12}^{(3)} + \left(1 + 3 \frac{\bar{c}_{55} h}{c_{55} \bar{h}} \right) A_{13}^{(3)} + \ldots + \left[1 + \frac{n(n-1)}{2} \right] \frac{\bar{c}_{55} h}{c_{55} \bar{h}} A_{1n}^{(3)} \right\} \\
&\quad + hk \left(1 - \frac{\bar{c}_{55}}{c_{55}} \right) \left(B_{21}^{(3)} + B_{22}^{(3)} + \ldots + B_{2n}^{(3)} \right) \\
A_{12}^{(3)} &= \frac{c_{55} \bar{h}}{\bar{c}_{55} h} \left[A_{12}^{(2)} - 3A_{13}^{(2)} - 6A_{15}^{(2)} + \ldots + (-1)^{n-1} \frac{n(n-1)}{2} A_{1n}^{(2)} \right] \\
&\quad + \left[A_{12}^{(3)} + 3A_{13}^{(3)} + \ldots + \frac{n(n-1)}{2} A_{1n}^{(3)} \right] \\
&\quad + hk \left(1 - \frac{\bar{c}_{55}}{c_{55}} \right) \left(B_{31}^{(3)} + B_{32}^{(3)} + \ldots + B_{3n}^{(3)} \right) \\
B_{11}^{(3)} &= \left\{ B_{11}^{(2)} - 2B_{13}^{(2)} + 5B_{15}^{(2)} + \ldots + (-1)^n \left[\frac{n(n-1)}{2} - 1 \right] B_{1n}^{(2)} \right\} \\
&\quad - \left\{ \left(1 + \frac{\bar{c}_{55} h}{c_{55} \bar{h}} \right) B_{12}^{(3)} + \left(1 + 3 \frac{\bar{c}_{55} h}{c_{55} \bar{h}} \right) B_{13}^{(3)} + \ldots + \left[1 + \frac{n(n-1)}{2} \right] \frac{\bar{c}_{55} h}{c_{55} \bar{h}} B_{1n}^{(3)} \right\} \\
&\quad + hk \left(1 - \frac{\bar{c}_{55}}{c_{55}} \right) \left(A_{31}^{(3)} + A_{32}^{(3)} + \ldots + A_{3n}^{(3)} \right) \\
B_{12}^{(3)} &= \frac{c_{55} \bar{h}}{\bar{c}_{55} h} \left[B_{12}^{(2)} - 3B_{13}^{(2)} - 6B_{15}^{(2)} + \ldots + (-1)^{n-1} \frac{n(n-1)}{2} B_{1n}^{(2)} \right] \\
&\quad + \left[B_{12}^{(3)} + 3B_{13}^{(3)} + \ldots + \frac{n(n-1)}{2} B_{1n}^{(3)} \right] \\
&\quad - \bar{h}k \left(\frac{c_{55}}{\bar{c}_{55}} - 1 \right) \left(A_{31}^{(3)} + A_{32}^{(3)} + \ldots + A_{3n}^{(3)} \right) \\
A_{31}^{(3)} &= \left\{ A_{31}^{(2)} - 2A_{33}^{(2)} + 5A_{35}^{(2)} + \ldots + (-1)^n \left[\frac{n(n-1)}{2} - 1 \right] A_{3n}^{(2)} \right\}
\end{aligned}
\tag{4.16}
$$

$$
\begin{aligned}
&- \left\{ \left(1+\frac{\bar{c}_{33}h}{c_{33}\bar{h}}\right) A_{32}^{(3)} + \left(1+3\frac{\bar{c}_{33}h}{c_{33}\bar{h}}\right) A_{33}^{(3)} + \ldots + \left[1+\frac{n\,(n-1)}{2}\frac{\bar{c}_{33}h}{c_{33}\bar{h}}\right] A_{3n}^{(3)} \right\} \\
&+ hk \left(1-\frac{\bar{c}_{33}}{c_{33}}\right) \left(B_{11}^{(3)} + B_{12}^{(3)} + \ldots + B_{1n}^{(3)}\right) \\
A_{32}^{(3)} &= \frac{c_{33}\bar{h}}{\bar{c}_{33}h} \left[A_{32}^{(2)} - 3A_{33}^{(2)} - 6A_{35}^{(2)} + \ldots + (-1)^{n-1}\,\frac{n\,(n-1)}{2} A_{3n}^{(2)}\right] \\
&+ \left[A_{32}^{(3)} + 3A_{33}^{(3)} + \ldots + \frac{n\,(n-1)}{2} A_{3n}^{(3)}\right] \\
&- \bar{h}k \left(\frac{c_{33}}{\bar{c}_{33}} - 1\right) \left(B_{11}^{(3)} + B_{12}^{(3)} + \ldots + B_{1n}^{(3)}\right) \\
B_{31}^{(3)} &= \left\{ B_{31}^{(2)} - 2B_{33}^{(2)} + 5B_{35}^{(2)} + \ldots + (-1)^{n} \left[\frac{n\,(n-1)}{2} - 1\right] B_{3n}^{(2)} \right\} \\
&+ \left[B_{32}^{(3)} + 3B_{33}^{(3)} + \ldots + \frac{n\,(n-1)}{2} B_{3n}^{(3)}\right] \\
&+ hk \left(1-\frac{\bar{c}_{33}}{c_{33}}\right) \left(A_{11}^{(3)} + A_{12}^{(3)} + \ldots + A_{1n}^{(3)}\right) \\
B_{32}^{(3)} &= \frac{c_{33}\bar{h}}{\bar{c}_{33}h} \left[B_{32}^{(2)} - 3B_{33}^{(2)} - 6B_{35}^{(2)} + \ldots + (-1)^{n-1}\,\frac{n\,(n-1)}{2} B_{3n}^{(2)}\right] \\
&+ \left[B_{32}^{(3)} + 3B_{33}^{(3)} + \ldots + \frac{n\,(n-1)}{2} B_{3n}^{(3)}\right] \\
&- \bar{h}k \left(\frac{c_{33}}{\bar{c}_{33}} - 1\right) \left(A_{11}^{(3)} + A_{12}^{(3)} + \ldots + A_{1n}^{(3)}\right) \\
A_{11}^{(4)} &= -A_{12}^{(4)} - A_{13}^{(4)} - \ldots - A_{1n}^{(4)} - A_{11}^{(2)} - A_{12}^{(2)} - \ldots - A_{1n}^{(2)} \\
B_{11}^{(4)} &= -B_{12}^{(4)} - B_{13}^{(4)} - \ldots - B_{1n}^{(4)} + B_{11}^{(2)} + B_{12}^{(2)} + \ldots + B_{1n}^{(2)} \\
A_{31}^{(4)} &= -A_{32}^{(4)} - A_{33}^{(4)} - \ldots - A_{3n}^{(4)} - A_{31}^{(2)} - A_{32}^{(2)} - \ldots - A_{3n}^{(2)} \\
B_{31}^{(4)} &= -B_{32}^{(4)} - B_{33}^{(4)} - \ldots - B_{3n}^{(4)} + B_{31}^{(2)} + B_{32}^{(2)} + \ldots + B_{3n}^{(2)}
\end{aligned}
\qquad (4.16)
$$

When only Eq. 4.7a is considered, that is:

$$\begin{cases} \bar{c}_{13}\frac{\partial u_3^{(3)}}{\partial x_3}+\bar{c}_{11}\frac{\partial u_1^{(3)}}{\partial x_1}=0 \\ \bar{c}_{55}\left(\frac{\partial u_3^{(3)}}{\partial x_1}+\frac{\partial u_1^{(3)}}{\partial x_3}\right)=0 \end{cases}, z\in\left[-\bar{h},0\right] \tag{4.17}$$

Substituting the displacement functions Eqs. 4.1 to 4.4 and Eq. 4.14 into 4.17, obtain:

$$\begin{aligned}
A_{11}^{(1)} &= -A_{12}^{(1)}-A_{13}^{(1)}-\ldots-A_{1n}^{(1)}-A_{11}^{(2)}-A_{12}^{(2)}-\ldots-A_{1n}^{(2)} \\
B_{11}^{(1)} &= -B_{12}^{(1)}-B_{13}^{(1)}-\ldots-B_{1n}^{(1)}+B_{11}^{(2)}+B_{12}^{(2)}+\ldots+B_{1n}^{(2)} \\
A_{31}^{(1)} &= -A_{32}^{(1)}-A_{33}^{(1)}-\ldots-A_{3n}^{(1)}-A_{31}^{(2)}-A_{32}^{(2)}-\ldots-A_{3n}^{(2)} \\
B_{31}^{(1)} &= -B_{32}^{(1)}-B_{33}^{(1)}-\ldots-B_{3n}^{(1)}+B_{31}^{(2)}+B_{32}^{(2)}+\ldots+B_{3n}^{(2)} \\
A_{11}^{(3)} &= \frac{2a_1^2\bar{c}_{13}}{2a_1^2\bar{c}_{13}+\bar{c}_{11}\bar{h}^2k^2}\left[A_{11}^{(2)}-A_{12}^{(2)}+\ldots+(-1)^{n-1}A_{1n}^{(2)}\right] \\
&\quad -\frac{a_1\bar{c}_{13}\bar{h}k}{2a_1^2\bar{c}_{13}+\bar{c}_{11}\bar{h}^2k^2}\left[B_{31}^{(2)}-B_{32}^{(2)}+\ldots+(-1)^{n-1}B_{3n}^{(2)}\right] \\
&\quad -\frac{2a_1^2\bar{c}_{13}}{2a_1^2\bar{c}_{13}+\bar{c}_{11}\bar{h}^2k^2}\left\{4A_{13}^{(3)}-5A_{14}^{(3)}+\ldots+\left[\frac{(-1)^{n-1}n(n-1)}{2}+1\right]A_{1n}^{(3)}\right\} \\
A_{12}^{(3)} &= \frac{\bar{c}_{11}\bar{h}^2k^2}{2a_1^2\bar{c}_{13}+\bar{c}_{11}\bar{h}^2k^2}\left[A_{11}^{(2)}-A_{12}^{(2)}+\ldots+(-1)^{n-1}A_{1n}^{(2)}\right] \\
&\quad +\frac{a_1\bar{c}_{13}\bar{h}k}{2a_1^2\bar{c}_{13}+\bar{c}_{11}\bar{h}^2k^2}\left[B_{31}^{(2)}-B_{32}^{(2)}+\ldots+(-1)^{n-1}B_{3n}^{(2)}\right] \\
&\quad +\frac{2a_1^2\bar{c}_{13}}{2a_1^2\bar{c}_{13}+\bar{c}_{11}\bar{h}^2k^2}\left[3A_{13}^{(3)}-6A_{14}^{(3)}+\ldots+\frac{(-1)^{n-1}n(n-1)}{2}A_{1n}^{(3)}\right] \\
&\quad -\frac{\bar{c}_{11}\bar{h}^2k^2}{2a_1^2\bar{c}_{13}+\bar{c}_{11}\bar{h}^2k^2}\left[A_{13}^{(3)}+A_{14}^{(3)}+\ldots+A_{1n}^{(3)}\right] \\
B_{11}^{(3)} &= \frac{2\left(3a_1^2\bar{c}_{33}+\bar{c}_{31}\bar{h}^2k^2\right)}{3\left(2a_1^2\bar{c}_{33}+\bar{c}_{31}\bar{h}^2k^2\right)}\left[B_{11}^{(2)}-B_{12}^{(2)}+\ldots+(-1)^{n-1}B_{1n}^{(2)}\right] \\
&\quad +\frac{\bar{h}k\left(6a_1^2\bar{c}_{33}+\bar{c}_{31}\bar{h}^2k^2\right)}{6a_1\left(2a_1^2\bar{c}_{33}+\bar{c}_{31}\bar{h}^2k^2\right)}\left[A_{31}^{(2)}-A_{32}^{(2)}+\ldots+(-1)^{n-1}A_{3n}^{(2)}\right]
\end{aligned} \tag{4.18}$$

$$
\begin{aligned}
& -\frac{1}{3}\left\{5B_{14}^{(3)}+14B_{16}^{(3)}+\ldots+\left[\frac{n(n-1)}{2}-1\right]B_{1n}^{(3)}\right\} \\
& +\frac{1}{3}\left\{7B_{15}^{(3)}+18B_{17}^{(3)}+\ldots+\left[\frac{n(n-1)}{2}-3\right]B_{1n}^{(3)}\right\} \\
& -\frac{2a_1^2\bar{c}_{33}\bar{h}k}{3a_1\left(2a_1^2\bar{c}_{33}+\bar{c}_{31}\bar{h}^2k^2\right)}\left\{5A_{33}^{(3)}+12A_{35}^{(3)}+\ldots+\left[\frac{n(n-1)}{2}+2\right]A_{3n}^{(3)}\right\} \\
& +\frac{2a_1^2\bar{c}_{33}\bar{h}k}{3a_1\left(2a_1^2\bar{c}_{33}+\bar{c}_{31}\bar{h}^2k^2\right)}\left\{5A_{34}^{(3)}+14A_{36}^{(3)}+\ldots+\left[\frac{n(n-1)}{2}-1\right]A_{3n}^{(3)}\right\} \\
& -\frac{\bar{c}_{31}\bar{h}^3k^3}{3a_1\left(2a_1^2\bar{c}_{33}+\bar{c}_{31}\bar{h}^2k^2\right)}\left(A_{33}^{(3)}+A_{35}^{(3)}+\ldots+A_{3n}^{(3)}\right) \\
B_{13}^{(3)} = & -\frac{\bar{c}_{31}\bar{h}^2k^2}{6\left(2a_1^2\bar{c}_{33}+\bar{c}_{31}\bar{h}^2k^2\right)}\left[B_{11}^{(2)}-B_{12}^{(2)}+\ldots+(-1)^{n-1}B_{1n}^{(2)}\right] \\
& -\frac{\bar{c}_{31}\bar{h}^3k^3}{6a_1\left(2a_1^2\bar{c}_{33}+\bar{c}_{31}\bar{h}^2k^2\right)}\left[A_{31}^{(2)}-A_{32}^{(2)}+\ldots+(-1)^{n-1}A_{3n}^{(2)}\right] \\
& +\frac{1}{3}\left\{5B_{14}^{(3)}+14B_{16}^{(3)}+\ldots+\left[\frac{n(n-1)}{2}-1\right]B_{1n}^{(3)}\right\} \\
& -\frac{1}{3}\left[10B_{15}^{(3)}+21B_{17}^{(3)}+\ldots+\frac{n(n-1)}{2}B_{1n}^{(3)}\right] \\
& -\frac{a_1\bar{c}_{33}\bar{h}k}{3\left(2a_1^2\bar{c}_{33}+\bar{c}_{31}\bar{h}^2k^2\right)}\left\{2A_{33}^{(3)}-5A_{34}^{(3)}+\ldots+(-1)^{n-1}\left[\frac{n(n-1)}{2}-1\right]A_{3n}^{(3)}\right\} \\
& +\frac{\bar{c}_{31}\bar{h}^3k^3}{3a_1\left(2a_1^2\bar{c}_{33}+\bar{c}_{31}\bar{h}^2k^2\right)}\left(A_{33}^{(3)}+A_{35}^{(3)}+\ldots+A_{3n}^{(3)}\right) \\
A_{31}^{(3)} = & -\frac{a_1\bar{c}_{31}\bar{h}k}{\left(2a_1^2\bar{c}_{33}+\bar{c}_{31}\bar{h}^2k^2\right)}\left[B_{11}^{(2)}-B_{12}^{(2)}+\ldots+(-1)^{n-1}B_{1n}^{(2)}\right] \\
& +\frac{2a_1^2\bar{c}_{33}}{\left(2a_1^2\bar{c}_{33}+\bar{c}_{31}\bar{h}^2k^2\right)}\left[A_{31}^{(2)}-A_{32}^{(2)}+\ldots+(-1)^{n-1}A_{3n}^{(2)}\right] \\
& -\frac{2a_1^2\bar{c}_{33}}{\left(2a_1^2\bar{c}_{33}+\bar{c}_{31}\bar{h}^2k^2\right)}\left\{4A_{33}^{(3)}-5A_{34}^{(3)}+\ldots+\left[(-1)^{n-1}\frac{n(n-1)}{2}+1\right]A_{3n}^{(3)}\right\}
\end{aligned}
\tag{4.18}
$$

$$
\begin{aligned}
A_{32}^{(3)} = & \frac{a_1 \bar{c}_{31} \bar{h} k}{\left(2a_1^2 \bar{c}_{33} + \bar{c}_{31} \bar{h}^2 k^2\right)} \left[B_{11}^{(2)} - B_{12}^{(2)} + \ldots + (-1)^{n-1} B_{1n}^{(2)}\right] \\
& + \frac{\bar{c}_{31} \bar{h}^2 k^2}{\left(2a_1^2 \bar{c}_{33} + \bar{c}_{31} \bar{h}^2 k^2\right)} \left[A_{31}^{(2)} - A_{32}^{(2)} + \ldots + (-1)^{n-1} A_{3n}^{(2)}\right] \\
& + \frac{2a_1^2 \bar{c}_{33}}{\left(2a_1^2 \bar{c}_{33} + \bar{c}_{31} \bar{h}^2 k^2\right)} \left[3A_{33}^{(3)} - 6A_{34}^{(3)} + \ldots + (-1)^{n-1} \frac{n(n-1)}{2} A_{3n}^{(3)}\right] \\
& - \frac{\bar{c}_{31} \bar{h}^2 k^2}{\left(2a_1^2 \bar{c}_{33} + \bar{c}_{31} \bar{h}^2 k^2\right)} \left(A_{33}^{(3)} + A_{34}^{(3)} + \ldots + A_{3n}^{(3)}\right) \\
& - \frac{4a_1 \bar{c}_{11} \bar{h} k}{3\left(2a_1^2 \bar{c}_{13} + \bar{c}_{11} \bar{h}^2 k^2\right)} \left\{4A_{13}^{(3)} - 5A_{14}^{(3)} + \ldots + \left[(-1)^{n-1} \frac{n(n-1)}{2} + 1\right] A_{1n}^{(3)}\right\} \\
& + \frac{2a_1 \bar{c}_{13} \bar{c}_{31} \bar{h} k}{3\bar{c}_{33}\left(2a_1^2 \bar{c}_{13} + \bar{c}_{11} \bar{h}^2 k^2\right)} \left[3A_{13}^{(3)} + 10A_{15}^{(3)} + \ldots + \frac{n(n-1)}{2} A_{1n}^{(3)}\right] \\
& - \frac{2a_1 \bar{c}_{13} \bar{c}_{31} \bar{h} k}{3\bar{c}_{33}\left(2a_1^2 \bar{c}_{13} + \bar{c}_{11} \bar{h}^2 k^2\right)} \left\{5A_{14}^{(3)} + 14A_{16}^{(3)} + \ldots + \left[\frac{n(n-1)}{2} - 1\right] A_{1n}^{(3)}\right\} \\
& - \frac{\bar{c}_{11} \bar{c}_{31} \bar{h}^3 k^3}{3a_1 \bar{c}_{33}\left(2a_1^2 \bar{c}_{13} + \bar{c}_{11} \bar{h}^2 k^2\right)} \left(A_{13}^{(3)} + A_{15}^{(3)} + \ldots + A_{1n}^{(3)}\right) \\
& - \frac{1}{3} \left\{5B_{34}^{(3)} + 14B_{36}^{(3)} + \ldots + \left[(-1)^{n-1} \frac{n(n-1)}{2} - 1\right] B_{3n}^{(3)}\right\} \\
& + \frac{1}{3} \left\{7B_{35}^{(3)} + 18B_{37}^{(3)} + \ldots + \left[(-1)^{n-1} \frac{n(n-1)}{2} - 3\right] B_{3n}^{(3)}\right\}
\end{aligned} \tag{4.18}
$$

$$
\begin{aligned}
B_{32}^{(3)} = & -\frac{a_1 \bar{c}_{11} \bar{h} k}{\left(2a_1^2 \bar{c}_{13} + \bar{c}_{11} \bar{h}^2 k^2\right)} \left[A_{11}^{(2)} - A_{12}^{(2)} + \ldots + (-1)^{n-1} A_{1n}^{(2)}\right] \\
& + \frac{\bar{c}_{11} \bar{h}^2 k^2}{2\left(2a_1^2 \bar{c}_{13} + \bar{c}_{11} \bar{h}^2 k^2\right)} \left[B_{31}^{(2)} - B_{32}^{(2)} + \ldots + (-1)^{n-1} B_{3n}^{(2)}\right] \\
& + \frac{a_1 \bar{c}_{11} \bar{h} k}{2a_1^2 \bar{c}_{13} + \bar{c}_{11} \bar{h}^2 k^2} \left[3A_{13}^{(3)} - 6A_{14}^{(3)} + 10A_{15}^{(3)} + \ldots + (-1)^{n-1} \frac{n(n-1)}{2} A_{1n}^{(3)}\right] \\
& + \frac{a_1 \bar{c}_{11} \bar{h} k}{\left(2a_1^2 \bar{c}_{13} + \bar{c}_{11} \bar{h}^2 k^2\right)} \left(A_{13}^{(3)} + A_{14}^{(3)} + \ldots + A_{1n}^{(3)}\right) - B_{34}^{(3)} - B_{36}^{(3)} - \ldots - B_{3n}^{(3)}
\end{aligned}
$$

$$
B_{33}^{(3)} = -\frac{\bar{h} k \left[a_1^2 \left(2\bar{c}_{11} \bar{c}_{33} - 2\bar{c}_{13} \bar{c}_{31}\right) + \bar{c}_{11} \bar{c}_{31} \bar{h}^2 k^2\right]}{6a_1 \bar{c}_{33}\left(2a_1^2 \bar{c}_{13} + \bar{c}_{11} \bar{h}^2 k^2\right)}
$$

$$\left[A_{11}^{(2)}-A_{12}^{(2)}+\ldots+(-1)^{n-1}A_{1n}^{(2)}\right]$$

$$+\frac{(\bar{c}_{11}\bar{c}_{33}-2\bar{c}_{13}\bar{c}_{31})\bar{h}^2k^2}{6\bar{c}_{33}\left(2a_1^2\bar{c}_{13}+\bar{c}_{11}\bar{h}^2k^2\right)}\left[B_{31}^{(2)}-B_{32}^{(2)}+\ldots+(-1)^{n-1}B_{3n}^{(2)}\right]$$

$$+\frac{a_1\bar{c}_{11}\bar{h}k}{3\left(2a_1^2\bar{c}_{13}+\bar{c}_{11}\bar{h}^2k^2\right)}\left\{4A_{13}^{(3)}-5A_{14}^{(3)}+\ldots+\left[(-1)^{n-1}\frac{n(n-1)}{2}+1\right]A_{1n}^{(3)}\right\}$$

$$-\frac{2a_1\bar{c}_{13}\bar{c}_{31}\bar{h}k}{3\bar{c}_{33}\left(2a_1^2\bar{c}_{13}+\bar{c}_{11}\bar{h}^2k^2\right)}\left[3A_{13}^{(3)}+10A_{15}^{(3)}+\ldots+\frac{n(n-1)}{2}A_{1n}^{(3)}\right]$$

$$+\frac{2a_1\bar{c}_{13}\bar{c}_{31}\bar{h}k}{3\bar{c}_{33}\left(2a_1^2\bar{c}_{13}+\bar{c}_{11}\bar{h}^2k^2\right)}\left\{5A_{14}^{(3)}+14A_{16}^{(3)}+\ldots+\left[\frac{n(n-1)}{2}-1\right]A_{1n}^{(3)}\right\}$$

$$B_{31}^{(3)}=-\frac{\bar{h}k\left[a_1^2(8\bar{c}_{11}\bar{c}_{33}-2\bar{c}_{13}\bar{c}_{31})+\bar{c}_{11}\bar{c}_{31}\bar{h}^2k^2\right]}{6a_1\bar{c}_{33}\left(2a_1^2\bar{c}_{13}+\bar{c}_{11}\bar{h}^2k^2\right)}$$

$$\left[A_{11}^{(2)}-A_{12}^{(2)}+\ldots+(-1)^{n-1}A_{1n}^{(2)}\right]$$

$$+\frac{6a_1^2\bar{c}_{13}\bar{c}_{33}+(\bar{c}_{13}\bar{c}_{31}+\bar{c}_{11}\bar{c}_{33})\bar{h}^2k^2}{3\bar{c}_{33}\left(2a_1^2\bar{c}_{13}+\bar{c}_{11}\bar{h}^2k^2\right)}\left[B_{31}^{(2)}-B_{32}^{(2)}+\ldots+(-1)^{n-1}B_{3n}^{(2)}\right]$$

$$+\frac{\bar{c}_{11}\bar{c}_{31}\bar{h}^3k^3}{3a_1\bar{c}_{33}\left(2a_1^2\bar{c}_{13}+\bar{c}_{11}\bar{h}^2k^2\right)}\left(A_{13}^{(3)}+A_{15}^{(3)}+\ldots+A_{1n}^{(3)}\right)$$

$$+\frac{1}{3}\left\{5B_{34}^{(3)}+14B_{36}^{(3)}+\ldots+\left[(-1)^{n-1}\frac{n(n-1)}{2}-1\right]B_{3n}^{(3)}\right\}$$

$$-\frac{1}{3}\left\{10B_{35}^{(3)}+21B_{37}^{(3)}+\ldots+\left[(-1)^{n-1}\frac{n(n-1)}{2}\right]B_{3n}^{(3)}\right\}$$

$$A_{11}^{(4)}=-A_{12}^{(4)}-A_{13}^{(4)}-\ldots-A_{1n}^{(4)}-A_{11}^{(2)}-A_{12}^{(2)}-\ldots-A_{1n}^{(2)}$$

$$B_{11}^{(4)}=-B_{12}^{(4)}-B_{13}^{(4)}-\ldots-B_{1n}^{(4)}+B_{11}^{(2)}+B_{12}^{(2)}+\ldots+B_{1n}^{(2)}$$

$$A_{31}^{(4)}=-A_{32}^{(4)}-A_{33}^{(4)}-\ldots-A_{3n}^{(4)}-A_{31}^{(2)}-A_{32}^{(2)}-\ldots-A_{3n}^{(2)}$$

$$B_{31}^{(4)}=-B_{32}^{(4)}-B_{33}^{(4)}-\ldots-B_{3n}^{(4)}+B_{31}^{(2)}+B_{32}^{(2)}+\ldots+B_{3n}^{(2)}$$

When considering Eq. 4.7b at the interface displacement and stress continuity, it can be obtained:

$$
\begin{aligned}
A_{11}^{(1)} &= -A_{12}^{(1)} - A_{13}^{(1)} - \ldots - A_{1n}^{(1)} - A_{11}^{(2)} - A_{12}^{(2)} - \ldots - A_{1n}^{(2)} \\
B_{11}^{(1)} &= -B_{12}^{(1)} - B_{13}^{(1)} - \ldots - B_{1n}^{(1)} + B_{11}^{(2)} + B_{12}^{(2)} + \ldots + B_{1n}^{(2)} \\
A_{31}^{(1)} &= -A_{32}^{(1)} - A_{33}^{(1)} - \ldots - A_{3n}^{(1)} - A_{31}^{(2)} - A_{32}^{(2)} - \ldots - A_{3n}^{(2)} \\
B_{31}^{(1)} &= -B_{32}^{(1)} - B_{33}^{(1)} - \ldots - B_{3n}^{(1)} + B_{31}^{(2)} + B_{32}^{(2)} + \ldots + B_{3n}^{(2)} \\
A_{11}^{(3)} &= \frac{6a_1^2\bar{c}_{13}}{6a_1^2\bar{c}_{13} + \bar{c}_{11}\bar{h}^2k^2}\left[A_{11}^{(2)} - A_{12}^{(2)} + \ldots + (-1)^{n-1}A_{1n}^{(2)}\right] \\
&- \frac{4a_1^2\bar{c}_{13}c_{55}\bar{h}}{\bar{c}_{55}h\left(6a_1^2\bar{c}_{13} + \bar{c}_{11}\bar{h}^2k^2\right)}\left[A_{12}^{(2)} - 3A_{13}^{(2)} + \ldots + \frac{(-1)^{n-1}n(n-1)}{2}A_{1n}^{(2)}\right] \\
&- \frac{a_1\bar{c}_{13}\bar{h}k(3\bar{c}_{55} - 2c_{55})}{\bar{c}_{55}\left(6a_1^2\bar{c}_{13} + \bar{c}_{11}\bar{h}^2k^2\right)}\left[B_{31}^{(2)} - B_{32}^{(2)} + \ldots + (-1)^{n-1}B_{3n}^{(2)}\right] \\
&+ \frac{6a_1^2\bar{c}_{13}}{6a_1^2\bar{c}_{13} + \bar{c}_{11}\bar{h}^2k^2}\left\{5A_{14}^{(3)} + 14A_{16}^{(3)} + \ldots + \left[\frac{n(n-1)}{2} - 1\right]A_{1n}^{(3)}\right\} \\
&+ \frac{2a_1^2\bar{c}_{13}}{6a_1^2\bar{c}_{13} + \bar{c}_{11}\bar{h}^2k^2}\left\{7A_{15}^{(3)} + 18A_{17}^{(3)} + \ldots + \left[\frac{n(n-1)}{2} - 3\right]A_{1n}^{(3)}\right\}
\end{aligned} \tag{4.19}
$$

$$
\begin{aligned}
A_{12}^{(3)} &= \frac{3\bar{c}_{11}\bar{h}^2k^2}{2\left(6a_1^2\bar{c}_{13} + \bar{c}_{11}\bar{h}^2k^2\right)}\left[A_{11}^{(2)} - A_{12}^{(2)} + \ldots + (-1)^{n-1}A_{1n}^{(2)}\right] \\
&- \frac{\left(\bar{c}_{11}\bar{h}^2k^2 - 6a_1^2\bar{c}_{13}\right)c_{55}\bar{h}}{2\bar{c}_{55}h\left(6a_1^2\bar{c}_{13} + \bar{c}_{11}\bar{h}^2k^2\right)}\left[A_{12}^{(2)} - 3A_{13}^{(2)} + \ldots + \frac{(-1)^{n-1}n(n-1)}{2}A_{1n}^{(2)}\right] \\
&+ \frac{\left[6a_1^2\bar{c}_{13}(2\bar{c}_{55} - c_{55}) + \bar{c}_{11}(c_{55} - \bar{c}_{55})\bar{h}^2k^2\right]\bar{h}k}{4a_1\bar{c}_{55}\left(6a_1^2\bar{c}_{13} + \bar{c}_{11}\bar{h}^2k^2\right)} \\
&\left[B_{31}^{(2)} - B_{32}^{(2)} + \ldots (-1)^{n-1}B_{3n}^{(2)}\right] \\
&+ \frac{\bar{c}_{11}\bar{h}^2k^2}{2\left(6a_1^2\bar{c}_{13} + \bar{c}_{11}\bar{h}^2k^2\right)}\left\{3A_{14}^{(3)} + 7A_{15}^{(3)} + \ldots + \left[\frac{n(n-1)}{2} - 3\right]A_{1n}^{(3)}\right\} \\
&- \frac{3a_1^2\bar{c}_{13}}{\left(6a_1^2\bar{c}_{13} + \bar{c}_{11}\bar{h}^2k^2\right)}\left[12A_{14}^{(3)} + 30A_{16}^{(3)} + \ldots + n(n-1)A_{1n}^{(3)}\right]
\end{aligned}
$$

$$
A_{13}^{(3)} = -\frac{\bar{c}_{11}\bar{h}^2k^2}{2\left(6a_1^2\bar{c}_{13} + \bar{c}_{11}\bar{h}^2k^2\right)}\left[A_{11}^{(2)} - A_{12}^{(2)} + \ldots + (-1)^{n-1}A_{1n}^{(2)}\right]
$$

$$
\begin{aligned}
& -\frac{\left(2a_1{}^2\bar{c}_{13}+\bar{c}_{11}\bar{h}^2k^2\right)c_{55}\bar{h}}{2\bar{c}_{55}h\left(6a_1^2\bar{c}_{13}+\bar{c}_{11}\bar{h}^2k^2\right)}\left[A_{12}^{(2)}-3A_{13}^{(2)}+\ldots+\frac{(-1)^{n-1}n(n-1)}{2}A_{1n}^{(2)}\right] \\
& -\frac{\left[2a_1^2\bar{c}_{13}c_{55}+\bar{c}_{11}\left(c_{55}-\bar{c}_{55}\right)\bar{h}^2k^2\right]\bar{h}k}{4a_1\bar{c}_{55}\left(6a_1^2\bar{c}_{13}+\bar{c}_{11}\bar{h}^2k^2\right)}\left[B_{31}^{(2)}-B_{32}^{(2)}+\ldots+(-1)^{n-1}B_{3n}^{(2)}\right] \\
& -\frac{2a_1^2\bar{c}_{13}}{\left(6a_1^2\bar{c}_{13}+\bar{c}_{11}\bar{h}^2k^2\right)}\left[10A_{15}^{(3)}+15A_{17}^{(3)}+\ldots+\frac{n(n-1)}{2}A_{1n}^{(3)}\right] \\
& -\frac{\bar{c}_{11}\bar{h}^2k^2}{2\left(6a_1^2\bar{c}_{13}+\bar{c}_{11}\bar{h}^2k^2\right)}\left\{5A_{14}^{(3)}+9A_{15}^{(3)}+\ldots+\left[\frac{n(n-1)}{2}-1\right]A_{1n}^{(3)}\right\}
\end{aligned}
$$

$$
\begin{aligned}
B_{11}^{(3)} = & \frac{144a_1^4\bar{c}_{33}^2+18a_1^2\bar{c}_{33}c_{31}\bar{h}^2k^2+\bar{c}_{31}\left(c_{31}-\bar{c}_{31}\right)\bar{h}^4k^4}{24a_1^2\bar{c}_{33}\left(6a_1^2\bar{c}_{33}+\bar{c}_{31}\bar{h}^2k^2\right)} \\
& \left[B_{11}^{(2)}-B_{12}^{(2)}+\ldots+(-1)^{n-1}B_{1n}^{(2)}\right] \\
& +\frac{c_{55}\bar{h}}{6\bar{c}_{55}h}\left[B_{12}^{(2)}-3B_{13}^{(2)}+\ldots+\frac{(-1)^{n-1}n(n-1)}{2}B_{1n}^{(2)}\right] \\
& +\frac{\bar{h}k\left[6a_1^2\bar{c}_{33}\left(6\bar{c}_{55}-c_{55}\right)+\bar{c}_{31}\left(3\bar{c}_{55}-c_{55}\right)\bar{h}^2k^2\right]}{12a_1\bar{c}_{55}\left(6a_1^2\bar{c}_{33}+\bar{c}_{31}\bar{h}^2k^2\right)} \\
& \left[A_{31}^{(2)}-A_{32}^{(2)}+\ldots+(-1)^{n-1}A_{3n}^{(2)}\right] \\
& -\frac{c_{33}\bar{h}^2k\left(18a_1^2\bar{c}_{33}+\bar{c}_{31}\bar{h}^2k^2\right)}{12a_1\bar{c}_{33}h\left(6a_1^2\bar{c}_{33}+\bar{c}_{31}\bar{h}^2k^2\right)}\left[A_{32}^{(2)}-3A_{33}^{(2)}+\ldots+\frac{(-1)^{n-1}n(n-1)}{2}A_{3n}^{(2)}\right] \\
& +\frac{1}{3}\left\{7B_{15}^{(3)}+18B_{17}^{(3)}+\ldots+\left[\frac{n(n-1)}{2}-3\right]B_{1n}^{(3)}\right\} \\
& +\frac{24a_1^2\bar{c}_{33}\bar{h}k+\bar{c}_{31}\bar{h}^3k^3}{12a_1\left(6a_1^2\bar{c}_{33}+\bar{c}_{31}\bar{h}^2k^2\right)}\left\{5A_{34}^{(3)}+14A_{36}^{(3)}+\ldots+\left[\frac{n(n-1)}{2}-1\right]A_{3n}^{(3)}\right\} \\
& +\frac{12a_1^2\bar{c}_{33}\bar{h}k+\bar{c}_{31}\bar{h}^3k^3}{12a_1\left(6a_1^2\bar{c}_{33}+\bar{c}_{31}\bar{h}^2k^2\right)}\left\{7A_{35}^{(3)}+18A_{37}^{(3)}+\ldots+\left[\frac{n(n-1)}{2}-3\right]A_{3n}^{(3)}\right\} \\
B_{12}^{(3)} = & \frac{\bar{h}^2k^2\left[6a_1^2\bar{c}_{33}\left(10\bar{c}_{31}-7c_{31}\right)+\bar{c}_{31}\left(\bar{c}_{31}-c_{31}\right)\bar{h}^2k^2\right]}{40a_1^2\bar{c}_{33}\left(6a_1^2\bar{c}_{33}+\bar{c}_{31}\bar{h}^2k^2\right)}\left[B_{11}^{(2)}-B_{12}^{(2)}+\ldots\right. \\
& \left.+(-1)^{n-1}B_{1n}^{(2)}\right]+\frac{c_{55}\bar{h}}{10\bar{c}_{55}h}\left[B_{12}^{(2)}-3B_{13}^{(2)}+\ldots+\frac{(-1)^{n-1}n(n-1)}{2}B_{1n}^{(2)}\right]
\end{aligned}
\tag{4.19}
$$

$$
\begin{aligned}
&-\frac{\bar{h}k\left[6a_1^2\bar{c}_{33}\left(10\bar{c}_{55}+c_{55}\right)+\bar{c}_{31}\left(\bar{c}_{55}+c_{55}\right)\bar{h}^2k^2\right]}{20a_1\bar{c}_{55}\left(6a_1^2\bar{c}_{33}+\bar{c}_{31}\bar{h}^2k^2\right)}\\
&\left[A_{31}^{(2)}-A_{32}^{(2)}+\ldots+(-1)^{n-1}A_{3n}^{(2)}\right]\\
&+\frac{c_{33}\bar{h}^2k\left(42a_1^2\bar{c}_{33}+\bar{c}_{31}\bar{h}^2k^2\right)}{20a_1\bar{c}_{33}h\left(6a_1^2\bar{c}_{33}+\bar{c}_{31}\bar{h}^2k^2\right)}\left[A_{32}^{(2)}-3A_{33}^{(2)}+\ldots+\frac{(-1)^{n-1}n(n-1)}{2}A_{3n}^{(2)}\right]\\
&+\frac{1}{5}\left\{9B_{16}^{(3)}+22B_{18}^{(3)}+\ldots+\left[\frac{n(n-1)}{2}-6\right]B_{1n}^{(3)}\right\}\\
&-\frac{60a_1^2\bar{c}_{33}\bar{h}k+\bar{c}_{31}\bar{h}^3k^3}{20a_1\left(6a_1^2\bar{c}_{33}+\bar{c}_{31}\bar{h}^2k^2\right)}\left\{5A_{34}^{(3)}+14A_{36}^{(3)}+\ldots+\left[\frac{n(n-1)}{2}-1\right]A_{3n}^{(3)}\right\}\\
&-\frac{24a_1^2\bar{c}_{33}\bar{h}k+\bar{c}_{31}\bar{h}^3k^3}{20a_1\left(6a_1^2\bar{c}_{33}+\bar{c}_{31}\bar{h}^2k^2\right)}\left\{7A_{35}^{(3)}+18A_{37}^{(3)}+\ldots+\left[\frac{n(n-1)}{2}-3\right]A_{3n}^{(3)}\right\}
\end{aligned}
$$

$$
\begin{aligned}
B_{13}^{(3)}=&\frac{\bar{h}^2k^2\left[6a_1^2\bar{c}_{33}\left(c_{31}-2\bar{c}_{31}\right)+\bar{c}_{31}\left(\bar{c}_{31}-c_{31}\right)\bar{h}^2k^2\right]}{24a_1^2\bar{c}_{33}\left(6a_1^2\bar{c}_{33}+\bar{c}_{31}\bar{h}^2k^2\right)}\left[B_{11}^{(2)}-B_{12}^{(2)}+\ldots\right.\\
&\left.+(-1)^{n-1}B_{1n}^{(2)}\right]-\frac{c_{55}\bar{h}}{6\bar{c}_{55}h}\left[B_{12}^{(2)}-3B_{13}^{(2)}+\ldots+\frac{(-1)^{n-1}n(n-1)}{2}B_{1n}^{(2)}\right]\\
&+\frac{\bar{h}k\left[6a_1^2\bar{c}_{33}c_{55}+\bar{c}_{31}\left(c_{55}-3\bar{c}_{55}\right)\bar{h}^2k^2\right]}{12a_1\bar{c}_{55}\left(6a_1^2\bar{c}_{33}+\bar{c}_{31}\bar{h}^2k^2\right)}\left[A_{31}^{(2)}-A_{32}^{(2)}+\ldots+(-1)^{n-1}A_{3n}^{(2)}\right]\\
&-\frac{c_{33}\bar{h}^2k\left(\bar{c}_{31}\bar{h}^2k^2-6a_1^2\bar{c}_{33}\right)}{12a_1\bar{c}_{33}h\left(6a_1^2\bar{c}_{33}+\bar{c}_{31}\bar{h}^2k^2\right)}\left[A_{32}^{(2)}-3A_{33}^{(2)}+\ldots+\frac{(-1)^{n-1}n(n-1)}{2}A_{3n}^{(2)}\right]\\
&-\frac{1}{3}\left[10B_{15}^{(3)}+21B_{17}^{(3)}+\ldots+\frac{n(n-1)}{2}B_{1n}^{(3)}\right]\\
&+\frac{12a_1^2\bar{c}_{33}\bar{h}k-\bar{c}_{31}\bar{h}^3k^3}{12a_1\left(6a_1^2\bar{c}_{33}+\bar{c}_{31}\bar{h}^2k^2\right)}\left\{5A_{34}^{(3)}+14A_{36}^{(3)}+\ldots+\left[\frac{n(n-1)}{2}-1\right]A_{3n}^{(3)}\right\}\\
&-\frac{\bar{c}_{31}\bar{h}^3k^3}{12a_1\left(6a_1^2\bar{c}_{33}+\bar{c}_{31}\bar{h}^2k^2\right)}\left\{7A_{35}^{(3)}+18A_{37}^{(3)}+\ldots+\left[\frac{n(n-1)}{2}-3\right]A_{3n}^{(3)}\right\}
\end{aligned}
\tag{4.19}
$$

$$
\begin{aligned}
B_{14}^{(3)}=&\frac{\bar{h}^2k^2\left[2a_1^2\bar{c}_{33}c_{31}-\bar{c}_{31}\left(\bar{c}_{31}-c_{31}\right)\bar{h}^2k^2\right]}{40a_1^2\bar{c}_{33}\left(6a_1^2\bar{c}_{33}+\bar{c}_{31}\bar{h}^2k^2\right)}\left[B_{11}^{(2)}-B_{12}^{(2)}+\ldots+(-1)^{n-1}B_{1n}^{(2)}\right]\\
&-\frac{c_{55}\bar{h}}{10\bar{c}_{55}h}\left[B_{12}^{(2)}-3B_{13}^{(2)}+\ldots+\frac{(-1)^{n-1}n(n-1)}{2}B_{1n}^{(2)}\right]
\end{aligned}
$$

$$+\frac{\bar{h}k\left[6a_1^2\bar{c}_{33}c_{55}+\bar{c}_{31}\left(\bar{c}_{55}+c_{55}\right)\bar{h}^2k^2\right]}{20a_1\bar{c}_{55}\left(6a_1^2\bar{c}_{33}+\bar{c}_{31}\bar{h}^2k^2\right)}\left[A_{31}^{(2)}-A_{32}^{(2)}+\ldots+(-1)^{n-1}A_{3n}^{(2)}\right]$$

$$-\frac{c_{33}\bar{h}^2k\left(2a_1^2\bar{c}_{33}+\bar{c}_{31}\bar{h}^2k^2\right)}{20a_1\bar{c}_{33}h\left(6a_1^2\bar{c}_{33}+\bar{c}_{31}\bar{h}^2k^2\right)}\left[A_{32}^{(2)}-3A_{33}^{(2)}+\ldots+\frac{(-1)^{n-1}n(n-1)}{2}A_{3n}^{(2)}\right]$$

$$-\frac{1}{5}\left\{14B_{16}^{(3)}+27B_{18}^{(3)}+\ldots+\left[\frac{n(n-1)}{2}-1\right]B_{1n}^{(3)}\right\}$$

$$+\frac{\bar{h}k\left(4a_1^2\bar{c}_{33}+\bar{c}_{31}\bar{h}^2k^2\right)}{20a_1\left(6a_1^2\bar{c}_{33}+\bar{c}_{31}\bar{h}^2k^2\right)}\left\{7A_{35}^{(3)}+18A_{37}^{(3)}+\ldots+\left[\frac{n(n-1)}{2}-3\right]A_{3n}^{(3)}\right\}$$

$$+\frac{\bar{c}_{31}\bar{h}^3k^3}{20a_1\left(6a_1^2\bar{c}_{33}+\bar{c}_{31}\bar{h}^2k^2\right)}\left\{5A_{34}^{(3)}+14A_{36}^{(3)}+\ldots+\left[\frac{n(n-1)}{2}-1\right]A_{3n}^{(3)}\right\}$$

$$\begin{aligned}
A_{31}^{(3)}&=-\frac{a_1\left(3\bar{c}_{31}-2c_{31}\right)\bar{h}k}{\left(6a_1^2\bar{c}_{33}+\bar{c}_{31}\bar{h}^2k^2\right)}\left[B_{11}^{(2)}-B_{12}^{(2)}+\ldots+(-1)^{n-1}B_{1n}^{(2)}\right]\\
&+\frac{6a_1^2\bar{c}_{33}}{\left(6a_1^2\bar{c}_{33}+\bar{c}_{31}\bar{h}^2k^2\right)}\left[A_{31}^{(2)}-A_{32}^{(2)}+\ldots+(-1)^{n-1}A_{3n}^{(2)}\right]\\
&-\frac{4a_1^2c_{33}\bar{h}}{h\left(6a_1^2\bar{c}_{33}+\bar{c}_{31}\bar{h}^2k^2\right)}\left[A_{32}^{(2)}-3A_{33}^{(2)}+\ldots+\frac{(-1)^{n-1}n(n-1)}{2}A_{3n}^{(2)}\right]\\
&+\frac{6a_1^2\bar{c}_{33}}{\left(6a_1^2\bar{c}_{33}+\bar{c}_{31}\bar{h}^2k^2\right)}\left\{5A_{34}^{(3)}+14A_{36}^{(3)}+\ldots+\left[\frac{n(n-1)}{2}-1\right]A_{3n}^{(3)}\right\}\\
&+\frac{2a_1^2\bar{c}_{33}}{\left(6a_1^2\bar{c}_{33}+\bar{c}_{31}\bar{h}^2k^2\right)}\left\{7A_{35}^{(3)}+18A_{37}^{(3)}+\ldots+\left[\frac{n(n-1)}{2}-3\right]A_{3n}^{(3)}\right\}
\end{aligned}\tag{4.19}$$

$$\begin{aligned}
A_{32}^{(3)}&=\frac{\left[6a_1^2\bar{c}_{33}\left(2\bar{c}_{31}-c_{31}\right)+\bar{c}_{31}\left(c_{31}-\bar{c}_{31}\right)\bar{h}^2k^2\right]\bar{h}k}{4a_1\bar{c}_{33}\left(6a_1^2\bar{c}_{33}+\bar{c}_{31}\bar{h}^2k^2\right)}\left[B_{11}^{(2)}-B_{12}^{(2)}+\ldots\right.\\
&\left.+(-1)^{n-1}B_{1n}^{(2)}\right]+\frac{3\bar{c}_{31}\bar{h}^2k^2}{2\left(6a_1^2\bar{c}_{33}+\bar{c}_{31}\bar{h}^2k^2\right)}\left[A_{31}^{(2)}-A_{32}^{(2)}+\ldots+(-1)^{n-1}A_{3n}^{(2)}\right]\\
&+\frac{c_{33}\bar{h}\left(6a_1^2\bar{c}_{33}-\bar{c}_{31}\bar{h}^2k^2\right)}{2\bar{c}_{33}h\left(6a_1^2\bar{c}_{33}+\bar{c}_{31}\bar{h}^2k^2\right)}\left[A_{32}^{(2)}-3A_{33}^{(2)}+\ldots+\frac{(-1)^{n-1}n(n-1)}{2}A_{3n}^{(2)}\right]\\
&+\frac{\bar{c}_{31}\bar{h}^2k^2}{2\left(6a_1^2\bar{c}_{33}+\bar{c}_{31}\bar{h}^2k^2\right)}\left\{3A_{34}^{(3)}+7A_{35}^{(3)}+\ldots+\left[\frac{n(n-1)}{2}-3\right]A_{3n}^{(3)}\right\}
\end{aligned}$$

$$- \frac{6a_1^2\bar{c}_{33}}{\left(6a_1^2\bar{c}_{33}+\bar{c}_{31}\bar{h}^2k^2\right)}\left[6A_{34}^{(3)}+15A_{36}^{(3)}+\ldots+\frac{n\,(n-1)}{2}A_{3n}^{(3)}\right]$$

$$A_{32}^{(3)} = \frac{\left[6a_1^2\bar{c}_{33}\,(2\bar{c}_{31}-c_{31})+\bar{c}_{31}\,(c_{31}-\bar{c}_{31})\,\bar{h}^2k^2\right]\bar{h}k}{4a_1\bar{c}_{33}\left(6a_1^2\bar{c}_{33}+\bar{c}_{31}\bar{h}^2k^2\right)}\left[B_{11}^{(2)}-B_{12}^{(2)}+\ldots\right.$$

$$\left.+(-1)^{n-1}B_{1n}^{(2)}\right]+\frac{3\bar{c}_{31}\bar{h}^2k^2}{2\left(6a_1^2\bar{c}_{33}+\bar{c}_{31}\bar{h}^2k^2\right)}\left[A_{31}^{(2)}-A_{32}^{(2)}+\ldots+(-1)^{n-1}A_{3n}^{(2)}\right]$$

$$+\frac{c_{33}\bar{h}\left(6a_1^2\bar{c}_{33}-\bar{c}_{31}\bar{h}^2k^2\right)}{2\bar{c}_{33}h\left(6a_1^2\bar{c}_{33}+\bar{c}_{31}\bar{h}^2k^2\right)}\left[A_{32}^{(2)}-3A_{33}^{(2)}+\ldots+\frac{(-1)^{n-1}\,n\,(n-1)}{2}A_{3n}^{(2)}\right]$$

$$+\frac{\bar{c}_{31}\bar{h}^2k^2}{2\left(6a_1^2\bar{c}_{33}+\bar{c}_{31}\bar{h}^2k^2\right)}\left\{3A_{34}^{(3)}+7A_{35}^{(3)}+\ldots+\left[\frac{n\,(n-1)}{2}-3\right]A_{3n}^{(3)}\right\}$$

$$-\frac{6a_1^2\bar{c}_{33}}{\left(6a_1^2\bar{c}_{33}+\bar{c}_{31}\bar{h}^2k^2\right)}\left[6A_{34}^{(3)}+15A_{36}^{(3)}+\ldots+\frac{n\,(n-1)}{2}A_{3n}^{(3)}\right]$$

$$A_{33}^{(3)} = -\frac{\left[2a_1^2\bar{c}_{33}c_{31}+\bar{c}_{31}\,(c_{31}-\bar{c}_{31})\,\bar{h}^2k^2\right]\bar{h}k}{4a_1\bar{c}_{33}\left(6a_1^2\bar{c}_{33}+\bar{c}_{31}\bar{h}^2k^2\right)}\left[B_{11}^{(2)}-B_{12}^{(2)}+\ldots\right.$$

$$\left.+(-1)^{n-1}B_{1n}^{(2)}\right]-\frac{\bar{c}_{31}\bar{h}^2k^2}{2\left(6a_1^2\bar{c}_{33}+\bar{c}_{31}\bar{h}^2k^2\right)}\left[A_{31}^{(2)}-A_{32}^{(2)}+\ldots+(-1)^{n-1}A_{3n}^{(2)}\right] \quad (4.19)$$

$$+\frac{c_{33}\bar{h}\left(2a_1^2\bar{c}_{33}+\bar{c}_{31}\bar{h}^2k^2\right)}{2\bar{c}_{33}h\left(6a_1^2\bar{c}_{33}+\bar{c}_{31}\bar{h}^2k^2\right)}\left[A_{32}^{(2)}-3A_{33}^{(2)}+\ldots+\frac{(-1)^{n-1}\,n\,(n-1)}{2}A_{3n}^{(2)}\right]$$

$$-\frac{\bar{c}_{31}\bar{h}^2k^2}{2\left(6a_1^2\bar{c}_{33}+\bar{c}_{31}\bar{h}^2k^2\right)}\left\{5A_{34}^{(3)}+9A_{35}^{(3)}+14A_{36}^{(3)}+\ldots+\left[\frac{n\,(n-1)}{2}-1\right]A_{3n}^{(3)}\right\}$$

$$-\frac{a_1^2\bar{c}_{33}}{\left(6a_1^2\bar{c}_{33}+\bar{c}_{31}\bar{h}^2k^2\right)}\left[20A_{35}^{(3)}+42A_{37}^{(3)}+\ldots+n(n-1)A_{3n}^{(3)}\right]$$

$$B_{31}^{(3)} = \frac{\bar{h}k\left[6a_1^2\,(6\bar{c}_{11}\bar{c}_{33}-\bar{c}_{13}\bar{c}_{31})+\bar{c}_{11}\,(3\bar{c}_{31}-c_{31})\,\bar{h}^2k^2\right]}{12a_1\bar{c}_{33}\left(6a_1^2\bar{c}_{13}+\bar{c}_{11}\bar{h}^2k^2\right)}$$

$$\left[A_{11}^{(2)}-A_{12}^{(2)}+\ldots+(-1)^{n-1}A_{1n}^{(2)}\right]$$

$$+\frac{c_{55}\bar{h}^2k\left[6a_1^2\,(\bar{c}_{13}\bar{c}_{31}-4\bar{c}_{11}\bar{c}_{33})-\bar{c}_{11}\bar{c}_{31}\bar{h}^2k^2\right]}{12a_1\bar{c}_{33}\bar{c}_{55}h\left(6a_1^2\bar{c}_{13}+\bar{c}_{11}\bar{h}^2k^2\right)}$$

$$\left[A_{12}^{(2)}-3A_{13}^{(2)}+\ldots+\frac{(-1)^{n-1}\,n\,(n-1)}{2}A_{1n}^{(2)}\right]$$

$$+\left\{\frac{144a_1^4\bar{c}_{13}\bar{c}_{33}\bar{c}_{55}-6a_1^2\left[2\bar{c}_{11}\bar{c}_{33}\left(\bar{c}_{55}-2c_{55}\right)+\bar{c}_{13}\bar{c}_{31}\left(c_{55}-2\bar{c}_{55}\right)\right]\bar{h}^2k^2}{24a_1^2\bar{c}_{55}\bar{c}_{33}\left(6a_1^2\bar{c}_{13}+\bar{c}_{11}\bar{h}^2k^2\right)}\right.$$

$$\left.+\frac{\bar{c}_{11}\bar{c}_{31}\left(c_{55}-\bar{c}_{55}\right)\bar{h}^4k^4}{24a_1^2\bar{c}_{55}\bar{c}_{33}\left(6a_1^2\bar{c}_{13}+\bar{c}_{11}\bar{h}^2k^2\right)}\right\}\left[B_{31}^{(2)}-B_{32}^{(2)}+\ldots+(-1)^{n-1}B_{3n}^{(2)}\right]$$

$$-\frac{c_{33}\bar{h}}{6\bar{c}_{33}h}\left[B_{32}^{(2)}-3B_{33}^{(2)}+\ldots+\frac{(-1)^{n-1}n(n-1)}{2}B_{3n}^{(2)}\right]$$

$$+\frac{36a_1^2\bar{c}_{33}\bar{c}_{11}\bar{h}k+\bar{c}_{11}\bar{c}_{31}\bar{h}^3k^3-12a_1^2\bar{c}_{13}\bar{c}_{31}\bar{h}k}{12a_1\bar{c}_{33}\left(6a_1^2\bar{c}_{13}+\bar{c}_{11}\bar{h}^2k^2\right)}$$

$$\left\{5A_{14}^{(3)}+14A_{16}^{(3)}+\ldots+\left[\frac{n(n-1)}{2}-1\right]A_{1n}^{(3)}\right\}$$

$$+\frac{12a_1^2\bar{c}_{11}\bar{c}_{33}\bar{h}k+\bar{c}_{11}\bar{c}_{31}\bar{h}^3k^3}{12a_1\bar{c}_{33}\left(6a_1^2\bar{c}_{13}+\bar{c}_{11}\bar{h}^2k^2\right)}\left\{7A_{15}^{(3)}+18A_{17}^{(3)}+\ldots+\left[\frac{n(n-1)}{2}-3\right]A_{1n}^{(3)}\right\}$$

$$+\frac{1}{3}\left\{7B_{35}^{(3)}+18B_{37}^{(3)}+\ldots+\left[\frac{n(n-1)}{2}-3\right]B_{3n}^{(3)}\right\}$$

$$B_{32}^{(3)}=-\frac{\bar{h}k\left\{6a_1^2\left[12\bar{c}_{11}\bar{c}_{33}+\bar{c}_{13}\left(c_{31}-2\bar{c}_{31}\right)\right]+\bar{c}_{11}\left(\bar{c}_{31}+c_{31}\right)\bar{h}^2k^2\right\}}{20a_1\bar{c}_{33}\left(6a_1^2\bar{c}_{13}+\bar{c}_{11}\bar{h}^2k^2\right)} \tag{4.19}$$

$$\left[A_{11}^{(2)}-A_{12}^{(2)}+\ldots+(-1)^{n-1}A_{1n}^{(2)}\right]$$

$$\left[A_{12}^{(2)}-3A_{13}^{(2)}+\ldots+\frac{(-1)^{n-1}n(n-1)}{2}A_{1n}^{(2)}\right]$$

$$-\bar{h}^2k^2\left\{\frac{6a_1^2\left[\bar{c}_{13}\bar{c}_{31}\left(2\bar{c}_{55}-c_{55}\right)+4\bar{c}_{11}\bar{c}_{33}\left(2c_{55}-3\bar{c}_{55}\right)\right]}{40a_1^2\bar{c}_{55}\bar{c}_{33}\left(6a_1^2\bar{c}_{13}+\bar{c}_{11}\bar{h}^2k^2\right)}\right.$$

$$\left.+\frac{\bar{c}_{11}\bar{c}_{31}\left(c_{55}-\bar{c}_{55}\right)\bar{h}^2k^2}{40a_1^2\bar{c}_{55}\bar{c}_{33}\left(6a_1^2\bar{c}_{13}+\bar{c}_{11}\bar{h}^2k^2\right)}\right\}\left[B_{31}^{(2)}-B_{32}^{(2)}+\ldots+(-1)^{n-1}B_{3n}^{(2)}\right]$$

$$-\frac{c_{33}\bar{h}}{10\bar{c}_{33}h}\left[B_{32}^{(2)}-3B_{33}^{(2)}+\ldots+\frac{(-1)^{n-1}n(n-1)}{2}B_{3n}^{(2)}\right]$$

$$-\frac{72\bar{c}_{11}\bar{c}_{33}\bar{h}ka_1^2+\bar{c}_{11}\bar{c}_{31}\bar{h}^3k^3-12\bar{c}_{13}\bar{c}_{31}\bar{h}ka_1^2}{20a_1\bar{c}_{33}\left(6a_1^2\bar{c}_{33}+\bar{c}_{31}\bar{h}^2k^2\right)}$$

$$\left\{5A_{14}^{(3)}+14A_{16}^{(3)}+\ldots+\left[\frac{n(n-1)}{2}-1\right]A_{1n}^{(3)}\right\}$$

$$- \frac{24\bar{c}_{11}\bar{c}_{33}\bar{h}ka_1^2 + \bar{c}_{11}\bar{c}_{31}\bar{h}^3k^3}{20a_1\bar{c}_{33}\left(6a_1^2\bar{c}_{33} + \bar{c}_{31}\bar{h}^2k^2\right)} \left\{7A_{15}^{(3)} + 18A_{17}^{(3)} + \ldots + \left[\frac{n(n-1)}{2} - 3\right] A_{1n}^{(3)}\right\}$$

$$+ \frac{1}{5}\left\{9B_{36}^{3} + 22B_{38}^{3} + \ldots + \left[\frac{n(n-1)}{2} - 6\right] B_{3n}^{3}\right\}$$

$$\begin{aligned}
B_{33}^{(3)} = {} & \frac{\bar{h}k\left[6a_1^2\bar{c}_{13}c_{31} + \bar{c}_{11}\left(c_{31} - 3\bar{c}_{31}\right)\bar{h}^2k^2\right]}{12a_1\bar{c}_{33}\left(6a_1^2\bar{c}_{13} + \bar{c}_{11}\bar{h}^2k^2\right)} \left[A_{11}^{(2)} - A_{12}^{(2)} + \ldots + (-1)^{n-1} A_{1n}^{(2)}\right] \\
& + \frac{\bar{c}_{31}c_{55}\bar{h}^2k\left(\bar{c}_{11}\bar{h}^2k^2 - 6a_1^2\bar{c}_{13}\right)}{12a_1\bar{c}_{33}\bar{c}_{55}h\left(6a_1^2\bar{c}_{13} + \bar{c}_{11}\bar{h}^2k^2\right)} \left[A_{12}^{2} - 3A_{13}^{2} + \ldots + (-1)^{n-1}\frac{n(n-1)}{2}A_{1n}^{2}\right] \\
& + \frac{\bar{c}_{31}\bar{h}^2k^2\left[6a_1^2\bar{c}_{13}\left(c_{55} - 2\bar{c}_{55}\right) + \bar{c}_{11}\left(\bar{c}_{55} - c_{55}\right)\bar{h}^2k^2\right]}{24a_1^2\bar{c}_{55}\bar{c}_{33}\left(6a_1^2\bar{c}_{13} + \bar{c}_{11}\bar{h}^2k^2\right)} \\
& \left[B_{31}^{(2)} - B_{32}^{(2)} + \ldots + (-1)^{n-1} B_{3n}^{(2)}\right] \\
& + \frac{c_{33}\bar{h}}{6\bar{c}_{33}h}\left[B_{32}^{(2)} - 3B_{33}^{(2)} + \ldots + \frac{(-1)^{n-1}n(n-1)}{2}B_{3n}^{(2)}\right] \\
& - \frac{\bar{c}_{11}\bar{c}_{31}\bar{h}^3k^3 - 12\bar{c}_{13}\bar{c}_{31}\bar{h}ka_1^2}{12a_1\bar{c}_{33}\left(6a_1^2\bar{c}_{13} + \bar{c}_{11}\bar{h}^2k^2\right)} \left\{5A_{14}^{(3)} + 14A_{16}^{(3)} + \ldots + \left[\frac{n(n-1)}{2} - 1\right] A_{1n}^{(3)}\right\} \\
& - \frac{\bar{c}_{11}\bar{c}_{31}\bar{h}^3k^3}{12a_1\bar{c}_{33}\left(6a_1^2\bar{c}_{13} + \bar{c}_{11}\bar{h}^2k^2\right)} \left\{7A_{15}^{(3)} + 18A_{17}^{(3)} + \ldots + \left[\frac{n(n-1)}{2} - 3\right] A_{1n}^{(3)}\right\} \\
& - \frac{1}{3}\left[10B_{35}^{(3)} + 21B_{37}^{(3)} + \ldots + \frac{n(n-1)}{2}B_{3n}^{(3)}\right]
\end{aligned} \tag{4.19}$$

$$\begin{aligned}
B_{34}^{(3)} = {} & -\frac{\bar{h}k\left\{6a_1^2\left[2\bar{c}_{11}\bar{c}_{33} + \bar{c}_{13}\left(c_{31} - 2\bar{c}_{31}\right)\right] + \bar{c}_{11}\left(\bar{c}_{31} + c_{31}\right)\bar{h}^2k^2\right\}}{20a_1\bar{c}_{33}\left(6a_1^2\bar{c}_{13} + \bar{c}_{11}\bar{h}^2k^2\right)} \\
& \left[A_{11}^{(2)} - A_{12}^{(2)} + \ldots + (-1)^{n-1} A_{1n}^{(2)}\right] \\
& + \bar{h}^2k^2\left[\frac{2a_1^2\left(6\bar{c}_{13}\bar{c}_{31}\bar{c}_{55} - 6\bar{c}_{11}\bar{c}_{33}\bar{c}_{55} - 3\bar{c}_{13}\bar{c}_{31}c_{55} + 4\bar{c}_{11}\bar{c}_{33}c_{55}\right)}{40a_1^2\bar{c}_{55}\bar{c}_{33}\left(6a_1^2\bar{c}_{13} + \bar{c}_{11}\bar{h}^2k^2\right)}\right. \\
& \left. + \frac{\bar{c}_{11}\bar{c}_{31}\left(c_{55} - \bar{c}_{55}\right)\bar{h}^2k^2}{40a_1^2\bar{c}_{55}\bar{c}_{33}\left(6a_1^2\bar{c}_{13} + \bar{c}_{11}\bar{h}^2k^2\right)}\right] \left[B_{31}^{(2)} - B_{32}^{(2)} + \ldots + (-1)^{n-1} B_{3n}^{(2)}\right] \\
& + \frac{c_{33}\bar{h}}{10\bar{c}_{33}h}\left[B_{32}^{(2)} - 3B_{33}^{(2)} + \ldots + \frac{(-1)^{n-1}n(n-1)}{2}B_{3n}^{(2)}\right]
\end{aligned}$$

$$
\begin{aligned}
&+\frac{12a_1^2\bar{c}_{11}\bar{c}_{33}\bar{h}k+\bar{c}_{11}\bar{c}_{31}\bar{h}^3k^3-12a_1^2\bar{c}_{13}\bar{c}_{31}\bar{h}k}{20a_1\bar{c}_{33}\left(6a_1^2\bar{c}_{13}+\bar{c}_{11}\bar{h}^2k^2\right)}\\
&\left\{5A_{14}^{(3)}+14A_{16}^{(3)}+\ldots+\left[\frac{n(n-1)}{2}-1\right]A_{1n}^{(3)}\right\}\\
&+\frac{4a_1^2\bar{c}_{11}\bar{c}_{33}\bar{h}k+\bar{c}_{11}\bar{c}_{31}\bar{h}^3k^3}{20a_1\bar{c}_{33}\left(6a_1^2\bar{c}_{13}+\bar{c}_{11}\bar{h}^2k^2\right)}\left\{7A_{15}^{(3)}+18A_{17}^{(3)}+\ldots+\left[\frac{n(n-1)}{2}-3\right]A_{1n}^{(3)}\right\}\\
&-\frac{1}{5}\left\{14B_{36}^{(3)}+27B_{38}^{(3)}+\ldots+\left[\frac{n(n-1)}{2}-1\right]B_{3n}^{(3)}\right\}
\end{aligned}
\tag{4.19}
$$

$$
\begin{aligned}
A_{11}^{(4)}&=-A_{12}^{(4)}-A_{13}^{(4)}-\ldots-A_{1n}^{(4)}-A_{11}^{(2)}-A_{12}^{(2)}-\ldots-A_{1n}^{(2)}\\
B_{11}^{(4)}&=-B_{12}^{(4)}-B_{13}^{(4)}-\ldots-B_{1n}^{(4)}+B_{11}^{(2)}+B_{12}^{(2)}+\ldots+B_{1n}^{(2)}\\
A_{31}^{(4)}&=-A_{32}^{(4)}-A_{33}^{(4)}-\ldots-A_{3n}^{(4)}-A_{31}^{(2)}-A_{32}^{(2)}-\ldots-A_{3n}^{(2)}\\
B_{31}^{(4)}&=-B_{32}^{(4)}-B_{33}^{(4)}-\ldots-B_{3n}^{(4)}+B_{31}^{(2)}+B_{32}^{(2)}+\ldots+B_{3n}^{(2)}
\end{aligned}
$$

The independent unknown coefficients exhibited in the right-hand side of the equation in Eq. 4.19 can be set to the new unknown vector, $\{\bar{\alpha}\}$:

$$
\begin{aligned}
&\{\alpha\}=[S_1]\{\bar{\alpha}\}\\
&\{\alpha\}=\left\{\left[A_1^{(1)}\right]\ \left[B_1^{(1)}\right]\ \left[A_3^{(1)}\right]\ \left[B_3^{(1)}\right]\ \left[A_1^{(2)}\right]\ \cdots\ \left[A_1^{(4)}\right]\ \left[B_1^{(4)}\right]\ \left[A_3^{(4)}\right]\ \left[B_3^{(4)}\right]\right\}^T\\
&\{\bar{\alpha}\}=\left\{\left[\tilde{A}_1^{(1)}\right]\ \left[\tilde{B}_1^{(1)}\right]\ \left[\tilde{A}_3^{(1)}\right]\ \left[\tilde{B}_3^{(1)}\right]\ \left[A_1^{(2)}\right]\ \cdots\ \left[\tilde{A}_1^{(4)}\right]\ \left[\tilde{B}_1^{(4)}\right]\ \left[\tilde{A}_3^{(4)}\right]\ \left[\tilde{B}_3^{(4)}\right]\right\}^T
\end{aligned}
\tag{4.20}
$$

where

$$
\begin{aligned}
\left\{A_1^{(1)}\right\}&=\left[A_{11}^{(1)}\ \ A_{12}^{(1)}\ \ \ldots\ \ A_{1n}^{(1)}\right]^T\\
\left\{B_1^{(1)}\right\}&=\left[B_{11}^{(1)}\ \ B_{12}^{(1)}\ \ \ldots\ \ B_{1n}^{(1)}\right]^T
\end{aligned}
$$

$$
\begin{aligned}
\left\{A_3^{(1)}\right\} &= \left[A_{31}^{(1)} \quad A_{32}^{(1)} \quad \ldots \quad A_{3n}^{(1)}\right]^T \\
\left\{B_3^{(1)}\right\} &= \left[B_{31}^{(1)} \quad B_{32}^{(1)} \quad \ldots \quad B_{3n}^{(1)}\right]^T \\
\left\{A_1^{(2)}\right\} &= \left[A_{11}^{(2)} \quad A_{12}^{(2)} \quad \ldots \quad A_{1n}^{(2)}\right]^T \\
\left\{B_1^{(2)}\right\} &= \left[B_{11}^{(2)} \quad B_{12}^{(2)} \quad \ldots \quad B_{1n}^{(2)}\right]^T \\
\left\{A_3^{(2)}\right\} &= \left[A_{31}^{(2)} \quad A_{32}^{(2)} \quad \ldots \quad A_{3n}^{(2)}\right]^T \\
\left\{B_3^{(2)}\right\} &= \left[B_{31}^{(2)} \quad B_{32}^{(2)} \quad \ldots \quad B_{3n}^{(2)}\right]^T \\
\left\{A_1^{(3)}\right\} &= \left[A_{11}^{(3)} \quad A_{12}^{(3)} \quad \ldots \quad A_{1n}^{(3)}\right]^T \\
\left\{B_1^{(3)}\right\} &= \left[B_{11}^{(3)} \quad B_{12}^{(3)} \quad \ldots \quad B_{1n}^{(3)}\right]^T \\
\left\{A_3^{(3)}\right\} &= \left[A_{31}^{(3)} \quad A_{32}^{(3)} \quad \ldots \quad A_{3n}^{(3)}\right]^T \\
\left\{B_3^{(3)}\right\} &= \left[B_{31}^{(3)} \quad B_{32}^{(3)} \quad \ldots \quad B_{3n}^{(3)}\right]^T \\
\left\{A_1^{(4)}\right\} &= \left[A_{11}^{(4)} \quad A_{12}^{(4)} \quad \ldots \quad A_{1n}^{(4)}\right]^T \\
\left\{B_1^{(4)}\right\} &= \left[B_{11}^{(4)} \quad B_{12}^{(4)} \quad \ldots \quad B_{1n}^{(4)}\right]^T \\
\left\{A_3^{(4)}\right\} &= \left[A_{31}^{(4)} \quad A_{32}^{(4)} \quad \ldots \quad A_{3n}^{(4)}\right]^T \\
\left\{B_3^{(4)}\right\} &= \left[B_{31}^{(4)} \quad B_{32}^{(4)} \quad \ldots \quad B_{3n}^{(4)}\right]^T \\
\left\{\tilde{A}_1^{(1)}\right\} &= \left[A_{12}^{(1)} \quad A_{13}^{(1)} \quad \ldots \quad A_{1n}^{(1)}\right]^T \\
\left\{\tilde{B}_1^{(1)}\right\} &= \left[B_{12}^{(1)} \quad B_{13}^{(1)} \quad \ldots \quad B_{1n}^{(1)}\right]^T \\
\left\{\tilde{A}_3^{(1)}\right\} &= \left[A_{32}^{(1)} \quad A_{33}^{(1)} \quad \ldots \quad A_{3n}^{(1)}\right]^T \\
\left\{\tilde{B}_3^{(1)}\right\} &= \left[B_{32}^{(1)} \quad B_{33}^{(1)} \quad \ldots \quad B_{3n}^{(1)}\right]^T
\end{aligned}
\tag{4.21}
$$

$$
\begin{aligned}
\left\{\tilde{A}_1^{(3)}\right\} &= \left[A_{13}^{(3)} \quad A_{14}^{(3)} \quad \ldots \quad A_{1n}^{(3)}\right]^T \\
\left\{\tilde{B}_1^{(3)}\right\} &= \left[B_{14}^{(3)} \quad B_{15}^{(3)} \quad \ldots \quad B_{1n}^{(3)}\right]^T \\
\left\{\tilde{A}_3^{(3)}\right\} &= \left[A_{33}^{(3)} \quad A_{34}^{(3)} \quad \ldots \quad A_{3n}^{(3)}\right]^T \\
\left\{\tilde{B}_3^{(3)}\right\} &= \left[B_{34}^{(3)} \quad B_{34}^{(3)} \quad \ldots \quad B_{3n}^{(3)}\right]^T \\
\left\{\tilde{A}_1^{(4)}\right\} &= \left[A_{12}^{(4)} \quad A_{13}^{(4)} \quad \ldots \quad A_{1n}^{(4)}\right]^T \\
\left\{\tilde{B}_1^{(4)}\right\} &= \left[B_{12}^{(4)} \quad B_{13}^{(4)} \quad \ldots \quad B_{1n}^{(4)}\right]^T \\
\left\{\tilde{A}_3^{(4)}\right\} &= \left[A_{32}^{(4)} \quad A_{33}^{(4)} \quad \ldots \quad A_{3n}^{(4)}\right]^T \\
\left\{\tilde{B}_3^{(4)}\right\} &= \left[B_{32}^{(4)} \quad B_{33}^{(4)} \quad \ldots \quad B_{3n}^{(4)}\right]^T
\end{aligned}
\tag{4.21}
$$

The matrix $[S_1]$ can be acquired according to Eq. 4.19.

When the bottom of the substrate is fixed, then $f^{(}(r))(x_3) = (1 - \frac{x_3}{h})$, $r = 1,2,4$. According to the previous chapter, it can be obtained that the transfer matrix obtained by considering other boundary conditions without considering the stress continuity at the interface between the covering layer and the substrate is consistent with the results of the previous section. Therefore, this section will not be repeated in this section and only the case of stress continuity on the intersection with $x_3 = 0$ is discussed below.

Substituting the displacement functions into Eqs. 4.5, 4.6 and 4.7, obtained:

$$
\begin{aligned}
A_{11}^{(1)} &= -A_{12}^{(1)} - A_{13}^{(1)} - \ldots - A_{1n}^{(1)} - A_{11}^{(2)} - A_{12}^{(2)} - \ldots - A_{1n}^{(2)} \\
B_{11}^{(1)} &= -B_{12}^{(1)} - B_{13}^{(1)} - \ldots - B_{1n}^{(1)} + B_{11}^{(2)} + B_{12}^{(2)} + \ldots + B_{1n}^{(2)} \\
A_{31}^{(1)} &= -A_{32}^{(1)} - A_{33}^{(1)} - \ldots - A_{3n}^{(1)} - A_{31}^{(2)} - A_{32}^{(2)} - \ldots - A_{3n}^{(2)} \\
B_{31}^{(1)} &= -B_{32}^{(1)} - B_{33}^{(1)} - \ldots - B_{3n}^{(1)} + B_{31}^{(2)} + B_{32}^{(2)} + \ldots + B_{3n}^{(2)} \\
A_{11}^{(3)} &= \frac{6a_1^2\bar{c}_{13}}{6a_1^2\bar{c}_{13} + \bar{c}_{11}\bar{h}^2k^2} \left[A_{11}^{(2)} - A_{12}^{(2)} + \ldots + (-1)^{n-1} A_{1n}^{(2)}\right]
\end{aligned}
$$

$$
\begin{aligned}
&+\frac{2a_1^2\bar{c}_{13}c_{55}\bar{h}}{\bar{c}_{55}h\left(6a_1^2\bar{c}_{13}+\bar{c}_{11}\bar{h}^2k^2\right)}\left\{A_{11}^{(2)}-3A_{12}^{(2)}+7A_{13}^{(2)}+\ldots\right.\\
&\left.+(-1)^{n-1}\left[n(n-1)+1\right]A_{1n}^{(2)}\right\}\\
&-\frac{a_1\bar{c}_{13}\bar{h}k\left(3\bar{c}_{55}-2c_{55}\right)}{\bar{c}_{55}\left(6a_1^2\bar{c}_{13}+\bar{c}_{11}\bar{h}^2k^2\right)}\left[B_{31}^{(2)}-B_{32}^{(2)}+\ldots+(-1)^{n-1}B_{3n}^{(2)}\right]\\
&-\frac{a_1\bar{c}_{13}\bar{h}k\left(3\bar{c}_{55}-2c_{55}\right)}{\bar{c}_{55}\left(6a_1^2\bar{c}_{13}+\bar{c}_{11}\bar{h}^2k^2\right)}\left[B_{31}^{(2)}-B_{32}^{(2)}+\ldots+(-1)^{n-1}B_{3n}^{(2)}\right]\\
&+\frac{2a_1^2\bar{c}_{13}}{6a_1^2\bar{c}_{13}+\bar{c}_{11}\bar{h}^2k^2}\left\{7A_{15}^{(3)}+18A_{17}^{(3)}+\ldots+\left[\frac{n(n-1)}{2}-3\right]A_{1n}^{(3)}\right\}\\
A_{12}^{(3)}&=\frac{3\bar{c}_{11}\bar{h}^2k^2}{2\left(6a_1^2\bar{c}_{13}+\bar{c}_{11}\bar{h}^2k^2\right)}\left[A_{11}^{(2)}-A_{12}^{(2)}+\ldots+(-1)^{n-1}A_{1n}^{(2)}\right]\\
&+\frac{\left(\bar{c}_{11}\bar{h}^2k^2-6a_1^2\bar{c}_{13}\right)c_{55}\bar{h}}{4\bar{c}_{55}h\left(6a_1^2\bar{c}_{13}+\bar{c}_{11}\bar{h}^2k^2\right)}\left\{A_{11}^{(2)}-3A_{12}^{(2)}+7A_{13}^{(2)}+\ldots\right.\\
&\left.+(-1)^{n-1}\left[n(n-1)+1\right]A_{1n}^{(2)}\right\}\\
&+\frac{\left[6a_1^2\bar{c}_{13}\left(2\bar{c}_{55}-c_{55}\right)+\bar{c}_{11}\left(c_{55}-\bar{c}_{55}\right)\bar{h}^2k^2\right]\bar{h}k}{4a_1\bar{c}_{55}\left(6a_1^2\bar{c}_{13}+\bar{c}_{11}\bar{h}^2k^2\right)}\\
&\left[B_{31}^{(2)}-B_{32}^{(2)}+\ldots+(-1)^{n-1}B_{3n}^{(2)}\right]\\
&+\frac{\bar{c}_{11}\bar{h}^2k^2}{2\left(6a_1^2\bar{c}_{13}+\bar{c}_{11}\bar{h}^2k^2\right)}\left\{3A_{14}^{(3)}+7A_{15}^{(3)}+\ldots+\left[\frac{n(n-1)}{2}-3\right]A_{1n}^{(3)}\right\}\\
&-\frac{3a_1^2\bar{c}_{13}}{\left(6a_1^2\bar{c}_{13}+\bar{c}_{11}\bar{h}^2k^2\right)}\left[12A_{14}^{(3)}+30A_{16}^{(3)}+\ldots+n(n-1)A_{1n}^{(3)}\right]\\
A_{13}^{(3)}&=-\frac{\bar{c}_{11}\bar{h}^2k^2}{2\left(6a_1^2\bar{c}_{13}+\bar{c}_{11}\bar{h}^2k^2\right)}\left[A_{11}^{(2)}-A_{12}^{(2)}+\ldots+(-1)^{n-1}A_{1n}^{(2)}\right]\\
&-\frac{\left(2{a_1}^2\bar{c}_{13}+\bar{c}_{11}\bar{h}^2k^2\right)c_{55}\bar{h}}{4\bar{c}_{55}h\left(6a_1^2\bar{c}_{13}+\bar{c}_{11}\bar{h}^2k^2\right)}\left\{A_{11}^{(2)}-3A_{12}^{(2)}+7A_{13}^{(2)}+\ldots\right.\\
&\left.+(-1)^{n-1}\left[n(n-1)+1\right]A_{1n}^{(2)}\right\}\\
&-\frac{\left[2a_1^2\bar{c}_{13}c_{55}+\bar{c}_{11}\left(c_{55}-\bar{c}_{55}\right)\bar{h}^2k^2\right]\bar{h}k}{4a_1\bar{c}_{55}\left(6a_1^2\bar{c}_{13}+\bar{c}_{11}\bar{h}^2k^2\right)}\left[B_{31}^{(2)}-B_{32}^{(2)}+\ldots+(-1)^{n-1}B_{3n}^{(2)}\right]
\end{aligned}
\tag{4.22}
$$

$$- \frac{2a_1^2\bar{c}_{13}}{\left(6a_1^2\bar{c}_{13}+\bar{c}_{11}\bar{h}^2k^2\right)}\left[10A_{15}^{(3)}+15A_{17}^{(3)}+\ldots+\frac{n\,(n-1)}{2}A_{1n}^{(3)}\right]$$

$$- \frac{\bar{c}_{11}\bar{h}^2k^2}{2\left(6a_1^2\bar{c}_{13}+\bar{c}_{11}\bar{h}^2k^2\right)}\left\{5A_{14}^{(3)}+9A_{15}^{(3)}+\ldots+\left[\frac{n\,(n-1)}{2}-1\right]A_{1n}^{(3)}\right\}$$

$$B_{11}^{(3)} = \frac{144a_1^4\bar{c}_{33}^2+18a_1^2\bar{c}_{33}c_{31}\bar{h}^2k^2+\bar{c}_{31}\,(c_{31}-\bar{c}_{31})\,\bar{h}^4k^4}{24a_1^2\bar{c}_{33}\left(6a_1^2\bar{c}_{33}+\bar{c}_{31}\bar{h}^2k^2\right)}\left[B_{11}^{(2)}-B_{12}^{(2)}+\ldots\right.$$

$$\left.+\,(-1)^{n-1}B_{1n}^{(2)}\right]+\frac{c_{55}\bar{h}}{12\bar{c}_{55}h}\left[B_{11}^{(2)}-3B_{12}^{(2)}+\ldots+\frac{(-1)^{n-1}\,n\,(n-1)}{2}B_{1n}^{(2)}\right]$$

$$+\frac{\bar{h}k\left[6a_1^2\bar{c}_{33}\,(6\bar{c}_{55}-c_{55})+\bar{c}_{31}\,(3\bar{c}_{55}-c_{55})\,\bar{h}^2k^2\right]}{12a_1\bar{c}_{55}\left(6a_1^2\bar{c}_{33}+\bar{c}_{31}\bar{h}^2k^2\right)}$$

$$\left[A_{31}^{(2)}-A_{32}^{(2)}+\ldots+(-1)^{n-1}A_{3n}^{(2)}\right]$$

$$-\frac{c_{33}\bar{h}^2k\left(18a_1^2\bar{c}_{33}+\bar{c}_{31}\bar{h}^2k^2\right)}{12a_1\bar{c}_{33}h\left(6a_1^2\bar{c}_{33}+\bar{c}_{31}\bar{h}^2k^2\right)}\left[A_{32}^{(2)}-3A_{33}^{(2)}+\ldots+\frac{(-1)^{n-1}\,n\,(n-1)}{2}A_{3n}^{(2)}\right]$$

$$+\frac{1}{3}\left\{7B_{15}^{(3)}+18B_{17}^{(3)}+\ldots+\left[\frac{n\,(n-1)}{2}-3\right]B_{1n}^{(3)}\right\} \tag{4.22}$$

$$+\frac{24a_1^2\bar{c}_{33}\bar{h}k+\bar{c}_{31}\bar{h}^3k^3}{12a_1\left(6a_1^2\bar{c}_{33}+\bar{c}_{31}\bar{h}^2k^2\right)}\left\{5A_{34}^{(3)}+14A_{36}^{(3)}+\ldots+\left[\frac{n\,(n-1)}{2}-1\right]A_{3n}^{(3)}\right\}$$

$$+\frac{12a_1^2\bar{c}_{33}\bar{h}k+\bar{c}_{31}\bar{h}^3k^3}{12a_1\left(6a_1^2\bar{c}_{33}+\bar{c}_{31}\bar{h}^2k^2\right)}\left\{7A_{35}^{(3)}+18A_{37}^{(3)}+\ldots+\left[\frac{n\,(n-1)}{2}-3\right]A_{3n}^{(3)}\right\}$$

$$B_{12}^{(3)} = \frac{\bar{h}^2k^2\left[6a_1^2\bar{c}_{33}\,(10\bar{c}_{31}-7c_{31})+\bar{c}_{31}\,(\bar{c}_{31}-c_{31})\,\bar{h}^2k^2\right]}{40a_1^2\bar{c}_{33}\left(6a_1^2\bar{c}_{33}+\bar{c}_{31}\bar{h}^2k^2\right)}\left[B_{11}^{(2)}-B_{12}^{(2)}+\ldots\right.$$

$$\left.+\,(-1)^{n-1}B_{1n}^{(2)}\right]+\frac{c_{55}\bar{h}}{10\bar{c}_{55}h}\left[B_{12}^{(2)}-3B_{13}^{(2)}+\ldots+\frac{(-1)^{n-1}\,n\,(n-1)}{2}B_{1n}^{(2)}\right]$$

$$-\frac{\bar{h}k\left[6a_1^2\bar{c}_{33}\,(10\bar{c}_{55}+c_{55})+\bar{c}_{31}\,(\bar{c}_{55}+c_{55})\,\bar{h}^2k^2\right]}{20a_1\bar{c}_{55}\left(6a_1^2\bar{c}_{33}+\bar{c}_{31}\bar{h}^2k^2\right)}$$

$$\left[A_{31}^{(2)}-A_{32}^{(2)}+\ldots+(-1)^{n-1}A_{3n}^{(2)}\right]$$

$$+\frac{c_{33}\bar{h}^2k\left(42a_1^2\bar{c}_{33}+\bar{c}_{31}\bar{h}^2k^2\right)}{20a_1\bar{c}_{33}h\left(6a_1^2\bar{c}_{33}+\bar{c}_{31}\bar{h}^2k^2\right)}\left[A_{32}^{(2)}-3A_{33}^{(2)}+\ldots+\frac{(-1)^{n-1}\,n\,(n-1)}{2}A_{3n}^{(2)}\right]$$

$$+\frac{1}{5}\left\{9B_{16}^{(3)}+22B_{18}^{(3)}+\ldots+\left[\frac{n(n-1)}{2}-6\right]B_{1n}^{(3)}\right\}$$
$$-\frac{60a_1^2\bar{c}_{33}\bar{h}k+\bar{c}_{31}\bar{h}^3k^3}{20a_1\left(6a_1^2\bar{c}_{33}+\bar{c}_{31}\bar{h}^2k^2\right)}\left\{5A_{34}^{(3)}+14A_{36}^{(3)}+\ldots+\left[\frac{n(n-1)}{2}-1\right]A_{3n}^{(3)}\right\}$$
$$-\frac{24a_1^2\bar{c}_{33}\bar{h}k+\bar{c}_{31}\bar{h}^3k^3}{20a_1\left(6a_1^2\bar{c}_{33}+\bar{c}_{31}\bar{h}^2k^2\right)}\left\{7A_{35}^{(3)}+18A_{37}^{(3)}+\ldots+\left[\frac{n(n-1)}{2}-3\right]A_{3n}^{(3)}\right\}$$

$$B_{13}^{(3)}=\frac{\bar{h}^2k^2\left[6a_1^2\bar{c}_{33}\left(c_{31}-2\bar{c}_{31}\right)+\bar{c}_{31}\left(\bar{c}_{31}-c_{31}\right)\bar{h}^2k^2\right]}{24a_1^2\bar{c}_{33}\left(6a_1^2\bar{c}_{33}+\bar{c}_{31}\bar{h}^2k^2\right)}\left[B_{11}^{(2)}-B_{12}^{(2)}+\ldots\right.$$
$$\left.+(-1)^{n-1}B_{1n}^{(2)}\right]-\frac{c_{55}\bar{h}}{6\bar{c}_{55}h}\left[B_{12}^{(2)}-3B_{13}^{(2)}+\ldots+\frac{(-1)^{n-1}n(n-1)}{2}B_{1n}^{(2)}\right]$$
$$+\frac{\bar{h}k\left[6a_1^2\bar{c}_{33}c_{55}+\bar{c}_{31}\left(c_{55}-3\bar{c}_{55}\right)\bar{h}^2k^2\right]}{12a_1\bar{c}_{55}\left(6a_1^2\bar{c}_{33}+\bar{c}_{31}\bar{h}^2k^2\right)}\left[A_{31}^{(2)}-A_{32}^{(2)}+\ldots+(-1)^{n-1}A_{3n}^{(2)}\right]$$
$$-\frac{c_{33}\bar{h}^2k\left(\bar{c}_{31}\bar{h}^2k^2-6a_1^2\bar{c}_{33}\right)}{12a_1\bar{c}_{33}h\left(6a_1^2\bar{c}_{33}+\bar{c}_{31}\bar{h}^2k^2\right)}\left[A_{32}^{(2)}-3A_{33}^{(2)}+\ldots+\frac{(-1)^{n-1}n(n-1)}{2}A_{3n}^{(2)}\right]$$
$$-\frac{1}{3}\left[10B_{15}^{(3)}+21B_{17}^{(3)}+\ldots+\frac{n(n-1)}{2}B_{1n}^{(3)}\right] \tag{4.22}$$
$$+\frac{12a_1^2\bar{c}_{33}\bar{h}k-\bar{c}_{31}\bar{h}^3k^3}{12a_1\left(6a_1^2\bar{c}_{33}+\bar{c}_{31}\bar{h}^2k^2\right)}\left\{5A_{34}^{(3)}+14A_{36}^{(3)}+\ldots+\left[\frac{n(n-1)}{2}-1\right]A_{3n}^{(3)}\right\}$$
$$-\frac{\bar{c}_{31}\bar{h}^3k^3}{12a_1\left(6a_1^2\bar{c}_{33}+\bar{c}_{31}\bar{h}^2k^2\right)}\left\{7A_{35}^{(3)}+18A_{37}^{(3)}+\ldots+\left[\frac{n(n-1)}{2}-3\right]A_{3n}^{(3)}\right\}$$

$$B_{14}^{(3)}=\frac{\bar{h}^2k^2\left[2a_1^2\bar{c}_{33}c_{31}-\bar{c}_{31}\left(\bar{c}_{31}-c_{31}\right)\bar{h}^2k^2\right]}{40a_1^2\bar{c}_{33}\left(6a_1^2\bar{c}_{33}+\bar{c}_{31}\bar{h}^2k^2\right)}\left[B_{11}^{(2)}-B_{12}^{(2)}+\ldots+(-1)^{n-1}B_{1n}^{(2)}\right]$$
$$-\frac{c_{55}\bar{h}}{10\bar{c}_{55}h}\left[B_{12}^{(2)}-3B_{13}^{(2)}+\ldots+\frac{(-1)^{n-1}n(n-1)}{2}B_{1n}^{(2)}\right]$$
$$+\frac{\bar{h}k\left[6a_1^2\bar{c}_{33}c_{55}+\bar{c}_{31}\left(\bar{c}_{55}+c_{55}\right)\bar{h}^2k^2\right]}{20a_1\bar{c}_{55}\left(6a_1^2\bar{c}_{33}+\bar{c}_{31}\bar{h}^2k^2\right)}\left[A_{31}^{(2)}-A_{32}^{(2)}+\ldots+(-1)^{n-1}A_{3n}^{(2)}\right]$$
$$-\frac{c_{33}\bar{h}^2k\left(2a_1^2\bar{c}_{33}+\bar{c}_{31}\bar{h}^2k^2\right)}{20a_1\bar{c}_{33}h\left(6a_1^2\bar{c}_{33}+\bar{c}_{31}\bar{h}^2k^2\right)}\left[A_{32}^{(2)}-3A_{33}^{(2)}+\ldots+\frac{(-1)^{n-1}n(n-1)}{2}A_{3n}^{(2)}\right]$$
$$-\frac{1}{5}\left\{14B_{16}^{(3)}+27B_{18}^{(3)}+\ldots+\left[\frac{n(n-1)}{2}-1\right]B_{1n}^{(3)}\right\}$$

$$+\frac{\bar{h}k\left(4a_1^2\bar{c}_{33}+\bar{c}_{31}\bar{h}^2k^2\right)}{20a_1\left(6a_1^2\bar{c}_{33}+\bar{c}_{31}\bar{h}^2k^2\right)}\left\{7A_{35}^{(3)}+18A_{37}^{(3)}+\ldots+\left[\frac{n(n-1)}{2}-3\right]A_{3n}^{(3)}\right\}$$

$$+\frac{\bar{c}_{31}\bar{h}^3k^3}{20a_1\left(6a_1^2\bar{c}_{33}+\bar{c}_{31}\bar{h}^2k^2\right)}\left\{5A_{34}^{(3)}+14A_{36}^{(3)}+\ldots+\left[\frac{n(n-1)}{2}-1\right]A_{3n}^{(3)}\right\}$$

$$A_{31}^{(3)}=-\frac{a_1(3\bar{c}_{31}-2c_{31})\bar{h}k}{\left(6a_1^2\bar{c}_{33}+\bar{c}_{31}\bar{h}^2k^2\right)}\left[B_{11}^{(2)}-B_{12}^{(2)}+\ldots+(-1)^{n-1}B_{1n}^{(2)}\right]$$

$$+\frac{6a_1^2\bar{c}_{33}}{\left(6a_1^2\bar{c}_{33}+\bar{c}_{31}\bar{h}^2k^2\right)}\left[A_{31}^{(2)}-A_{32}^{(2)}+\ldots+(-1)^{n-1}A_{3n}^{(2)}\right]$$

$$-\frac{4a_1^2c_{33}\bar{h}}{h\left(6a_1^2\bar{c}_{33}+\bar{c}_{31}\bar{h}^2k^2\right)}\left[A_{32}^{(2)}-3A_{33}^{(2)}+\ldots+\frac{(-1)^{n-1}n(n-1)}{2}A_{3n}^{(2)}\right]$$

$$+\frac{6a_1^2\bar{c}_{33}}{\left(6a_1^2\bar{c}_{33}+\bar{c}_{31}\bar{h}^2k^2\right)}\left\{5A_{34}^{(3)}+14A_{36}^{(3)}+\ldots+\left[\frac{n(n-1)}{2}-1\right]A_{3n}^{(3)}\right\}$$

$$+\frac{2a_1^2\bar{c}_{33}}{\left(6a_1^2\bar{c}_{33}+\bar{c}_{31}\bar{h}^2k^2\right)}\left\{7A_{35}^{(3)}+18A_{37}^{(3)}+\ldots+\left[\frac{n(n-1)}{2}-3\right]A_{3n}^{(3)}\right\} \tag{4.22}$$

$$A_{32}^{(3)}=\frac{\left[6a_1^2\bar{c}_{33}(2\bar{c}_{31}-c_{31})+\bar{c}_{31}(c_{31}-\bar{c}_{31})\bar{h}^2k^2\right]\bar{h}k}{4a_1\bar{c}_{33}\left(6a_1^2\bar{c}_{33}+\bar{c}_{31}\bar{h}^2k^2\right)}\left[B_{11}^{(2)}-B_{12}^{(2)}+\ldots\right.$$

$$\left.+(-1)^{n-1}B_{1n}^{(2)}\right]+\frac{3\bar{c}_{31}\bar{h}^2k^2}{2\left(6a_1^2\bar{c}_{33}+\bar{c}_{31}\bar{h}^2k^2\right)}\left[A_{31}^{(2)}-A_{32}^{(2)}+\ldots+(-1)^{n-1}A_{3n}^{(2)}\right]$$

$$+\frac{c_{33}\bar{h}\left(6a_1^2\bar{c}_{33}-\bar{c}_{31}\bar{h}^2k^2\right)}{2\bar{c}_{33}h\left(6a_1^2\bar{c}_{33}+\bar{c}_{31}\bar{h}^2k^2\right)}\left[A_{32}^{(2)}-3A_{33}^{(2)}+\ldots+\frac{(-1)^{n-1}n(n-1)}{2}A_{3n}^{(2)}\right]$$

$$+\frac{\bar{c}_{31}\bar{h}^2k^2}{2\left(6a_1^2\bar{c}_{33}+\bar{c}_{31}\bar{h}^2k^2\right)}\left\{3A_{34}^{(3)}+7A_{35}^{(3)}+\ldots+\left[\frac{n(n-1)}{2}-3\right]A_{3n}^{(3)}\right\}$$

$$-\frac{6a_1^2\bar{c}_{33}}{\left(6a_1^2\bar{c}_{33}+\bar{c}_{31}\bar{h}^2k^2\right)}\left[6A_{34}^{(3)}+15A_{36}^{(3)}+\ldots+\frac{n(n-1)}{2}A_{3n}^{(3)}\right]$$

$$A_{33}^{(3)}=-\frac{\left[2a_1^2\bar{c}_{33}c_{31}+\bar{c}_{31}(c_{31}-\bar{c}_{31})\bar{h}^2k^2\right]\bar{h}k}{4a_1\bar{c}_{33}\left(6a_1^2\bar{c}_{33}+\bar{c}_{31}\bar{h}^2k^2\right)}\left[B_{11}^{(2)}-B_{12}^{(2)}+\ldots+(-1)^{n-1}B_{1n}^{(2)}\right]$$

$$-\frac{\bar{c}_{31}\bar{h}^2k^2}{2\left(6a_1^2\bar{c}_{33}+\bar{c}_{31}\bar{h}^2k^2\right)}\left[A_{31}^{(2)}-A_{32}^{(2)}+\ldots+(-1)^{n-1}A_{3n}^{(2)}\right]$$

$$
\begin{aligned}
&+\frac{c_{33}\bar{h}\left(2a_1^2\bar{c}_{33}+\bar{c}_{31}\bar{h}^2k^2\right)}{2\bar{c}_{33}h\left(6a_1^2\bar{c}_{33}+\bar{c}_{31}\bar{h}^2k^2\right)}\left[A_{32}^{(2)}-3A_{33}^{(2)}+\ldots+\frac{(-1)^{n-1}n(n-1)}{2}A_{3n}^{(2)}\right]\\
&-\frac{\bar{c}_{31}\bar{h}^2k^2}{2\left(6a_1^2\bar{c}_{33}+\bar{c}_{31}\bar{h}^2k^2\right)}\left\{5A_{34}^{(3)}+9A_{35}^{(3)}+14A_{36}^{(3)}+\ldots+\left[\frac{n(n-1)}{2}-1\right]A_{3n}^{(3)}\right\}\\
&-\frac{a_1^2\bar{c}_{33}}{\left(6a_1^2\bar{c}_{33}+\bar{c}_{31}\bar{h}^2k^2\right)}\left[20A_{35}^{(3)}+42A_{37}^{(3)}+\ldots+n(n-1)A_{3n}^{(3)}\right]\\
B_{31}^{(3)}=&\frac{\bar{h}k\left[6a_1^2\left(6\bar{c}_{11}\bar{c}_{33}-\bar{c}_{13}\bar{c}_{31}\right)+\bar{c}_{11}\left(3\bar{c}_{31}-c_{31}\right)\bar{h}^2k^2\right]}{12a_1\bar{c}_{33}\left(6a_1^2\bar{c}_{13}+\bar{c}_{11}\bar{h}^2k^2\right)}\left[A_{11}^{(2)}-A_{12}^{(2)}+\ldots\right.\\
&\left.+(-1)^{n-1}A_{1n}^{(2)}\right]+\frac{c_{55}\bar{h}^2k\left[6a_1^2\left(\bar{c}_{13}\bar{c}_{31}-4\bar{c}_{11}\bar{c}_{33}\right)-\bar{c}_{11}\bar{c}_{31}\bar{h}^2k^2\right]}{12a_1\bar{c}_{33}\bar{c}_{55}h\left(6a_1^2\bar{c}_{13}+\bar{c}_{11}\bar{h}^2k^2\right)}\\
&\left[A_{12}^{(2)}-3A_{13}^{(2)}+\ldots+\frac{(-1)^{n-1}n(n-1)}{2}A_{1n}^{(2)}\right]\\
&+\left\{\frac{144a_1^4\bar{c}_{13}\bar{c}_{33}\bar{c}_{55}-6a_1^2\left[2\bar{c}_{11}\bar{c}_{33}\left(\bar{c}_{55}-2c_{55}\right)+\bar{c}_{13}\bar{c}_{31}\left(c_{55}-2\bar{c}_{55}\right)\right]\bar{h}^2k^2}{24a_1^2\bar{c}_{55}\bar{c}_{33}\left(6a_1^2\bar{c}_{13}+\bar{c}_{11}\bar{h}^2k^2\right)}\right.\\
&\left.+\frac{\bar{c}_{11}\bar{c}_{31}\left(c_{55}-\bar{c}_{55}\right)\bar{h}^4k^4}{24a_1^2\bar{c}_{55}\bar{c}_{33}\left(6a_1^2\bar{c}_{13}+\bar{c}_{11}\bar{h}^2k^2\right)}\right\}\left[B_{31}^{(2)}-B_{32}^{(2)}+\ldots+(-1)^{n-1}B_{3n}^{(2)}\right]\\
&+\frac{c_{33}\bar{h}}{12\bar{c}_{33}h}\left\{B_{21}^{(2)}-3B_{22}^{(2)}+\ldots+(-1)^{n-1}\left[n(n-1)+1\right]B_{2n}^{(2)}\right\}\\
&+\frac{36a_1^2\bar{c}_{33}\bar{c}_{11}\bar{h}k+\bar{c}_{11}\bar{c}_{31}\bar{h}^3k^3-12a_1^2\bar{c}_{13}\bar{c}_{31}\bar{h}k}{12a_1\bar{c}_{33}\left(6a_1^2\bar{c}_{13}+\bar{c}_{11}\bar{h}^2k^2\right)}\\
B_{32}^{(3)}=&-\frac{\bar{h}k\left\{6a_1^2\left[12\bar{c}_{11}\bar{c}_{33}+\bar{c}_{13}\left(c_{31}-2\bar{c}_{31}\right)\right]+\bar{c}_{11}\left(\bar{c}_{31}+c_{31}\right)\bar{h}^2k^2\right\}}{20a_1\bar{c}_{33}\left(6a_1^2\bar{c}_{13}+\bar{c}_{11}\bar{h}^2k^2\right)}\\
&\left[A_{11}^{(2)}-A_{12}^{(2)}+\ldots+(-1)^{n-1}A_{1n}^{(2)}\right]\\
&+\frac{c_{55}\bar{h}^2k\left[-6a_1^2\left(\bar{c}_{13}\bar{c}_{31}-8\bar{c}_{11}\bar{c}_{33}\right)+\bar{c}_{11}\bar{c}_{31}\bar{h}^2k^2\right]}{20a_1\bar{c}_{33}\bar{c}_{55}h\left(6a_1^2\bar{c}_{13}+\bar{c}_{11}\bar{h}^2k^2\right)}\\
&\left[A_{12}^{(2)}-3A_{13}^{(2)}+\ldots+\frac{(-1)^{n-1}n(n-1)}{2}A_{1n}^{(2)}\right]
\end{aligned}
\tag{4.22}
$$

$$
\begin{aligned}
& -\bar{h}^2k^2\left\{\frac{6a_1^2\left[\bar{c}_{13}\bar{c}_{31}\left(2\bar{c}_{55}-c_{55}\right)+4\bar{c}_{11}\bar{c}_{33}\left(2c_{55}-3\bar{c}_{55}\right)\right]}{40a_1^2\bar{c}_{55}\bar{c}_{33}\left(6a_1^2\bar{c}_{13}+\bar{c}_{11}\bar{h}^2k^2\right)}\right.\\
& \left.+\frac{\bar{c}_{11}\bar{c}_{31}\left(c_{55}-\bar{c}_{55}\right)\bar{h}^2k^2}{40a_1^2\bar{c}_{55}\bar{c}_{33}\left(6a_1^2\bar{c}_{13}+\bar{c}_{11}\bar{h}^2k^2\right)}\right\}\left[B_{31}^{(2)}-B_{32}^{(2)}+\ldots+(-1)^{n-1}B_{3n}^{(2)}\right]\\
& +\frac{c_{33}\bar{h}}{20\bar{c}_{33}h}\left\{B_{21}^{(2)}-3B_{22}^{(2)}+\ldots+(-1)^{n-1}\left[n\left(n-1\right)+1\right]B_{2n}^{(2)}\right\}\\
& -\frac{72\bar{c}_{11}\bar{c}_{33}\bar{h}ka_1^2+\bar{c}_{11}\bar{c}_{31}\bar{h}^3k^3-12\bar{c}_{13}\bar{c}_{31}\bar{h}ka_1^2}{20a_1\bar{c}_{33}\left(6a_1^2\bar{c}_{33}+\bar{c}_{31}\bar{h}^2k^2\right)}\\
& \left\{5A_{14}^{(3)}+14A_{16}^{(3)}+\ldots+\left[\frac{n\left(n-1\right)}{2}-1\right]A_{1n}^{(3)}\right\}\\
& -\frac{24\bar{c}_{11}\bar{c}_{33}\bar{h}ka_1^2+\bar{c}_{11}\bar{c}_{31}\bar{h}^3k^3}{20a_1\bar{c}_{33}\left(6a_1^2\bar{c}_{33}+\bar{c}_{31}\bar{h}^2k^2\right)}\left\{7A_{15}^{(3)}+18A_{17}^{(3)}+\ldots+\left[\frac{n\left(n-1\right)}{2}-3\right]A_{1n}^{(3)}\right\}\\
& +\frac{1}{5}\left\{9B_{36}^{(3)}+22B_{38}^{(3)}+\ldots+\left[\frac{n\left(n-1\right)}{2}-6\right]B_{3n}^{(3)}\right\}
\end{aligned}
\tag{4.22}
$$

$$
\begin{aligned}
B_{33}^{(3)}= & \frac{\bar{h}k\left[6a_1^2\bar{c}_{13}c_{31}+\bar{c}_{11}\left(c_{31}-3\bar{c}_{31}\right)\bar{h}^2k^2\right]}{12a_1\bar{c}_{33}\left(6a_1^2\bar{c}_{13}+\bar{c}_{11}\bar{h}^2k^2\right)}\\
& \left[A_{11}^{(2)}-A_{12}^{(2)}+\ldots+(-1)^{n-1}A_{1n}^{(2)}\right]\\
& +\frac{\bar{c}_{31}c_{55}\bar{h}^2k\left(\bar{c}_{11}\bar{h}^2k^2-6a_1^2\bar{c}_{13}\right)}{12a_1\bar{c}_{33}\bar{c}_{55}h\left(6a_1^2\bar{c}_{13}+\bar{c}_{11}\bar{h}^2k^2\right)}\left[A_{12}^{(2)}-3A_{13}^{(2)}+\ldots\right.\\
& \left.+(-1)^{n-1}\frac{n\left(n-1\right)}{2}A_{1n}^{(2)}\right]\\
& +\frac{\bar{c}_{31}\bar{h}^2k^2\left[6a_1^2\bar{c}_{13}\left(c_{55}-2\bar{c}_{55}\right)+\bar{c}_{11}\left(\bar{c}_{55}-c_{55}\right)\bar{h}^2k^2\right]}{24a_1^2\bar{c}_{55}\bar{c}_{33}\left(6a_1^2\bar{c}_{13}+\bar{c}_{11}\bar{h}^2k^2\right)}\\
& \left[B_{31}^{(2)}-B_{32}^{(2)}+\ldots+(-1)^{n-1}B_{3n}^{(2)}\right]\\
& -\frac{c_{33}\bar{h}}{12\bar{c}_{33}h}\left\{B_{31}^{(2)}-3B_{32}^{(2)}+\ldots+(-1)^{n-1}\left[n\left(n-1\right)+1\right]B_{3n}^{(2)}\right\}
\end{aligned}
$$

$$
\begin{aligned}
&-\frac{\bar{c}_{11}\bar{c}_{31}\bar{h}^3k^3-12\bar{c}_{13}\bar{c}_{31}\bar{h}ka_1^2}{12a_1\bar{c}_{33}\left(6a_1^2\bar{c}_{13}+\bar{c}_{11}\bar{h}^2k^2\right)}\left\{5A_{14}^{(3)}+14A_{16}^{(3)}+\ldots+\left[\frac{n(n-1)}{2}-1\right]A_{1n}^{(3)}\right\}\\
&-\frac{\bar{c}_{11}\bar{c}_{31}\bar{h}^3k^3}{12a_1\bar{c}_{33}\left(6a_1^2\bar{c}_{13}+\bar{c}_{11}\bar{h}^2k^2\right)}\left\{7A_{15}^{(3)}+18A_{17}^{(3)}+\ldots+\left[\frac{n(n-1)}{2}-3\right]A_{1n}^{(3)}\right\}\\
&-\frac{1}{3}\left[10B_{35}^{(3)}+21B_{37}^{(3)}+\ldots+\frac{n(n-1)}{2}B_{3n}^{(3)}\right]\\
B_{34}^{(3)}=&-\frac{\bar{h}k\left\{6a_1^2\left[2\bar{c}_{11}\bar{c}_{33}+\bar{c}_{13}\left(c_{31}-2\bar{c}_{31}\right)\right]+\bar{c}_{11}\left(\bar{c}_{31}+c_{31}\right)\bar{h}^2k^2\right\}}{20a_1\bar{c}_{33}\left(6a_1^2\bar{c}_{13}+\bar{c}_{11}\bar{h}^2k^2\right)}\\
&\left[A_{11}^{(2)}-A_{12}^{(2)}+\ldots+(-1)^{n-1}A_{1n}^{(2)}\right]\\
&-\frac{c_{55}\bar{h}^2k\left[a_1^2\left(8\bar{c}_{11}\bar{c}_{33}-6\bar{c}_{13}\bar{c}_{31}\right)+\bar{c}_{11}\bar{c}_{31}\bar{h}^2k^2\right]}{20a_1\bar{c}_{33}\bar{c}_{55}h\left(6a_1^2\bar{c}_{13}+\bar{c}_{11}\bar{h}^2k^2\right)}\\
&\left[A_{12}^{(2)}-3A_{13}^{(2)}+\ldots+\frac{(-1)^{n-1}n(n-1)}{2}A_{1n}^{(2)}\right]\\
&+\bar{h}^2k^2\left[\frac{2a_1^2\left(6\bar{c}_{13}\bar{c}_{31}\bar{c}_{55}-6\bar{c}_{11}\bar{c}_{33}\bar{c}_{55}-3\bar{c}_{13}\bar{c}_{31}c_{55}+4\bar{c}_{11}\bar{c}_{33}c_{55}\right)}{40a_1^2\bar{c}_{55}\bar{c}_{33}\left(6a_1^2\bar{c}_{13}+\bar{c}_{11}\bar{h}^2k^2\right)}\right.\\
&\left.+\frac{\bar{c}_{11}\bar{c}_{31}\left(c_{55}-\bar{c}_{55}\right)\bar{h}^2k^2}{40a_1^2\bar{c}_{55}\bar{c}_{33}\left(6a_1^2\bar{c}_{13}+\bar{c}_{11}\bar{h}^2k^2\right)}\right]\left[B_{31}^2-B_{32}^2+\ldots+(-1)^{n-1}B_{3n}^2\right]\\
&-\frac{c_{33}\bar{h}}{20\bar{c}_{33}h}\left\{B_{31}^{(2)}-3B_{32}^{(2)}+\ldots+(-1)^{n-1}\left[n(n-1)+1\right]B_{3n}^{(2)}\right\}\\
&+\frac{12a_1^2\bar{c}_{11}\bar{c}_{33}\bar{h}k+\bar{c}_{11}\bar{c}_{31}\bar{h}^3k^3-12a_1^2\bar{c}_{13}\bar{c}_{31}\bar{h}k}{20a_1\bar{c}_{33}\left(6a_1^2\bar{c}_{13}+\bar{c}_{11}\bar{h}^2k^2\right)}\\
&\left\{5A_{14}^{(3)}+14A_{16}^{(3)}+\ldots+\left[\frac{n(n-1)}{2}-1\right]A_{1n}^{(3)}\right\}\\
&+\frac{4a_1^2\bar{c}_{11}\bar{c}_{33}\bar{h}k+\bar{c}_{11}\bar{c}_{31}\bar{h}^3k^3}{20a_1\bar{c}_{33}\left(6a_1^2\bar{c}_{13}+\bar{c}_{11}\bar{h}^2k^2\right)}\left\{7A_{15}^{(3)}+18A_{17}^{(3)}+\ldots+\left[\frac{n(n-1)}{2}-3\right]A_{1n}^{(3)}\right\}\\
&-\frac{1}{5}\left\{14B_{36}^{(3)}+27B_{38}^{(3)}+\ldots+\left[\frac{n(n-1)}{2}-1\right]B_{3n}^{(3)}\right\}\\
A_{11}^{(4)}=&-A_{12}^{(4)}-A_{13}^{(4)}-\ldots-A_{1n}^{(4)}-A_{11}^{(2)}-A_{12}^{(2)}-\ldots-A_{1n}^{(2)}
\end{aligned}
\tag{4.22}
$$

$$B_{11}^{(4)} = -B_{12}^{(4)} - B_{13}^{(4)} - \ldots - B_{1n}^{(4)} + B_{11}^{(2)} + B_{12}^{(2)} + \ldots + B_{1n}^{(2)}$$

$$A_{31}^{(4)} = -A_{32}^{(4)} - A_{33}^{(4)} - \ldots - A_{3n}^{(4)} - A_{31}^{(2)} - A_{32}^{(2)} - \ldots - A_{3n}^{(2)}$$

$$B_{31}^{(4)} = -B_{32}^{(4)} - B_{33}^{(4)} - \ldots - B_{3n}^{(4)} + B_{31}^{(2)} + B_{32}^{(2)} + \ldots + B_{3n}^{(2)}$$

The transfer matrix, $\{S_1\}$ for the corresponding boundary conditions can be obtained according to Eq. 4.21, which leads to the corresponding characteristic equation.

Chapter 5

Propagation characteristics of low-order SAWs in a finite plate covered by periodic electrodes

Nowadays, because the overall model of the SAW device structure is mostly complex, it is difficult to directly obtain an accurate solution through the analytical method, so the design and research of the SAW device are generally carried out by numerical analysis methods, among which the FEM is more commonly used one of the means. In actual SAW devices, there are often hundreds of electrodes. The larger the number of units, the more computational cost will undoubtedly be invested. Therefore, in order to control the computational cost, only one of them is usually analyzed separately in most research work.

The Rayleigh-Ritz method can obtain the stiffness matrix and mass matrix of each part of the structure, store them in the matrix in the form of symbolic functions, and then directly call the corresponding functions through various parameters to quickly obtain the required values. In this way, the calculation consumption of a single branch is saved to a large extent. However, through the boundary conditions between the parts in the structure, the transfer matrix between two adjacent parts can be obtained relatively easily. According to the order of distribution of each part in the structure, any two points can be obtained by multiplying the matrices sequentially. The relationship between parts can be sorted out to obtain the transfer matrix of the whole structure, and the stiffness matrix and mass matrix of each part are connected to obtain the characteristic equation of the whole structure. In general, the more comprehensive the boundary conditions considered, the more unknown coefficients can be solved, that is, the smaller the obtained transfer matrix.

To the best of the author's knowledge, there are no studies on the propagation properties of SAWs in finite-size elastic plate structures covered with periodic electrodes by the Rayleigh-

Ritz method. In this chapter, the Rayleigh-Ritz method is still used to obtain the stiffness matrix and mass matrix of each part of the model, and then the transfer matrix is used to connect the various parts to obtain the characteristic equation that characterizes the entire structure. On the basis of the previous two chapters, this chapter also analyzes the dispersion characteristics of the low-order SAWs in the finite structure covered with multi-electrodes under different combinations of the covering layer materials.

This chapter mainly studies the propagation characteristics of low-order SAWs in isotropic substrates in the case of multiple elements. First, based on the conclusions obtained in the previous chapter, this chapter considers the stress boundary conditions corresponding to each free surface in the model and the stress continuity condition on the interface between the upper and lower layers, and uses the bottom surface of the substrate as a fixed boundary condition, thus deriving The transfer matrix corresponding to the general multi-electrode structure is obtained, and the characteristic equation of the overall structure is further obtained; then, the dispersion relationship in the structure composed of multiple electrodes is numerically calculated; finally, the structure of two and three electrode combinations is taken as an example , adopting different permutations and combinations of covering materials, the influence of the combination of the covering layer materials on the velocity dispersion characteristics of low-order SAWs in the structure is analyzed.

5.1 Problem description

The model structure used in this chapter is shown in Fig. 5.1. The unit size used in this chapter is the same as that in the previous chapter. The whole structure is composed of multiple units connected along the x_1 direction.

If the structure only includes a few electrodes at this time, as shown in Fig. 5.1, it is advisable to set the boundary between $x_1 = -\frac{a}{2}$ and $x_1 = \frac{a}{2}$ as a periodic boundary, $\lambda = 2a_1$.

Let the displacement function form of the covering layer be:

$$\begin{aligned}\bar{u}_i^{(r)} = \bar{f}(x_3)\left\{\bar{A}_{in}^{(r)} P_n\left(\frac{2x_3}{\bar{h}}+1\right)\sin\left\{\frac{k}{a_1}\left[x_1 - \frac{(r-3)\lambda}{2}\right]\right\}\right. \\ \left. +\bar{B}_{in}^{(r)} P_n\left(\frac{2x_3}{\bar{h}}+1\right)\cos\left\{\frac{k}{a_1}\left[x_1 - \frac{(r-3)\lambda}{2}\right]\right\}\right\} e^{j\omega t}\end{aligned} \tag{5.1}$$

The displacement function of the substrate takes the form as:

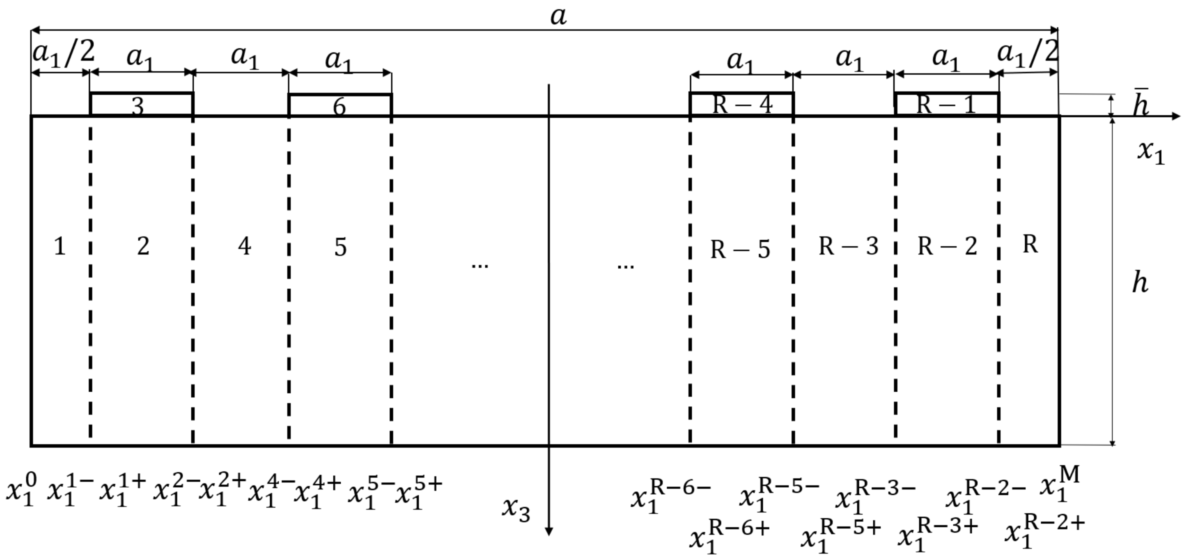

Fig. 5.1 A finite solid covered by periodic electrodes

$$
\begin{aligned}
u_i^{(r)} = f(x_3)\Bigg\{ & A_{in}^{(r)} P_n\left(\frac{2x_3}{h}-1\right)\sin\left\{\frac{2k}{\lambda-a_1}\left[x_1-\frac{(r-2)\lambda+a_1}{4}\right]\right\} \\
& +B_{in}^{(r)} P_n\left(\frac{2x_3}{h}-1\right)\cos\left\{\frac{2k}{\lambda-a_1}\left[x_1-\frac{(r-2)\lambda+a_1}{4}\right]\right\}\Bigg\} e^{j\omega t}
\end{aligned}
\tag{5.2}
$$

where $r = 1,2,3,...R$, denotes the numbering of the individual parts of the unit and the substrate, and $f(x_3)$ and $\bar{f}(x_3)$ are the boundary functions in the x_3 direction. In this chapter, we mainly analyze the propagation characteristics of the SAWs in the structure under the fixed boundary conditions of the substrate bottom surface, and $f(x_3) = \left(1-\frac{x_3}{h}\right)$, $\bar{f}(x_3) = 1$.

According to the conclusion of Chapter 4, this model only considers the following boundary conditions:

(1) Continuous displacement at the interface

$$
u_i^{(r)}(x_3 = 0) = \bar{u}_i^{(r)}(x_3 = 0) \tag{5.3}
$$

(2) Continuous stress at the interface

$$
\sigma_{3i}^{(r)}(x_3 = 0) = \bar{\sigma}_{3i}^{(r)}(x_3 = 0) \tag{5.4}
$$

(3) Free boundary conditions

$$\bar{\sigma}_{3i}^{(r)}\left(x_3=-\bar{h}\right)=0 \tag{5.5}$$

(4) Fixed boundary condition at the bottom of the substrate

$$u_i^{(r)}\left(x_3=h\right)=0 \tag{5.6}$$

5.2 Equation derivation

According to the model, the structure is divided into R parts for calculation, so according to the previous chapter, the kinetic energy and potential energy of this structure can be expressed as:

$$T=T^{(1)}+T^{(2)}+T^{(3)}+\ldots+T^{(R)} \tag{5.7}$$

$$V=V^{(1)}+V^{(2)}+V^{(3)}+\ldots+V^{(R)} \tag{5.8}$$

The steps are the same as in the previous chapter. After sorting, the form of the characteristic equation Eq. 3.15 is still obtained, but the stiffness matrix and mass matrix have certain changes:

$$[K]=\begin{bmatrix}[K]^{(1)} & [0] & \ldots & [0]\\ [0] & [K]^{(2)} & \ldots & [0]\\ \vdots & \vdots & \ddots & \vdots\\ [0] & [0] & \ldots & [K]^{(R)}\end{bmatrix}$$

$$[M]=\begin{bmatrix}[M]^{(1)} & [0] & \ldots & [0]\\ [0] & [M]^{(2)} & \ldots & [0]\\ \vdots & \vdots & \ddots & \vdots\\ [0] & [0] & \ldots & [M]^{(R)}\end{bmatrix} \tag{5.9}$$

$$\{\alpha\}=\begin{Bmatrix}\{\alpha\}^{(1)}\\ \{\alpha\}^{(2)}\\ \vdots\\ \{\alpha\}^{(R)}\end{Bmatrix}$$

The boundary conditions, known as Eqs. 5.3 to 5.6, are used to obtain the transfer matrix $[S_1]$, and the characteristic equations of the computational model are obtained via Eq. 4.12.

In order to fit the actual situation, on the basis of the conclusion in the previous chapter, this chapter adopts the boundary condition that the bottom surface of the substrate is fixed. And in this chapter, the simple transfer matrix method is still used to connect the various parts together according to the boundary conditions to form the characteristic equation of the structure.

The transfer matrix connecting each part of this structure can be abbreviated as:

$$\begin{Bmatrix} A_{1n}^{(r)} \\ B_{1n}^{(r)} \\ A_{3n}^{(r)} \\ B_{3n}^{(r)} \end{Bmatrix} = [S_{r\ r-1}] \begin{Bmatrix} A_{1n}^{(r-1)} \\ B_{1n}^{(r-1)} \\ A_{3n}^{(r-1)} \\ B_{3n}^{(r-1)} \end{Bmatrix} + [S_{r\ r}] \begin{Bmatrix} \tilde{A}_{1n}^{(r)} \\ \tilde{B}_{1n}^{(r)} \\ \tilde{A}_{3n}^{(r)} \\ \tilde{B}_{3n}^{(r)} \end{Bmatrix} \tag{5.10}$$

In Eq. 5.10, $r \neq 2$, when $r = 2$, the formula is written as:

$$\begin{Bmatrix} A_{1n}^{(2)} \\ B_{1n}^{(2)} \\ A_{3n}^{(2)} \\ B_{3n}^{(2)} \end{Bmatrix} = [I] \begin{Bmatrix} A_{1n}^{(2)} \\ B_{1n}^{(2)} \\ A_{3n}^{(2)} \\ B_{3n}^{(2)} \end{Bmatrix} \tag{5.11}$$

where $[I]$ is the identity matrix. And $\left\{ \tilde{A}_{1n}^{(r)} \quad \tilde{B}_{1n}^{(r)} \quad \tilde{A}_{3n}^{(r)} \quad \tilde{B}_{3n}^{(r)} \right\}^T$ means that in addition to the known coefficients A new vector of unknown coefficients composed of other unknown coefficients.

According to the layer matrix relationship between each part, combined with Eq. 5.10, the transfer matrix of the $r(r \geq 5)$ part of the base can be expressed as:

$$\begin{aligned} \begin{Bmatrix} A_{1n}^{(r)} \\ B_{1n}^{(r)} \\ A_{3n}^{(r)} \\ B_{3n}^{(r)} \end{Bmatrix} &= [S_{r\ r-1}][S_{r-1\ r-2}]\ldots[S_{32}] \begin{Bmatrix} A_{1n}^{(2)} \\ B_{1n}^{(2)} \\ A_{3n}^{(2)} \\ B_{3n}^{(2)} \end{Bmatrix} + \ldots \\ &+ [S_{r\ r-1}][S_{r-1\ r-1}] \begin{Bmatrix} A_{1n}^{(r-1)} \\ B_{1n}^{(r-1)} \\ A_{3n}^{(r-1)} \\ B_{3n}^{(r-1)} \end{Bmatrix} + [S_{r\ r}] \begin{Bmatrix} \tilde{A}_{1n}^{(r)} \\ \tilde{B}_{1n}^{(r)} \\ \tilde{A}_{3n}^{(r)} \\ \tilde{B}_{3n}^{(r)} \end{Bmatrix} \end{aligned} \tag{5.12}$$

$$= [S_{r\,2}] \begin{Bmatrix} A_{1n}^{(2)} \\ B_{1n}^{(2)} \\ A_{3n}^{(2)} \\ B_{3n}^{(2)} \end{Bmatrix} + \ldots + [\bar{S}_{r\,r-1}] \begin{Bmatrix} A_{1n}^{(r-1)} \\ B_{1n}^{(r-1)} \\ A_{3n}^{(r-1)} \\ B_{3n}^{(r-1)} \end{Bmatrix} + [S_{r\,r}] \begin{Bmatrix} \tilde{A}_{1n}^{(r)} \\ \tilde{B}_{1n}^{(r)} \\ \tilde{A}_{3n}^{(r)} \\ \tilde{B}_{3n}^{(r)} \end{Bmatrix}$$

Matrix coefficients such as $[S_{r\,r-1}]$, $[S_{r-1\,r-1}]$, $[S_{32}]$, $[S_{r\,r}]$, etc. in Eqs. 5.10 to 5.12 are obtained by substituting the displacement function into The relationship between the unknown coefficients is obtained after the boundary conditions are obtained. After sorting, new matrices $[S_{r\,2}]$, $[\bar{S}_{rr-1}]$, etc. can be obtained. Finally, combine the matrix between the unknown coefficients of each part, and then obtain the obtained transfer matrix according to the distribution order of each part in the stiffness matrix and mass matrix, and the matrix includes the boundary conditions in the structure, the size parameters of each part, and the materials used The physical parameters and other factors play an important role in the analysis of wave propagation problems in structures.

$$[S_1] = \begin{bmatrix} [S_{11}] & [S_{12}] & [0] & \ldots & [0] \\ [0] & [I] & [0] & \ldots & [0] \\ [0] & [S_{32}] & [S_{33}] & \ldots & [0] \\ \vdots & \vdots & \vdots & \ddots & \vdots \\ [0] & [S_{r-1\,2}] & [0] & \ldots & [0] \\ [0] & [S_{r2}] & [0] & \ldots & [S_{rr}] \end{bmatrix} \tag{5.13}$$

In the appendix of this chapter, the relationship between the unknown coefficients in the case of three unit combinations is listed.

5.3 Numerical results and discussion

In this section, we investigate the effect of the number of electrodes and the combination of different covering materials on the SAW propagation characteristics in this structural model. In the following case studies, a fixed boundary condition at the base of the structure is used to In the following case studies, fixed boundary conditions on the bottom surface of the structure are used to better match the situation of the actual SAW device.

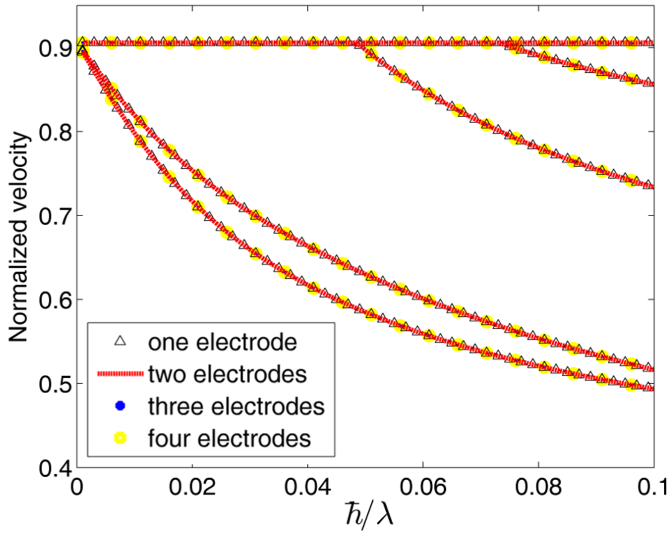

Fig. 5.2 Dispersion curves with the different number of Au electrodes

5.3.1 Effect of the number of elements on the dispersion curve of low-order SAWs

In this subsection, the parameters of Au and Al_2O_3 are used for the overlay material respectively, and the material parameters of fused quartz are still used for the substrate . This section examines whether the number of units has an effect on the propagation of the SAWs in the structure when analysed by the above method. As can be seen from Figs. 5.2 and 5.3, the number of electrodes in the structure has almost no effect on the dispersion curve of the SAWs in this model for the same covering parameters. Since Fig. 5.1 is actually made up of several models as in Fig. 4.1, the number of electrodes has no effect on the wave velocity of the lower order SAWs in the structure, provided that the dimensions and materials of each cell model are the same and the stiffness and mass matrices of each part of the cell are the same.

5.3.2 Dispersion characteristics of low-order SAWs in structures with different covering material combinations

This section mainly studies the propagation characteristics of SAWs in a structure covered with multiple electrodes, where the material of the electrode layer is different but the size of the structure is the same. First, the structure covered with two electrodes is taken as an example. At this time, there are four kinds of combination forms, and two of them are selected here in which the covering layer is made of different materials, that is, the covering

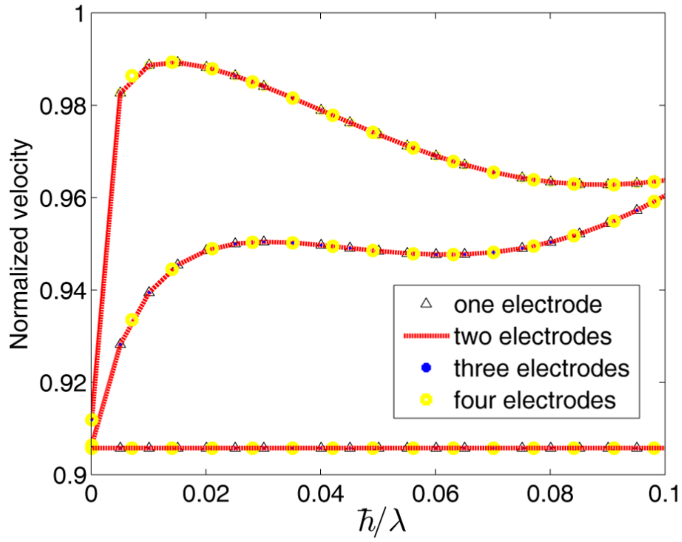

Fig. 5.3 Dispersion curves with different numbers of Al_2O_3 electrodes

material of one unit is Au, and the other is Al_2O_3. The corresponding dispersion curve is shown in Fig. 5.4. For the model covered with three electrodes, there are 8 different material combination modes, only some combinations are listed here: $Au + Al_2O_3 + Al_2O_3$, $Al_2O_3 + Au + Au$, $Au + Al_2O_3 + Au$ and $Al_2O_3 + Au + Al_2O_3$, the dispersion curves of each combination are shown in Fig. 5.5 in turn.

Compared with the model with only one covering material in the previous section, the dispersion curve changes significantly, and the difference becomes more obvious as the thickness of the upper layer increases.

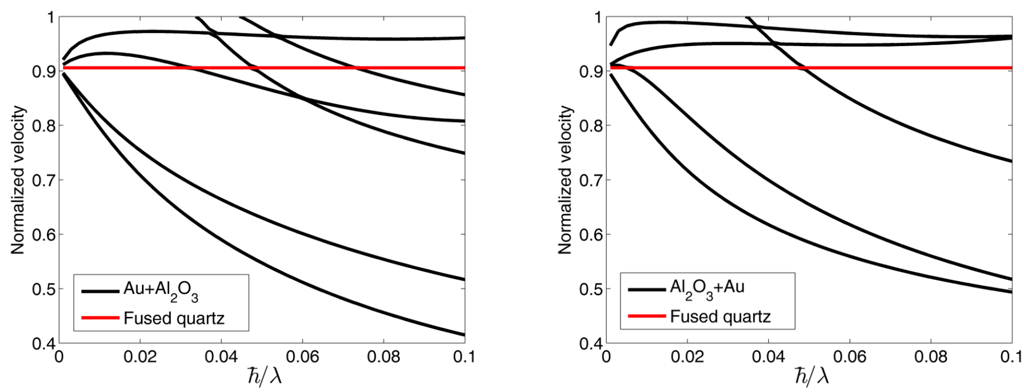

(a) (b)

Fig. 5.4 Dispersion curves for the structure with two electrodes: (a) $Au + Al_2O_3$; (b) $Al_2O_3 + Au$

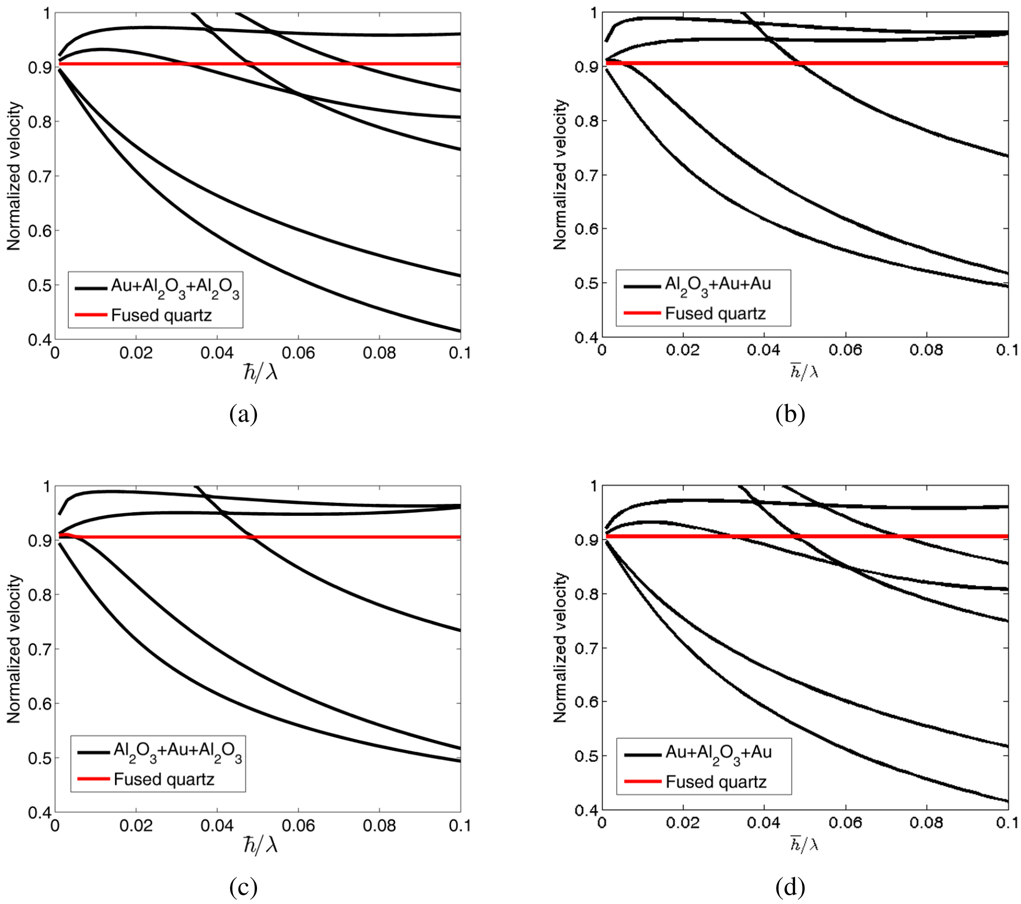

Fig. 5.5 Dispersion curves for structure with three electrodes: (a) $Au + Al_2O_3 + Al_2O_3$; (b) $Al_2O_3 + Au + Au$; (c) $Al_2O_3 + Au + Al_2O_3$; (d) $Au + Al_2O_3 + Au$

5.4 Summary

In this chapter, a simple transfer matrix is derived for a structure covered with multiple periodic electrodes under fixed bottom surface conditions, leading to a reconstruction of the characteristic equations of the structure and a numerical discussion of the effect of the number of electrodes and the material combination of the electrode layers on the dispersion characteristics of the low-order wave velocity in the structure. The specific conclusions are as follows:

(1) In this calculation model, a combination of trigonometric functions and Legendre polynomials is used as the displacement function, and the boundary condition that the bottom edge of the base is fixed is considered. According to the research results, in this calculation model, the number of electrodes in the structure will not have a significant impact on the propagation velocity of the low-order SAWs in the model.

(2) For a structure covered with multiple electrodes, and the materials of the electrode layers are different, the combination of different materials will have a certain influence on the dispersion characteristics of the low-order SAWs in the structure. According to the research results in this chapter, it is found that the combination sequence of materials is the main influencing factor.

5.5 Appendix

This shows the coefficient relationship when there are three unit combinations:

$$A_{11}^{(1)} = -A_{12}^{(1)} - A_{13}^{(1)} - \ldots - A_{1n}^{(1)} - A_{11}^{(2)} - A_{12}^{(2)} - \ldots - A_{1n}^{(2)}$$

$$B_{11}^{(1)} = -B_{12}^{(1)} - B_{13}^{(1)} - \ldots - B_{1n}^{(1)} + B_{11}^{(2)} + B_{12}^{(2)} + \ldots + B_{1n}^{(2)}$$

$$A_{31}^{(1)} = -A_{32}^{(1)} - A_{33}^{(1)} - \ldots - A_{3n}^{(1)} - A_{31}^{(2)} - A_{32}^{(2)} - \ldots - A_{3n}^{(2)}$$

$$B_{31}^{(1)} = -B_{32}^{(1)} - B_{33}^{(1)} - \ldots - B_{3n}^{(1)} + B_{31}^{(2)} + B_{32}^{(2)} + \ldots + B_{3n}^{(2)}$$

$$A_{11}^{(3)} = \frac{6a_1^2\bar{c}_{13}}{6a_1^2\bar{c}_{13} + \bar{c}_{11}\bar{h}^2k^2}\left[A_{11}^{(2)} - A_{12}^{(2)} + \ldots + (-1)^{n-1}A_{1n}^{(2)}\right]$$
$$+ \frac{2a_1^2\bar{c}_{13}c_{55}\bar{h}}{\bar{c}_{55}h\left(6a_1^2\bar{c}_{13} + \bar{c}_{11}\bar{h}^2k^2\right)}\left\{A_{11}^{(2)} - 3A_{12}^{(2)} + 7A_{13}^{(2)} + \ldots\right.$$
$$\left. + (-1)^{n-1}\left[n(n-1)+1\right]A_{1n}^{(2)}\right\}$$

$$
\begin{aligned}
&-\frac{a_1\bar{c}_{13}\bar{h}k\left(3\bar{c}_{55}-2c_{55}\right)}{\bar{c}_{55}\left(6a_1^2\bar{c}_{13}+\bar{c}_{11}\bar{h}^2k^2\right)}\left[B_{31}^{(2)}-B_{32}^{(2)}+\ldots+(-1)^{n-1}B_{3n}^{(2)}\right]\\
&+\frac{6a_1^2\bar{c}_{13}}{6a_1^2\bar{c}_{13}+\bar{c}_{11}\bar{h}^2k^2}\left\{5A_{14}^{(3)}+14A_{16}^{(3)}+\ldots+\left[\frac{n\,(n-1)}{2}-1\right]A_{1n}^{(3)}\right\}\\
&+\frac{2a_1^2\bar{c}_{13}}{6a_1^2\bar{c}_{13}+\bar{c}_{11}\bar{h}^2k^2}\left\{7A_{15}^{(3)}+18A_{17}^{(3)}+\ldots+\left[\frac{n\,(n-1)}{2}-3\right]A_{1n}^{(3)}\right\}
\end{aligned}
$$

$$
\begin{aligned}
A_{12}^{(3)}=&\frac{3\bar{c}_{11}\bar{h}^2k^2}{2\left(6a_1^2\bar{c}_{13}+\bar{c}_{11}\bar{h}^2k^2\right)}\left[A_{11}^{(2)}-A_{12}^{(2)}+\ldots+(-1)^{n-1}A_{1n}^{(2)}\right]\\
&+\frac{\left(\bar{c}_{11}\bar{h}^2k^2-6a_1^2\bar{c}_{13}\right)c_{55}\bar{h}}{4\bar{c}_{55}h\left(6a_1^2\bar{c}_{13}+\bar{c}_{11}\bar{h}^2k^2\right)}\left\{A_{11}^{(2)}-3A_{12}^{(2)}+7A_{13}^{(2)}+\ldots\right.\\
&\left.+(-1)^{n-1}\left[n\,(n-1)+1\right]A_{1n}^{(2)}\right\}\\
&+\frac{\left[6a_1^2\bar{c}_{13}\left(2\bar{c}_{55}-c_{55}\right)+\bar{c}_{11}\left(c_{55}-\bar{c}_{55}\right)\bar{h}^2k^2\right]\bar{h}k}{4a_1\bar{c}_{55}\left(6a_1^2\bar{c}_{13}+\bar{c}_{11}\bar{h}^2k^2\right)}\\
&\left[B_{31}^{(2)}-B_{32}^{(2)}+\ldots+(-1)^{n-1}B_{3n}^{(2)}\right]\\
&+\frac{\bar{c}_{11}\bar{h}^2k^2}{2\left(6a_1^2\bar{c}_{13}+\bar{c}_{11}\bar{h}^2k^2\right)}\left\{3A_{14}^{(3)}+7A_{15}^{(3)}+\ldots+\left[\frac{n\,(n-1)}{2}-3\right]A_{1n}^{(3)}\right\}\\
&-\frac{3a_1^2\bar{c}_{13}}{\left(6a_1^2\bar{c}_{13}+\bar{c}_{11}\bar{h}^2k^2\right)}\left[12A_{14}^{(3)}+30A_{16}^{(3)}+\ldots+n\,(n-1)A_{1n}^{(3)}\right]
\end{aligned}
\tag{5.14}
$$

$$
\begin{aligned}
A_{13}^{(3)}=&-\frac{\bar{c}_{11}\bar{h}^2k^2}{2\left(6a_1^2\bar{c}_{13}+\bar{c}_{11}\bar{h}^2k^2\right)}\left[A_{11}^{(2)}-A_{12}^{(2)}+\ldots+(-1)^{n-1}A_{1n}^{(2)}\right]\\
&-\frac{\left(2{a_1}^2\bar{c}_{13}+\bar{c}_{11}\bar{h}^2k^2\right)c_{55}\bar{h}}{2\bar{c}_{55}h\left(6a_1^2\bar{c}_{13}+\bar{c}_{11}\bar{h}^2k^2\right)}\left\{A_{12}^{(2)}-3A_{13}^{(2)}+12A_{14}^{(2)}+\ldots\right.\\
&\left.+\frac{(-1)^{n-1}\left[n\,(n-1)\right]}{2}A_{1n}^{(2)}\right\}\\
&-\frac{\left[2a_1^2\bar{c}_{13}c_{55}+\bar{c}_{11}\left(c_{55}-\bar{c}_{55}\right)\bar{h}^2k^2\right]\bar{h}k}{4a_1\bar{c}_{55}\left(6a_1^2\bar{c}_{13}+\bar{c}_{11}\bar{h}^2k^2\right)}\left[B_{31}^{(2)}-B_{32}^{(2)}+\ldots+(-1)^{n-1}B_{3n}^{(2)}\right]
\end{aligned}
$$

$$
\begin{aligned}
&-\frac{2a_1^2\bar{c}_{13}}{\left(6a_1^2\bar{c}_{13}+\bar{c}_{11}\bar{h}^2k^2\right)}\left[10A_{15}^{(3)}+15A_{17}^{(3)}+\ldots+\frac{n\,(n-1)}{2}A_{1n}^{(3)}\right]\\
&-\frac{\bar{c}_{11}\bar{h}^2k^2}{2\left(6a_1^2\bar{c}_{13}+\bar{c}_{11}\bar{h}^2k^2\right)}\left\{5A_{14}^{(3)}+9A_{15}^{(3)}+\ldots+\left[\frac{n\,(n-1)}{2}-1\right]A_{1n}^{(3)}\right\}\\
B_{11}^{(3)}=&\ \frac{144a_1^4\bar{c}_{33}^2+18a_1^2\bar{c}_{33}c_{31}\bar{h}^2k^2+\bar{c}_{31}\left(c_{31}-\bar{c}_{31}\right)\bar{h}^4k^4}{24a_1^2\bar{c}_{33}\left(6a_1^2\bar{c}_{33}+\bar{c}_{31}\bar{h}^2k^2\right)}\left[B_{11}^{(2)}-B_{12}^{(2)}+\ldots\right.\\
&\left.+\left(-1\right)^{n-1}B_{1n}^{(2)}\right]+\frac{c_{55}\bar{h}}{12\bar{c}_{55}h}\left[B_{11}^{(2)}-3B_{12}^{(2)}+\ldots+\frac{\left(-1\right)^{n-1}n\,(n-1)}{2}B_{1n}^{(2)}\right]\\
&+\frac{\bar{h}k\left[6a_1^2\bar{c}_{33}\left(6\bar{c}_{55}-c_{55}\right)+\bar{c}_{31}\left(3\bar{c}_{55}-c_{55}\right)\bar{h}^2k^2\right]}{12a_1\bar{c}_{55}\left(6a_1^2\bar{c}_{33}+\bar{c}_{31}\bar{h}^2k^2\right)}\\
&\left[A_{31}^{(2)}-A_{32}^{(2)}+\ldots+\left(-1\right)^{n-1}A_{3n}^{(2)}\right]\\
&-\frac{c_{33}\bar{h}^2k\left(18a_1^2\bar{c}_{33}+\bar{c}_{31}\bar{h}^2k^2\right)}{12a_1\bar{c}_{33}h\left(6a_1^2\bar{c}_{33}+\bar{c}_{31}\bar{h}^2k^2\right)}\left[A_{32}^{(2)}-3A_{33}^{(2)}+\ldots+\frac{\left(-1\right)^{n-1}n\,(n-1)}{2}A_{3n}^{(2)}\right]\\
&+\frac{1}{3}\left\{7B_{15}^{(3)}+18B_{17}^{(3)}+\ldots+\left[\frac{n\,(n-1)}{2}-3\right]B_{1n}^{(3)}\right\} \qquad (5.14)\\
&+\frac{24a_1^2\bar{c}_{33}\bar{h}k+\bar{c}_{31}\bar{h}^3k^3}{12a_1\left(6a_1^2\bar{c}_{33}+\bar{c}_{31}\bar{h}^2k^2\right)}\left\{5A_{34}^{(3)}+14A_{36}^{(3)}+\ldots+\left[\frac{n\,(n-1)}{2}-1\right]A_{3n}^{(3)}\right\}\\
&+\frac{12a_1^2\bar{c}_{33}\bar{h}k+\bar{c}_{31}\bar{h}^3k^3}{12a_1\left(6a_1^2\bar{c}_{33}+\bar{c}_{31}\bar{h}^2k^2\right)}\left\{7A_{35}^{(3)}+18A_{37}^{(3)}+\ldots+\left[\frac{n\,(n-1)}{2}-3\right]A_{3n}^{(3)}\right\}\\
B_{12}^{(3)}=&\ \frac{\bar{h}^2k^2\left[6a_1^2\bar{c}_{33}\left(10\bar{c}_{31}-7c_{31}\right)+\bar{c}_{31}\left(\bar{c}_{31}-c_{31}\right)\bar{h}^2k^2\right]}{40a_1^2\bar{c}_{33}\left(6a_1^2\bar{c}_{33}+\bar{c}_{31}\bar{h}^2k^2\right)}\left[B_{11}^{(2)}-B_{12}^{(2)}+\ldots\right.\\
&\left.+\left(-1\right)^{n-1}B_{1n}^{(2)}\right]+\frac{c_{55}\bar{h}}{10\bar{c}_{55}h}\left[B_{12}^{(2)}-3B_{13}^{(2)}+\ldots+\frac{\left(-1\right)^{n-1}n\,(n-1)}{2}B_{1n}^{(2)}\right]\\
&-\frac{\bar{h}k\left[6a_1^2\bar{c}_{33}\left(10\bar{c}_{55}+c_{55}\right)+\bar{c}_{31}\left(\bar{c}_{55}+c_{55}\right)\bar{h}^2k^2\right]}{20a_1\bar{c}_{55}\left(6a_1^2\bar{c}_{33}+\bar{c}_{31}\bar{h}^2k^2\right)}\\
&\left[A_{31}^{(2)}-A_{32}^{(2)}+\ldots+\left(-1\right)^{n-1}A_{3n}^{(2)}\right]\\
&+\frac{c_{33}\bar{h}^2k\left(42a_1^2\bar{c}_{33}+\bar{c}_{31}\bar{h}^2k^2\right)}{20a_1\bar{c}_{33}h\left(6a_1^2\bar{c}_{33}+\bar{c}_{31}\bar{h}^2k^2\right)}\left[A_{32}^{(2)}-3A_{33}^{(2)}+\ldots+\frac{\left(-1\right)^{n-1}n\,(n-1)}{2}A_{3n}^{(2)}\right]
\end{aligned}
$$

$$
\begin{aligned}
&+\frac{1}{5}\left\{9B_{16}^{(3)}+22B_{18}^{(3)}+\ldots+\left[\frac{n\,(n-1)}{2}-6\right]B_{1n}^{(3)}\right\}\\
&-\frac{60a_1^2\bar{c}_{33}\bar{h}k+\bar{c}_{31}\bar{h}^3k^3}{20a_1\left(6a_1^2\bar{c}_{33}+\bar{c}_{31}\bar{h}^2k^2\right)}\left\{5A_{34}^{(3)}+14A_{36}^{(3)}+\ldots+\left[\frac{n\,(n-1)}{2}-1\right]A_{3n}^{(3)}\right\}\\
&-\frac{24a_1^2\bar{c}_{33}\bar{h}k+\bar{c}_{31}\bar{h}^3k^3}{20a_1\left(6a_1^2\bar{c}_{33}+\bar{c}_{31}\bar{h}^2k^2\right)}\left\{7A_{35}^{(3)}+18A_{37}^{(3)}+\ldots+\left[\frac{n\,(n-1)}{2}-3\right]A_{3n}^{(3)}\right\}\\
&+(-1)^{n-1}B_{1n}^{(2)}\Big]-\frac{c_{55}\bar{h}}{6\bar{c}_{55}h}\left[B_{12}^{(2)}-3B_{13}^{(2)}+\ldots+\frac{(-1)^{n-1}n\,(n-1)}{2}B_{1n}^{(2)}\right]\\
&+\frac{\bar{h}k\left[6a_1^2\bar{c}_{33}c_{55}+\bar{c}_{31}\left(c_{55}-3\bar{c}_{55}\right)\bar{h}^2k^2\right]}{12a_1\bar{c}_{55}\left(6a_1^2\bar{c}_{33}+\bar{c}_{31}\bar{h}^2k^2\right)}\left[A_{31}^{(2)}-A_{32}^{(2)}+\ldots+(-1)^{n-1}A_{3n}^{(2)}\right]\\
&-\frac{c_{33}\bar{h}^2k\left(\bar{c}_{31}\bar{h}^2k^2-6a_1^2\bar{c}_{33}\right)}{12a_1\bar{c}_{33}h\left(6a_1^2\bar{c}_{33}+\bar{c}_{31}\bar{h}^2k^2\right)}\left[A_{32}^{(2)}-3A_{33}^{(2)}+\ldots+\frac{(-1)^{n-1}n\,(n-1)}{2}A_{3n}^{(2)}\right]\\
&-\frac{1}{3}\left[10B_{15}^{(3)}+21B_{17}^{(3)}+\ldots+\frac{n\,(n-1)}{2}B_{1n}^{(3)}\right]\\
&+\frac{12a_1^2\bar{c}_{33}\bar{h}k-\bar{c}_{31}\bar{h}^3k^3}{12a_1\left(6a_1^2\bar{c}_{33}+\bar{c}_{31}\bar{h}^2k^2\right)}\left\{5A_{34}^{(3)}+14A_{36}^{(3)}+\ldots+\left[\frac{n\,(n-1)}{2}-1\right]A_{3n}^{(3)}\right\}\\
&-\frac{\bar{c}_{31}\bar{h}^3k^3}{12a_1\left(6a_1^2\bar{c}_{33}+\bar{c}_{31}\bar{h}^2k^2\right)}\left\{7A_{35}^{(3)}+18A_{37}^{(3)}+\ldots+\left[\frac{n\,(n-1)}{2}-3\right]A_{3n}^{(3)}\right\}
\end{aligned}
\tag{5.14}
$$

$$
\begin{aligned}
B_{14}^{(3)}=&\frac{\bar{h}^2k^2\left[2a_1^2\bar{c}_{33}c_{31}-\bar{c}_{31}\left(\bar{c}_{31}-c_{31}\right)\bar{h}^2k^2\right]}{40a_1^2\bar{c}_{33}\left(6a_1^2\bar{c}_{33}+\bar{c}_{31}\bar{h}^2k^2\right)}\left[B_{11}^{(2)}-B_{12}^{(2)}+\ldots+(-1)^{n-1}B_{1n}^{(2)}\right]\\
&-\frac{c_{55}\bar{h}}{10\bar{c}_{55}h}\left[B_{12}^{(2)}-3B_{13}^{(2)}+\ldots+\frac{(-1)^{n-1}n\,(n-1)}{2}B_{1n}^{(2)}\right]\\
&+\frac{\bar{h}k\left[6a_1^2\bar{c}_{33}c_{55}+\bar{c}_{31}\left(\bar{c}_{55}+c_{55}\right)\bar{h}^2k^2\right]}{20a_1\bar{c}_{55}\left(6a_1^2\bar{c}_{33}+\bar{c}_{31}\bar{h}^2k^2\right)}\left[A_{31}^{(2)}-A_{32}^{(2)}+\ldots+(-1)^{n-1}A_{3n}^{(2)}\right]\\
&-\frac{c_{33}\bar{h}^2k\left(2a_1^2\bar{c}_{33}+\bar{c}_{31}\bar{h}^2k^2\right)}{20a_1\bar{c}_{33}h\left(6a_1^2\bar{c}_{33}+\bar{c}_{31}\bar{h}^2k^2\right)}\left[A_{32}^{(2)}-3A_{33}^{(2)}+\ldots+\frac{(-1)^{n-1}n\,(n-1)}{2}A_{3n}^{(2)}\right]\\
&-\frac{1}{5}\left\{14B_{16}^{(3)}+27B_{18}^{(3)}+\ldots+\left[\frac{n\,(n-1)}{2}-1\right]B_{1n}^{(3)}\right\}
\end{aligned}
$$

$$+\frac{\bar{h}k\left(4a_1^2\bar{c}_{33}+\bar{c}_{31}\bar{h}^2k^2\right)}{20a_1\left(6a_1^2\bar{c}_{33}+\bar{c}_{31}\bar{h}^2k^2\right)}\left\{7A_{35}^{(3)}+18A_{37}^{(3)}+\ldots+\left[\frac{n(n-1)}{2}-3\right]A_{3n}^{(3)}\right\}$$

$$+\frac{\bar{c}_{31}\bar{h}^3k^3}{20a_1\left(6a_1^2\bar{c}_{33}+\bar{c}_{31}\bar{h}^2k^2\right)}\left\{5A_{34}^{(3)}+14A_{36}^{(3)}+\ldots+\left[\frac{n(n-1)}{2}-1\right]A_{3n}^{(3)}\right\}$$

$$A_{31}^{(3)}=-\frac{a_1(3\bar{c}_{31}-2c_{31})\bar{h}k}{\left(6a_1^2\bar{c}_{33}+\bar{c}_{31}\bar{h}^2k^2\right)}\left[B_{11}^{(2)}-B_{12}^{(2)}+\ldots+(-1)^{n-1}B_{1n}^{(2)}\right]$$

$$+\frac{6a_1^2\bar{c}_{33}}{\left(6a_1^2\bar{c}_{33}+\bar{c}_{31}\bar{h}^2k^2\right)}\left[A_{31}^{(2)}-A_{32}^{(2)}+\ldots+(-1)^{n-1}A_{3n}^{(2)}\right]$$

$$-\frac{4a_1^2c_{33}\bar{h}}{h\left(6a_1^2\bar{c}_{33}+\bar{c}_{31}\bar{h}^2k^2\right)}\left[A_{32}^{(2)}-3A_{33}^{(2)}+\ldots+\frac{(-1)^{n-1}n(n-1)}{2}A_{3n}^{(2)}\right]$$

$$+\frac{6a_1^2\bar{c}_{33}}{\left(6a_1^2\bar{c}_{33}+\bar{c}_{31}\bar{h}^2k^2\right)}\left\{5A_{34}^{(3)}+14A_{36}^{(3)}+\ldots+\left[\frac{n(n-1)}{2}-1\right]A_{3n}^{(3)}\right\}$$

$$+\frac{2a_1^2\bar{c}_{33}}{\left(6a_1^2\bar{c}_{33}+\bar{c}_{31}\bar{h}^2k^2\right)}\left\{7A_{35}^{(3)}+18A_{37}^{(3)}+\ldots+\left[\frac{n(n-1)}{2}-3\right]A_{3n}^{(3)}\right\}$$

$$A_{32}^{(3)}=\frac{\left[6a_1^2\bar{c}_{33}(2\bar{c}_{31}-c_{31})+\bar{c}_{31}(c_{31}-\bar{c}_{31})\bar{h}^2k^2\right]\bar{h}k}{4a_1\bar{c}_{33}\left(6a_1^2\bar{c}_{33}+\bar{c}_{31}\bar{h}^2k^2\right)}\left[B_{11}^{(2)}-B_{12}^{(2)}+\ldots\right. \tag{5.14}$$

$$\left.+(-1)^{n-1}B_{1n}^{(2)}\right]+\frac{3\bar{c}_{31}\bar{h}^2k^2}{2\left(6a_1^2\bar{c}_{33}+\bar{c}_{31}\bar{h}^2k^2\right)}\left[A_{31}^{(2)}-A_{32}^{(2)}+\ldots+(-1)^{n-1}A_{3n}^{(2)}\right]$$

$$+\frac{c_{33}\bar{h}\left(6a_1^2\bar{c}_{33}-\bar{c}_{31}\bar{h}^2k^2\right)}{2\bar{c}_{33}h\left(6a_1^2\bar{c}_{33}+\bar{c}_{31}\bar{h}^2k^2\right)}\left[A_{32}^{(2)}-3A_{33}^{(2)}+\ldots+\frac{(-1)^{n-1}n(n-1)}{2}A_{3n}^{(2)}\right]$$

$$+\frac{\bar{c}_{31}\bar{h}^2k^2}{2\left(6a_1^2\bar{c}_{33}+\bar{c}_{31}\bar{h}^2k^2\right)}\left\{3A_{34}^{(3)}+7A_{35}^{(3)}+\ldots+\left[\frac{n(n-1)}{2}-3\right]A_{3n}^{(3)}\right\}$$

$$-\frac{6a_1^2\bar{c}_{33}}{\left(6a_1^2\bar{c}_{33}+\bar{c}_{31}\bar{h}^2k^2\right)}\left[6A_{34}^{(3)}+15A_{36}^{(3)}+\ldots+\frac{n(n-1)}{2}A_{3n}^{(3)}\right]$$

$$A_{33}^{(3)}=-\frac{\left[2a_1^2\bar{c}_{33}c_{31}+\bar{c}_{31}(c_{31}-\bar{c}_{31})\bar{h}^2k^2\right]\bar{h}k}{4a_1\bar{c}_{33}\left(6a_1^2\bar{c}_{33}+\bar{c}_{31}\bar{h}^2k^2\right)}\left[B_{11}^{(2)}-B_{12}^{(2)}+\ldots+(-1)^{n-1}B_{1n}^{(2)}\right]$$

$$-\frac{\bar{c}_{31}\bar{h}^2k^2}{2\left(6a_1^2\bar{c}_{33}+\bar{c}_{31}\bar{h}^2k^2\right)}\left[A_{31}^{(2)}-A_{32}^{(2)}+\ldots+(-1)^{n-1}A_{3n}^{(2)}\right]$$

$$+\frac{c_{33}\bar{h}\left(2a_1^2\bar{c}_{33}+\bar{c}_{31}\bar{h}^2k^2\right)}{2\bar{c}_{33}h\left(6a_1^2\bar{c}_{33}+\bar{c}_{31}\bar{h}^2k^2\right)}\left[A_{32}^{(2)}-3A_{33}^{(2)}+\ldots+\frac{(-1)^{n-1}n(n-1)}{2}A_{3n}^{(2)}\right]$$

$$
\begin{aligned}
& -\frac{\bar{c}_{31}\bar{h}^2k^2}{2\left(6a_1^2\bar{c}_{33}+\bar{c}_{31}\bar{h}^2k^2\right)}\left\{5A_{34}^{(3)}+9A_{35}^{(3)}+14A_{36}^{(3)}+\ldots+\left[\frac{n\,(n-1)}{2}-1\right]A_{3n}^{(3)}\right\} \\
& -\frac{a_1^2\bar{c}_{33}}{\left(6a_1^2\bar{c}_{33}+\bar{c}_{31}\bar{h}^2k^2\right)}\left[20A_{35}^{(3)}+42A_{37}^{(3)}+\ldots+n\,(n-1)\,A_{3n}^{(3)}\right] \\
B_{31}^{(3)} = & \frac{\bar{h}k\left[6a_1^2\,(6\bar{c}_{11}\bar{c}_{33}-\bar{c}_{13}\bar{c}_{31})+\bar{c}_{11}\,(3\bar{c}_{31}-c_{31})\,\bar{h}^2k^2\right]}{12a_1\bar{c}_{33}\left(6a_1^2\bar{c}_{13}+\bar{c}_{11}\bar{h}^2k^2\right)} \\
& \left[A_{11}^{(2)}-A_{12}^{(2)}+\ldots+(-1)^{n-1}A_{1n}^{(2)}\right] \\
& +\frac{c_{55}\bar{h}^2k\left[6a_1^2\,(\bar{c}_{13}\bar{c}_{31}-4\bar{c}_{11}\bar{c}_{33})-\bar{c}_{11}\bar{c}_{31}\bar{h}^2k^2\right]}{12a_1\bar{c}_{33}\bar{c}_{55}h\left(6a_1^2\bar{c}_{13}+\bar{c}_{11}\bar{h}^2k^2\right)} \\
& \left[A_{12}^{(2)}-3A_{13}^{(2)}+\ldots+\frac{(-1)^{n-1}\,n\,(n-1)}{2}A_{1n}^{(2)}\right] \\
& +\left\{\frac{144a_1^4\bar{c}_{13}\bar{c}_{33}\bar{c}_{55}-6a_1^2\left[2\bar{c}_{11}\bar{c}_{33}\,(\bar{c}_{55}-2c_{55})+\bar{c}_{13}\bar{c}_{31}\,(c_{55}-2\bar{c}_{55})\right]\bar{h}^2k^2}{24a_1^2\bar{c}_{55}\bar{c}_{33}\left(6a_1^2\bar{c}_{13}+\bar{c}_{11}\bar{h}^2k^2\right)}\right. \\
& \left.+\frac{\bar{c}_{11}\bar{c}_{31}\,(c_{55}-\bar{c}_{55})\,\bar{h}^4k^4}{24a_1^2\bar{c}_{55}\bar{c}_{33}\left(6a_1^2\bar{c}_{13}+\bar{c}_{11}\bar{h}^2k^2\right)}\right\}\left[B_{31}^{(2)}-B_{32}^{(2)}+\ldots+(-1)^{n-1}B_{3n}^{(2)}\right] \\
& +\frac{c_{33}\bar{h}}{12\bar{c}_{33}h}\left\{B_{21}^{(2)}-3B_{22}^{(2)}+\ldots+(-1)^{n-1}\left[n\,(n-1)+1\right]B_{2n}^{(2)}\right\} \\
& \frac{36a_1^2\bar{c}_{33}\bar{c}_{11}\bar{h}k+\bar{c}_{11}\bar{c}_{31}\bar{h}^3k^3-12a_1^2\bar{c}_{13}\bar{c}_{31}\bar{h}k}{12a_1\bar{c}_{33}\left(6a_1^2\bar{c}_{13}+\bar{c}_{11}\bar{h}^2k^2\right)} \\
& \left\{5A_{14}^{(3)}+14A_{16}^{(3)}+\ldots+\left[\frac{n\,(n-1)}{2}-1\right]A_{1n}^{(3)}\right\} \\
& +\frac{12a_1^2\bar{c}_{11}\bar{c}_{33}\bar{h}k+\bar{c}_{11}\bar{c}_{31}\bar{h}^3k^3}{12a_1\bar{c}_{33}\left(6a_1^2\bar{c}_{13}+\bar{c}_{11}\bar{h}^2k^2\right)}\left\{7A_{15}^{(3)}+18A_{17}^{(3)}+\ldots+\left[\frac{n\,(n-1)}{2}-3\right]A_{1n}^{(3)}\right\} \\
& +\frac{1}{3}\left\{7B_{35}^{(3)}+18B_{37}^{(3)}+\ldots+\left[\frac{n\,(n-1)}{2}-3\right]B_{3n}^{(3)}\right\} \\
B_{32}^{(3)} = & -\frac{\bar{h}k\left\{6a_1^2\left[12\bar{c}_{11}\bar{c}_{33}+\bar{c}_{13}\,(c_{31}-2\bar{c}_{31})\right]+\bar{c}_{11}\,(\bar{c}_{31}+c_{31})\,\bar{h}^2k^2\right\}}{20a_1\bar{c}_{33}\left(6a_1^2\bar{c}_{13}+\bar{c}_{11}\bar{h}^2k^2\right)} \\
& \left[A_{11}^{(2)}-A_{12}^{(2)}+\ldots+(-1)^{n-1}A_{1n}^{(2)}\right] \\
& +\frac{c_{55}\bar{h}^2k\left[-6a_1^2\,(\bar{c}_{13}\bar{c}_{31}-8\bar{c}_{11}\bar{c}_{33})+\bar{c}_{11}\bar{c}_{31}\bar{h}^2k^2\right]}{20a_1\bar{c}_{33}\bar{c}_{55}h\left(6a_1^2\bar{c}_{13}+\bar{c}_{11}\bar{h}^2k^2\right)}
\end{aligned}
\tag{5.14}
$$

$$\left[A_{12}^{(2)}-3A_{13}^{(2)}+\ldots+\frac{(-1)^{n-1}n(n-1)}{2}A_{1n}^{(2)}\right]$$

$$-\bar{h}^2k^2\left\{\frac{6a_1^2\left[\bar{c}_{13}\bar{c}_{31}(2\bar{c}_{55}-c_{55})+4\bar{c}_{11}\bar{c}_{33}(2c_{55}-3\bar{c}_{55})\right]}{40a_1^2\bar{c}_{55}\bar{c}_{33}\left(6a_1^2\bar{c}_{13}+\bar{c}_{11}\bar{h}^2k^2\right)}\right.$$

$$\left.+\frac{\bar{c}_{11}\bar{c}_{31}(c_{55}-\bar{c}_{55})\bar{h}^2k^2}{40a_1^2\bar{c}_{55}\bar{c}_{33}\left(6a_1^2\bar{c}_{13}+\bar{c}_{11}\bar{h}^2k^2\right)}\right\}\left[B_{31}^{(2)}-B_{32}^{(2)}+\ldots+(-1)^{n-1}B_{3n}^{(2)}\right]$$

$$+\frac{c_{33}\bar{h}}{20\bar{c}_{33}h}\left\{B_{21}^{(2)}-3B_{22}^{(2)}+\ldots+(-1)^{n-1}\left[n(n-1)+1\right]B_{2n}^{(2)}\right\}$$

$$-\frac{72\bar{c}_{11}\bar{c}_{33}\bar{h}ka_1^2+\bar{c}_{11}\bar{c}_{31}\bar{h}^3k^3-12\bar{c}_{13}\bar{c}_{31}\bar{h}ka_1^2}{20a_1\bar{c}_{33}\left(6a_1^2\bar{c}_{33}+\bar{c}_{31}\bar{h}^2k^2\right)}$$

$$\left\{5A_{14}^{(3)}+14A_{16}^{(3)}+\ldots+\left[\frac{n(n-1)}{2}-1\right]A_{1n}^{(3)}\right\}$$

$$-\frac{24\bar{c}_{11}\bar{c}_{33}\bar{h}ka_1^2+\bar{c}_{11}\bar{c}_{31}\bar{h}^3k^3}{20a_1\bar{c}_{33}\left(6a_1^2\bar{c}_{33}+\bar{c}_{31}\bar{h}^2k^2\right)}\left\{7A_{15}^{(3)}+18A_{17}^{(3)}+\ldots\right.$$

$$\left.+\left[\frac{n(n-1)}{2}-3\right]A_{1n}^{(3)}\right\}+\frac{1}{5}\left\{9B_{36}^{(3)}+22B_{38}^{(3)}+\ldots+\left[\frac{n(n-1)}{2}-6\right]B_{3n}^{(3)}\right\} \tag{5.14}$$

$$B_{33}^{(3)}=\frac{\bar{h}k\left[6a_1^2\bar{c}_{13}c_{31}+\bar{c}_{11}(c_{31}-3\bar{c}_{31})\bar{h}^2k^2\right]}{12a_1\bar{c}_{33}\left(6a_1^2\bar{c}_{13}+\bar{c}_{11}\bar{h}^2k^2\right)}\left[A_{11}^{(2)}-A_{12}^{(2)}+\ldots+(-1)^{n-1}A_{1n}^{(2)}\right]$$

$$+\frac{\bar{c}_{31}c_{55}\bar{h}^2k\left(\bar{c}_{11}\bar{h}^2k^2-6a_1^2\bar{c}_{13}\right)}{12a_1\bar{c}_{33}\bar{c}_{55}h\left(6a_1^2\bar{c}_{13}+\bar{c}_{11}\bar{h}^2k^2\right)}$$

$$\left[A_{12}^{(2)}-3A_{13}^{(2)}+\ldots+(-1)^{n-1}\frac{n(n-1)}{2}A_{1n}^{(2)}\right]$$

$$+\frac{\bar{c}_{31}\bar{h}^2k^2\left[6a_1^2\bar{c}_{13}(c_{55}-2\bar{c}_{55})+\bar{c}_{11}(\bar{c}_{55}-c_{55})\bar{h}^2k^2\right]}{24a_1^2\bar{c}_{55}\bar{c}_{33}\left(6a_1^2\bar{c}_{13}+\bar{c}_{11}\bar{h}^2k^2\right)}$$

$$\left[B_{31}^{(2)}-B_{32}^{(2)}+\ldots+(-1)^{n-1}B_{3n}^{(2)}\right]$$

$$-\frac{c_{33}\bar{h}}{12\bar{c}_{33}h}\left\{B_{31}^{(2)}-3B_{32}^{(2)}+\ldots+(-1)^{n-1}\left[n(n-1)+1\right]B_{3n}^{(2)}\right\}$$

$$-\frac{\bar{c}_{11}\bar{c}_{31}\bar{h}^3k^3-12\bar{c}_{13}\bar{c}_{31}\bar{h}ka_1^2}{12a_1\bar{c}_{33}\left(6a_1^2\bar{c}_{13}+\bar{c}_{11}\bar{h}^2k^2\right)}\left\{5A_{14}^{(3)}+14A_{16}^{(3)}+\ldots+\left[\frac{n(n-1)}{2}-1\right]A_{1n}^{(3)}\right\}$$

$$-\frac{\bar{c}_{11}\bar{c}_{31}\bar{h}^3k^3}{12a_1\bar{c}_{33}\left(6a_1^2\bar{c}_{13}+\bar{c}_{11}\bar{h}^2k^2\right)}\left\{7A_{15}^{(3)}+18A_{17}^{(3)}+\ldots+\left[\frac{n(n-1)}{2}-3\right]A_{1n}^{(3)}\right\}$$
$$-\frac{1}{3}\left[10B_{35}^{(3)}+21B_{37}^{(3)}+\ldots+\frac{n(n-1)}{2}B_{3n}^{(3)}\right]$$

$$\begin{aligned}
B_{34}^{(3)} =& -\frac{\bar{h}k\left\{6a_1^2\left[2\bar{c}_{11}\bar{c}_{33}+\bar{c}_{13}\left(c_{31}-2\bar{c}_{31}\right)\right]+\bar{c}_{11}\left(\bar{c}_{31}+c_{31}\right)\bar{h}^2k^2\right\}}{20a_1\bar{c}_{33}\left(6a_1^2\bar{c}_{13}+\bar{c}_{11}\bar{h}^2k^2\right)}\\
&\left[A_{11}^{(2)}-A_{12}^{(2)}+\ldots+(-1)^{n-1}A_{1n}^{(2)}\right]\\
&-\frac{c_{55}\bar{h}^2k\left[a_1^2\left(8\bar{c}_{11}\bar{c}_{33}-6\bar{c}_{13}\bar{c}_{31}\right)+\bar{c}_{11}\bar{c}_{31}\bar{h}^2k^2\right]}{20a_1\bar{c}_{33}\bar{c}_{55}h\left(6a_1^2\bar{c}_{13}+\bar{c}_{11}\bar{h}^2k^2\right)}\\
&\left[A_{12}^{(2)}-3A_{13}^{(2)}+\ldots+\frac{(-1)^{n-1}n(n-1)}{2}A_{1n}^{(2)}\right]\\
&+\bar{h}^2k^2\left[\frac{2a_1^2\left(6\bar{c}_{13}\bar{c}_{31}\bar{c}_{55}-6\bar{c}_{11}\bar{c}_{33}\bar{c}_{55}-3\bar{c}_{13}\bar{c}_{31}c_{55}+4\bar{c}_{11}\bar{c}_{33}c_{55}\right)}{40a_1^2\bar{c}_{55}\bar{c}_{33}\left(6a_1^2\bar{c}_{13}+\bar{c}_{11}\bar{h}^2k^2\right)}\right.\\
&\left.+\frac{\bar{c}_{11}\bar{c}_{31}\left(c_{55}-\bar{c}_{55}\right)\bar{h}^2k^2}{40a_1^2\bar{c}_{55}\bar{c}_{33}\left(6a_1^2\bar{c}_{13}+\bar{c}_{11}\bar{h}^2k^2\right)}\right]\left[B_{31}^2-B_{32}^2+\ldots+(-1)^{n-1}B_{3n}^2\right]\\
&-\frac{c_{33}\bar{h}}{20\bar{c}_{33}h}\left\{B_{31}^{(2)}-3B_{32}^{(2)}+\ldots+(-1)^{n-1}\left[n(n-1)+1\right]B_{3n}^{(2)}\right\}\\
&+\frac{12a_1^2\bar{c}_{11}\bar{c}_{33}\bar{h}k+\bar{c}_{11}\bar{c}_{31}\bar{h}^3k^3-12a_1^2\bar{c}_{13}\bar{c}_{31}\bar{h}k}{20a_1\bar{c}_{33}\left(6a_1^2\bar{c}_{13}+\bar{c}_{11}\bar{h}^2k^2\right)}\\
&\left\{5A_{14}^{(3)}+14A_{16}^{(3)}+\ldots+\left[\frac{n(n-1)}{2}-1\right]A_{1n}^{(3)}\right\}\\
&+\frac{4a_1^2\bar{c}_{11}\bar{c}_{33}\bar{h}k+\bar{c}_{11}\bar{c}_{31}\bar{h}^3k^3}{20a_1\bar{c}_{33}\left(6a_1^2\bar{c}_{13}+\bar{c}_{11}\bar{h}^2k^2\right)}\left\{7A_{15}^{(3)}+18A_{17}^{(3)}+\ldots+\left[\frac{n(n-1)}{2}-3\right]A_{1n}^{(3)}\right\}\\
&-\frac{1}{5}\left\{14B_{36}^{(3)}+27B_{38}^{(3)}+\ldots+\left[\frac{n(n-1)}{2}-1\right]B_{3n}^{(3)}\right\}
\end{aligned} \tag{5.14}$$

$$A_{11}^{(4)}=-A_{12}^{(4)}-A_{13}^{(4)}-\ldots-A_{1n}^{(4)}-A_{11}^{(2)}-A_{12}^{(2)}-\ldots-A_{1n}^{(2)}$$
$$B_{11}^{(4)}=-B_{12}^{(4)}-B_{13}^{(4)}-\ldots-B_{1n}^{(4)}+B_{11}^{(2)}+B_{12}^{(2)}+\ldots+B_{1n}^{(2)}$$
$$A_{31}^{(4)}=-A_{32}^{(4)}-A_{33}^{(4)}-\ldots-A_{3n}^{(4)}-A_{31}^{(2)}-A_{32}^{(2)}-\ldots-A_{3n}^{(2)}$$
$$B_{31}^{(4)}=-B_{32}^{(4)}-B_{33}^{(4)}-\ldots-B_{3n}^{(4)}+B_{31}^{(2)}+B_{32}^{(2)}+\ldots+B_{3n}^{(2)}$$
$$A_{11}^{(5)}=-A_{12}^{(5)}-A_{13}^{(5)}-\ldots-A_{1n}^{(5)}+A_{11}^{(2)}+A_{12}^{(2)}+\ldots+A_{1n}^{(2)}$$
$$B_{11}^{(5)}=-B_{12}^{(5)}-B_{13}^{(5)}-\ldots-B_{1n}^{(5)}+B_{11}^{(2)}+B_{12}^{(2)}+\ldots+B_{1n}^{(2)}$$

$$A_{31}^{(5)} = -A_{32}^{(5)} - A_{33}^{(5)} - \ldots - A_{3n}^{(5)} + A_{31}^{(2)} + A_{32}^{(2)} + \ldots + A_{3n}^{(2)}$$

$$B_{31}^{(5)} = -B_{32}^{(5)} - B_{33}^{(5)} - \ldots - B_{3n}^{(5)} + B_{31}^{(2)} + B_{32}^{(2)} + \ldots + B_{3n}^{(2)}$$

$$\begin{aligned}
A_{11}^{(6)} = & \frac{6a_1^2\bar{c}_{13}}{6a_1^2\bar{c}_{13} + \bar{c}_{11}\bar{h}^2k^2}\left(A_{11}^{(2)} + A_{12}^{(2)} + \ldots + A_{1n}^{(2)}\right) \\
& - \frac{a_1\bar{c}_{13}\bar{h}k\,(3\bar{c}_{55} - 2c_{55})}{\bar{c}_{55}\left(6a_1^2\bar{c}_{13} + \bar{c}_{11}\bar{h}^2k^2\right)}\left(B_{31}^{(2)} + B_{32}^{(2)} + \ldots + B_{3n}^{(2)}\right) \\
& - \frac{12a_1^2\bar{c}_{13}}{6a_1^2\bar{c}_{13} + \bar{c}_{11}\bar{h}^2k^2}\left(A_{12}^{(5)} + A_{14}^{(5)} + \ldots + A_{1n}^{(5)}\right) \\
& - \frac{4a_1^2\bar{c}_{13}c_{55}\bar{h}}{\bar{c}_{55}h\left(6a_1^2\bar{c}_{13} + \bar{c}_{11}\bar{h}^2k^2\right)}\left[A_{12}^{(5)} - 3A_{13}^{(5)} + 6A_{14}^{(5)} + \ldots \right. \\
& \left. + (-1)^{n-1}\frac{n(n-1)}{2}A_{1n}^{(5)}\right] + \frac{2a_1\bar{c}_{13}\bar{h}k\,(3\bar{c}_{55} - 2c_{55})}{\bar{c}_{55}\left(6a_1^2\bar{c}_{13} + \bar{c}_{11}\bar{h}^2k^2\right)}\left(B_{32}^{(5)} + B_{34}^{(5)} + \ldots + B_{3n}^{(5)}\right) \\
& + \frac{6a_1^2\bar{c}_{13}}{6a_1^2\bar{c}_{13} + \bar{c}_{11}\bar{h}^2k^2}\left\{5A_{14}^{(6)} + 14A_{16}^{(6)} + \ldots + \left[\frac{n(n-1)}{2} - 1\right]A_{1n}^{(6)}\right\} \\
& + \frac{2a_1^2\bar{c}_{13}}{6a_1^2\bar{c}_{13} + \bar{c}_{11}\bar{h}^2k^2}\left\{7A_{15}^{(6)} + 18A_{17}^{(6)} + \ldots + \left[\frac{n(n-1)}{2} - 3\right]A_{1n}^{(6)}\right\}
\end{aligned} \tag{5.14}$$

$$\begin{aligned}
A_{12}^{(6)} = & \frac{3\bar{c}_{11}\bar{h}^2k^2}{2\left(6a_1^2\bar{c}_{13} + \bar{c}_{11}\bar{h}^2k^2\right)}\left(A_{11}^{(2)} + A_{12}^{(2)} + \ldots + A_{1n}^{(2)}\right) \\
& + \frac{\left[6a_1^2\bar{c}_{13}\,(2\bar{c}_{55} - c_{55}) + \bar{c}_{11}\,(c_{55} - \bar{c}_{55})\,\bar{h}^2k^2\right]\bar{h}k}{4a_1\bar{c}_{55}\left(6a_1^2\bar{c}_{13} + \bar{c}_{11}\bar{h}^2k^2\right)}\left(B_{31}^{(2)} + B_{32}^{(2)} + \ldots + B_{3n}^{(2)}\right) \\
& - \frac{3\bar{c}_{11}\bar{h}^2k^2}{6a_1^2\bar{c}_{13} + \bar{c}_{11}\bar{h}^2k^2}\left(A_{12}^{(5)} + A_{14}^{(5)} + \ldots + A_{1n}^{(5)}\right) - \frac{c_{55}\bar{h}\left(-6a_1^2\bar{c}_{13} + \bar{c}_{11}\bar{h}^2k^2\right)}{2\bar{c}_{55}h\left(6a_1^2\bar{c}_{13} + \bar{c}_{11}\bar{h}^2k^2\right)} \\
& \left[A_{12}^{(5)} - 3A_{13}^{(5)} + 6A_{14}^{(5)} + \ldots + (-1)^{n-1}\frac{n(n-1)}{2}A_{1n}^{(5)}\right] \\
& + \frac{\bar{h}k\left[6a_1^2\bar{c}_{13}\,(-2\bar{c}_{55} + c_{55}) + \bar{c}_{11}\,(\bar{c}_{55} - c_{55})\,\bar{h}^2k^2\right]}{2a_1\bar{c}_{55}\left(6a_1^2\bar{c}_{13} + \bar{c}_{11}\bar{h}^2k^2\right)}\left(B_{32}^{(5)} + B_{34}^{(5)} + \ldots + B_{3n}^{(5)}\right) \\
& - \frac{6a_1^2\bar{c}_{13}}{6a_1^2\bar{c}_{13} + \bar{c}_{11}\bar{h}^2k^2}\left\{6A_{14}^{(6)} + 15A_{16}^{(6)} + \ldots + \frac{n(n-1)}{2}A_{1n}^{(6)}\right\}
\end{aligned}$$

$$
\begin{aligned}
&+\frac{\bar{c}_{11}\bar{h}^2k^2}{2\left(6a_1^2\bar{c}_{13}+\bar{c}_{11}\bar{h}^2k^2\right)}\left\{3A_{14}^{(6)}+7A_{15}^{(6)}+\ldots+\left[\frac{n(n-1)}{2}-3\right]A_{1n}^{(6)}\right\}\\
A_{13}^{(6)} &= -\frac{\bar{c}_{11}\bar{h}^2k^2}{2\left(6a_1^2\bar{c}_{13}+\bar{c}_{11}\bar{h}^2k^2\right)}\left(A_{11}^{(2)}+A_{12}^{(2)}+\ldots+A_{1n}^{(2)}\right)\\
&-\frac{\left[2a_1^2\bar{c}_{13}c_{55}+\bar{c}_{11}\left(c_{55}-\bar{c}_{55}\right)\bar{h}^2k^2\right]\bar{h}k}{4a_1\bar{c}_{55}\left(6a_1^2\bar{c}_{13}+\bar{c}_{11}\bar{h}^2k^2\right)}\left(B_{31}^{(2)}+B_{32}^{(2)}+\ldots+B_{3n}^{(2)}\right)\\
&+\frac{\bar{c}_{11}\bar{h}^2k^2}{6a_1^2\bar{c}_{13}+\bar{c}_{11}\bar{h}^2k^2}\left(A_{12}^{(5)}+A_{14}^{(5)}+\ldots+A_{1n}^{(5)}\right)+\frac{c_{55}\bar{h}\left(2a_1^2\bar{c}_{13}+\bar{c}_{11}\bar{h}^2k^2\right)}{2a_1\bar{c}_{55}h\left(6a_1^2\bar{c}_{13}+\bar{c}_{11}\bar{h}^2k^2\right)}\\
&\left[A_{12}^{(5)}-3A_{13}^{(5)}+6A_{14}^{(5)}+\ldots+(-1)^{n-1}\frac{n(n-1)}{2}A_{1n}^{(5)}\right]\\
&+\frac{\bar{h}k\left[2a_1^2\bar{c}_{13}c_{55}+\bar{c}_{11}\left(-\bar{c}_{55}+c_{55}\right)\bar{h}^2k^2\right]}{2a_1\bar{c}_{55}\left(6a_1^2\bar{c}_{13}+\bar{c}_{11}\bar{h}^2k^2\right)}\left(B_{32}^{(5)}+B_{34}^{(5)}+\ldots+B_{3n}^{(5)}\right)\\
&-\frac{a_1^2\bar{c}_{13}}{6a_1^2\bar{c}_{13}+\bar{c}_{11}\bar{h}^2k^2}\left[20A_{15}^{(6)}+42A_{17}^{(6)}+\ldots+n(n-1)A_{1n}^{(6)}\right]\\
&-\frac{\bar{c}_{11}\bar{h}^2k^2}{2\left(6a_1^2\bar{c}_{13}+\bar{c}_{11}\bar{h}^2k^2\right)}\left\{5A_{14}^{(6)}+9A_{15}^{(6)}+\ldots+\left[\frac{n(n-1)}{2}-1\right]A_{1n}^{(6)}\right\}\\
B_{11}^{(6)} &= \frac{144a_1^4\bar{c}_{33}^2+18a_1^2\bar{c}_{33}c_{31}\bar{h}^2k^2+\bar{c}_{31}\left(c_{31}-\bar{c}_{31}\right)\bar{h}^4k^4}{24a_1^2\bar{c}_{33}\left(6a_1^2\bar{c}_{33}+\bar{c}_{31}\bar{h}^2k^2\right)}\left(B_{11}^{(2)}+B_{12}^{(2)}+\ldots+B_{1n}^{(2)}\right)\\
&+\frac{\bar{h}k\left[6a_1^2\bar{c}_{33}\left(6\bar{c}_{55}-c_{55}\right)+\bar{c}_{31}\left(3\bar{c}_{55}-c_{55}\right)\bar{h}^2k^2\right]}{12a_1\bar{c}_{55}\left(6a_1^2\bar{c}_{33}+\bar{c}_{31}\bar{h}^2k^2\right)}\left(A_{31}^{(2)}+A_{32}^{(2)}+\ldots+A_{3n}^{(2)}\right)\\
&-\frac{c_{55}\bar{h}}{6\bar{c}_{55}h}\left[B_{12}^{(5)}-B_{13}^{(5)}+\ldots+(-1)^{n-1}\frac{n(n-1)}{2}B_{1n}^{(5)}\right]\\
&-\frac{144a_1^4\bar{c}_{33}^2+18a_1^2\bar{c}_{33}c_{31}\bar{h}^2k^2+\bar{c}_{31}\left(c_{31}-\bar{c}_{31}\right)\bar{h}^4k^4}{12a_1^2\bar{c}_{33}\left(6a_1^2\bar{c}_{33}+\bar{c}_{31}\bar{h}^2k^2\right)}\left(B_{12}^{(5)}+B_{14}^{(5)}+\ldots+B_{1n}^{(5)}\right)\\
&-\frac{c_{33}\bar{h}^2k\left(18a_1^2\bar{c}_{33}+\bar{c}_{31}\bar{h}^2k^2\right)}{12a_1\bar{c}_{33}h\left(6a_1^2\bar{c}_{33}+\bar{c}_{31}\bar{h}^2k^2\right)}\left[A_{32}^{(5)}-A_{33}^{(5)}+\ldots+(-1)^{n-1}\frac{n(n-1)}{2}A_{3n}^{(5)}\right]\\
&-\frac{\bar{h}k\left[6a_1^2\bar{c}_{33}\left(6\bar{c}_{55}-c_{55}\right)+\bar{c}_{31}\left(3\bar{c}_{55}-c_{55}\right)\bar{h}^2k^2\right]}{6a_1\bar{c}_{55}\left(6a_1^2\bar{c}_{33}+\bar{c}_{31}\bar{h}^2k^2\right)}\left(A_{32}^{(5)}+A_{34}^{(5)}+\ldots+A_{3n}^{(5)}\right)\\
&+\frac{1}{3}\left\{7B_{15}^{(6)}+18B_{17}^{(6)}+\ldots+\left[\frac{n(n-1)}{2}-3\right]B_{1n}^{(6)}\right\}\\
&+\frac{24a_1^2\bar{c}_{33}\bar{h}k+\bar{c}_{31}\bar{h}^3k^3}{12a_1\left(6a_1^2\bar{c}_{33}+\bar{c}_{31}\bar{h}^2k^2\right)}\left\{5A_{34}^{(6)}+14A_{36}^{(6)}+\ldots+\left[\frac{n(n-1)}{2}-1\right]A_{3n}^{(6)}\right\}
\end{aligned}
\tag{5.14}
$$

$$+\frac{12a_1^2\bar{c}_{33}\bar{h}k+\bar{c}_{31}\bar{h}^3k^3}{12a_1\left(6a_1^2\bar{c}_{33}+\bar{c}_{31}\bar{h}^2k^2\right)}\left\{7A_{35}^{(6)}+18A_{37}^{(6)}+\ldots+\left[\frac{n(n-1)}{2}-3\right]A_{3n}^{(6)}\right\}$$

$$\begin{aligned}
B_{12}^{(6)}=&\frac{\bar{h}^2k^2\left[6a_1^2\bar{c}_{33}\left(10\bar{c}_{31}-7c_{31}\right)+\bar{c}_{31}\left(\bar{c}_{31}-c_{31}\right)\bar{h}^2k^2\right]}{40a_1^2\bar{c}_{33}\left(6a_1^2\bar{c}_{33}+\bar{c}_{31}\bar{h}^2k^2\right)}\\
&\left(B_{11}^{(2)}+B_{12}^{(2)}+\ldots+B_{1n}^{(2)}\right)\\
&-\frac{\bar{h}k\left[6a_1^2\bar{c}_{33}\left(10\bar{c}_{55}+c_{55}\right)+\bar{c}_{31}\left(\bar{c}_{55}+c_{55}\right)\bar{h}^2k^2\right]}{20a_1\bar{c}_{55}\left(6a_1^2\bar{c}_{33}+\bar{c}_{31}\bar{h}^2k^2\right)}\left(A_{31}^{(2)}+A_{32}^{(2)}+\ldots+A_{3n}^{(2)}\right)\\
&-\frac{c_{55}\bar{h}}{10\bar{c}_{55}h}\left[B_{12}^{(5)}-B_{13}^{(5)}+\ldots+(-1)^{n-1}\frac{n(n-1)}{2}B_{1n}^{(5)}\right]\\
&-\frac{\bar{h}^2k^2\left[6a_1^2\bar{c}_{33}\left(10\bar{c}_{31}-7c_{31}\right)+\bar{c}_{31}\left(\bar{c}_{31}-c_{31}\right)\bar{h}^2k^2\right]}{20a_1^2\bar{c}_{33}\left(6a_1^2\bar{c}_{33}+\bar{c}_{31}\bar{h}^2k^2\right)}\\
&\left(B_{12}^{(5)}+B_{14}^{(5)}+\ldots+B_{1n}^{(5)}\right)-\frac{c_{33}\bar{h}^2k\left(42a_1^2\bar{c}_{33}+\bar{c}_{31}\bar{h}^2k^2\right)}{20a_1\bar{c}_{33}h\left(6a_1^2\bar{c}_{33}+\bar{c}_{31}\bar{h}^2k^2\right)}\\
&\left[A_{32}^{(5)}-A_{33}^{(5)}+\ldots+(-1)^{n-1}\frac{n(n-1)}{2}A_{3n}^{(5)}\right]\\
&-\frac{\bar{h}k\left[6a_1^2\bar{c}_{33}\left(10\bar{c}_{55}-c_{55}\right)+\bar{c}_{31}\left(\bar{c}_{55}+c_{55}\right)\bar{h}^2k^2\right]}{10a_1\bar{c}_{55}\left(6a_1^2\bar{c}_{33}+\bar{c}_{31}\bar{h}^2k^2\right)}\left(A_{32}^{(5)}+A_{34}^{(5)}+\ldots+A_{3n}^{(5)}\right)\\
&+\frac{1}{5}\left\{9B_{16}^{(6)}+22B_{18}^{(6)}+\ldots+\left[\frac{n(n-1)}{2}-6\right]B_{1n}^{(6)}\right\}\\
&-\frac{60a_1^2\bar{c}_{33}\bar{h}k+\bar{c}_{31}\bar{h}^3k^3}{20a_1\left(6a_1^2\bar{c}_{33}+\bar{c}_{31}\bar{h}^2k^2\right)}\left\{5A_{34}^{(6)}+14A_{36}^{(6)}+\ldots+\left[\frac{n(n-1)}{2}-1\right]A_{3n}^{(6)}\right\}\\
&-\frac{24a_1^2\bar{c}_{33}\bar{h}k+\bar{c}_{31}\bar{h}^3k^3}{20a_1\left(6a_1^2\bar{c}_{33}+\bar{c}_{31}\bar{h}^2k^2\right)}\left\{7A_{35}^{(6)}+18A_{37}^{(6)}+\ldots+\left[\frac{n(n-1)}{2}-3\right]A_{3n}^{(6)}\right\}
\end{aligned}\tag{5.14}$$

$$\begin{aligned}
B_{13}^{(6)}=&\frac{\bar{h}^2k^2\left[6a_1^2\bar{c}_{33}\left(c_{31}-2\bar{c}_{31}\right)+\bar{c}_{31}\left(\bar{c}_{31}-c_{31}\right)\bar{h}^2k^2\right]}{24a_1^2\bar{c}_{33}\left(6a_1^2\bar{c}_{33}+\bar{c}_{31}\bar{h}^2k^2\right)}\left(B_{11}^{(2)}+B_{12}^{(2)}+\ldots+B_{1n}^{(2)}\right)\\
&+\frac{\bar{h}k\left[6a_1^2\bar{c}_{33}c_{55}+\bar{c}_{31}\left(c_{55}-3\bar{c}_{55}\right)\bar{h}^2k^2\right]}{12a_1\bar{c}_{55}\left(6a_1^2\bar{c}_{33}+\bar{c}_{31}\bar{h}^2k^2\right)}\left(A_{31}^{(2)}+A_{32}^{(2)}+\ldots+A_{3n}^{(2)}\right)\\
&+\frac{c_{55}\bar{h}}{6\bar{c}_{55}h}\left[B_{12}^{(5)}-B_{13}^{(5)}+\ldots+(-1)^{n-1}\frac{n(n-1)}{2}B_{1n}^{(5)}\right]\\
&-\frac{\bar{h}^2k^2\left[a_1^2\left(6\bar{c}_{31}\bar{c}_{33}-3\bar{c}_{33}c_{31}\right)+\bar{c}_{31}\left(c_{31}-\bar{c}_{31}\right)\bar{h}^2k^2\right]}{6a_1^2\bar{c}_{33}\left(6a_1^2\bar{c}_{33}+\bar{c}_{31}\bar{h}^2k^2\right)}
\end{aligned}$$

$$\left(B_{12}^{(5)}+B_{14}^{(5)}+\ldots+B_{1n}^{(5)}\right)+\frac{c_{33}\bar{h}^2k\left(-6a_1^2\bar{c}_{33}+\bar{c}_{31}\bar{h}^2k^2\right)}{12a_1\bar{c}_{33}h\left(6a_1^2\bar{c}_{33}+\bar{c}_{31}\bar{h}^2k^2\right)}$$

$$\left[A_{32}^{(5)}-A_{33}^{(5)}+\ldots+(-1)^{n-1}\frac{n(n-1)}{2}A_{3n}^{(5)}\right]$$

$$-\frac{\bar{h}k\left[6a_1^2\bar{c}_{33}c_{55}+\bar{c}_{31}\left(-3\bar{c}_{55}+c_{55}\right)\bar{h}^2k^2\right]}{6a_1\bar{c}_{55}\left(6a_1^2\bar{c}_{33}+\bar{c}_{31}\bar{h}^2k^2\right)}\left(A_{32}^{(5)}+A_{34}^{(5)}+\ldots+A_{3n}^{(5)}\right)$$

$$-\frac{1}{3}\left[10B_{15}^{(6)}+21B_{17}^{(6)}+\ldots+\frac{n(n-1)}{2}B_{1n}^{(6)}\right]$$

$$+\frac{12a_1^2\bar{c}_{33}\bar{h}k-\bar{c}_{31}\bar{h}^3k^3}{12a_1\left(6a_1^2\bar{c}_{33}+\bar{c}_{31}\bar{h}^2k^2\right)}\left\{5A_{34}^{(6)}+14A_{36}^{(6)}+\ldots+\left[\frac{n(n-1)}{2}-1\right]A_{3n}^{(6)}\right\}$$

$$-\frac{\bar{c}_{31}\bar{h}^3k^3}{12a_1\left(6a_1^2\bar{c}_{33}+\bar{c}_{31}\bar{h}^2k^2\right)}\left\{7A_{35}^{(6)}+18A_{37}^{(6)}+\ldots+\left[\frac{n(n-1)}{2}-3\right]A_{3n}^{(6)}\right\}$$

$$B_{14}^{(6)}=\frac{\bar{h}^2k^2\left[2a_1^2\bar{c}_{33}c_{31}-\bar{c}_{31}\left(\bar{c}_{31}-c_{31}\right)\bar{h}^2k^2\right]}{40a_1^2\bar{c}_{33}\left(6a_1^2\bar{c}_{33}+\bar{c}_{31}\bar{h}^2k^2\right)}\left(B_{11}^{(2)}+B_{12}^{(2)}+\ldots+B_{1n}^{(2)}\right)$$

$$+\frac{\bar{h}k\left[6a_1^2\bar{c}_{33}c_{55}+\bar{c}_{31}\left(\bar{c}_{55}+c_{55}\right)\bar{h}^2k^2\right]}{20a_1\bar{c}_{55}\left(6a_1^2\bar{c}_{33}+\bar{c}_{31}\bar{h}^2k^2\right)}\left(A_{31}^{(2)}+A_{32}^{(2)}+\ldots+A_{3n}^{(2)}\right)$$

$$+\frac{c_{55}\bar{h}}{10\bar{c}_{55}h}\left[B_{12}^{(5)}-B_{13}^{(5)}+\ldots+(-1)^{n-1}\frac{n(n-1)}{2}B_{1n}^{(5)}\right] \quad (5.14)$$

$$-\frac{\bar{h}^2k^2\left[2a_1^2\bar{c}_{33}c_{31}+\bar{c}_{31}\left(c_{31}-\bar{c}_{31}\right)\bar{h}^2k^2\right]}{20a_1^2\bar{c}_{33}\left(6a_1^2\bar{c}_{33}+\bar{c}_{31}\bar{h}^2k^2\right)}\left(B_{12}^{(5)}+B_{14}^{(5)}+\ldots+B_{1n}^{(5)}\right)$$

$$-\frac{c_{33}\bar{h}^2k\left(2a_1^2\bar{c}_{33}+\bar{c}_{31}\bar{h}^2k^2\right)}{20a_1\bar{c}_{33}h\left(6a_1^2\bar{c}_{33}+\bar{c}_{31}\bar{h}^2k^2\right)}\left[A_{32}^{(5)}-A_{33}^{(5)}+\ldots+(-1)^{n-1}\frac{n(n-1)}{2}A_{3n}^{(5)}\right]$$

$$-\frac{\bar{h}k\left[6a_1^2\bar{c}_{33}c_{55}+\bar{c}_{31}\left(\bar{c}_{55}+c_{55}\right)\bar{h}^2k^2\right]}{10a_1\bar{c}_{55}\left(6a_1^2\bar{c}_{33}+\bar{c}_{31}\bar{h}^2k^2\right)}\left(A_{32}^{(5)}+A_{34}^{(5)}+\ldots+A_{3n}^{(5)}\right)$$

$$-\frac{1}{5}\left\{14B_{16}^{(6)}+27B_{18}^{(6)}+\ldots+\left[\frac{n(n-1)}{2}-1\right]B_{1n}^{(6)}\right\}$$

$$+\frac{4a_1^2\bar{c}_{33}\bar{h}k+\bar{c}_{31}\bar{h}^3k^3}{20a_1\left(6a_1^2\bar{c}_{33}+\bar{c}_{31}\bar{h}^2k^2\right)}\left\{7A_{35}^{(6)}+18A_{37}^{(6)}+\ldots+\left[\frac{n(n-1)}{2}-3\right]A_{3n}^{(6)}\right\}$$

$$+\frac{\bar{c}_{31}\bar{h}^3k^3}{20a_1\left(6a_1^2\bar{c}_{33}+\bar{c}_{31}\bar{h}^2k^2\right)}\left\{5A_{34}^{(6)}+14A_{36}^{(6)}+\ldots+\left[\frac{n(n-1)}{2}-1\right]A_{3n}^{(6)}\right\}$$

$$A_{31}^{(6)}=-\frac{a_1\left(3\bar{c}_{31}-2c_{31}\right)\bar{h}k}{\left(6a_1^2\bar{c}_{33}+\bar{c}_{31}\bar{h}^2k^2\right)}\left(B_{11}^{(2)}+B_{12}^{(2)}+\ldots+B_{1n}^{(2)}\right)$$

$$
\begin{aligned}
&+\frac{6a_1^2\bar{c}_{33}}{\left(6a_1^2\bar{c}_{33}+\bar{c}_{31}\bar{h}^2k^2\right)}\left(A_{31}^{(2)}+A_{32}^{(2)}+\ldots+A_{3n}^{(2)}\right)\\
&-\frac{2a_1\bar{h}k\left(3\bar{c}_{31}-2c_{31}\right)}{\left(6a_1^2\bar{c}_{33}+\bar{c}_{31}\bar{h}^2k^2\right)}\left(B_{12}^{(5)}+B_{14}^{(5)}+\ldots+B_{1n}^{(5)}\right)\\
&-\frac{4a_1^2c_{33}\bar{h}}{h\left(6a_1^2\bar{c}_{33}+\bar{c}_{31}\bar{h}^2k^2\right)}\left[A_{32}^{(5)}-3A_{33}^{(5)}+\ldots+(-1)^{n-1}\frac{n\left(n-1\right)}{2}A_{3n}^{(5)}\right]\\
&-\frac{12a_1^2\bar{c}_{33}}{\left(6a_1^2\bar{c}_{33}+\bar{c}_{31}\bar{h}^2k^2\right)}\left(A_{32}^{(5)}+A_{34}^{(5)}+\ldots+A_{3n}^{(5)}\right)\\
&+\frac{2a_1^2\bar{c}_{33}}{20a_1\left(6a_1^2\bar{c}_{33}+\bar{c}_{31}\bar{h}^2k^2\right)}\left\{7A_{35}^{(6)}+18A_{37}^{(6)}+\ldots+\left[\frac{n\left(n-1\right)}{2}-3\right]A_{3n}^{(6)}\right\}\\
&+\frac{6a_1^2\bar{c}_{33}}{\left(6a_1^2\bar{c}_{33}+\bar{c}_{31}\bar{h}^2k^2\right)}\left\{5A_{34}^{(6)}+14A_{36}^{(6)}+\ldots+\left[\frac{n\left(n-1\right)}{2}-1\right]A_{3n}^{(6)}\right\}
\end{aligned}
$$

$$
\begin{aligned}
A_{32}^{(6)}=&\frac{\left[6a_1^2\bar{c}_{33}\left(2\bar{c}_{31}-c_{31}\right)+\bar{c}_{31}\left(c_{31}-\bar{c}_{31}\right)\bar{h}^2k^2\right]\bar{h}k}{4a_1\bar{c}_{33}\left(6a_1^2\bar{c}_{33}+\bar{c}_{31}\bar{h}^2k^2\right)}\left(B_{11}^{(2)}+B_{12}^{(2)}+\ldots+B_{1n}^{(2)}\right)\\
&+\frac{3\bar{c}_{31}\bar{h}^2k^2}{2\left(6a_1^2\bar{c}_{33}+\bar{c}_{31}\bar{h}^2k^2\right)}\left(A_{31}^{(2)}+A_{32}^{(2)}+\ldots+A_{3n}^{(2)}\right)\\
&+\frac{\bar{h}k\left[6a_1^2\bar{c}_{33}\left(c_{31}-2\bar{c}_{31}\right)+\bar{c}_{31}\left(\bar{c}_{31}-c_{31}\right)\bar{h}^2k^2\right]}{2a_1\bar{c}_{33}\left(6a_1^2\bar{c}_{33}+\bar{c}_{31}\bar{h}^2k^2\right)}\left(B_{12}^{(5)}+B_{14}^{(5)}+\ldots+B_{1n}^{(5)}\right)\\
&+\frac{c_{33}\bar{h}\left(6a_1^2\bar{c}_{33}-\bar{c}_{31}\bar{h}^2k^2\right)}{2\bar{c}_{33}h\left(6a_1^2\bar{c}_{33}+\bar{c}_{31}\bar{h}^2k^2\right)}\left[A_{32}^{(5)}-3A_{33}^{(5)}+\ldots+(-1)^{n-1}\frac{n\left(n-1\right)}{2}A_{3n}^{(5)}\right]\\
&-\frac{3\bar{c}_{31}\bar{h}^2k^2}{\left(6a_1^2\bar{c}_{33}+\bar{c}_{31}\bar{h}^2k^2\right)}\left(A_{32}^{(5)}+A_{34}^{(5)}+\ldots+A_{3n}^{(5)}\right)\\
&+\frac{\bar{c}_{31}\bar{h}^2k^2}{2\left(6a_1^2\bar{c}_{33}+\bar{c}_{31}\bar{h}^2k^2\right)}\left\{3A_{34}^{(6)}+7A_{35}^{(6)}+\ldots+\left[\frac{n\left(n-1\right)}{2}-3\right]A_{3n}^{(6)}\right\}\\
&-\frac{6a_1^2\bar{c}_{33}}{\left(6a_1^2\bar{c}_{33}+\bar{c}_{31}\bar{h}^2k^2\right)}\left[6A_{34}^{(6)}+15A_{36}^{(6)}+\ldots+\frac{n\left(n-1\right)}{2}A_{3n}^{(6)}\right]
\end{aligned}
\tag{5.14}
$$

$$
A_{33}^{(6)}=-\frac{\left[2a_1^2\bar{c}_{33}c_{31}+\bar{c}_{31}\left(c_{31}-\bar{c}_{31}\right)\bar{h}^2k^2\right]\bar{h}k}{4a_1\bar{c}_{33}\left(6a_1^2\bar{c}_{33}+\bar{c}_{31}\bar{h}^2k^2\right)}\left(B_{11}^{(2)}+B_{12}^{(2)}+\ldots+B_{1n}^{(2)}\right)
$$

$$
\begin{aligned}
&- \frac{\bar{c}_{31}\bar{h}^2k^2}{2\left(6a_1^2\bar{c}_{33}+\bar{c}_{31}\bar{h}^2k^2\right)}\left(A_{31}^{(2)}+A_{32}^{(2)}+\ldots+A_{3n}^{(2)}\right)\\
&+ \frac{\bar{h}k\left[2a_1^2\bar{c}_{33}c_{31}-\bar{c}_{31}\left(\bar{c}_{31}-c_{31}\right)\bar{h}^2k^2\right]}{2a_1\bar{c}_{33}\left(6a_1^2\bar{c}_{33}+\bar{c}_{31}\bar{h}^2k^2\right)}\left(B_{12}^{(5)}+B_{14}^{(5)}+\ldots+B_{1n}^{(5)}\right)\\
&+ \frac{c_{33}\bar{h}\left(2a_1^2\bar{c}_{33}+\bar{c}_{31}\bar{h}^2k^2\right)}{2\bar{c}_{33}h\left(6a_1^2\bar{c}_{33}+\bar{c}_{31}\bar{h}^2k^2\right)}\left[A_{32}^{(5)}-3A_{33}^{(5)}+\ldots+(-1)^{n-1}\frac{n\left(n-1\right)}{2}A_{3n}^{(5)}\right]\\
&+ \frac{\bar{c}_{31}\bar{h}^2k^2}{\left(6a_1^2\bar{c}_{33}+\bar{c}_{31}\bar{h}^2k^2\right)}\left(A_{32}^{(5)}+A_{34}^{(5)}+\ldots+A_{3n}^{(5)}\right)\\
&- \frac{\bar{c}_{31}\bar{h}^2k^2}{2\left(6a_1^2\bar{c}_{33}+\bar{c}_{31}\bar{h}^2k^2\right)}\left\{5A_{34}^{(6)}+9A_{35}^{(6)}+14A_{36}^{(6)}+\ldots+\left[\frac{n\left(n-1\right)}{2}-1\right]A_{3n}^{(6)}\right\}\\
&- \frac{a_1^2\bar{c}_{33}}{\left(6a_1^2\bar{c}_{33}+\bar{c}_{31}\bar{h}^2k^2\right)}\left[20A_{35}^{(6)}+42A_{37}^{(6)}+\ldots+n(n-1)A_{3n}^{(6)}\right]
\end{aligned}
$$

$$
\begin{aligned}
B_{31}^{(6)} =& \frac{\bar{h}k\left[6a_1^2\left(6\bar{c}_{11}\bar{c}_{33}-\bar{c}_{13}\bar{c}_{31}\right)+\bar{c}_{11}\left(3\bar{c}_{31}-c_{31}\right)\bar{h}^2k^2\right]}{12a_1\bar{c}_{33}\left(6a_1^2\bar{c}_{13}+\bar{c}_{11}\bar{h}^2k^2\right)}\\
&\left(A_{11}^{(2)}+A_{12}^{(2)}+\ldots+A_{1n}^{(2)}\right)+\left(B_{31}^{(2)}+B_{32}^{(2)}+\ldots+B_{3n}^{(2)}\right)\\
&\left\{\frac{144a_1^4\bar{c}_{13}\bar{c}_{33}\bar{c}_{55}+\bar{c}_{11}\bar{c}_{31}\left(c_{55}-\bar{c}_{55}\right)\bar{h}^4k^4}{24a_1^2\bar{c}_{55}\bar{c}_{33}\left(6a_1^2\bar{c}_{13}+\bar{c}_{11}\bar{h}^2k^2\right)}\right.\\
&\left.-\frac{6a_1^2\left[2\bar{c}_{11}\bar{c}_{33}\left(\bar{c}_{55}-2c_{55}\right)+\bar{c}_{13}\bar{c}_{31}\left(c_{55}-2\bar{c}_{55}\right)\right]\bar{h}^2k^2}{24a_1^2\bar{c}_{55}\bar{c}_{33}\left(6a_1^2\bar{c}_{13}+\bar{c}_{11}\bar{h}^2k^2\right)}\right\}\\
&+\frac{\bar{h}k\left[a_1^2\left(6\bar{c}_{13}c_{31}-36\bar{c}_{11}\bar{c}_{33}\right)+\bar{c}_{11}\left(c_{31}-3\bar{c}_{31}\right)\bar{h}^2k^2\right]}{6a_1\bar{c}_{33}\left(6a_1^2\bar{c}_{13}+\bar{c}_{11}\bar{h}^2k^2\right)}\\
&\left(A_{12}^{(5)}+A_{14}^{(5)}+\ldots+A_{1n}^{(5)}\right)+\frac{c_{55}\bar{h}^2k\left(6a_1^2\left(\bar{c}_{13}\bar{c}_{31}-4\bar{c}_{11}\bar{c}_{33}\right)-\bar{c}_{11}\bar{c}_{31}\bar{h}^2k^2\right)}{12a_1\bar{c}_{33}\bar{c}_{55}h\left(6a_1^2\bar{c}_{13}+\bar{c}_{11}\bar{h}^2k^2\right)}\\
&\left[A_{12}^{(5)}-3A_{13}^{(5)}+\ldots+(-1)^{n-1}\frac{n\left(n-1\right)}{2}A_{1n}^{(5)}\right]\\
&-\left(B_{32}^{(5)}+B_{34}^{(5)}+\ldots+B_{3n}^{(5)}\right)\left\{\frac{144a_1^4\bar{c}_{13}\bar{c}_{33}\bar{c}_{55}+\bar{c}_{11}\bar{c}_{31}\left(c_{55}-\bar{c}_{55}\right)\bar{h}^4k^4}{12a_1^2\bar{c}_{55}\bar{c}_{33}\left(6a_1^2\bar{c}_{13}+\bar{c}_{11}\bar{h}^2k^2\right)}\right.\\
&\left.+\frac{6a_1^2\left[2\bar{c}_{11}\bar{c}_{33}\left(\bar{c}_{55}-2c_{55}\right)+\bar{c}_{13}\bar{c}_{31}\left(c_{55}-2\bar{c}_{55}\right)\right]\bar{h}^2k^2}{12a_1^2\bar{c}_{55}\bar{c}_{33}\left(6a_1^2\bar{c}_{13}+\bar{c}_{11}\bar{h}^2k^2\right)}\right\}
\end{aligned}
\tag{5.14}
$$

$$
\begin{aligned}
& -\frac{c_{33}\bar{h}}{6\bar{c}_{33}h}\left[B_{32}^{(5)}-3B_{33}^{(5)}+\ldots+(-1)^{n-1}\frac{n(n-1)}{2}B_{3n}^{(5)}\right] \\
& +\frac{12a_1^2\bar{c}_{11}\bar{c}_{33}\bar{h}k+\bar{c}_{11}\bar{c}_{31}\bar{h}^3k^3}{12a_1\bar{c}_{33}\left(6a_1^2\bar{c}_{13}+\bar{c}_{11}\bar{h}^2k^2\right)}\left\{7A_{15}^{(6)}+18A_{17}^{(6)}+\ldots+\left[\frac{n(n-1)}{2}-3\right]A_{1n}^{(6)}\right\} \\
& +\frac{36a_1^2\bar{c}_{11}\bar{c}_{33}\bar{h}k+\bar{c}_{11}\bar{c}_{31}\bar{h}^3k^3-12a_1^2\bar{c}_{13}\bar{c}_{31}\bar{h}k}{12a_1\bar{c}_{33}\left(6a_1^2\bar{c}_{13}+\bar{c}_{11}\bar{h}^2k^2\right)} \\
& \left\{5A_{14}^{(6)}+14A_{16}^{(6)}+\ldots+\left[\frac{n(n-1)}{2}-1\right]A_{1n}^{(6)}\right\} \\
& +\frac{1}{3}\left\{7B_{35}^{(6)}+18B_{37}^{(6)}+\ldots+\left[\frac{n(n-1)}{2}-3\right]B_{3n}^{(6)}\right\} \\
B_{32}^{(6)} = & -\frac{\bar{h}k\left\{6a_1^2\left[12\bar{c}_{11}\bar{c}_{33}+\bar{c}_{13}\left(c_{31}-2\bar{c}_{31}\right)\right]+\bar{c}_{11}\left(\bar{c}_{31}+c_{31}\right)\bar{h}^2k^2\right\}}{20a_1\bar{c}_{33}\left(6a_1^2\bar{c}_{13}+\bar{c}_{11}\bar{h}^2k^2\right)} \\
& \left(A_{11}^{(2)}+A_{12}^{(2)}+\ldots+A_{1n}^{(2)}\right) \\
& -\bar{h}^2k^2\left\{\frac{6a_1^2\left[\bar{c}_{13}\bar{c}_{31}\left(2\bar{c}_{55}-c_{55}\right)+4\bar{c}_{11}\bar{c}_{33}\left(2c_{55}-3\bar{c}_{55}\right)\right]}{40a_1^2\bar{c}_{55}\bar{c}_{33}\left(6a_1^2\bar{c}_{13}+\bar{c}_{11}\bar{h}^2k^2\right)}\right. \\
& \left.+\frac{\bar{c}_{11}\bar{c}_{31}\left(c_{55}-\bar{c}_{55}\right)\bar{h}^2k^2}{40a_1^2\bar{c}_{55}\bar{c}_{33}\left(6a_1^2\bar{c}_{13}+\bar{c}_{11}\bar{h}^2k^2\right)}\right\}\left(B_{31}^{(2)}+B_{32}^{(2)}+\ldots+B_{3n}^{(2)}\right) \\
& +\frac{\bar{h}k\left\{6a_1^2\left[12\bar{c}_{11}\bar{c}_{33}+\bar{c}_{13}\left(c_{31}-2\bar{c}_{31}\right)\right]+\bar{c}_{11}\left(\bar{c}_{31}+c_{31}\right)\bar{h}^2k^2\right\}}{10a_1\bar{c}_{33}\left(6a_1^2\bar{c}_{13}+\bar{c}_{11}\bar{h}^2k^2\right)} \\
& \left(A_{12}^{(5)}+A_{14}^{(5)}+\ldots+A_{1n}^{(5)}\right) \\
& +\frac{c_{55}\bar{h}^2k\left[-6a_1^2\left(\bar{c}_{13}\bar{c}_{31}-8\bar{c}_{11}\bar{c}_{33}\right)+\bar{c}_{11}\bar{c}_{31}\bar{h}^2k^2\right]}{20a_1\bar{c}_{33}\bar{c}_{55}h\left(6a_1^2\bar{c}_{13}+\bar{c}_{11}\bar{h}^2k^2\right)} \\
& \left[A_{12}^{(5)}-3A_{13}^{(5)}+\ldots+(-1)^{n-1}\frac{n(n-1)}{2}A_{1n}^{(5)}\right] \\
& -\bar{h}^2k^2\left\{\frac{6a_1^2\left[\bar{c}_{13}\bar{c}_{31}\left(2\bar{c}_{55}-c_{55}\right)+4\bar{c}_{11}\bar{c}_{33}\left(2c_{55}-3\bar{c}_{55}\right)\right]}{20a_1^2\bar{c}_{55}\bar{c}_{33}\left(6a_1^2\bar{c}_{13}+\bar{c}_{11}\bar{h}^2k^2\right)}\right. \\
& \left.+\frac{\bar{c}_{11}\bar{c}_{31}\left(c_{55}-\bar{c}_{55}\right)\bar{h}^2k^2}{20a_1^2\bar{c}_{55}\bar{c}_{33}\left(6a_1^2\bar{c}_{13}+\bar{c}_{11}\bar{h}^2k^2\right)}\right\}\left(B_{31}^{(5)}+B_{32}^{(5)}+\ldots+B_{3n}^{(5)}\right) \\
& -\frac{c_{33}\bar{h}}{10\bar{c}_{33}h}\left[B_{32}^{(5)}-3B_{33}^{(5)}+\ldots+(-1)^{n-1}\frac{n(n-1)}{2}B_{3n}^{(5)}\right]
\end{aligned}
\tag{5.14}
$$

$$
\begin{aligned}
&-\frac{72\bar{c}_{11}\bar{c}_{33}\bar{h}ka_1^2+\bar{c}_{11}\bar{c}_{31}\bar{h}^3k^3-12a_1^2\bar{c}_{13}\bar{c}_{31}\bar{h}k}{20a_1\bar{c}_{33}\left(6a_1^2\bar{c}_{13}+\bar{c}_{11}\bar{h}^2k^2\right)}\\
&\left\{5A_{14}^{(6)}+14A_{16}^{(6)}+\ldots+\left[\frac{n(n-1)}{2}-1\right]A_{1n}^{(6)}\right\}\\
&-\frac{24\bar{c}_{11}\bar{c}_{33}\bar{h}ka_1^2+\bar{c}_{11}\bar{c}_{31}\bar{h}^3k^3}{20a_1\bar{c}_{33}\left(6a_1^2\bar{c}_{13}+\bar{c}_{11}\bar{h}^2k^2\right)}\left\{7A_{15}^{(6)}+18A_{17}^{(6)}+\ldots+\left[\frac{n(n-1)}{2}-3\right]A_{1n}^{(6)}\right\}\\
&+\frac{1}{5}\left\{9B_{36}^{(6)}+22B_{38}^{(6)}+\ldots+\left[\frac{n(n-1)}{2}-6\right]B_{3n}^{(6)}\right\}
\end{aligned}
$$

$$
\begin{aligned}
B_{23}^{(6)}=&\frac{\bar{h}k\left[6a_1^2\bar{c}_{13}c_{31}+\bar{c}_{11}\left(c_{31}-3\bar{c}_{31}\right)\bar{h}^2k^2\right]}{12a_1\bar{c}_{33}\left(6a_1^2\bar{c}_{13}+\bar{c}_{11}\bar{h}^2k^2\right)}\left(A_{11}^{(2)}+A_{12}^{(2)}+\ldots+A_{1n}^{(2)}\right)\\
&+\frac{\bar{c}_{31}c_{55}\bar{h}^2k\left(\bar{c}_{11}\bar{h}^2k^2-6a_1^2\bar{c}_{13}\right)}{12a_1\bar{c}_{33}\bar{c}_{55}h\left(6a_1^2\bar{c}_{13}+\bar{c}_{11}\bar{h}^2k^2\right)}\left(B_{31}^{(2)}+B_{32}^{(2)}+\ldots+B_{3n}^{(2)}\right)\\
&+\frac{\bar{h}k\left[6a_1^2\bar{c}_{13}c_{31}+\bar{c}_{11}\left(-3\bar{c}_{31}+c_{31}\right)\bar{h}^2k^2\right]}{6a_1\bar{c}_{33}\left(6a_1^2\bar{c}_{13}+\bar{c}_{11}\bar{h}^2k^2\right)}\left(A_{12}^{(5)}+A_{14}^{(5)}+\ldots+A_{1n}^{(5)}\right)\\
&+\frac{\bar{c}_{31}c_{55}\bar{h}^2k\left(-6a_1^2\bar{c}_{13}+\bar{c}_{11}\bar{h}^2k^2\right)}{12a_1\bar{c}_{33}\bar{c}_{55}h\left(6a_1^2\bar{c}_{13}+\bar{c}_{11}\bar{h}^2k^2\right)}\left[A_{12}^{(5)}-3A_{13}^{(5)}+\ldots(-1)^{n-1}\frac{n(n-1)}{2}A_{1n}^{(5)}\right]\\
&-\frac{\bar{c}_{31}\bar{h}^2k^2\left\{6a_1^2\bar{c}_{13}\left(2\bar{c}_{55}-c_{55}\right)+\bar{c}_{11}\left(c_{55}-\bar{c}_{55}\right)\bar{h}^2k^2\right\}}{12a_1^2\bar{c}_{55}\bar{c}_{33}\left(6a_1^2\bar{c}_{13}+\bar{c}_{11}\bar{h}^2k^2\right)}\\
&\left(B_{31}^{(5)}+B_{32}^{(5)}+\ldots+B_{3n}^{(5)}\right)\\
&-\frac{c_{33}\bar{h}}{6\bar{c}_{33}h}\left[B_{32}^{(5)}-3B_{33}^{(5)}+\ldots+(-1)^{n-1}\frac{n(n-1)}{2}B_{3n}^{(5)}\right]\\
&-\frac{\bar{c}_{11}\bar{c}_{31}\bar{h}^3k^3-12a_1^2\bar{c}_{13}\bar{c}_{31}\bar{h}k}{12a_1\bar{c}_{33}\left(6a_1^2\bar{c}_{13}+\bar{c}_{11}\bar{h}^2k^2\right)}\left\{5A_{14}^{(6)}+14A_{16}^{(6)}+\ldots+\left[\frac{n(n-1)}{2}-1\right]A_{1n}^{(6)}\right\}\\
&-\frac{\bar{c}_{11}\bar{c}_{31}\bar{h}^3k^3}{20a_1\bar{c}_{33}\left(6a_1^2\bar{c}_{13}+\bar{c}_{11}\bar{h}^2k^2\right)}\left\{7A_{15}^{(6)}+18A_{17}^{(6)}+\ldots+\left[\frac{n(n-1)}{2}-3\right]A_{1n}^{(6)}\right\}\\
&-\frac{1}{3}\left[10B_{36}^{(6)}+21B_{38}^{(6)}+\ldots+\frac{n(n-1)}{2}B_{3n}^{(6)}\right]
\end{aligned}
\tag{5.14}
$$

$$
\begin{aligned}
B_{34}^{(6)}=&-\frac{\bar{h}k\left\{6a_1^2\left[2\bar{c}_{11}\bar{c}_{33}+\bar{c}_{13}\left(c_{31}-2\bar{c}_{31}\right)\right]+\bar{c}_{11}\left(\bar{c}_{31}+c_{31}\right)\bar{h}^2k^2\right\}}{20a_1\bar{c}_{33}\left(6a_1^2\bar{c}_{13}+\bar{c}_{11}\bar{h}^2k^2\right)}\\
&\left(A_{11}^{(2)}+A_{12}^{(2)}+\ldots+A_{1n}^{(2)}\right)
\end{aligned}
$$

$$
\begin{aligned}
&+\left[\frac{2a_1^2\left(6\bar{c}_{13}\bar{c}_{31}\bar{c}_{55}-6\bar{c}_{11}\bar{c}_{33}\bar{c}_{55}-3\bar{c}_{13}\bar{c}_{31}c_{55}+4\bar{c}_{11}\bar{c}_{33}c_{55}\right)}{40a_1^2\bar{c}_{55}\bar{c}_{33}\left(6a_1^2\bar{c}_{13}+\bar{c}_{11}\bar{h}^2k^2\right)}\right.\\
&+\left.\frac{\bar{c}_{11}\bar{c}_{31}\left(c_{55}-\bar{c}_{55}\right)\bar{h}^2k^2}{40a_1^2\bar{c}_{55}\bar{c}_{33}\left(6a_1^2\bar{c}_{13}+\bar{c}_{11}\bar{h}^2k^2\right)}\right]\bar{h}^2k^2\left(B_{31}^{(2)}+B_{32}^{(2)}+\ldots+B_{3n}^{(2)}\right)\\
&+\frac{\bar{h}k\left\{6a_1^2\left[12\bar{c}_{11}\bar{c}_{33}+\bar{c}_{13}\left(c_{31}-2\bar{c}_{31}\right)\right]+\bar{c}_{11}\left(\bar{c}_{31}+c_{31}\right)\bar{h}^2k^2\right\}}{10a_1\bar{c}_{33}\left(6a_1^2\bar{c}_{13}+\bar{c}_{11}\bar{h}^2k^2\right)}\\
&\left(A_{12}^{(5)}+A_{14}^{(5)}+\ldots+A_{1n}^{(5)}\right)\\
&+\frac{c_{55}\bar{h}^2k\left(-6a_1^2\left(\bar{c}_{13}\bar{c}_{31}-8\bar{c}_{11}\bar{c}_{33}\right)+\bar{c}_{11}\bar{c}_{31}\bar{h}^2k^2\right)}{20a_1\bar{c}_{33}\bar{c}_{55}h\left(6a_1^2\bar{c}_{13}+\bar{c}_{11}\bar{h}^2k^2\right)}\\
&\left[A_{12}^{(5)}-3A_{13}^{(5)}+\ldots+(-1)^{n-1}\frac{n\left(n-1\right)}{2}A_{1n}^{(5)}\right]\\
&-\left\{\frac{2a_1^2\left[6\bar{c}_{13}\bar{c}_{31}\bar{c}_{55}+4\bar{c}_{11}\bar{c}_{33}c_{55}-3\bar{c}_{13}\bar{c}_{31}c_{55}\right]}{20a_1^2\bar{c}_{55}\bar{c}_{33}\left(6a_1^2\bar{c}_{13}+\bar{c}_{11}\bar{h}^2k^2\right)}\right.\\
&+\left.\frac{\bar{c}_{11}\bar{c}_{31}\left(c_{55}-\bar{c}_{55}\right)\bar{h}^2k^2}{20a_1^2\bar{c}_{55}\bar{c}_{33}\left(6a_1^2\bar{c}_{13}+\bar{c}_{11}\bar{h}^2k^2\right)}\right\}\bar{h}^2k^2\left(B_{31}^{(5)}+B_{32}^{(5)}+\ldots+B_{3n}^{(5)}\right)\\
&+\frac{c_{33}\bar{h}}{10\bar{c}_{33}h}\left[B_{32}^{(5)}-3B_{33}^{(5)}+\ldots+(-1)^{n-1}\frac{n\left(n-1\right)}{2}B_{3n}^{(5)}\right]\\
&+\frac{12\bar{c}_{11}\bar{c}_{33}\bar{h}ka_1^2+\bar{c}_{11}\bar{c}_{31}\bar{h}^3k^3-12a_1^2\bar{c}_{13}\bar{c}_{31}\bar{h}k}{20a_1\bar{c}_{33}\left(6a_1^2\bar{c}_{13}+\bar{c}_{11}\bar{h}^2k^2\right)}\\
&\left\{5A_{14}^{(6)}+14A_{16}^{(6)}+\ldots+\left[\frac{n\left(n-1\right)}{2}-1\right]A_{1n}^{(6)}\right\}\\
&+\frac{4\bar{c}_{11}\bar{c}_{33}\bar{h}ka_1^2+\bar{c}_{11}\bar{c}_{31}\bar{h}^3k^3}{20a_1\bar{c}_{33}\left(6a_1^2\bar{c}_{13}+\bar{c}_{11}\bar{h}^2k^2\right)}\left\{7A_{15}^{(6)}+18A_{17}^{(6)}+\ldots+\left[\frac{n\left(n-1\right)}{2}-3\right]A_{1n}^{(6)}\right\}\\
&-\frac{1}{5}\left\{14B_{36}^{(6)}+27B_{38}^{(6)}+\ldots+\left[\frac{n\left(n-1\right)}{2}-1\right]B_{3n}^{(6)}\right\}
\end{aligned}
\tag{5.14}
$$

$$A_{11}^{(7)}=-A_{12}^{(7)}-A_{13}^{(7)}-\ldots-A_{1n}^{(7)}-A_{11}^{(2)}-A_{12}^{(2)}-\ldots-A_{1n}^{(2)}$$

$$B_{11}^{(7)}=-B_{12}^{(7)}-B_{13}^{(7)}-\ldots-B_{1n}^{(7)}+B_{11}^{(2)}+B_{12}^{(2)}+\ldots+B_{1n}^{(2)}$$

$$A_{31}^{(7)}=-A_{32}^{(7)}-A_{33}^{(7)}-\ldots-A_{3n}^{(7)}-A_{31}^{(2)}-A_{32}^{(2)}-\ldots-A_{3n}^{(2)}$$

$$B_{31}^{(7)}=-B_{32}^{(7)}-B_{33}^{(7)}-\ldots-B_{3n}^{(7)}+B_{31}^{(2)}+B_{32}^{(2)}+\ldots+B_{3n}^{(2)}$$

$$A_{11}^{(8)}=-A_{12}^{(8)}-A_{13}^{(8)}-\ldots-A_{1n}^{(8)}+A_{11}^{(2)}+A_{12}^{(2)}+\ldots+A_{1n}^{(2)}$$

$$B_{11}^{(8)} = -B_{12}^{(8)} - B_{13}^{(8)} - \ldots - B_{1n}^{(8)} + B_{11}^{(2)} + B_{12}^{(2)} + \ldots + B_{1n}^{(2)}$$

$$A_{31}^{(8)} = -A_{32}^{(8)} - A_{33}^{(8)} - \ldots - A_{3n}^{(8)} + A_{31}^{(2)} + A_{32}^{(2)} + \ldots + A_{3n}^{(2)}$$

$$B_{31}^{(8)} = -B_{32}^{(8)} - B_{33}^{(8)} - \ldots - B_{3n}^{(8)} + B_{31}^{(2)} + B_{32}^{(2)} + \ldots + B_{3n}^{(2)}$$

$$\begin{aligned}
A_{11}^{(9)} = & \frac{6a_1^2\bar{c}_{13}}{6a_1^2\bar{c}_{13} + \bar{c}_{11}\bar{h}^2k^2}\left(A_{11}^{(2)} + A_{12}^{(2)} + \ldots + A_{1n}^{(2)}\right) \\
& - \frac{a_1\bar{c}_{13}\bar{h}k\left(3\bar{c}_{55} - 2c_{55}\right)}{\bar{c}_{55}\left(6a_1^2\bar{c}_{13} + \bar{c}_{11}\bar{h}^2k^2\right)}\left(B_{31}^{(2)} + B_{32}^{(2)} + \ldots + B_{3n}^{(2)}\right) \\
& - \frac{12a_1^2\bar{c}_{13}}{6a_1^2\bar{c}_{13} + \bar{c}_{11}\bar{h}^2k^2}\left(A_{12}^{(6)} + A_{14}^{(6)} + \ldots + A_{1n}^{(6)}\right) \\
& - \frac{4a_1^2\bar{c}_{13}c_{55}\bar{h}}{\bar{c}_{55}h\left(6a_1^2\bar{c}_{13} + \bar{c}_{11}\bar{h}^2k^2\right)}\left[A_{12}^{(8)} - 3A_{13}^{(8)} + 6A_{14}^{(8)} + \ldots\right. \\
& \left. + (-1)^{n-1}\frac{n(n-1)}{2}A_{1n}^{(8)}\right] + \frac{2a_1\bar{c}_{13}\bar{h}k\left(3\bar{c}_{55} - 2c_{55}\right)}{\bar{c}_{55}\left(6a_1^2\bar{c}_{13} + \bar{c}_{11}\bar{h}^2k^2\right)}\left(B_{22}^{(8)} + B_{24}^{(8)} + \ldots + B_{2n}^{(8)}\right) \\
& + \frac{6a_1^2\bar{c}_{13}}{6a_1^2\bar{c}_{13} + \bar{c}_{11}\bar{h}^2k^2}\left\{5A_{14}^{(9)} + 14A_{16}^{(9)} + \ldots + \left[\frac{n(n-1)}{2} - 1\right]A_{1n}^{(9)}\right\} \\
& + \frac{2a_1^2\bar{c}_{13}}{6a_1^2\bar{c}_{13} + \bar{c}_{11}\bar{h}^2k^2}\left\{7A_{15}^{(9)} + 18A_{17}^{(9)} + \ldots + \left[\frac{n(n-1)}{2} - 3\right]A_{1n}^{(9)}\right\}
\end{aligned} \tag{5.14}$$

$$\begin{aligned}
A_{12}^{(9)} = & \frac{3\bar{c}_{11}\bar{h}^2k^2}{2\left(6a_1^2\bar{c}_{13} + \bar{c}_{11}\bar{h}^2k^2\right)}\left(A_{11}^{(2)} + A_{12}^{(2)} + \ldots + A_{1n}^{(2)}\right) \\
& + \frac{\left[6a_1^2\bar{c}_{13}\left(2\bar{c}_{55} - c_{55}\right) + \bar{c}_{11}\left(c_{55} - \bar{c}_{55}\right)\bar{h}^2k^2\right]\bar{h}k}{4a_1\bar{c}_{55}\left(6a_1^2\bar{c}_{13} + \bar{c}_{11}\bar{h}^2k^2\right)} \\
& \left(B_{31}^{(2)} + B_{32}^{(2)} + \ldots + B_{3n}^{(2)}\right) - \frac{3\bar{c}_{11}\bar{h}^2k^2}{6a_1^2\bar{c}_{13} + \bar{c}_{11}\bar{h}^2k^2} \\
& \left(A_{12}^{(8)} + A_{14}^{(8)} + \ldots + A_{1n}^{(8)}\right) - \frac{c_{55}\bar{h}\left(-6a_1^2\bar{c}_{13} + \bar{c}_{11}\bar{h}^2k^2\right)}{2\bar{c}_{55}h\left(6a_1^2\bar{c}_{13} + \bar{c}_{11}\bar{h}^2k^2\right)} \\
& \left[A_{12}^{(8)} - 3A_{13}^{(8)} + 6A_{14}^{(8)} + \ldots + (-1)^{n-1}\frac{n(n-1)}{2}A_{1n}^{(8)}\right]
\end{aligned}$$

$$+\frac{\bar{h}k\left[6a_1^2\bar{c}_{13}\left(-2\bar{c}_{55}+c_{55}\right)+\bar{c}_{11}\left(\bar{c}_{55}-c_{55}\right)\bar{h}^2k^2\right]}{2a_1\bar{c}_{55}\left(6a_1^2\bar{c}_{13}+\bar{c}_{11}\bar{h}^2k^2\right)}\left(B_{22}^{(8)}+B_{24}^{(8)}+\ldots+B_{2n}^{(8)}\right)$$

$$-\frac{6a_1^2\bar{c}_{13}}{6a_1^2\bar{c}_{13}+\bar{c}_{11}\bar{h}^2k^2}\left\{6A_{14}^{(9)}+15A_{16}^{(9)}+\ldots+\frac{n\left(n-1\right)}{2}A_{1n}^{(9)}\right\}$$

$$+\frac{\bar{c}_{11}\bar{h}^2k^2}{2\left(6a_1^2\bar{c}_{13}+\bar{c}_{11}\bar{h}^2k^2\right)}\left\{3A_{14}^{(9)}+7A_{15}^{(9)}+\ldots+\left[\frac{n\left(n-1\right)}{2}-3\right]A_{1n}^{(9)}\right\}$$

$$\begin{aligned}
A_{13}^{(9)}= & -\frac{\bar{c}_{11}\bar{h}^2k^2}{2\left(6a_1^2\bar{c}_{13}+\bar{c}_{11}\bar{h}^2k^2\right)}\left(A_{11}^{(2)}+A_{12}^{(2)}+\ldots+A_{1n}^{(2)}\right) \\
& -\frac{\left[2a_1^2\bar{c}_{13}c_{55}+\bar{c}_{11}\left(c_{55}-\bar{c}_{55}\right)\bar{h}^2k^2\right]\bar{h}k}{4a_1\bar{c}_{55}\left(6a_1^2\bar{c}_{13}+\bar{c}_{11}\bar{h}^2k^2\right)}\left(B_{31}^{(2)}+B_{32}^{(2)}+\ldots+B_{3n}^{(2)}\right) \\
& +\frac{\bar{c}_{11}\bar{h}^2k^2}{6a_1^2\bar{c}_{13}+\bar{c}_{11}\bar{h}^2k^2}\left(A_{12}^{(8)}+A_{14}^{(8)}+\ldots+A_{1n}^{(8)}\right) \\
& +\frac{c_{55}\bar{h}\left(2a_1^2\bar{c}_{13}+\bar{c}_{11}\bar{h}^2k^2\right)}{2a_1\bar{c}_{55}h\left(6a_1^2\bar{c}_{13}+\bar{c}_{11}\bar{h}^2k^2\right)}\left[A_{12}^{(8)}-3A_{13}^{(8)}+6A_{14}^{(8)}+\ldots\right. \\
& \left.+\left(-1\right)^{n-1}\frac{n\left(n-1\right)}{2}A_{1n}^{(8)}\right]+\frac{\bar{h}k\left[2a_1^2\bar{c}_{13}c_{55}+\bar{c}_{11}\left(-\bar{c}_{55}+c_{55}\right)\bar{h}^2k^2\right]}{2a_1\bar{c}_{55}\left(6a_1^2\bar{c}_{13}+\bar{c}_{11}\bar{h}^2k^2\right)} \\
& \left(B_{22}^{(8)}+B_{24}^{(8)}+\ldots+B_{2n}^{(8)}\right)-\frac{a_1^2\bar{c}_{13}}{6a_1^2\bar{c}_{13}+\bar{c}_{11}\bar{h}^2k^2} \\
& \left[20A_{15}^{(9)}+42A_{17}^{(9)}+\ldots+n\left(n-1\right)A_{1n}^{(9)}\right] \\
& -\frac{\bar{c}_{11}\bar{h}^2k^2}{2\left(6a_1^2\bar{c}_{13}+\bar{c}_{11}\bar{h}^2k^2\right)}\left\{5A_{14}^{(9)}+9A_{15}^{(9)}+\ldots+\left[\frac{n\left(n-1\right)}{2}-1\right]A_{1n}^{(9)}\right\}
\end{aligned} \tag{5.14}$$

$$\begin{aligned}
B_{11}^{(9)}= & \frac{144a_1^4\bar{c}_{33}^2+18a_1^2\bar{c}_{33}c_{31}\bar{h}^2k^2+\bar{c}_{31}\left(c_{31}-\bar{c}_{31}\right)\bar{h}^4k^4}{24a_1^2\bar{c}_{33}\left(6a_1^2\bar{c}_{33}+\bar{c}_{31}\bar{h}^2k^2\right)}\left(B_{11}^{(2)}+B_{12}^{(2)}+\ldots+B_{1n}^{(2)}\right) \\
& +\frac{\bar{h}k\left[6a_1^2\bar{c}_{33}\left(6\bar{c}_{55}-c_{55}\right)+\bar{c}_{31}\left(3\bar{c}_{55}-c_{55}\right)\bar{h}^2k^2\right]}{12a_1\bar{c}_{55}\left(6a_1^2\bar{c}_{33}+\bar{c}_{31}\bar{h}^2k^2\right)}\left(A_{31}^{(2)}+A_{32}^{(2)}+\ldots+A_{3n}^{(2)}\right) \\
& -\frac{c_{55}\bar{h}}{6\bar{c}_{55}h}\left[B_{12}^{(8)}-B_{13}^{(8)}+\ldots+\left(-1\right)^{n-1}\frac{n\left(n-1\right)}{2}B_{1n}^{(8)}\right] \\
& -\frac{144a_1^4\bar{c}_{33}^2+18a_1^2\bar{c}_{33}c_{31}\bar{h}^2k^2+\bar{c}_{31}\left(c_{31}-\bar{c}_{31}\right)\bar{h}^4k^4}{12a_1^2\bar{c}_{33}\left(6a_1^2\bar{c}_{33}+\bar{c}_{31}\bar{h}^2k^2\right)}\left(B_{12}^{(8)}+B_{14}^{(8)}+\ldots+B_{1n}^{(8)}\right)
\end{aligned}$$

$$
\begin{aligned}
&-\frac{c_{33}\bar{h}^2k\left(18a_1^2\bar{c}_{33}+\bar{c}_{31}\bar{h}^2k^2\right)}{12a_1\bar{c}_{33}h\left(6a_1^2\bar{c}_{33}+\bar{c}_{31}\bar{h}^2k^2\right)}\left[A_{32}^{(8)}-A_{33}^{(8)}+\ldots+(-1)^{n-1}\frac{n(n-1)}{2}A_{3n}^{(8)}\right]\\
&-\frac{\bar{h}k\left[6a_1^2\bar{c}_{33}\left(6\bar{c}_{55}-c_{55}\right)+\bar{c}_{31}\left(3\bar{c}_{55}-c_{55}\right)\bar{h}^2k^2\right]}{6a_1\bar{c}_{55}\left(6a_1^2\bar{c}_{33}+\bar{c}_{31}\bar{h}^2k^2\right)}\left(A_{32}^{(8)}+A_{34}^{(8)}+\ldots+A_{3n}^{(8)}\right)\\
&+\frac{1}{3}\left\{7B_{15}^{(9)}+18B_{17}^{(9)}+\ldots+\left[\frac{n(n-1)}{2}-3\right]B_{1n}^{(9)}\right\}\\
&+\frac{24a_1^2\bar{c}_{33}\bar{h}k+\bar{c}_{31}\bar{h}^3k^3}{12a_1\left(6a_1^2\bar{c}_{33}+\bar{c}_{31}\bar{h}^2k^2\right)}\left\{5A_{34}^{(9)}+14A_{36}^{(9)}+\ldots+\left[\frac{n(n-1)}{2}-1\right]A_{3n}^{(9)}\right\}\\
&+\frac{12a_1^2\bar{c}_{33}\bar{h}k+\bar{c}_{31}\bar{h}^3k^3}{12a_1\left(6a_1^2\bar{c}_{33}+\bar{c}_{31}\bar{h}^2k^2\right)}\left\{7A_{35}^{(9)}+18A_{37}^{(9)}+\ldots+\left[\frac{n(n-1)}{2}-3\right]A_{3n}^{(9)}\right\}\\
B_{12}^{(9)}=&\frac{\bar{h}^2k^2\left[6a_1^2\bar{c}_{33}\left(10\bar{c}_{31}-7c_{31}\right)+\bar{c}_{31}\left(\bar{c}_{31}-c_{31}\right)\bar{h}^2k^2\right]}{40a_1^2\bar{c}_{33}\left(6a_1^2\bar{c}_{33}+\bar{c}_{31}\bar{h}^2k^2\right)}\\
&\left(B_{11}^{(2)}+B_{12}^{(2)}+\ldots+B_{1n}^{(2)}\right)\\
&-\frac{\bar{h}k\left[6a_1^2\bar{c}_{33}\left(10\bar{c}_{55}+c_{55}\right)+\bar{c}_{31}\left(\bar{c}_{55}+c_{55}\right)\bar{h}^2k^2\right]}{20a_1\bar{c}_{55}\left(6a_1^2\bar{c}_{33}+\bar{c}_{31}\bar{h}^2k^2\right)}\left(A_{31}^{(2)}+A_{32}^{(2)}+\ldots+A_{3n}^{(2)}\right)\\
&-\frac{\bar{h}^2k^2\left[6a_1^2\bar{c}_{33}\left(10\bar{c}_{31}-7c_{31}\right)+\bar{c}_{31}\left(\bar{c}_{31}-c_{31}\right)\bar{h}^2k^2\right]}{20a_1^2\bar{c}_{33}\left(6a_1^2\bar{c}_{33}+\bar{c}_{31}\bar{h}^2k^2\right)}\\
&\left(B_{12}^{(8)}+B_{14}^{(8)}+\ldots+B_{1n}^{(8)}\right)-\frac{c_{33}\bar{h}^2k\left(42a_1^2\bar{c}_{33}+\bar{c}_{31}\bar{h}^2k^2\right)}{20a_1\bar{c}_{33}h\left(6a_1^2\bar{c}_{33}+\bar{c}_{31}\bar{h}^2k^2\right)}\\
&\left[A_{32}^{(8)}-A_{33}^{(8)}+\ldots+(-1)^{n-1}\frac{n(n-1)}{2}A_{3n}^{(8)}\right]\\
&-\frac{\bar{h}k\left[6a_1^2\bar{c}_{33}\left(10\bar{c}_{55}-c_{55}\right)+\bar{c}_{31}\left(\bar{c}_{55}+c_{55}\right)\bar{h}^2k^2\right]}{10a_1\bar{c}_{55}\left(6a_1^2\bar{c}_{33}+\bar{c}_{31}\bar{h}^2k^2\right)}\\
&\left(A_{32}^{(8)}+A_{34}^{(8)}+\ldots+A_{3n}^{(8)}\right)+\frac{1}{5}\left\{9B_{16}^{(9)}+22B_{18}^{(9)}+\ldots+\left[\frac{n(n-1)}{2}-6\right]B_{1n}^{(9)}\right\}\\
&-\frac{60a_1^2\bar{c}_{33}\bar{h}k+\bar{c}_{31}\bar{h}^3k^3}{20a_1\left(6a_1^2\bar{c}_{33}+\bar{c}_{31}\bar{h}^2k^2\right)}\left\{5A_{24}^{(9)}+14A_{26}^{(9)}+\ldots+\left[\frac{n(n-1)}{2}-1\right]A_{2n}^{(9)}\right\}\\
&-\frac{24a_1^2\bar{c}_{33}\bar{h}k+\bar{c}_{31}\bar{h}^3k^3}{20a_1\left(6a_1^2\bar{c}_{33}+\bar{c}_{31}\bar{h}^2k^2\right)}\left\{7A_{25}^{(9)}+18A_{27}^{(9)}+\ldots+\left[\frac{n(n-1)}{2}-3\right]A_{2n}^{(9)}\right\}\\
B_{13}^{(9)}=&\frac{\bar{h}^2k^2\left[6a_1^2\bar{c}_{33}\left(c_{31}-2\bar{c}_{31}\right)+\bar{c}_{31}\left(\bar{c}_{31}-c_{31}\right)\bar{h}^2k^2\right]}{24a_1^2\bar{c}_{33}\left(6a_1^2\bar{c}_{33}+\bar{c}_{31}\bar{h}^2k^2\right)}
\end{aligned}
\tag{5.14}
$$

$$
\begin{aligned}
&\left(B_{11}^{(2)}+B_{12}^{(2)}+\ldots+B_{1n}^{(2)}\right)+\frac{\bar{h}k\left[6a_1^2\bar{c}_{33}c_{55}+\bar{c}_{31}\left(c_{55}-3\bar{c}_{55}\right)\bar{h}^2k^2\right]}{12a_1\bar{c}_{55}\left(6a_1^2\bar{c}_{33}+\bar{c}_{31}\bar{h}^2k^2\right)}\\
&\left(A_{31}^{(2)}+A_{32}^{(2)}+\ldots+A_{3n}^{(2)}\right)\\
&+\frac{c_{55}\bar{h}}{6\bar{c}_{55}h}\left[B_{12}^{(8)}-B_{13}^{(8)}+\ldots+(-1)^{n-1}\frac{n(n-1)}{2}B_{1n}^{(8)}\right]\\
&-\frac{\bar{h}^2k^2\left[a_1^2\left(6\bar{c}_{31}\bar{c}_{33}-3\bar{c}_{33}c_{31}\right)+\bar{c}_{31}\left(c_{31}-\bar{c}_{31}\right)\bar{h}^2k^2\right]}{6a_1^2\bar{c}_{33}\left(6a_1^2\bar{c}_{33}+\bar{c}_{31}\bar{h}^2k^2\right)}\\
&\left(B_{12}^{(8)}+B_{14}^{(8)}+\ldots+B_{1n}^{(8)}\right)+\frac{c_{33}\bar{h}^2k\left(-6a_1^2\bar{c}_{33}+\bar{c}_{31}\bar{h}^2k^2\right)}{12a_1\bar{c}_{33}h\left(6a_1^2\bar{c}_{33}+\bar{c}_{31}\bar{h}^2k^2\right)}\\
&\left[A_{32}^{(6)}-A_{33}^{(6)}+\ldots+(-1)^{n-1}\frac{n(n-1)}{2}A_{3n}^{(6)}\right]\\
&-\frac{\bar{h}k\left[6a_1^2\bar{c}_{33}c_{55}+\bar{c}_{31}\left(-3\bar{c}_{55}+c_{55}\right)\bar{h}^2k^2\right]}{6a_1\bar{c}_{55}\left(6a_1^2\bar{c}_{33}+\bar{c}_{31}\bar{h}^2k^2\right)}\left(A_{32}^{(8)}+A_{34}^{(8)}+\ldots+A_{3n}^{(8)}\right)\\
&-\frac{1}{3}\left[10B_{15}^{(9)}+21B_{17}^{(9)}+\ldots+\frac{n(n-1)}{2}B_{1n}^{(9)}\right]\\
&+\frac{12a_1^2\bar{c}_{33}\bar{h}k-\bar{c}_{31}\bar{h}^3k^3}{12a_1\left(6a_1^2\bar{c}_{33}+\bar{c}_{31}\bar{h}^2k^2\right)}\left\{5A_{24}^{(9)}+14A_{26}^{(9)}+\ldots+\left[\frac{n(n-1)}{2}-1\right]A_{2n}^{(9)}\right\}\\
&-\frac{\bar{c}_{31}\bar{h}^3k^3}{12a_1\left(6a_1^2\bar{c}_{33}+\bar{c}_{31}\bar{h}^2k^2\right)}\left\{7A_{25}^{(9)}+18A_{27}^{(9)}+\ldots+\left[\frac{n(n-1)}{2}-3\right]A_{2n}^{(9)}\right\}
\end{aligned}
\tag{5.14}
$$

$$
\begin{aligned}
B_{14}^{(9)}=&\frac{\bar{h}^2k^2\left[2a_1^2\bar{c}_{33}c_{31}-\bar{c}_{31}\left(\bar{c}_{31}-c_{31}\right)\bar{h}^2k^2\right]}{40a_1^2\bar{c}_{33}\left(6a_1^2\bar{c}_{33}+\bar{c}_{31}\bar{h}^2k^2\right)}\left(B_{11}^{(2)}+B_{12}^{(2)}+\ldots+B_{1n}^{(2)}\right)\\
&+\frac{\bar{h}k\left[6a_1^2\bar{c}_{33}c_{55}+\bar{c}_{31}\left(\bar{c}_{55}+c_{55}\right)\bar{h}^2k^2\right]}{20a_1\bar{c}_{55}\left(6a_1^2\bar{c}_{33}+\bar{c}_{31}\bar{h}^2k^2\right)}\left(A_{31}^{(2)}+A_{32}^{(2)}+\ldots+A_{3n}^{(2)}\right)\\
&+\frac{c_{55}\bar{h}}{10\bar{c}_{55}h}\left[B_{12}^{(8)}-B_{13}^{(8)}+\ldots+(-1)^{n-1}\frac{n(n-1)}{2}B_{1n}^{(8)}\right]\\
&-\frac{\bar{h}^2k^2\left[2a_1^2\bar{c}_{33}c_{31}+\bar{c}_{31}\left(c_{31}-\bar{c}_{31}\right)\bar{h}^2k^2\right]}{20a_1^2\bar{c}_{33}\left(6a_1^2\bar{c}_{33}+\bar{c}_{31}\bar{h}^2k^2\right)}\left(B_{12}^{(8)}+B_{14}^{(8)}+\ldots+B_{1n}^{(8)}\right)\\
&-\frac{c_{33}\bar{h}^2k\left(2a_1^2\bar{c}_{33}+\bar{c}_{31}\bar{h}^2k^2\right)}{20a_1\bar{c}_{33}h\left(6a_1^2\bar{c}_{33}+\bar{c}_{31}\bar{h}^2k^2\right)}\left[A_{32}^{(8)}-A_{33}^{(8)}+\ldots+(-1)^{n-1}\frac{n(n-1)}{2}A_{3n}^{(8)}\right]
\end{aligned}
$$

$$
\begin{aligned}
& -\frac{\bar{h}k\left[6a_1^2\bar{c}_{33}c_{55}+\bar{c}_{31}\left(\bar{c}_{55}+c_{55}\right)\bar{h}^2k^2\right]}{10a_1\bar{c}_{55}\left(6a_1^2\bar{c}_{33}+\bar{c}_{31}\bar{h}^2k^2\right)}\left(A_{32}^{(8)}+A_{34}^{(8)}+\ldots+A_{3n}^{(8)}\right) \\
& -\frac{1}{5}\left\{14B_{16}^{(9)}+27B_{18}^{(9)}+\ldots+\left[\frac{n(n-1)}{2}-1\right]B_{1n}^{(9)}\right\} \\
& +\frac{4a_1^2\bar{c}_{33}\bar{h}k+\bar{c}_{31}\bar{h}^3k^3}{20a_1\left(6a_1^2\bar{c}_{33}+\bar{c}_{31}\bar{h}^2k^2\right)}\left\{7A_{25}^{(9)}+18A_{27}^{(9)}+\ldots+\left[\frac{n(n-1)}{2}-3\right]A_{2n}^{(9)}\right\} \\
& +\frac{\bar{c}_{31}\bar{h}^3k^3}{20a_1\left(6a_1^2\bar{c}_{33}+\bar{c}_{31}\bar{h}^2k^2\right)}\left\{5A_{24}^{(9)}+14A_{26}^{(9)}+\ldots+\left[\frac{n(n-1)}{2}-1\right]A_{2n}^{(9)}\right\} \\
A_{31}^{(9)} = & -\frac{a_1\left(3\bar{c}_{31}-2c_{31}\right)\bar{h}k}{\left(6a_1^2\bar{c}_{33}+\bar{c}_{31}\bar{h}^2k^2\right)}\left(B_{11}^{(2)}+B_{12}^{(2)}+\ldots+B_{1n}^{(2)}\right) \\
& +\frac{6a_1^2\bar{c}_{33}}{\left(6a_1^2\bar{c}_{33}+\bar{c}_{31}\bar{h}^2k^2\right)}\left(A_{31}^{(2)}+A_{32}^{(2)}+\ldots+A_{3n}^{(2)}\right) \\
& -\frac{2a_1\bar{h}k\left(3\bar{c}_{31}-2c_{31}\right)}{\left(6a_1^2\bar{c}_{33}+\bar{c}_{31}\bar{h}^2k^2\right)}\left(B_{12}^{(6)}+B_{14}^{(6)}+\ldots+B_{1n}^{(6)}\right) \\
& -\frac{4a_1^2c_{33}\bar{h}}{h\left(6a_1^2\bar{c}_{33}+\bar{c}_{31}\bar{h}^2k^2\right)}\left[A_{32}^{(8)}-A_{33}^{(8)}+\ldots+(-1)^{n-1}\frac{n(n-1)}{2}A_{3n}^{(8)}\right] \\
& -\frac{12a_1^2\bar{c}_{33}}{\left(6a_1^2\bar{c}_{33}+\bar{c}_{31}\bar{h}^2k^2\right)}\left(A_{32}^{(8)}+A_{34}^{(8)}+\ldots+A_{3n}^{(8)}\right) \\
& +\frac{2a_1^2\bar{c}_{33}}{20a_1\left(6a_1^2\bar{c}_{33}+\bar{c}_{31}\bar{h}^2k^2\right)}\left\{7A_{25}^{(9)}+18A_{27}^{(9)}+\ldots+\left[\frac{n(n-1)}{2}-3\right]A_{2n}^{(9)}\right\} \\
& +\frac{6a_1^2\bar{c}_{33}}{\left(6a_1^2\bar{c}_{33}+\bar{c}_{31}\bar{h}^2k^2\right)}\left\{5A_{24}^{(9)}+14A_{26}^{(9)}+\ldots+\left[\frac{n(n-1)}{2}-1\right]A_{2n}^{(9)}\right\} \\
A_{32}^{(9)} = & \frac{\left[6a_1^2\bar{c}_{33}\left(2\bar{c}_{31}-c_{31}\right)+\bar{c}_{31}\left(c_{31}-\bar{c}_{31}\right)\bar{h}^2k^2\right]\bar{h}k}{4a_1\bar{c}_{33}\left(6a_1^2\bar{c}_{33}+\bar{c}_{31}\bar{h}^2k^2\right)}\left(B_{11}^{(2)}+B_{12}^{(2)}+\ldots+B_{1n}^{(2)}\right) \\
& +\frac{3\bar{c}_{31}\bar{h}^2k^2}{2\left(6a_1^2\bar{c}_{33}+\bar{c}_{31}\bar{h}^2k^2\right)}\left(A_{31}^{(2)}+A_{32}^{(2)}+\ldots+A_{3n}^{(2)}\right) \\
& +\frac{\bar{h}k\left[6a_1^2\bar{c}_{33}\left(c_{31}-2\bar{c}_{31}\right)+\bar{c}_{31}\left(\bar{c}_{31}-c_{31}\right)\bar{h}^2k^2\right]}{2a_1\bar{c}_{33}\left(6a_1^2\bar{c}_{33}+\bar{c}_{31}\bar{h}^2k^2\right)}\left(B_{12}^{(8)}+B_{14}^{(8)}+\ldots+B_{1n}^{(8)}\right)
\end{aligned} \tag{5.14}
$$

$$
\begin{aligned}
&+\frac{c_{33}\bar{h}\left(6a_1^2\bar{c}_{33}-\bar{c}_{31}\bar{h}^2k^2\right)}{2\bar{c}_{33}h\left(6a_1^2\bar{c}_{33}+\bar{c}_{31}\bar{h}^2k^2\right)}\left[A_{32}^{(8)}-A_{33}^{(8)}+\ldots+(-1)^{n-1}\frac{n(n-1)}{2}A_{3n}^{(8)}\right]\\
&-\frac{3\bar{c}_{31}\bar{h}^2k^2}{\left(6a_1^2\bar{c}_{33}+\bar{c}_{31}\bar{h}^2k^2\right)}\left(A_{32}^{(8)}+A_{34}^{(8)}+\ldots+A_{3n}^{(8)}\right)\\
&+\frac{\bar{c}_{31}\bar{h}^2k^2}{2\left(6a_1^2\bar{c}_{33}+\bar{c}_{31}\bar{h}^2k^2\right)}\left\{3A_{34}^{(9)}+7A_{35}^{(9)}+\ldots+\left[\frac{n(n-1)}{2}-3\right]A_{3n}^{(9)}\right\}\\
&-\frac{6a_1^2\bar{c}_{33}}{\left(6a_1^2\bar{c}_{33}+\bar{c}_{31}\bar{h}^2k^2\right)}\left[6A_{34}^{(9)}+15A_{36}^{(9)}+\ldots+\frac{n(n-1)}{2}A_{3n}^{(9)}\right]
\end{aligned}
$$

$$
\begin{aligned}
A_{33}^{(9)}=&-\frac{\left[2a_1^2\bar{c}_{33}c_{31}+\bar{c}_{31}\left(c_{31}-\bar{c}_{31}\right)\bar{h}^2k^2\right]\bar{h}k}{4a_1\bar{c}_{33}\left(6a_1^2\bar{c}_{33}+\bar{c}_{31}\bar{h}^2k^2\right)}\left(B_{11}^{(2)}+B_{12}^{(2)}+\ldots+B_{1n}^{(2)}\right)\\
&-\frac{\bar{c}_{31}\bar{h}^2k^2}{2\left(6a_1^2\bar{c}_{33}+\bar{c}_{31}\bar{h}^2k^2\right)}\left(A_{31}^{(2)}+A_{32}^{(2)}+\ldots+A_{3n}^{(2)}\right)\\
&+\frac{\bar{h}k\left[2a_1^2\bar{c}_{33}c_{31}-\bar{c}_{31}\left(\bar{c}_{31}-c_{31}\right)\bar{h}^2k^2\right]}{2a_1\bar{c}_{33}\left(6a_1^2\bar{c}_{33}+\bar{c}_{31}\bar{h}^2k^2\right)}\left(B_{12}^{(8)}+B_{14}^{(8)}+\ldots+B_{1n}^{(8)}\right)\\
&+\frac{c_{33}\bar{h}\left(2a_1^2\bar{c}_{33}+\bar{c}_{31}\bar{h}^2k^2\right)}{2\bar{c}_{33}h\left(6a_1^2\bar{c}_{33}+\bar{c}_{31}\bar{h}^2k^2\right)}\left[A_{32}^{(8)}-A_{33}^{(8)}+\ldots+(-1)^{n-1}\frac{n(n-1)}{2}A_{3n}^{(8)}\right]\\
&+\frac{\bar{c}_{31}\bar{h}^2k^2}{\left(6a_1^2\bar{c}_{33}+\bar{c}_{31}\bar{h}^2k^2\right)}\left(A_{32}^{(8)}+A_{34}^{(8)}+\ldots+A_{3n}^{(8)}\right)\\
&-\frac{\bar{c}_{31}\bar{h}^2k^2}{2\left(6a_1^2\bar{c}_{33}+\bar{c}_{31}\bar{h}^2k^2\right)}\left\{5A_{34}^{(9)}+9A_{35}^{(9)}+14A_{36}^{(9)}+\ldots+\left[\frac{n(n-1)}{2}-1\right]A_{3n}^{(9)}\right\}\\
&-\frac{a_1^2\bar{c}_{33}}{\left(6a_1^2\bar{c}_{33}+\bar{c}_{31}\bar{h}^2k^2\right)}\left[20A_{35}^{(9)}+42A_{37}^{(9)}+\ldots+n(n-1)A_{3n}^{(9)}\right]
\end{aligned}
\tag{5.14}
$$

$$
\begin{aligned}
B_{31}^{(9)}=&\frac{\bar{h}k\left[6a_1^2\left(6\bar{c}_{11}\bar{c}_{33}-\bar{c}_{13}\bar{c}_{31}\right)+\bar{c}_{11}\left(3\bar{c}_{31}-c_{31}\right)\bar{h}^2k^2\right]}{12a_1\bar{c}_{33}\left(6a_1^2\bar{c}_{13}+\bar{c}_{11}\bar{h}^2k^2\right)}\Big(A_{11}^{(2)}+A_{12}^{(2)}+\\
&\ldots+A_{1n}^{(2)}\Big)+\left\{\frac{-6a_1^2\left[2\bar{c}_{11}\bar{c}_{33}\left(\bar{c}_{55}-2c_{55}\right)+\bar{c}_{13}\bar{c}_{31}\left(c_{55}-2\bar{c}_{55}\right)\right]\bar{h}^2k^2}{24a_1^2\bar{c}_{55}\bar{c}_{33}\left(6a_1^2\bar{c}_{13}+\bar{c}_{11}\bar{h}^2k^2\right)}\right.\\
&\left.+\frac{144a_1^4\bar{c}_{13}\bar{c}_{33}\bar{c}_{55}+\bar{c}_{11}\bar{c}_{31}\left(c_{55}-\bar{c}_{55}\right)\bar{h}^4k^4}{24a_1^2\bar{c}_{55}\bar{c}_{33}\left(6a_1^2\bar{c}_{13}+\bar{c}_{11}\bar{h}^2k^2\right)}\right\}\left(B_{31}^{(2)}+B_{32}^{(2)}+\ldots+B_{3n}^{(2)}\right)
\end{aligned}
$$

$$
\begin{aligned}
&+\frac{\bar{h}k\left[a_1^2\left(6\bar{c}_{13}c_{31}-36\bar{c}_{11}\bar{c}_{33}\right)+\bar{c}_{11}\left(c_{31}-3\bar{c}_{31}\right)\bar{h}^2k^2\right]}{6a_1\bar{c}_{33}\left(6a_1^2\bar{c}_{13}+\bar{c}_{11}\bar{h}^2k^2\right)}\\
&\left(A_{12}^{(8)}+A_{14}^{(8)}+\ldots+A_{1n}^{(8)}\right)+\frac{c_{55}\bar{h}^2k\left(6a_1^2\left(\bar{c}_{13}\bar{c}_{31}-4\bar{c}_{11}\bar{c}_{33}\right)-\bar{c}_{11}\bar{c}_{31}\bar{h}^2k^2\right)}{12a_1\bar{c}_{33}\bar{c}_{55}h\left(6a_1^2\bar{c}_{13}+\bar{c}_{11}\bar{h}^2k^2\right)}\\
&\left[A_{12}^{(8)}-3A_{13}^{(8)}+\ldots+(-1)^{n-1}\frac{n(n-1)}{2}A_{1n}^{(8)}\right]\\
&-\left\{\frac{-6a_1^2\left[2\bar{c}_{11}\bar{c}_{33}\left(\bar{c}_{55}-2c_{55}\right)+\bar{c}_{13}\bar{c}_{31}\left(c_{55}-2\bar{c}_{55}\right)\right]\bar{h}^2k^2}{24a_1^2\bar{c}_{55}\bar{c}_{33}\left(6a_1^2\bar{c}_{13}+\bar{c}_{11}\bar{h}^2k^2\right)}\right.\\
&\left.+\frac{144a_1^4\bar{c}_{13}\bar{c}_{33}\bar{c}_{55}+\bar{c}_{11}\bar{c}_{31}\left(c_{55}-\bar{c}_{55}\right)\bar{h}^4k^4}{24a_1^2\bar{c}_{55}\bar{c}_{33}\left(6a_1^2\bar{c}_{13}+\bar{c}_{11}\bar{h}^2k^2\right)}\right\}\left(B_{32}^{(8)}+B_{34}^{(8)}+\ldots+B_{3n}^{(8)}\right)\\
&-\frac{c_{33}\bar{h}}{6\bar{c}_{33}h}\left[B_{32}^{(8)}-3B_{33}^{(8)}+\ldots+(-1)^{n-1}\frac{n(n-1)}{2}B_{3n}^{(8)}\right]\\
&+\frac{12a_1^2\bar{c}_{11}\bar{c}_{33}\bar{h}k+\bar{c}_{11}\bar{c}_{31}\bar{h}^3k^3}{12a_1\bar{c}_{33}\left(6a_1^2\bar{c}_{13}+\bar{c}_{11}\bar{h}^2k^2\right)}\left\{7A_{15}^{(9)}+18A_{17}^{(9)}+\ldots\right.\\
&\left.+\left[\frac{n(n-1)}{2}-3\right]A_{1n}^{(9)}\right\}+\frac{36a_1^2\bar{c}_{11}\bar{c}_{33}\bar{h}k+\bar{c}_{11}\bar{c}_{31}\bar{h}^3k^3-12a_1^2\bar{c}_{13}\bar{c}_{31}\bar{h}k}{12a_1\bar{c}_{33}\left(6a_1^2\bar{c}_{13}+\bar{c}_{11}\bar{h}^2k^2\right)}\\
&\left\{5A_{14}^{(9)}+14A_{16}^{(9)}+\ldots+\left[\frac{n(n-1)}{2}-1\right]A_{1n}^{(9)}\right\}\\
&+\frac{1}{3}\left\{7B_{35}^{(9)}+18B_{37}^{(9)}+\ldots+\left[\frac{n(n-1)}{2}-3\right]B_{3n}^{(9)}\right\}
\end{aligned}
\tag{5.14}
$$

$$
\begin{aligned}
B_{32}^{(9)}=&-\frac{\bar{h}k\left\{6a_1^2\left[12\bar{c}_{11}\bar{c}_{33}+\bar{c}_{13}\left(c_{31}-2\bar{c}_{31}\right)\right]+\bar{c}_{11}\left(\bar{c}_{31}+c_{31}\right)\bar{h}^2k^2\right\}}{20a_1\bar{c}_{33}\left(6a_1^2\bar{c}_{13}+\bar{c}_{11}\bar{h}^2k^2\right)}\\
&\left(A_{11}^{(2)}+A_{12}^{(2)}+\ldots+A_{1n}^{(2)}\right)\\
&-\bar{h}^2k^2\left\{\frac{6a_1^2\left[\bar{c}_{13}\bar{c}_{31}\left(2\bar{c}_{55}-c_{55}\right)+4\bar{c}_{11}\bar{c}_{33}\left(2c_{55}-3\bar{c}_{55}\right)\right]}{40a_1^2\bar{c}_{55}\bar{c}_{33}\left(6a_1^2\bar{c}_{13}+\bar{c}_{11}\bar{h}^2k^2\right)}\right.\\
&\left.+\frac{\bar{c}_{11}\bar{c}_{31}\left(c_{55}-\bar{c}_{55}\right)\bar{h}^2k^2}{40a_1^2\bar{c}_{55}\bar{c}_{33}\left(6a_1^2\bar{c}_{13}+\bar{c}_{11}\bar{h}^2k^2\right)}\right\}\left(B_{31}^{(2)}+B_{32}^{(2)}+\ldots+B_{3n}^{(2)}\right)\\
&+\frac{\bar{h}k\left\{6a_1^2\left[12\bar{c}_{11}\bar{c}_{33}+\bar{c}_{13}\left(c_{31}-2\bar{c}_{31}\right)\right]+\bar{c}_{11}\left(\bar{c}_{31}+c_{31}\right)\bar{h}^2k^2\right\}}{10a_1\bar{c}_{33}\left(6a_1^2\bar{c}_{13}+\bar{c}_{11}\bar{h}^2k^2\right)}
\end{aligned}
$$

$$
\begin{aligned}
&\left(A_{12}^{(8)}+A_{14}^{(8)}+\ldots+A_{1n}^{(8)}\right)\\
&+\frac{c_{55}\bar{h}^2k\left[-6a_1^2\left(\bar{c}_{13}\bar{c}_{31}-8\bar{c}_{11}\bar{c}_{33}\right)+\bar{c}_{11}\bar{c}_{31}\bar{h}^2k^2\right]}{20a_1\bar{c}_{33}\bar{c}_{55}h\left(6a_1^2\bar{c}_{13}+\bar{c}_{11}\bar{h}^2k^2\right)}\\
&\left[A_{12}^{(8)}-3A_{13}^{(8)}+\ldots+(-1)^{n-1}\frac{n(n-1)}{2}A_{1n}^{(8)}\right]\\
&-\bar{h}^2k^2\left\{\frac{6a_1^2\left[\bar{c}_{13}\bar{c}_{31}\left(2\bar{c}_{55}-c_{55}\right)+4\bar{c}_{11}\bar{c}_{33}\left(2c_{55}-3\bar{c}_{55}\right)\right]}{20a_1^2\bar{c}_{55}\bar{c}_{33}\left(6a_1^2\bar{c}_{13}+\bar{c}_{11}\bar{h}^2k^2\right)}\right.\\
&\left.+\frac{+\bar{c}_{11}\bar{c}_{31}\left(c_{55}-\bar{c}_{55}\right)\bar{h}^2k^2}{20a_1^2\bar{c}_{55}\bar{c}_{33}\left(6a_1^2\bar{c}_{13}+\bar{c}_{11}\bar{h}^2k^2\right)}\right\}\left(B_{32}^{(8)}+B_{34}^{(8)}+\ldots+B_{3n}^{(8)}\right)\\
&-\frac{c_{33}\bar{h}}{10\bar{c}_{33}h}\left[B_{32}^{(8)}-3B_{33}^{(8)}+\ldots+(-1)^{n-1}\frac{n(n-1)}{2}B_{3n}^{(8)}\right]\\
&-\frac{72\bar{c}_{11}\bar{c}_{33}\bar{h}ka_1^2+\bar{c}_{11}\bar{c}_{31}\bar{h}^3k^3-12a_1^2\bar{c}_{13}\bar{c}_{31}\bar{h}k}{20a_1\bar{c}_{33}\left(6a_1^2\bar{c}_{13}+\bar{c}_{11}\bar{h}^2k^2\right)}\\
&\left\{5A_{14}^{(9)}+14A_{16}^{(9)}+\ldots+\left[\frac{n(n-1)}{2}-1\right]A_{1n}^{(9)}\right\}\\
&-\frac{24\bar{c}_{11}\bar{c}_{33}\bar{h}ka_1^2+\bar{c}_{11}\bar{c}_{31}\bar{h}^3k^3}{20a_1\bar{c}_{33}\left(6a_1^2\bar{c}_{13}+\bar{c}_{11}\bar{h}^2k^2\right)}\left\{7B_{35}^{(9)}+18B_{37}^{(9)}+\ldots\right.\\
&\left.+\left[\frac{n(n-1)}{2}-3\right]B_{3n}^{(9)}\right\}+\frac{1}{5}\left\{9B_{36}^{(9)}+22B_{38}^{(9)}+\ldots+\left[\frac{n(n-1)}{2}-6\right]B_{3n}^{(9)}\right\}
\end{aligned}
\tag{5.14}
$$

$$
\begin{aligned}
B_{33}^{(9)}=&\frac{\bar{h}k\left[6a_1^2\bar{c}_{13}c_{31}+\bar{c}_{11}\left(c_{31}-3\bar{c}_{31}\right)\bar{h}^2k^2\right]}{12a_1\bar{c}_{33}\left(6a_1^2\bar{c}_{13}+\bar{c}_{11}\bar{h}^2k^2\right)}\left(A_{11}^{(2)}+A_{12}^{(2)}+\ldots+A_{1n}^{(2)}\right)\\
&+\frac{\bar{c}_{31}c_{55}\bar{h}^2k\left(\bar{c}_{11}\bar{h}^2k^2-6a_1^2\bar{c}_{13}\right)}{12a_1\bar{c}_{33}\bar{c}_{55}h\left(6a_1^2\bar{c}_{13}+\bar{c}_{11}\bar{h}^2k^2\right)}\left(B_{31}^{(2)}+B_{32}^{(2)}+\ldots+B_{3n}^{(2)}\right)\\
&+\frac{\bar{h}k\left[6a_1^2\bar{c}_{13}c_{31}+\bar{c}_{11}\left(-3\bar{c}_{31}+c_{31}\right)\bar{h}^2k^2\right]}{6a_1\bar{c}_{33}\left(6a_1^2\bar{c}_{13}+\bar{c}_{11}\bar{h}^2k^2\right)}\left(A_{12}^{(8)}+A_{14}^{(8)}+\ldots+A_{1n}^{(8)}\right)\\
&+\frac{\bar{c}_{31}c_{55}\bar{h}^2k\left(-6a_1^2\bar{c}_{13}+\bar{c}_{11}\bar{h}^2k^2\right)}{12a_1\bar{c}_{33}\bar{c}_{55}h\left(6a_1^2\bar{c}_{13}+\bar{c}_{11}\bar{h}^2k^2\right)}\\
&\left[A_{12}^{(8)}-3A_{13}^{(8)}+\ldots+(-1)^{n-1}\frac{n(n-1)}{2}A_{1n}^{(8)}\right]
\end{aligned}
$$

$$
\begin{aligned}
& - \frac{\bar{c}_{31}\bar{h}^2k^2\left\{6a_1^2\bar{c}_{13}\left(2\bar{c}_{55}-c_{55}\right)+\bar{c}_{11}\left(c_{55}-\bar{c}_{55}\right)\bar{h}^2k^2\right\}}{12a_1^2\bar{c}_{55}\bar{c}_{33}\left(6a_1^2\bar{c}_{13}+\bar{c}_{11}\bar{h}^2k^2\right)} \\
& \left(B_{32}^{(8)}+B_{34}^{(8)}+\ldots+B_{3n}^{(8)}\right) \\
& - \frac{c_{33}\bar{h}}{6\bar{c}_{33}h}\left[B_{32}^{(8)}-3B_{33}^{(8)}+\ldots+(-1)^{n-1}\frac{n(n-1)}{2}B_{3n}^{(8)}\right] \\
& - \frac{\bar{c}_{11}\bar{c}_{31}\bar{h}^3k^3-12a_1^2\bar{c}_{13}\bar{c}_{31}\bar{h}k}{12a_1\bar{c}_{33}\left(6a_1^2\bar{c}_{13}+\bar{c}_{11}\bar{h}^2k^2\right)}\left\{5A_{14}^{(9)}+14A_{16}^{(9)}+\ldots+\left[\frac{n(n-1)}{2}-1\right]A_{1n}^{(9)}\right\} \\
& - \frac{\bar{c}_{11}\bar{c}_{31}\bar{h}^3k^3}{20a_1\bar{c}_{33}\left(6a_1^2\bar{c}_{13}+\bar{c}_{11}\bar{h}^2k^2\right)}\left\{7B_{35}^{(9)}+18B_{37}^{(9)}+\ldots+\left[\frac{n(n-1)}{2}-3\right]B_{3n}^{(9)}\right\} \\
& - \frac{1}{3}\left[10B_{36}^{(9)}+21B_{38}^{(9)}+\ldots+\frac{n(n-1)}{2}B_{3n}^{(9)}\right]
\end{aligned}
$$

$$
\begin{aligned}
B_{34}^{(9)} = & -\frac{\bar{h}k\left\{6a_1^2\left[2\bar{c}_{11}\bar{c}_{33}+\bar{c}_{13}\left(c_{31}-2\bar{c}_{31}\right)\right]+\bar{c}_{11}\left(\bar{c}_{31}+c_{31}\right)\bar{h}^2k^2\right\}}{20a_1\bar{c}_{33}\left(6a_1^2\bar{c}_{13}+\bar{c}_{11}\bar{h}^2k^2\right)} \\
& \left(A_{11}^{(2)}+A_{12}^{(2)}+\ldots+A_{1n}^{(2)}\right) \\
& + \left[\frac{2a_1^2\left(6\bar{c}_{13}\bar{c}_{31}\bar{c}_{55}-6\bar{c}_{11}\bar{c}_{33}\bar{c}_{55}-3\bar{c}_{13}\bar{c}_{31}c_{55}+4\bar{c}_{11}\bar{c}_{33}c_{55}\right)}{40a_1^2\bar{c}_{55}\bar{c}_{33}\left(6a_1^2\bar{c}_{13}+\bar{c}_{11}\bar{h}^2k^2\right)}\right. \\
& \left. + \frac{\bar{c}_{11}\bar{c}_{31}\left(c_{55}-\bar{c}_{55}\right)\bar{h}^2k^2}{40a_1^2\bar{c}_{55}\bar{c}_{33}\left(6a_1^2\bar{c}_{13}+\bar{c}_{11}\bar{h}^2k^2\right)}\right]\bar{h}^2k^2\left(B_{31}^{(2)}+B_{32}^{(2)}+\ldots+B_{3n}^{(2)}\right) \\
& + \frac{\bar{h}k\left\{6a_1^2\left[12\bar{c}_{11}\bar{c}_{33}+\bar{c}_{13}\left(c_{31}-2\bar{c}_{31}\right)\right]+\bar{c}_{11}\left(\bar{c}_{31}+c_{31}\right)\bar{h}^2k^2\right\}}{10a_1\bar{c}_{33}\left(6a_1^2\bar{c}_{13}+\bar{c}_{11}\bar{h}^2k^2\right)} \\
& \left(A_{12}^{(8)}+A_{14}^{(8)}+\ldots+A_{1n}^{(8)}\right) \\
& + \frac{c_{55}\bar{h}^2k\left[-6a_1^2\left(\bar{c}_{13}\bar{c}_{31}-8\bar{c}_{11}\bar{c}_{33}\right)+\bar{c}_{11}\bar{c}_{31}\bar{h}^2k^2\right]}{20a_1\bar{c}_{33}\bar{c}_{55}h\left(6a_1^2\bar{c}_{13}+\bar{c}_{11}\bar{h}^2k^2\right)} \\
& \left[A_{12}^{(8)}-3A_{13}^{(8)}+\ldots+(-1)^{n-1}\frac{n(n-1)}{2}A_{1n}^{(8)}\right] \\
& - \left\{\frac{2a_1^2\left[6\bar{c}_{13}\bar{c}_{31}\bar{c}_{55}+4\bar{c}_{11}\bar{c}_{33}c_{55}-3\bar{c}_{13}\bar{c}_{31}c_{55}\right]}{20a_1^2\bar{c}_{55}\bar{c}_{33}\left(6a_1^2\bar{c}_{13}+\bar{c}_{11}\bar{h}^2k^2\right)}\right.
\end{aligned}
\tag{5.14}
$$

$$+\frac{\bar{c}_{11}\bar{c}_{31}\left(c_{55}-\bar{c}_{55}\right)\bar{h}^2k^2}{20a_1^2\bar{c}_{55}\bar{c}_{33}\left(6a_1^2\bar{c}_{13}+\bar{c}_{11}\bar{h}^2k^2\right)}\Bigg\}\bar{h}^2k^2\left(B_{32}^{(8)}+B_{34}^{(8)}+\ldots+B_{3n}^{(8)}\right)$$

$$+\frac{c_{33}\bar{h}}{10\bar{c}_{33}h}\left[B_{32}^{(8)}-3B_{33}^{(8)}+\ldots+(-1)^{n-1}\frac{n(n-1)}{2}B_{3n}^{(8)}\right]$$

$$+\frac{12\bar{c}_{11}\bar{c}_{33}\bar{h}ka_1^2+\bar{c}_{11}\bar{c}_{31}\bar{h}^3k^3-12a_1^2\bar{c}_{13}\bar{c}_{31}\bar{h}k}{20a_1\bar{c}_{33}\left(6a_1^2\bar{c}_{13}+\bar{c}_{11}\bar{h}^2k^2\right)}$$

$$\left\{5A_{14}^{(9)}+14A_{16}^{(9)}+\ldots+\left[\frac{n(n-1)}{2}-1\right]A_{1n}^{(9)}\right\}$$

$$+\frac{4\bar{c}_{11}\bar{c}_{33}\bar{h}ka_1^2+\bar{c}_{11}\bar{c}_{31}\bar{h}^3k^3}{20a_1\bar{c}_{33}\left(6a_1^2\bar{c}_{13}+\bar{c}_{11}\bar{h}^2k^2\right)}\left\{7B_{35}^{(9)}+18B_{37}^{(9)}+\ldots+\left[\frac{n(n-1)}{2}-3\right]B_{3n}^{(9)}\right\}$$

$$-\frac{1}{5}\left\{14B_{36}^{(9)}+27B_{38}^{(9)}+\ldots+\left[\frac{n(n-1)}{2}-1\right]B_{3n}^{(9)}\right\}$$

$$A_{11}^{(10)}=-A_{12}^{(10)}-A_{13}^{(10)}-\ldots-A_{1n}^{(10)}-A_{11}^{(2)}-A_{12}^{(2)}-\ldots-A_{1n}^{(2)}$$

$$B_{11}^{(10)}=-B_{12}^{(10)}-B_{13}^{(10)}-\ldots-B_{1n}^{(10)}+B_{11}^{(2)}+B_{12}^{(2)}+\ldots+B_{1n}^{(2)}$$

$$A_{31}^{(10)}=-A_{32}^{(10)}-A_{33}^{(10)}-\ldots-A_{3n}^{(10)}-A_{31}^{(2)}-A_{32}^{(2)}-\ldots-A_{3n}^{(2)}$$

$$B_{31}^{(10)}=-B_{32}^{(10)}-B_{33}^{(10)}-\ldots-B_{3n}^{(10)}+B_{31}^{(2)}+B_{32}^{(2)}+\ldots+B_{3n}^{(2)}$$

Chapter 6

Analysis of the propagation characteristics of low-order SAWs in the three-dimensional finite elastic structure by CUF

In the research of SAW devices, the FEM is one of the main tools. Due to the complex structure of the actual SAW devices, it is generally difficult to obtain an accurate solution directly through the analytical method, and the FEM is limited in the shape of the structure. It is small and can analyze more complex structures based on modeling, so it has a large number of applications in device research and design. Generally, hundreds of pairs of IDTs are arranged on the substrate of a SAW device along the wave propagation direction, so the size of the device along the wave propagation direction is often much larger than the size of the other two sides. As for a single unit structure (the unit structure in this chapter refers to the structure covering only one electrode), the width of the electrode and the distance between the fingers are close to the size of the SAW device in the direction of wave propagation. Therefore, in order to simplify the model and reduce the calculation cost, the characteristics of SAWs propagation can be used to replace the analysis of the entire structure by analyzing the propagation characteristics of SAWs in a unit cell under reasonable boundary conditions.

As the main tool for analyzing and designing SAW devices, the FEM has obvious advantages in analyzing complex structures, but its calculation cost will rise sharply with the increase of the complexity of the structure. In this chapter, CUF is used to transform the three-dimensional geometric model into a one-dimensional beam calculation model, so as to obtain a more streamlined stiffness matrix and mass matrix. On the basis of ensuring reliable calculation results, finite element calculations can be realized with fewer degrees of freedom;

By setting the viscous-spring artificial boundary on the boundary element, it is possible to use the finite-scale model to analyse the propagation characteristics of the SAWs.

The main feature of CUF is that it allows to deal with the expansion of arbitrary functions of unknown variables over the thickness/cross-section domain in a compact form, since the governing equations are actually obtained in terms of some basic kernels, which neither depend on the function expansion The order of , also does not depend on the basis function equation used. Therefore, it can be widely used in the dynamic, static and buckling mechanical behavior of beams, plates, shells and other structures. When using the CUF framework to analyze the mechanical properties in a multi-layer structure, the nodes on the interface are generally used to ensure the continuity of the displacement on the contact surface. For a structure with a large number of layers, it can also be analyzed in combination with the theory of multilayer boards.

Viscous-spring artificial boundary conditions can "absorb" waves on the boundary and prevent them from reflecting back to the structure by setting reasonable damping and spring coefficients. And because it acts on the nodes of the finite element, it can be matched with the nodes of the finite element constructed by the CUF framework. The spring stiffness matrix of the artificial boundary is added to the stiffness matrix of the structure itself, and the damping coefficients are organized into the form of a damping matrix, so that the generalized characteristic equation can be obtained. By solving this equation, the characteristic frequency of the structure can be obtained, and then the velocities of the low-order SAWs in the structure can be obtained by using the relationship between angular frequency, wave number and wave velocity.

In this chapter, by setting artificial boundaries on different sides of the model, the location of the necessary interface for adding artificial boundaries is analyzed; on this basis, the convergence of finite element calculations under different structures is analyzed; The influence of the size of each direction on the velocity of the low-order SAWs; the numerical analysis of the velocity and mode of the low-order SAWs in the structure under the influence of the T-shaped covering layer.

6.1 Problem description

In this chapter, a series of structural models as shown in Fig. 6.1 are applied. The thickness of the substrate (x_3 axis direction) is six wavelengths, the structure width (x_1 axis direction) is one wavelength, and the structure length (x_2 axis direction) for three wavelengths.

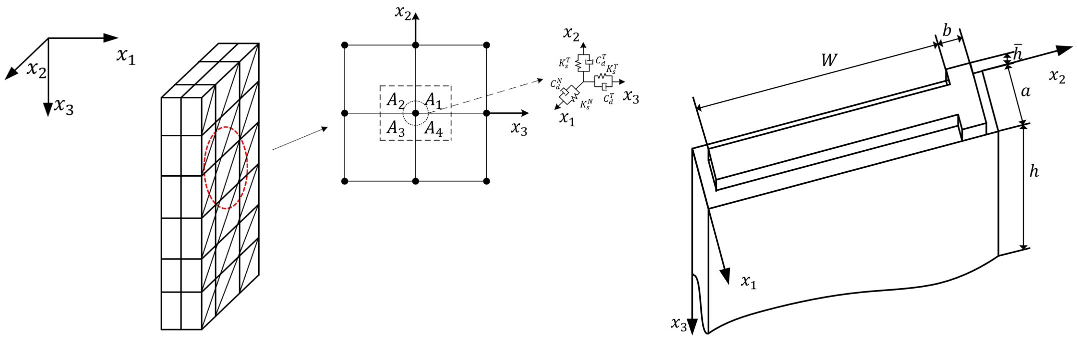

(a) (b)

Fig. 6.1 The schematic of the structure used in this chapter: (a) a finite elastic solid with artificial boundary on the boundary elements; (b) a finite solid covered by a T-plate

6.2 Related theories

6.2.1 One-dimensional beam model under CUF framework

This chapter uses the one-dimensional beam model in CUF to analyze the SAWs propagation characteristics in the above structure. First, the displacement function used here has the following form:

$$\mathbf{U}^{(r)}(x_1,x_2,x_3) = \begin{pmatrix} u_{x_1}^{(r)} & u_{x_2}^{(r)} & u_{x_3}^{(r)} \end{pmatrix}^T \tag{6.1}$$

$$\begin{aligned} &\mathbf{U}^{(r)}(x_1,x_2,x_3) = F_\tau(x_1,x_2)\,N_i(x_3)\,\mathbf{q}_{\tau i}^{(r)} \\ &\tau = 1,2,\ldots,\mathrm{T}; i = 1,2,\ldots,N_n \end{aligned} \tag{6.2}$$

where $r = 1,2$, where 1 refers to the base, 2 refers to the covering layer; $F_\tau(x_1,x_2)$ represents the section function, and $N_i(x_3)$ represents the $i-$order one-dimensional shape function, $\mathbf{q}_{\tau i}$ represents the nodal displacement vector. Under the framework of CUF, the displacement function of the multi-layer structure can be written as:

$$\begin{aligned} u^{(r)}(x_1,x_2,x_3) &= F_1(x_1,x_2)\,N_1(x_3)\,q_{11}^{(r)} + F_2(x_1,x_2)\,N_2(x_3)\,q_{22}^{(r)} + \ldots \\ &\quad + F_M(x_1,x_2)\,N_{N_n}(x_3)\,q_{MN_n}^{(r)} \\ u_2^{(r)}(x_1,x_2,x_3) &= F_1(x_1,x_2)\,N_1(x_3)\,q_{11}^{(r)} + F_2(x_1,x_2)\,N_2(x_3)\,q_{22}^{(r)} + \ldots \\ &\quad + F_M(x_1,x_2)\,N_{N_n}(x_3)\,q_{MN_n}^{(r)} \\ u_3^{(r)}(x_1,x_2,x_3) &= F_1(x_1,x_2)\,N_1(x_3)\,q_{11}^{(r)} + F_2(x_1,x_2)\,N_2(x_3)\,q_{22}^{(r)} + \ldots \\ &\quad + F_M(x_1,x_2)\,N_{N_n}(x_3)\,q_{MN_n}^{(r)} \end{aligned} \tag{6.3}$$

The stresses and strains in the structure can be written as:

$$\begin{aligned}\varepsilon^{(r)}\left(x_1,x_2,x_3\right) &= \mathrm{b}N_i\left(x_3\right)F_\tau\left(x_1,x_2\right)\mathbf{U}_{i\tau}^{(r)}\\ \sigma^{(r)}\left(x_1,x_2,x_3\right) &= \mathrm{Cb}N_i\left(x_3\right)F_\tau\left(x_1,x_2\right)\mathbf{U}_{i\tau}^{(r)}\end{aligned} \tag{6.4}$$

$[C]$ represents the elastic constant matrix, and $[b]$ is the Jacobian matrix.

$$[b]=\begin{bmatrix} 0 & \frac{\partial}{\partial x_2} & 0\\ \frac{\partial}{\partial x_1} & 0 & 0\\ 0 & 0 & \frac{\partial}{\partial x_3}\\ \frac{\partial}{\partial x_3} & 0 & \frac{\partial}{\partial x_1}\\ 0 & \frac{\partial}{\partial x_3} & \frac{\partial}{\partial x_2}\\ \frac{\partial}{\partial x_2} & \frac{\partial}{\partial x_1} & 0 \end{bmatrix} \tag{6.5}$$

According to the principle of virtual work, the variation of strain energy, δL_{int} can be expressed as:

$$\delta L_{int}=\delta \mathrm{u}^T[K]\mathrm{u} \tag{6.6}$$

The virtual work done by the elastic force, δL_{ine} can be expressed as:

$$\delta L_{int}=-\delta L_{ine}=\int_V \delta\mathbf{u}\rho\ddot{\mathbf{u}}dV \tag{6.7}$$

where $\mathbf{u}=\mathbf{U}e^{i\omega t}$. And Eq. 6.7 can be written in the form of characteristic equation:

$$\left([K]-\omega^2[M]\right)\{U\}=0 \tag{6.8}$$

The elements in the stiffness matrix here can be expressed as:

$$[K_{\mathbf{uu}}^{ij\tau s}]=\int_V \left([b]N_iF_\tau\right)^T[C]\left([b]N_jF_s\right)dV \tag{6.9}$$

The elements in the mass matrix can be written as:

$$[M_{\mathbf{uu}}^{ij\tau s}]=\int_V \left([I]N_iF_\tau\right)^T\rho\left([I]N_jF_s\right)dV \tag{6.10}$$

where $[I]$ represents the identity matrix.

In this chapter, the Lagrangian expansion is used as the section function, and the expression forms of the Lagrangian elements with different cut-off points are different, as shown in Fig. 6.2 for the four-node and nine-node Lagrangian elements, They are denoted as L4 and L9 respectively, and the corresponding $F_\tau(\alpha,\beta)$ are respectively written as:

$$\begin{aligned}
F_1(\alpha,\beta) &= \frac{1}{4}(1-\alpha)(1-\beta)\\
F_2(\alpha,\beta) &= \frac{1}{4}(1+\alpha)(1-\beta)\\
F_3(\alpha,\beta) &= \frac{1}{4}(1+\alpha)(1+\beta)\\
F_4(\alpha,\beta) &= \frac{1}{4}(1-\alpha)(1+\beta)\\
&\alpha,\beta \in [-1,1]
\end{aligned} \tag{6.11}$$

$$\begin{aligned}
&F_1(\alpha,\beta) = \tfrac{1}{4}\left(\alpha^2-\alpha\right)\left(\beta^2-\beta\right), F_2(\alpha,\beta) = \tfrac{1}{2}\left(\beta^2+\beta\right)\left(1-\alpha^2\right)\\
&F_3(\alpha,\beta) = \tfrac{1}{4}\left(\alpha^2-\alpha\right)\left(\beta^2+\beta\right), F_4(\alpha,\beta) = \tfrac{1}{2}\left(\alpha^2-\alpha\right)\left(1-\beta^2\right)\\
&F_5(\alpha,\beta) = \tfrac{1}{4}\left(\alpha^2+\alpha\right)\left(\beta^2+\beta\right), F_6(\alpha,\beta) = \tfrac{1}{2}\left(\beta^2-\beta\right)\left(1-\alpha^2\right)\\
&F_7(\alpha,\beta) = \tfrac{1}{4}\left(\alpha^2+\alpha\right)\left(\beta^2-\beta\right), F_8(\alpha,\beta) = \tfrac{1}{2}\left(\alpha^2+\alpha\right)\left(1-\beta^2\right)\\
&F_9(\alpha,\beta) = \left(1-\alpha^2\right)\left(1-\beta^2\right), \alpha,\beta \in [-1,1]
\end{aligned} \tag{6.12}$$

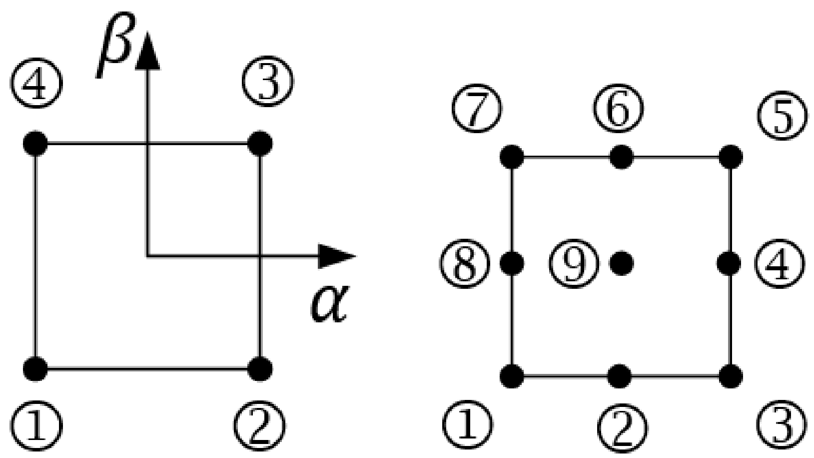

(a) (b)

Fig. 6.2 The schematic of different Lagrange element models: (a) four-node Lagrange element (L4); (b) nine-node Lagrange element (L9)

For the x_3 direction in the structure, the beam element is used, which is similar to the Lagrangian element. The corresponding function forms of beam elements with different numbers of nodes are also different. In the calculations in this chapter, two-node (B2) and three-node (B3) are mainly used, and four nodes (B4), the specific expression is as follows:

$$\begin{gathered} N_1(\zeta)=\frac{1}{2}(1-\zeta),\ N_2(\zeta)=\frac{1}{2}(1+\zeta), \\ \zeta_1=-1,\quad \zeta_2=1 \end{gathered} \tag{6.13}$$

$$\begin{aligned} &N_1(\zeta)=\frac{1}{2}r(1-\zeta),\ N_2=\frac{1}{2}\zeta(1+\zeta), \\ &N_3(\zeta)=-(1-\zeta)(1+\zeta), \\ &\quad \zeta_1=-1,\quad \zeta_2=1,\quad \zeta_3=0 \end{aligned} \tag{6.14}$$

$$\begin{aligned} &N_1(\zeta)=-\tfrac{9}{16}\left(\zeta+\tfrac{1}{3}\right)\left(\zeta-\tfrac{1}{3}\right)(\zeta-1) \\ &N_2(\zeta)=\tfrac{9}{16}\left(\zeta+\tfrac{1}{3}\right)\left(\zeta-\tfrac{1}{3}\right)(\zeta+1) \\ &N_3(\zeta)=\tfrac{27}{16}(\zeta+1)\left(\zeta-\tfrac{1}{3}\right)(\zeta-1) \\ &N_4(\zeta)=-\tfrac{27}{16}(\zeta+1)\left(\zeta+\tfrac{1}{3}\right)(\zeta-1) \\ &\zeta_1=-1,\quad \zeta_2=1,\quad \zeta_3=-\tfrac{1}{3},\quad \zeta_4=\tfrac{1}{3} \end{aligned} \tag{6.15}$$

6.2.2 Viscous-spring artificial boundary condition

As shown in Fig. 6.1, viscoelastic artificial boundaries are set on the unit nodes on the side of the base. By setting reasonable springs (K_s), dampers (C_d) and material coefficients (B), the boundaries can "absorb" fluctuations, thereby achieving a Suitable for solving periodic boundaries of SAWs in structures.

$$\begin{aligned} K_s^{N,T} &= \alpha^{N,T}\mu\Sigma A_i, \\ C_d^{N,T} &= \rho B c^{N,T}\Sigma A_i, \end{aligned} \tag{6.16}$$

N and T here represent the forward and tangential directions of the artificial boundary, respectively. The specific structural diagram is shown in Fig. 6.3.

After considering the artificial boundary conditions, the characteristic equation 6.8 is rewritten as:

$$[\tilde{K}][U]+[D][\dot{U}]+[M][\ddot{U}]=[0] \tag{6.17}$$

where $[\tilde{K}]=[K]+[K_S]$, through

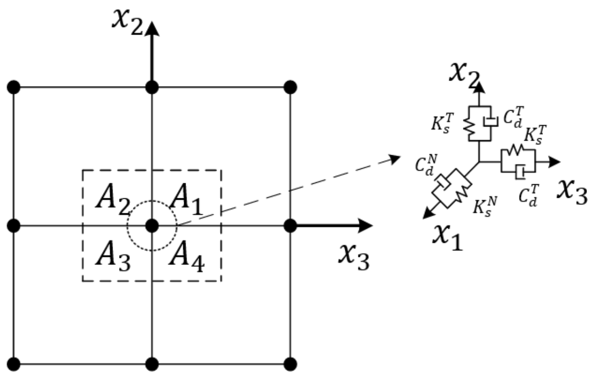

Fig. 6.3 The schematic of the viscous-spring artificial boundary condition

$$[q] = \begin{Bmatrix} \{U\} \\ \{\dot{U}\} \end{Bmatrix}, [\dot{q}] = \begin{Bmatrix} \{\dot{U}\} \\ \{\ddot{U}\} \end{Bmatrix} \tag{6.18}$$

Eq. 6.17 can be transformed into:

$$\begin{bmatrix} [K] & [D] \\ [0] & [I] \end{bmatrix} \begin{Bmatrix} \{U\} \\ \{\dot{U}\} \end{Bmatrix} - \begin{bmatrix} [0] & [M] \\ -[I] & [0] \end{bmatrix} \begin{Bmatrix} \{U\} \\ \{\ddot{U}\} \end{Bmatrix} = \begin{Bmatrix} [0] \\ [0] \end{Bmatrix} \tag{6.19}$$

obtain:

$$([A] + \omega[B])\,[q] = 0 \tag{6.20}$$

and $v_R = \frac{\omega}{k}$, where $k = \frac{2\pi}{\lambda}$, λ is wavelength.

6.3 Numerical results and discussions

In this chapter, the x_1-axis direction is the direction of wave propagation, and the x_3-axis is the thickness direction of the structure, that is, the direction of wave attenuation, as shown in Fig. 6.1. In this section, we use CUF combined with viscous-spring artificial boundaries to numerically analyze the propagation characteristics of SAWs in three-dimensional finite structures. The influence of SAW velocity, on this basis, the influence of adding covering layer on the wave velocity of low-order SAWs in the structure is analyzed, and when the covering layer is T-shaped, the change of low-order SAWs velocity in the structure is analyzed. Tab. 6.1 gives the physical parameters of the relevant materials involved in the calculations in this chapter, consistent with the previous three chapters, this section still uses the dimensionless wave velocity $\frac{v_R}{v_T}$, v_R represents the low-order SAWs velocity in the structure, $v_T = \sqrt{\frac{\mu}{\rho}}$, where μ and ρ represent the shear modulus and density of the substrate material, respectively.

Table 6.1 The material properties used in this section

Material	Elastic constants			Viscous-spring artificial boundary related parameters		
	ν	E(GPa)	ρ (kg/m^3)	α^N	α^T	B
Fused glass	0.21	73.1	2203	-0.125	-0.050	-0.010
Cu	0.35	110.0	8960	-0.002	-0.003	-0.053

6.3.1 Low-order SAWs in finite elastic plate

In this section, Cu is used as the structural material, and the SAWs velocities in the structure is calculated with artificial boundaries on all four sides of the elastic plate (T1) and artificial boundaries only on the side perpendicular to the wave propagation direction (T2) ; the convergence of different beam elements and section elements is analyzed; and the influence of each size parameter on the propagation of SAWs in the structure. When the T1 and T2 artificial boundary modes are used in the Fig. 6.1(a) model, 12 (2×6) L9 elements are used for the cross section, B4 is used for the beam element, and the ordinate is normalized The first-order SAW velocity of , the abscissa is the number of beam elements, and the calculation results are shown in Fig. 6.4.

It can be concluded from Fig. 6.4 that when the number of beam elements is greater than 4, the calculation results obtained by T1 and T2 modes are basically consistent. When analyzing the convergence of beam elements and cross-section elements, the T2 model is used, that is, artificial boundaries are only set on the surface perpendicular to the x_1 axis, so that the results shown in Fig. 6.5 can be obtained. According to (a) in Fig. 6.5, it is not difficult to find that in the case of the same cross-sectional unit (L4 is selected as the cross-sectional unit in this figure), the three beam units have good convergence; but under the same structural conditions , it is obvious that the more the number of nodes in the unit, the less the number of units needed to obtain the solution with the same accuracy, so in the subsequent calculation of the case, all B4 units are used in the x_3 direction; and according to (b) can be obtained, in this calculation case, for the same beam element (the B4 element selected here), the convergence effects of L9 and L4 as cross-section elements are similar, but in the case of the same degree of freedom, L9 can reduce the quantity.

When B4 is used as the beam unit and L4 is used as the cross-section unit, according to the characteristic that the SAW energy is concentrated near the surface of the elastic body, the wave velocity of the corresponding low-order SAWs can be determined through the displacement mode. Fig. 6.6 shows the same transverse In the case of section unit division,

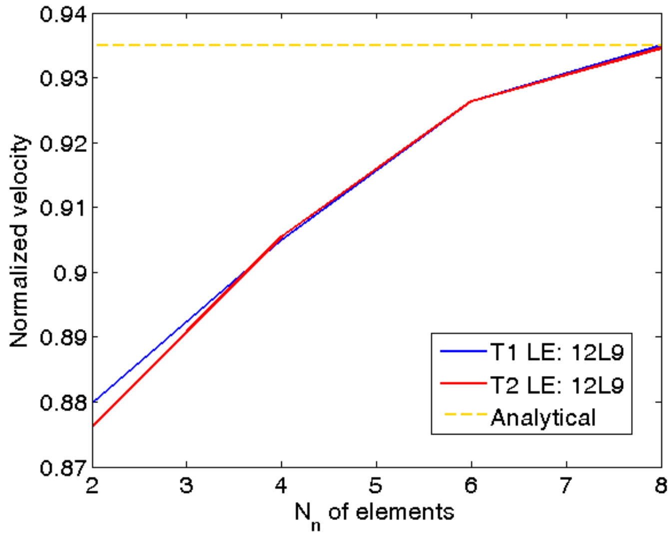

Fig. 6.4 The relationship between the number of beam elements and the velocity of the SAWs in the structure under T1 and T2

the displacement modes of the first-order Rayleigh wave corresponding to different numbers of B4 units.

According to Fig. 6.7(a), it can be concluded that the element needs to have a certain thickness to ensure the existence of stable Rayleigh waves in the structure. The calculation results have no obvious effect; according to Fig. 6.7(b), it can be obtained that when the structure width and thickness are constant, the size in the length direction of the model has little influence on the wave velocity of the low-order SAWs in the structure.

6.3.2 The low-order SAWs in the structure covered by a layer

According to the conclusion obtained in the previous section, a covering layer is added to the thick plate structure in this section, and the displacement continuity characteristic of the Lagrangian unit of CUF is used to make the structure meet the displacement continuity on the contact surface. In the calculation structure in this section, 12L9 is used as the section unit, 8B4 is used as the beam unit in the x_3 direction and the T2 boundary condition. The cover layer material is Cu, and the base material is fused glass. The specific material parameters are shown in Tab. 6.1. Here, the thickness of the base plate is six wavelengths, and the length is three wavelengths.

The dispersion curves of the first-order Rayleigh wave velocity under different cover thicknesses are shown in Fig. 6.8, and compared with the analytical solution, the two are in good agreement; the first-order Rayleigh wave velocity obtained under partial cover thickness

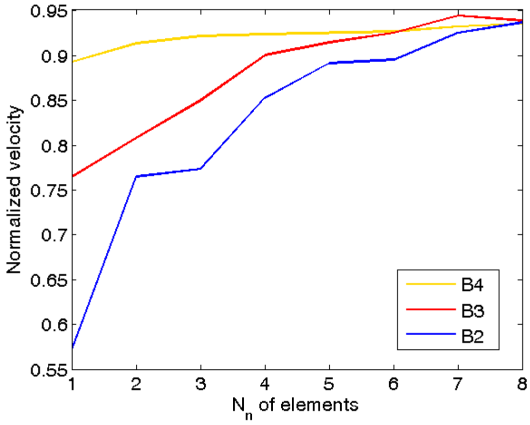

(a)

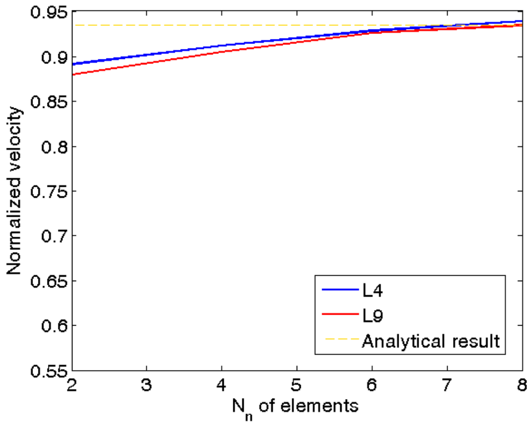

(b)

Fig. 6.5 Convergence analysis of the finite element with T2: (a) same cross-section element with different beam element; (b) same beam element with different cross-section element

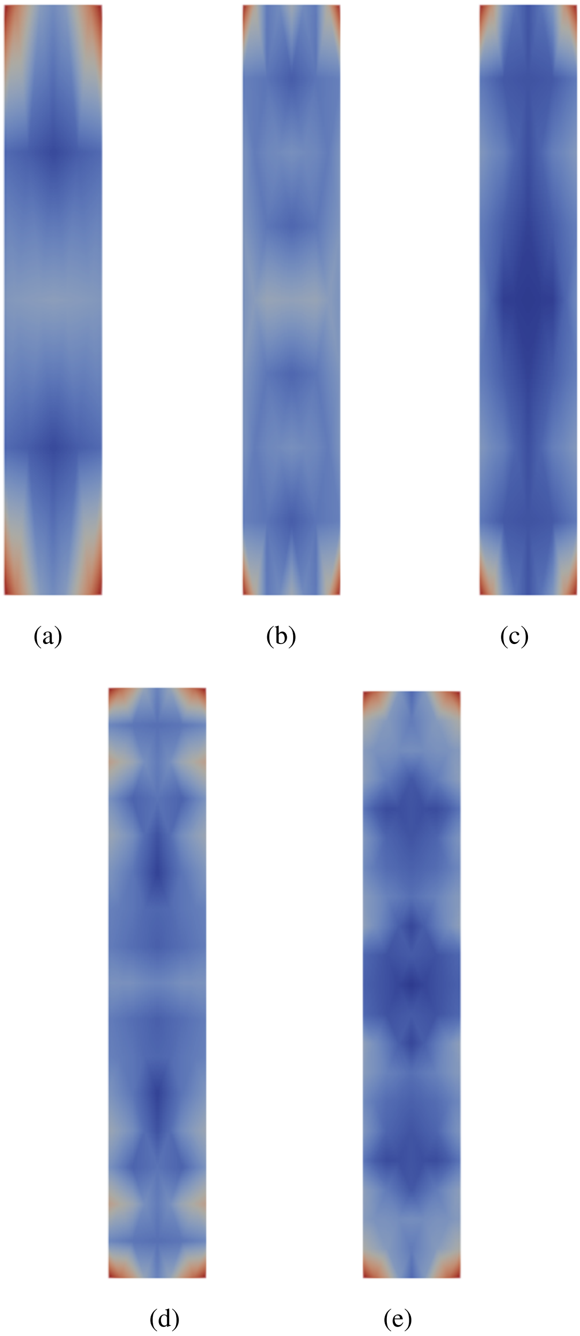

Fig. 6.6 The first velocity of the Rayleigh wave in the structure with different beam node elements: (a) 48L4, 2B4, $v_R = 0.8915$; (b) 48L4,4B4,$v_R = 0.9124$; (c) 48L4, 6B4, $v_R = 0.9292$; (d) 48L4, 8B4, $v_R = 0.9395$; (e)48L4, 10B4, $v_R = 0.9384$

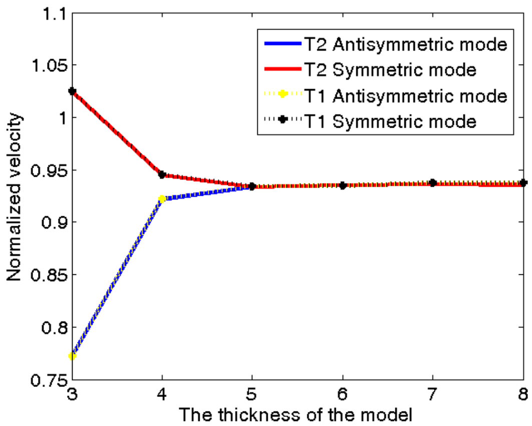

(a)

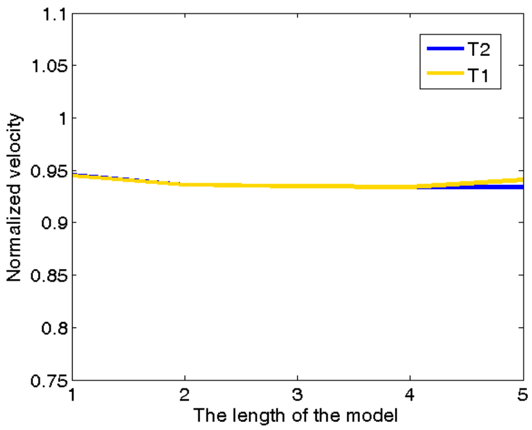

(b)

Fig. 6.7 Convergence analysis of the finite element in different sizes: (a) the length of model: 3λ, the width of model: λ; (b) the thickness of model: 6λ, the width of model: λ

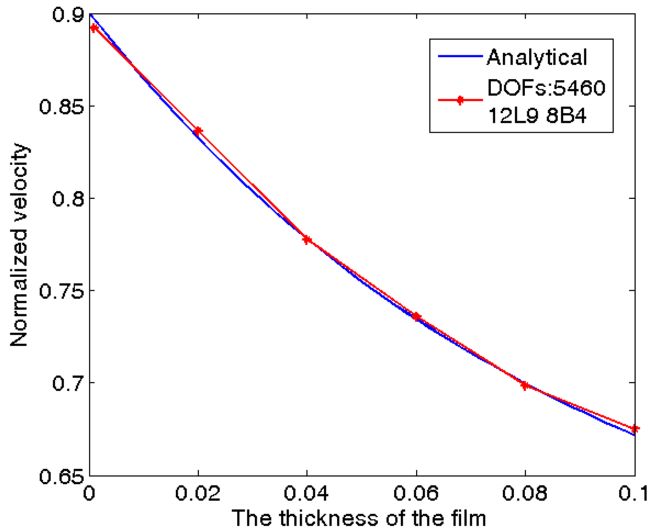

Fig. 6.8 Dispersion curves of the Rayleigh wave in the structure

The displacement mode of the wave velocity is shown in Fig. 6.9. At this time, the amplitude is mainly concentrated near the interface between the covering and the substrate. This result is basically the same as the result in Chapter 3.

6.3.3 The low-order SAWs in the structure when the covering is T-shaped

This section mainly studies the propagation characteristics of SAWs in the structure when the base is covered with a T-shaped thin layer. The size of the base and the material parameters used in the structure are as shown in the previous section. Since the upper thin layer is T-type, it is necessary to consider the appropriate unit division to ensure that the upper and lower layers correspond to the nodes on the interface, as shown in Fig. 6.10, where a_1, b_1, c_1 and d_1 represent the number of units on each edge of the T-type layer respectively. In this section, the effects of the dimensions of the T-shaped covering layer on the SAW propagation velocity in the structure are mainly considered.

The main advantage of the CUF formula is that it can often be calculated with fewer degrees of freedom while ensuring the accuracy of the results. Through the numerical analysis of the free vibration frequency of the model in this section, that is, without considering the artificial boundary conditions, and except for the interface between the upper and lower layers, the others are all free surfaces, and the five minimum frequencies listed in Tab. 6.2 can be obtained. Compared with the results obtained by COMSOL, according to the table below, CUF obtains relatively reliable calculation results with fewer DOFs.

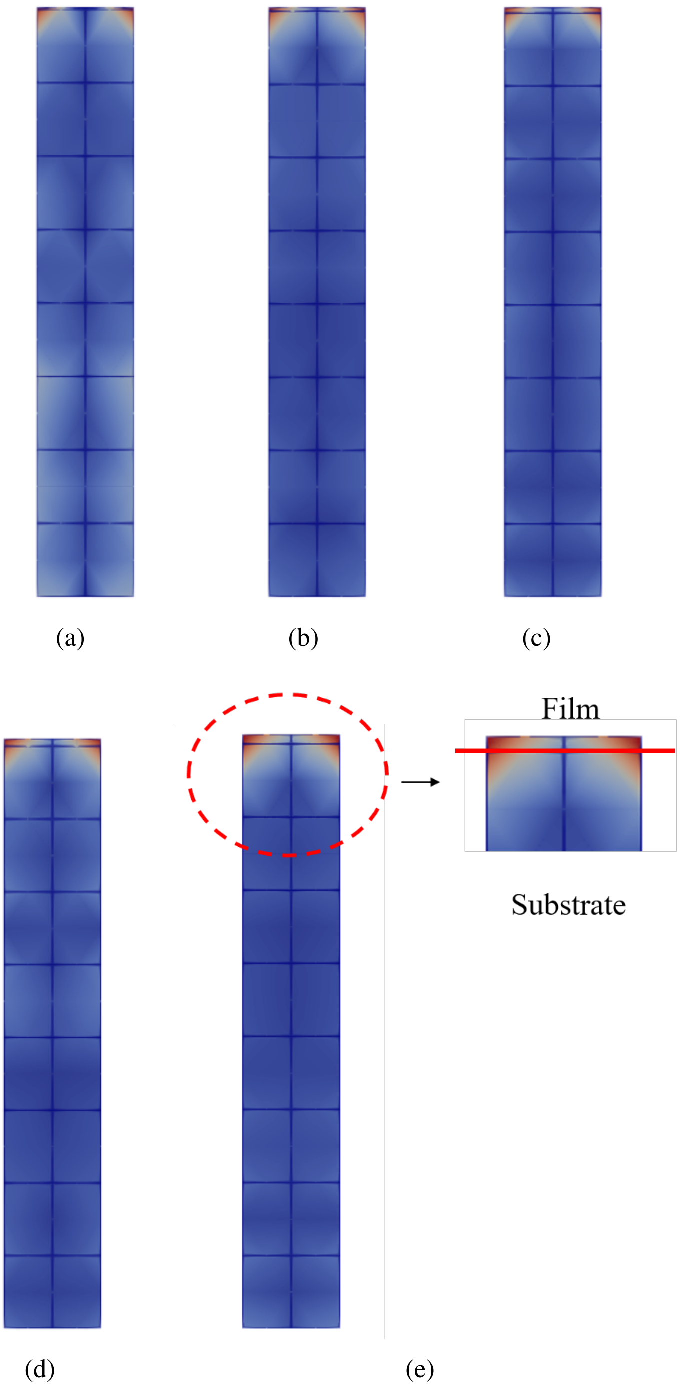

Fig. 6.9 Mode shapes of the first velocity of the SAW in the structure with different thickness of the covering: (a) 0.02λ, $v_R = 0.8922$; (b) 0.02λ,$v_R = 0.7777$; (c) 0.06λ, $v_R = 0.7358$; (d) 0.08λ, $v_R = 0.6985$; (e) 0.1λ, $v_R = 0.6751$

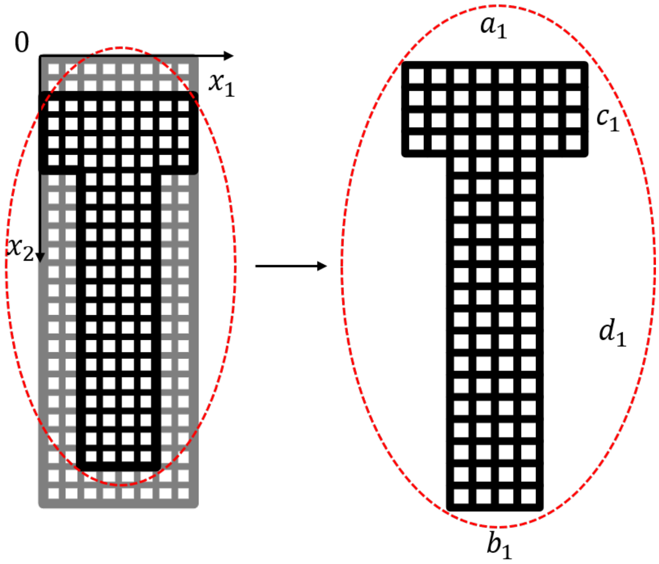

Fig. 6.10 The schematic diagram of the mesh on the cross-section of the T-plate

Table 6.2 Convergence analysis of frequency for the finite substrate covered a T-plate

Meshing in the substrate	Meshing in the covering	Frequencies (MHz)					DOFs
		f_1	f_2	f_3	f_4	f_5	
4×12	$4\times2\times2\times8$	143.20	173.03	301.91	348.75	355.34	4056
8×12	$8\times4\times2\times8$	142.96	172.49	301.89	347.24	354.03	7272
8×24	$8\times4\times4\times16$	142.92	172.07	301.73	347.60	353.74	13950
12×24	$12\times6\times4\times16$	142.87	171.96	301.73	346.29	353.48	20118
COMSOL		142.82	171.71	301.66	345.71	353.14	145320

Table 6.3 The first normalized velocity of the structure with different W

W	Meshing in the covering	DOFs	v_R
0.25λ	$8\times4\times4\times2$	13320	0.9020
0.50λ	$8\times4\times4\times4$	13410	0.9015
0.75λ	$8\times4\times4\times6$	13500	0.9010
1.00λ	$8\times4\times4\times8$	13590	0.9013
1.25λ	$8\times4\times4\times10$	13680	0.9010
1.50λ	$8\times4\times4\times12$	13770	0.9016
1.75λ	$8\times4\times4\times14$	13860	0.8985
2.00λ	$8\times4\times4\times16$	13950	0.8981
2.25λ	$8\times4\times4\times18$	14040	0.8950
2.50λ	$8\times4\times4\times20$	14130	0.8927

Table 6.4 The first normalized velocity of the structure with different b

b	Meshing in the covering	DOFs	v_R
0.25λ	$8\times2\times2\times18$	13554	0.8987
0.50λ	$8\times4\times4\times16$	13950	0.8981
0.75λ	$8\times6\times6\times14$	14274	0.8953
1.00λ	$8\times8\times8\times12$	14526	0.8975

When $b=0.5\lambda$, $\bar{h}=0.1\lambda$, and different W, L4 is used as the cross-section unit, B4 unit is used in the x_3 axis direction, and the artificial boundary is T2 mode. At this time, the results shown in Tab. 6.3 can be obtained. It can be seen from the table that the SAW velocity in the structure is not sensitive to the change of W. When W increases by 1000%, the wave velocity only decreases by 1.03%.

In the case of $W=2\lambda$, $\bar{h}=0.1\lambda$, and different b, L4 is used as the cross-section unit, B4 unit is used in the x_3 axis direction, and the artificial boundary is still T2 mode. At this time, the results shown in Tab. 6.4 can be obtained. According to the results in the table, it can be obtained that the velocity of SAW in this calculation model is not sensitive to the change of b. When b increases by 300%, the wave velocity only decreases by 0.1%.

In the case of $W=2\lambda$, $b=0.5\lambda$, and different $\bar{h}$, L4 is used as the cross-section unit, B4 unit is used in the x_3 axis direction, and the artificial boundary is still T2 mode. And the results are shown in Tab. 6.5. When the covering layer is extremely thin ($\bar{h}=0.001\lambda$), the first-order Rayleigh wave velocity at this time is close to the Rayleigh wave velocity in the base material. As the thickness of the covering layer increases, the first-order Rayleigh wave velocity in the structure The wave velocity decreases accordingly.

Table 6.5 The first normalized velocity of the structure with different $\bar{h}$

$\bar{h}$	Meshing in the covering	DOFs	v_R
0.001λ	$8\times4\times4\times16$	13950	0.9057
0.010λ	$8\times4\times4\times16$	13950	0.9049
0.050λ	$8\times4\times4\times16$	13950	0.9016
0.100λ	$8\times4\times4\times16$	13950	0.8981
0.200λ	$8\times4\times4\times16$	13950	0.8879

Fig. 6.11 shows the modes corresponding to the first-order Rayleigh wave velocity in the structure for the five T-plate thicknesses listed in Tab. 6.5. Different from the previous section, because the T-shaped plate does not completely cover the upper surface of the substrate, there will still be a large amplitude at the bottom of the substrate at this time, but as the thickness of the T-shaped plate increases, its influence on the SAW velocity in the substrate The amplitude at the bottom of the basement will gradually weaken as it increases, and the energy is mainly concentrated at the interface between the upper and lower layers.

6.4 Summary

According to the calculation results in this chapter, it can be seen that the combination of viscous-spring artificial boundary conditions and CUF can be used to analyze the propagation of SAW in three-dimensional finite structures. Specifically, this chapter has the following conclusions:

(1) The three-dimensional geometric model is transformed into a 1D beam calculation model through CUF, which can effectively reduce the calculation cost. Especially for complex structural models, CUF can obtain more reliable results with fewer degrees of freedom.

(2) In this case, there is not much difference in the accuracy of calculation results between L4 and L9 section elements, but under the same degree of freedom, the number of elements required to be set for L9 is generally less than that for L4 in the same model.

(3) Since the viscous-spring artificial boundary mainly acts on the unit nodes, it has a good match with the Lagrange expansion form in CUF. Based on the CUF framework, the simulation of the semi-infinite space is realized by using the "absorption" property of the artificial boundary, so that the propagation characteristics of the SAWs can be analyzed through the finite structure.

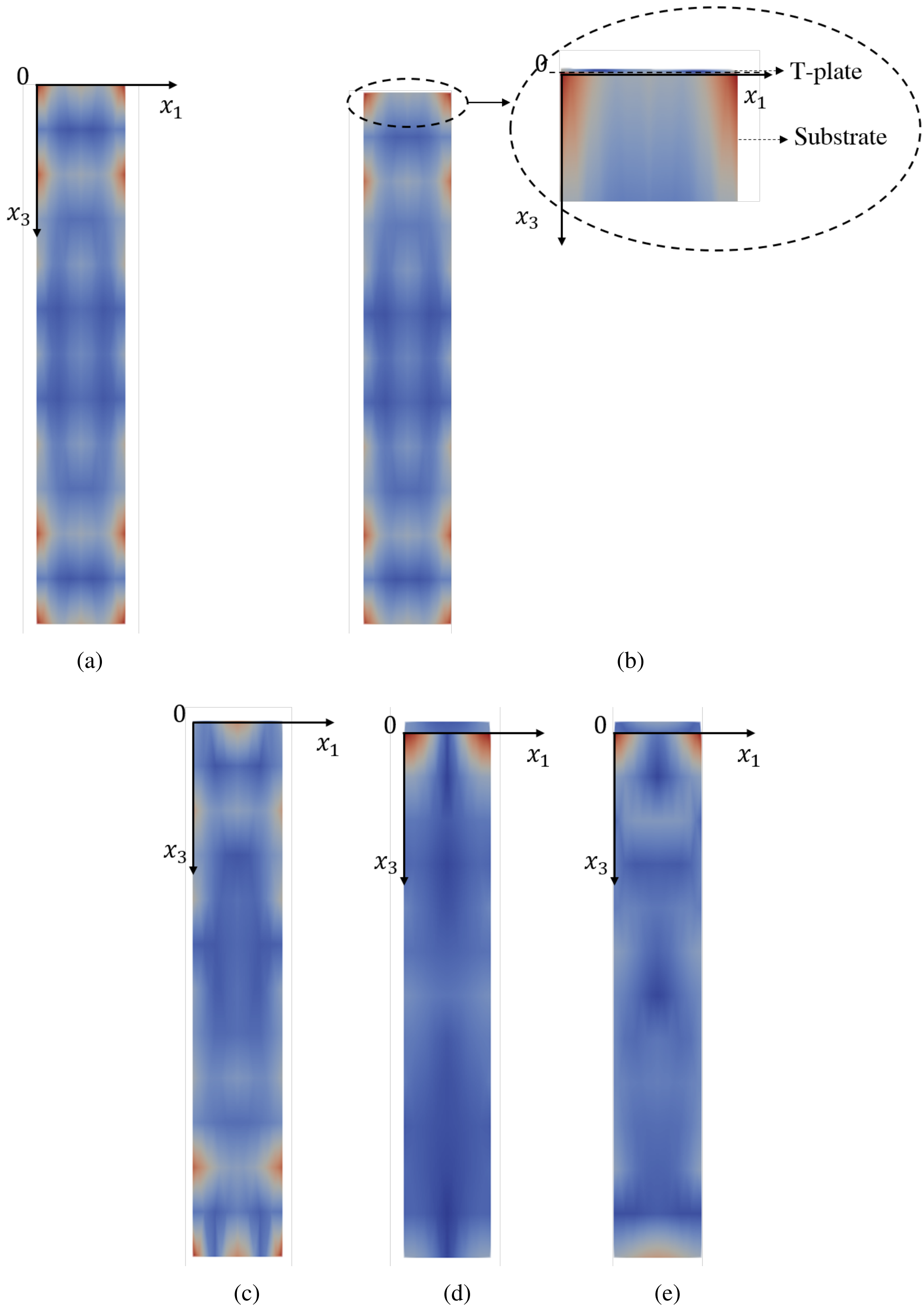

Fig. 6.11 Mode shapes of the first velocity of the Rayleigh wave in the structure with different thicknesses of the covering: (a) $\bar{h} = 0.001\lambda$; (b) $\bar{h} = 0.010\lambda$; (c) $\bar{h} = 0.050\lambda$; (d) $\bar{h} = 0.100\lambda$; (e) $\bar{h} = 0.200\lambda$

(4) And according to the calculation results in this chapter, the influence of T1 mode and T2 mode on the lowest velocity of SAW in the structure is basically the same, and the size in the x_2 axis direction has little influence on the low-order SAWs in the structure.

Chapter 7

Conclusions and prospects

7.1 Conclusions

In this paper, based on the combination of the Rayleigh-Ritz method and the transfer matrix, the trigonometric function is used to make the displacement functions satisfy the periodic boundary conditions, so as to analyze the propagation characteristics of the low-order SAWs in the two-dimensional finite elastic structure; through the CUF framework, the compact stiffness matrix form of the three-dimensional finite elastic structure, using the viscous-spring artificial boundary makes it possible to analyze the propagation characteristics of the SAWs through the finite structure. The specific research content includes: the propagation characteristics of the Rayleigh wave in the finite elastic plate; propagation characteristics of SAWs in finite structure covered with the thin layer on an isotropic substrate; propagation characteristics of SAWs in periodic structures when the width of the covering layer is smaller than that of the substrate; in the finite elastic plate covered with periodic electrodes propagation characteristics of SAWs; CUF is used to analyze the propagation characteristics of low-order SAWs in three-dimensional finite structure. Numerical examples show that the various boundary conditions in the structure, material and thickness of the covering will have a certain degree of influence on the propagation characteristics of low-order SAWs in the structure. This paper mainly obtains the following conclusions:

(1) To analyze the propagation characteristics of low-order Rayleigh waves in a finite elastic plate, the elastic plate must have a certain thickness and satisfy periodic boundary conditions. Only in a sufficiently thick elastic plate (this paper uses an elastic plate with a thickness of six wavelengths) can there be relatively stable Rayleigh wave propagation, and no matter whether the bottom surface of the structure is a free boundary condition or a fixed boundary condition, the Rayleigh wave velocity corresponds to the

stress modes of all conform to the corresponding stress boundary conditions, and the fixed bottom edge of the base can make the Rayleigh wave appear in the thinner elastic plate; in the case of a finite elastic plate with a small thickness, it is then generally assumed that Lamb waves are generated in the plate, when the stresses on the free surface of the structure may not be zero when the bottom edge of the substrate is a fixed boundary. In the Rayleigh-Ritz method, the displacement function can be made periodic by setting up a periodic function $f(x_1)$ (let the direction of x_1 be the wave propagation direction), so as to satisfy the periodic boundary conditions.

(2) In different finite elastic structures, the influence of boundary conditions on the propagation characteristics of low-order SAWs is also different. According to the calculation results from Chapter 2 to Chapter 4, it can be concluded that the more complex the structure, the greater the influence of stress boundary conditions on the velocity of low-order SAWs in the structure. For example, in a structure with the same width as the cover layer and the base, when the base thickness is large, the boundary conditions on the bottom edge of the base and the stress continuity boundary conditions on the contact surface of the upper and lower layers have little effect on the dispersion curves of the SAWs in the structure; in the structure described in Chapter 3, the stress continuum condition at the interface of the upper and lower layers will have a certain influence on the mode of the low-order SAWs and the corresponding stress distribution, but there is no significant effect on the velocity of low-order SAWs in the structure, and the dispersion curves obtained do not change significantly when the boundary conditions of the free surface of the cover layer in the structure are considered in the transfer matrix; the stress continuity conditions between the upper and lower layers in the adopted structure will not only affect the modes and stress distributions of the low-order SAWs in the structure, but also have a certain influence on the wave velocity of the low-order SAWs in the structure, and whether or not the stress boundary conditions on the free surface of the coatings are reflected in the transformation matrix also affects the calculation results.

(3) For covering materials with $\frac{\bar{v}_T}{v_T} < \frac{1}{\sqrt{2}}$, in the calculation results of this paper, the velocity of low-order SAWs in the structure decreases with the increase of covering thickness; but for $\frac{\bar{v}_T}{v_T} > \sqrt{2}$, the low-order SAWs velocity in the structure tends to increase with the increase of the covering thickness within the calculated thickness range ($\bar{h} \in [0, 0.1\lambda]$) used in this paper. However, regardless of the type of covering material, if the thickness of the substrate is sufficient, the boundary conditions on

the bottom edge of the substrate will not have a significant impact on the velocity of low-order SAWs in the structure.

(4) The CUF framework can effectively improve the finite element calculation efficiency of three-dimensional geometry. By combining appropriate boundary conditions, such as the viscous-spring artificial boundary used in this paper, the propagation characteristics of SAWs in the structure can be analyzed at a relatively small computational cost through a finite model. The research results show that in a three-dimensional structure, the dimension in the length direction of the structure (x_2 direction) has relatively little influence on the velocity of low-order SAWs in the structure, and the dimension in the thickness direction (x_3 direction) of the structure has a relatively small influence on the velocity of low-order SAWs in the structure. In the calculation model in Chapter 6, when the thickness of the substrate is five wavelengths, it is considered that Rayleigh waves appear in the substrate, and as the thickness of the covering layer increases, the velocity of low-order SAWs in the structure slowing shrieking.

7.2 Innovations

The innovations of this thesis research include:

(1) The Rayleigh-Ritz method is extended by considering the boundary conditions to obtain a modified structural stiffness matrix and mass matrix, and the effect of boundary conditions on the propagation characteristics of low-order SAWs in the structure was investigated and presented.

(2) With the extended Rayleigh-Ritz method, the SAW propagation characteristics of periodic composite structures are studied, revealing the influence of the number, shape, and material of electrodes on the dispersion curve of low-order SAWs.

(3) In the framework of Carrera's unified formulation, an artificial boundary with viscous-spring is added, and the analysis of the low-order SAWs propagation characteristics of three-dimensional elastic structures is completed by the modified finite element method with high computational efficiency.

7.3 Further work

For the actual SAW device structure, piezoelectric/piezoelectric semiconductor materials are generally used as the substrate, but the main material studied in this paper is isotropic elastic material. Therefore, the work of this paper is still a preliminary exploratory research. Based on the research in this paper, there are still many issues worthy of further exploration:

(1) The method adopted in this paper can be applied to the model where the substrate is a piezoelectric/piezoelectric semiconductor material, considering the propagation characteristics of low-order SAWs in the structure under the force-electric coupling effect.

(2) At present, in order to improve the performance of SAW devices, multi-layer material combinations are often used in the researched structures. Therefore, more boundary conditions need to be considered in the two-dimensional model, and the increase in components , will lead to an increase in the size of the matrix, and it is necessary to further consider how to effectively reduce the calculation cost on the basis of ensuring the reliability of the results.

(3) With the miniaturization of SAW devices, more and more attention has been paid to the nonlinear effects. Therefore, it can be considered to explore the nonlinear factors in the structure of SAW devices by introducing nonlinear terms in the above method. Influence of low-order SAWs propagation properties in structures.

References

[1] Won-Suk Ohm and Mark F. Hamilton. Evolution of nonlinear Rayleigh waves in a coated substrate. *The Journal of the Acoustical Society of America*, 115(6):2798–2806, June 2004. Publisher: Acoustical Society of America.

[2] O. C. Zienkiewicz, Robert Leroy Taylor, and David Dean Fox. *The finite element method for solid and structural mechanics*. Elsevier/Butterworth-Heinemann, Amsterdam Boston, 7th ed edition, 2014.

[3] Gou Endoh, Ken-ya Hashimoto Ken-ya Hashimoto, and Masatsune Yamaguchi Masatsune Yamaguchi. Surface Acoustic Wave Propagation Characterisation by Finite-Element Method and Spectral Domain Analysis. *Japanese Journal of Applied Physics*, 34(5S):2638, May 1995.

[4] M. Hofer, N. Finger, G. Kovacs, J. Schoberl, S. Zaglmayr, U. Langer, and R. Lerch. Finite-element simulation of wave propagation in periodic piezoelectric SAW structures. *IEEE Transactions on Ultrasonics, Ferroelectrics and Frequency Control*, 53(6):1192–1201, June 2006.

[5] M N Hamidon, S A Mousavi, M M Isa, A Ismail, and M A Mahdi. Finite Element Method on Mass Loading Effect for Gallium Phosphate Surface Acoustic Wave Resonators. volume I, page 6, London, U.K., 2009.

[6] Don W Dissanayake, Said Al-Sarawi, Tien-Fu Lu, and Derek Abbott. Finite element modelling of surface acoustic wave device based corrugated microdiaphragms. *Smart Materials and Structures*, 18(9):095030, September 2009.

[7] N. Ramakrishnan, Ashish K. Namdeo, Harshal B. Nemade, and Roy Paily Palathinkal. Simplified Model for FEM Simulation of SAW Delay Line Sensor. *Procedia Engineering*, 41:1022–1027, January 2012.

[8] P. Destuynder, L. Hervella-Nieto, P.M. López-Pérez, J. Orellana, and A. Prieto. A modal-based Partition of Unity Finite Element Method for elastic wave propagation problems in layered media. *Computers & Structures*, 265:106759, June 2022.

[9] Pu Chen, Guangxi Li, and Zhiyuan Zhu. Development and Application of SAW Filter. *Micromachines*, 13(5):656, May 2022. Number: 5 Publisher: Multidisciplinary Digital Publishing Institute.

[10] Fayçal Hadj-Larbi and Rafik Serhane. Sezawa SAW devices: Review of numerical-experimental studies and recent applications. *Sensors and Actuators A: Physical*, 292:169–197, June 2019.

[11] Ashish Tiwary, Shasanka Sekhar Rout, and Basudeba Behera. Design and Analysis of Various Characteristics of a MEMS-Based PIB/CNT/LiNbO3 Multilayered SAW Sensor for CO2 Gas Detection. *Transactions on Electrical and Electronic Materials*, 23(6):609–617, December 2022.

[12] Gurpreet Singh, Sihyeok Kim, and Keekeun Lee. Development of a highly sensitive and portable particulate matter SAW sensor and interface electronics. *Sensors and Actuators A: Physical*, 343:113641, August 2022.

[13] Yahui Tian, Litian Wang, Yuanyuan Wang, Yang Li, Haoxiang Wu, Lirong Qian, Honglang Li, Jinghui Wu, and Ji Wang. Research in Nonlinearity of Surface Acoustic Wave Devices. *Micromachines*, 12(12):1454, November 2021.

[14] Joshua Daw, Zhangxian Deng, and Shane Palmer. Characterization of Advanced Manufactured Surface Acoustic Wave Sensors for Temperature Measurement in Nuclear Applications. Technical report, Idaho National Laboratory, Idaho Falls, Idaho 83415, 2021.

[15] Tetsuya Kimura, Haruki Kyoya, Hiromu Okunaga, Masashi Omura, and Ken-ya Hashimoto. Observational and theoretical validation of longitudinal type surface acoustic wave devices. *Japanese Journal of Applied Physics*, 58(SG):SGGC04, July 2019.

[16] Xinyi Li, Jingfu Bao, Yulin Huang, Benfeng Zhang, Tatsuya Omori, and Ken-ya Hashimoto. Traveling wave excitation sources for FEM analysis of scattering in acoustic waveguide. *Microsystem Technologies*, 25(7):2783–2792, July 2019.

[17] Olgierd C. Zienkiewicz and Robert L. Taylor. *The finite element method for solid and structural mechanics*. Elsevier Butterworth-Heinemann, Amsterdam Heidelberg, 6. ed., repr edition, 2006.

[18] Zhangliang Xu and Yong J. Yuan. Implementation of guiding layers of surface acoustic wave devices: A review. *Biosensors and Bioelectronics*, 99:500–512, January 2018.

[19] Matthias Knapp, Alexey M. Lomonosov, Paul Warkentin, Philipp M. Jager, Werner Ruile, Hans-Peter Kirschner, Matthias Honal, Ingo Bleyl, Andreas P. Mayer, and Leonhard M. Reindl. Accurate characterization of SiO_2 thin films using surface acoustic waves. *IEEE Transactions on Ultrasonics, Ferroelectrics, and Frequency Control*, 62(4):736–743, April 2015.

[20] J. Koskela, P. Maniadis, B. A. Willemsen, P. J. Turner, R. B. Hammond, N. O. Fenzi, and V. Plessky. Hierarchical cascading in 2D FEM simulation of finite SAW devices with periodic block structure. In *2016 IEEE International Ultrasonics Symposium (IUS)*, pages 1–4, September 2016. ISSN: 1948-5727.

[21] S. Maouhoub, Y. Aoura, and A. Mir. FEM simulation of AlN thin layers on diamond substrates for high frequency SAW devices. *Diamond and Related Materials*, 62:7–13, February 2016.

[22] Vladimír Kutiš, Gabriel Gálik, Viktor Královič, Ivan Rýger, Emil Mojto, and Tibor Lalinský. Modelling and Simulation of SAW Sensor Using FEM. *Procedia Engineering*, 48:332–337, January 2012.

[23] Huiling Ong, Huafeng Pang, Jian Zhou, Ran Tao, Prashant Agrawal, Hamdi Torun, Kunyapat Thummavichai, Jingting Luo, Kai Tao, Qiang Wu, Honglong Chang, and Yong-Qing Fu. ZnO/glass thin film surface acoustic waves for efficient digital acoustofluidics and active surface cleaning. *Materials Chemistry and Physics*, 287:126290, August 2022.

[24] Min Zhu, Zhirong Liu, wenqi Bao, Caihua Xu, and Liqiang Xie. A surface acoustic wave device with IDT/(002)ZnO/SiO_2/Si multilayer strucutre. *Chinese journal of sensors and actuators*, 34(10):1360–1365, 2021.

[25] Muhammad, C. W. Lim, J. N. Reddy, E. Carrera, Xinsheng Xu, and Zhenhuan Zhou. Surface elastic waves whispering gallery modes based subwavelength tunable waveguide and cavity modes of the phononic crystals. *Mechanics of Advanced Materials and Structures*, 27(13):1053–1064, July 2020.

[26] Ryo Nakagawa and Ken-ya Hashimoto. Influence of electrode width of interdigital transducer on third-order nonlinearity of surface acoustic wave devices on 42°YX-LiTaO $_3$ substrate. *Japanese Journal of Applied Physics*, 57(7S1):07LD18, July 2018.

[27] Yong Li, Zhilin Hou, Mourad Oudich, and M. Badreddine Assouar. Analysis of surface acoustic wave propagation in a two-dimensional phononic crystal. *Journal of Applied Physics*, 112(2):023524, July 2012.

[28] C. Enzevaee and H. M. Shodja. Surface/interface effect on the propagation of high-frequency SH surface waves in an ultra-thin FGP over-layer bonded to a substrate. *Acta Mechanica*, 232(12):4677–4689, December 2021.

[29] Xiang-Fa Wu and Yuris A. Dzenis. Antiplane surface acoustic waves propagating in elastic half-space coated with an anisotropic laminate. *Composites Science and Technology*, 65(11-12):1761–1768, September 2005.

[30] Hamdi Ezzin, Mohamed Mkaoir, and Morched Ben Amor. Rayleigh wave behavior in functionally graded magneto-electro-elastic material. *Superlattices and Microstructures*, 112:455–469, December 2017.

[31] Issam Ben Salah, Anouar Njeh, and Mohamed Hédi Ben Ghozlen. A theoretical study of the propagation of Rayleigh waves in a functionally graded piezoelectric material (FGPM). *Ultrasonics*, 52(2):306–314, February 2012.

[32] V. T. N. Anh and P. C. Vinh. The incompressible limit method and Rayleigh waves in incompressible layered nonlocal orthotropic elastic media. *Acta Mechanica*, September 2022.

[33] Davinder Kumar, Dilbag Singh, and S. K. Tomar. Surface waves in layered thermoelastic medium with double porosity structure: Rayleigh and Stoneley waves. *Mechanics of Advanced Materials and Structures*, 29(18):2680–2705, July 2022. Publisher: Taylor & Francis _eprint: https://doi.org/10.1080/15376494.2021.1876283.

[34] N.T.K. Linh, P. C. Vinh, T. T. Tuan, and L. T. Thang. The H/V ratio of Rayleigh waves in layered incompressible orthotropic half-spaces and the incompressible limit method. *Waves in Random and Complex Media*, 32(1):103–119, January 2022.

[35] Joseph L. Rose. *Ultrasonic Guided Waves in Solid Media*. Cambridge University Press, August 2014.

[36] E. C. Leong and A. M. W. Aung. Weighted average velocity forward modelling of Rayleigh surface waves. *Soil Dynamics and Earthquake Engineering*, 43:218–228, December 2012.

[37] Limin Wang, Yinhe Luo, and Yixian Xu. Numerical investigation of Rayleigh-wave propagation on topography surface. *Journal of Applied Geophysics*, 86:88–97, November 2012.

[38] Xuefeng Liu and Youhua Fan. On the characteristics of high-frequency Rayleigh waves in stratified half-space. *Geophysical Journal International*, 190(2):1041–1057, August 2012.

[39] DANIEL ROYER and Eugene Dieulesaint. *Elastic Waves in Solids I: Free and Guided Propagation*. Springer Science & Business Media, November 1999. Google-Books-ID: SzwQ1UYspyQC.

[40] Rakesh K. Kapania and Stefano Raciti. Recent advances in analysis of laminated beams and plates, Part II: Vibrations and wave propagation. *AIAA journal*, 27(7):935–946, 1989.

[41] E.L. Adler. Matrix methods applied to acoustic waves in multilayers. *IEEE Transactions on Ultrasonics, Ferroelectrics, and Frequency Control*, 37(6):485–490, November 1990. Conference Name: IEEE Transactions on Ultrasonics, Ferroelectrics, and Frequency Control.

[42] A.H. Fahmy and E. L. Adler. Propagation of acoustic surface waves in multilayers: A matrix description. *Applied Physics Letters*, 22(10):495–497, May 1973.

[43] Norman A Haskell. The dispersion of surface waves on multilayered media. *Bulletin of the seismological Society of America*, 43(1):17–34, 1953.

[44] G. Degrande, G. De Roeck, P. Van Den Broeck, and D. Smeulders. Wave propagation in layered dry, saturated and unsaturated poroelastic media. *International Journal of Solids and Structures*, 35(34):4753–4778, December 1998.

[45] Huayou Chai, Yujun Cui, and Dianji Zhang. Analysis of Surface Waves in Saturated Layered Poroelastic Half-Spaces Using the Thin Layer Method. *Pure and Applied Geophysics*, 175(3):899–915, March 2018.

[46] S. V. Kuznetsov. Weiskopf model for sandy materials: Rayleigh – Lamb wave dispersion. *Mechanics of Advanced Materials and Structures*, 29(25):3815–3820, October 2022. Publisher: Taylor & Francis _eprint: https://doi.org/10.1080/15376494.2021.1910389.

[47] A. J. Philippacopoulos. Waves in a partially saturated layered half-space: Analytic formulation. *Bulletin of the Seismological Society of America*, 77(5):1838–1853, October 1987.

[48] Rahmatullah Ibrahim Nuruddeen, R. Nawaz, and Q. M. Zaigham Zia. Investigating the viscous damping effects on the propagation of Rayleigh waves in a three-layered inhomogeneous plate. *Physica Scripta*, 95(6):065224, April 2020. Publisher: IOP Publishing.

[49] F. Zhang, L. Cheng, L.H. Yam, and L.M. Zhou. Modal characteristics of a simplified brake rotor model using semi-analytical Rayleigh–Ritz method. *Journal of Sound and Vibration*, 297(1-2):72–88, October 2006.

[50] Ji Wang. The extended Rayleigh-Ritz method for an analysis of nonlinear vibrations. *Mechanics of Advanced Materials and Structures*, pages 1–4, March 2021.

[51] Jinghui Wu, Ji Wang, Longtao Xie, Sergei Zhgoon, Rongxing Wu, Aibing Zhang, Tingfeng Ma, and Jianke Du. An analysis and experimental validation of natural frequencies of elastic ellipsoids with the Rayleigh–Ritz method. *Mechanics of Advanced Materials and Structures*, 0(0):1–11, May 2022. Publisher: Taylor & Francis _eprint: https://doi.org/10.1080/15376494.2022.2077486.

[52] Wenjie Guo and Qingsong Feng. Free Vibration Analysis of Arbitrary-Shaped Plates Based on the Improved Rayleigh–Ritz Method. *Advances in Civil Engineering*, 2019:1–14, October 2019.

[53] Yajuvindra Kumar. The Rayleigh–Ritz method for linear dynamic, static and buckling behavior of beams, shells and plates: A literature review. *Journal of Vibration and Control*, 24(7):1205–1227, April 2018.

[54] Vojin Jovanovic and Sergiy Koshkin. The Ritz Method for Boundary Problems with Essential Conditions as Constraints. *Advances in Mathematical Physics*, 2016:1–12, 2016.

[55] Ji Wang, Peng Hu, Bin Huang, Sergei A. Zhgoon, Ju-lian Shen, Min-chiang Chao, Tingfeng Ma, and Jianke Du. Free vibrations of finite quartz crystal cylinders with the Rayleigh-Ritz method. *2016 Symposium on Piezoelectricity, Acoustic Waves, and Device Applications (SPAWDA)*, pages 335–338, 2016.

[56] Sinniah Ilanko, Luis E. Monterrubio, and Yusuke Mochida. The Rayleigh–Ritz Method and Simple Applications. In *The Rayleigh–Ritz Method for Structural Analysis*, pages 21–31. John Wiley & Sons, Ltd, 2014. Section: 3 _eprint: https://onlinelibrary.wiley.com/doi/pdf/10.1002/9781118984444.ch3.

[57] XIE Longtao WANG Ji WU Jinghui, ZHAO Shengquan. Analysis of Vibration Frequencies of Piezoelectric Ceramic Rings as Ultrasonic Transducers in Welding of Facial Mask Production. *Transactions of Nanjing University of Aeronautics & Astronautics*, 38(1):124–131, 2021.

[58] Chao Ye and Yan Qing Wang. On the use of Chebyshev polynomials in the Rayleigh-Ritz method for vibration and buckling analyses of circular cylindrical three-dimensional graphene foam shells. *Mechanics Based Design of Structures and Machines*, 49(7):932–946, October 2021.

[59] Hakan Ozbasaran. Convergence of the Rayleigh–Ritz Method for buckling analysis of arbitrarily configured I-section beam–columns. *Archive of Applied Mechanics*, 89(12):2397–2414, December 2019.

[60] Jing-hui WU, Long-tao XIE, Ai-bing ZHANG, Jian-ke DU, Ken-ya HASHIMOTO, and Ji WANG. The Analysis of Surface Acoustic Waves in A Finite Solid with Electrodes by the Rayleigh-Ritz Method. In *2019 14th Symposium on Piezoelectrcity, Acoustic Waves and Device Applications (SPAWDA)*, pages 1–4, November 2019.

[61] Xiang-lin GONG, Jing-hui WU, Jian-ke DU, Jian-kang CHEN, and Ji WANG. An Analysis of Surface Acoustic Wave in Elastic Solids with Curved Boundary. In *2019 14th Symposium on Piezoelectrcity, Acoustic Waves and Device Applications (SPAWDA)*, pages 1–4, November 2019.

[62] Wei Tian, Zhichun Yang, and Tian Zhao. Analysis of Nonlinear Vibrations and Dynamic Responses in a Trapezoidal Cantilever Plate Using the Rayleigh-Ritz Approach Combined with the Affine Transformation. *Mathematical Problems in Engineering*, 2019:1–23, July 2019.

[63] Xianjie Shi, Chunli Li, Fengjun Wang, and Fayuan Wei. A unified formulation for free transverse vibration analysis of orthotropic plates of revolution with general boundary conditions. *Mechanics of Advanced Materials and Structures*, 25(2):87–99, January 2018.

[64] Soo-Min Ko and Jae-Hoon Kang. Free vibration analysis of shallow and deep ellipsoidal shells having variable thickness with and without a top opening. *Acta Mechanica*, 228(12):4391–4409, December 2017.

[65] Pavla Stoklasová, Petr Sedlák, Hanuš Seiner, and Michal Landa. Forward and inverse problems for surface acoustic waves in anisotropic media: A Ritz–Rayleigh method based approach. *Ultrasonics*, 56:381–389, February 2015.

[66] A. Pagani, E. Carrera, R. Augello, and D. Scano. Use of Lagrange polynomials to build refined theories for laminated beams, plates and shells. *Composite Structures*, 276:114505, November 2021.

[67] M Petrolo, MH Nagaraj, E Daneshkhah, R Augello, and E Carrera. Static analysis of thin-walled beams accounting for nonlinearities. *Proceedings of the Institution of Mechanical Engineers, Part C: Journal of Mechanical Engineering Science*, 236(6):2967–2980, March 2022. Publisher: IMECHE.

[68] B. Wu, A. Pagani, W. Q. Chen, and E. Carrera. Geometrically nonlinear refined shell theories by Carrera Unified Formulation. *Mechanics of Advanced Materials and Structures*, 28(16):1721–1741, August 2021.

[69] E. Carrera, A. Pagani, D. Giusa, and R. Augello. Nonlinear analysis of thin-walled beams with highly deformable sections. *International Journal of Non-Linear Mechanics*, 128:103613, January 2021.

[70] Guohong Li, Erasmo Carrera, Yuliang Hou, and Gennady M. Kulikov. Multi-layered plate finite element models with node-dependent kinematics for smart structures with piezoelectric components. *Chinese Journal of Aeronautics*, 34(8):164–175, 2021.

[71] G. Li, E. Carrera, M. Cinefra, A.G. de Miguel, A. Pagani, and E. Zappino. An adaptable refinement approach for shell finite element models based on node-dependent kinematics. *Composite Structures*, 210:1–19, 2019.

[72] E. Carrera, S. Valvano, and G. M Kulikov. Multilayered plate elements with node-dependent kinematics for electro-mechanical problems. *International Journal of Smart and Nano Materials*, 9(4):279–317, October 2018.

[73] E. Zappino, G. Li, A. Pagani, E. Carrera, and A.G. de Miguel. Use of higher-order Legendre polynomials for multilayered plate elements with node-dependent kinematics. *Composite Structures*, 202:222–232, 2018.

[74] E. Carrera, A. Pagani, and M. Petrolo. Use of Lagrange multipliers to combine 1D variable kinematic finite elements. *Computers & Structures*, 129:194–206, December 2013.

[75] Fangzhou Zhu, Riccardo Augello, Rodolfo Azzara, Alfonso Pagani, Erasmo Carrera, and Weiqiu Chen. Vibration Analysis of Curved Panel Subjected to Internal Pressure and Axial Compression. *AIAA Journal*, 12(60):6842–6853, 2022. Publisher: American Institute of Aeronautics and Astronautics.

[76] F. Moleiro, J.F.A. Madeira, E. Carrera, and A.J.M. Ferreira. Thermo-mechanical design optimization of symmetric and non-symmetric sandwich plates with ceramic-metal-ceramic functionally graded core to minimize stress, deformation and mass. *Composite Structures*, 276:114496, November 2021.

[77] Kouami Koutoati, Foudil Mohri, El Mostafa Daya, and Erasmo Carrera. A finite element approach for the static and vibration analyses of functionally graded material viscoelastic sandwich beams with nonlinear material behavior. *Composite Structures*, 274:114315, October 2021.

[78] M. Petrolo, I. Kaleel, G. De Pietro, and E. Carrera. Wave propagation in compact, thin-walled, layered, and heterogeneous structures using variable kinematics finite elements. *International Journal for Computational Methods in Engineering Science and Mechanics*, 19(3):207–220, May 2018.

[79] Steven G. Johnson. Notes on Perfectly Matched Layers (PMLs). *arXiv:2108.05348 [physics]*, August 2021. arXiv: 2108.05348.

[80] Simon Erlandsson. *Evaluation, adaption and implementations of Perfectly Matched Layers in COMSOL Multiphysics*. Student thesis, KTH ROYAL INSTITUTE OF TECHNOLOGY SCHOOL OF ENGINEERING SCIENCES, Stockholm, Sweden, 2020.

[81] Shaolin Liu, Xiaofan Li, Wenshuai Wang, and Youshan Liu. A mixed-grid finite element method with PML absorbing boundary conditions for seismic wave modelling. *Journal of Geophysics and Engineering*, 11(5):055009, October 2014.

[82] Barbara Kaltenbacher, Manfred Kaltenbacher, and Imbo Sim. A modified and stable version of a perfectly matched layer technique for the 3-d second order wave equation in time domain with an application to aeroacoustics. *Journal of Computational Physics*, 235:407–422, February 2013.

[83] Abdel-Rahman Mahmoud. *FE-PML Modeling of Guided Elastic Waves and its Applications to Ultrasonic NDE*. Degree of Doctor, University of Manitoba, Winnipeg, Manitoba, 2010.

[84] Suomin Cui and Daniel S. Weile. Analysis of electromagnetic scattering from periodic structures by FEM truncated by anisotropic PML boundary condition. *Microwave and Optical Technology Letters*, 35(2):106–110, 2002. _eprint: https://onlinelibrary.wiley.com/doi/pdf/10.1002/mop.10530.

[85] Frank D. Hastings, John B. Schneider, and Shira L. Broschat. Application of the perfectly matched layer (PML) absorbing boundary condition to elastic wave propagation. *The Journal of the Acoustical Society of America*, 100(5):3061–3069, November 1996. Publisher: Acoustical Society of America.

[86] Juan Song and Shu Cai Li. Numerical Analysis of Viscous-Spring Artificial Boundary Element for Underground Explosion. *Applied Mechanics and Materials*, 353-356:3345–3349, 2013. Conference Name: Advances in Civil and Industrial Engineering ISBN: 9783037857755 Publisher: Trans Tech Publications Ltd.

[87] Hong Yang Zhang, Li Wei Han, Zong Tao Tao, Liang Yao, Song Ping Li, and Xiang Dong He. Research of Viscous-Spring Artificial Boundary in Dynamic Analysis. *Applied Mechanics and Materials*, 238:227–230, 2012. Conference Name: Innovation in Civil Engineering, Architecture and Sustainable Infrastructure ISBN: 9783037855348 Publisher: Trans Tech Publications Ltd.

[88] L. I. Wei-Hua, L. I. U. Qing-Hua, and Zhao Cheng-Gang. Three-dimensional viscous-spring boundaries in time domain and dynamic analysis using explicit finite element method of saturated porous medium. *Chinese Journal of Geophysics*, 53(10):2460–2469, October 2010. Publisher: Chinese Journal of Geophysics.

[89] Jingbo Liu, Yixin Du, Xiuli Du, Zhenyu Wang, and Jun Wu. 3D viscous-spring artificial boundary in time domain. *Earthquake Engineering and Engineering Vibration*, 5(1):93–102, 2006.

[90] Jingbo Liu. A unified viscous-spring artificial boundary for 3-D static and dynamic applications. *Science in China Series E*, 48(5):570, 2005.

[91] Jie Deng, Ling Zheng, and Oriol Guasch. Acoustic Lenses Using Multiple Acoustic Black Holes Based on Gaussian Expansion Method in Plates. pages 1–8, 2021.

[92] Zhidong Gao, Mi Zhao, Xiuli Du, and Zilan Zhong. A generalized response spectrum method for seismic response analysis of underground structure combined with viscous-spring artificial boundary. *Soil Dynamics and Earthquake Engineering*, 140:106451, 2021. Publisher: Elsevier.

[93] Lord Rayleigh. On Waves Propagated along the Plane Surface of an Elastic Solid. *Proceedings of the London Mathematical Society*, s1-17(1):4–11, 1885. _eprint: https://onlinelibrary.wiley.com/doi/pdf/10.1112/plms/s1-17.1.4.

[94] DM Barnett and J Lothe. Free surface (Rayleigh) waves in anisotropic elastic half-spaces: the surface impedance method. *Proceedings of the Royal Society of London. A. Mathematical and Physical Sciences*, 402(1822):135–152, December 1985.

[95] J. M. Carcione, D. Kosloff, and R. Kosloff. Wave propagation simulation in a linear viscoelastic medium. *Geophysical Journal International*, 95(3):597–611, December 1988.

[96] M. D. Sharma. Rayleigh Waves in Isotropic Viscoelastic Solid Half-Space. *Journal of Elasticity*, 139(1):163–175, April 2020.

[97] Pham Chi Vinh, Tran Thanh Tuan, and Le Thi Hue. Formulas for the H/V ratio (ellipticity) of Rayleigh waves in orthotropic elastic half-spaces. *Waves in Random and Complex Media*, 29(4):759–774, October 2019.

[98] Wenjun Yang, Xu Liang, Qian Deng, and Shengping Shen. Rayleigh wave propagation in a homogeneous centrosymmetric flexoelectric half-space. *Ultrasonics*, 103:106105, April 2020.

[99] Chapter 4 - Surface Waves and Free Oscillations. In Thorne Lay and Terry C. Wallace, editors, *Modern Global Seismology*, volume 58 of *International Geophysics*, pages 116–172. Academic Press, 1995.

[100] Zhaolun Liu, Jing Li, Sherif M. Hanafy, and Gerard Schuster. 3D wave-equation dispersion inversion of Rayleigh waves. *GEOPHYSICS*, 84(5):R673–R691, September 2019.

[101] Baljeet Singh and Ritu Sindhu. On Propagation of Rayleigh Type Surface Wave in a Micropolar Piezoelectric Medium. *Open Journal of Acoustics*, 06(04):35–44, 2016.

[102] Lalith Sai Srinivas Pillarisetti, Cliff J. Lissenden, and Parisa Shokouhi. Control of Rayleigh wave propagation through imposing Mindlin boundary conditions on the surface. *Journal of Sound and Vibration*, 530:116931, 2022. Publisher: Elsevier.

[103] Ru Tian, Jinxi Liu, Ernian Pan, Yuesheng Wang, and Ai Kah Soh. Some characteristics of elastic waves in a piezoelectric semiconductor plate. *Journal of Applied Physics*, 126(12):125701, September 2019.

[104] H. F. Tiersten. Elastic Surface Waves Guided by Thin Films. *Journal of Applied Physics*, 40(2):770–789, 1969.

[105] Ken-ya Hashimoto. Simulation of Surface Acoustic Wave Devices. *Japanese Journal of Applied Physics*, 45(5B):4423–4428, May 2006.

[106] Yinhui Chen, Hui Zhang, and Yingbin Zheng. Research progress on the theory of Surface Acoustic Wave filters. *Journal of Terahertz Science and Electronic Information Technology*, 14(3):467–473, 2016.

[107] David A. Powell, Kourosh Kalantar-zadeh, and Wojtek Wlodarski. Numerical calculation of SAW sensitivity: application to ZnO/LiTaO3 transducers. *Sensors and Actuators A: Physical*, 115(2-3):456–461, September 2004.

[108] G.T. Piliposian and Z.N. Danoyan. Surface electro-elastic Love waves in a layered structure with a piezoelectric substrate and two isotropic layers. *International Journal of Solids and Structures*, 46(6):1345–1353, March 2009.

[109] Hamdi Ezzin, Morched Ben Amor, and Mohamed Hédi Ben Ghozlen. Love waves propagation in a transversely isotropic piezoelectric layer on a piezomagnetic half-space. *Ultrasonics*, 69:83–89, July 2016.

[110] Soniya Chaudhary, Sanjeev A. Sahu, and Abhinav Singhal. Analytic model for Rayleigh wave propagation in piezoelectric layer overlaid orthotropic substratum. *Acta Mechanica*, 228(2):495–529, February 2017.

[111] Mahargha Biswas and Sanjeev A. Sahu. Surface wave dispersion in imperfectly bonded flexoelectric-piezoelectric/FGPM bi-composite in contact of Newtonian liquid. *Mechanics of Advanced Materials and Structures*, pages 1–18, May 2022.

[112] M. Pasternak. An Analytical Solution of Rayleigh Wave Propagation Problem on Elastic Substrate with Nonconductive Viscoelastic Layer. *Acta Physica Polonica A*, 116(3):371–374, September 2009.

[113] Ding Wang and Jing Tang. 3D analysis of Rayleigh-type surface wave in fractured media: Insights into anisotropic characteristics. *Journal of Sound and Vibration*, 537:117195, 2022. Publisher: Elsevier.

[114] Rei Goto, Hiroyuki Nakamura, and Ken-ya Hashimoto. The modeling of the transverse mode in TC-SAW using SiO_2 /$LiNbO_3$ structure. *Japanese Journal of Applied Physics*, 58(SG):SGGC07, July 2019.

[115] M. Buchner, W. Ruile, A. Dietz, and R. Dill. FEM analysis of the reflection coefficient of SAWs in an infinite periodic array. In *IEEE 1991 Ultrasonics Symposium,*, pages 371–375 vol.1, December 1991.

[116] M. R. Maheri and R. D. Adams. Modal Vibration Damping of Anisotropic FRP Laminates Using the Rayleigh–Ritz Energy Minimization Scheme. *Journal of Sound and Vibration*, 259(1):17–29, January 2003.

[117] A. Fasana and S. Marchesiello. Rayleigh-Ritz analysis of sandwich beams. *Journal of Sound and Vibration*, 241(4):643–652, April 2001.

[118] L. Meirovitch and M. K. Kwak. Rayleigh-Ritz based substructure synthesis for flexible multibody systems. *AIAA Journal*, 29(10):1709–1719, October 1991.

[119] Zhao Jing, Qin Sun, Yongjie Zhang, and Ke Liang. Fundamental frequency maximization of composite rectangular plates by sequential permutation search algorithm. *Mechanics of Advanced Materials and Structures*, pages 1–17, July 2021.

[120] Sinwoo Jeong and Hong Hee Yoo. Generalized classical Ritz method for modeling geometrically nonlinear flexible multibody systems having a general topology. *International Journal of Mechanical Sciences*, 181:105687, September 2020.

[121] Bijuan Yan, Huijun Liang, Minjie Jin, Zhanlong Li, and Yong Song. Vibration-damping characteristic analysis of constrained stand-off layer damping cylindrical shell using Rayleigh-Ritz method. *Engineering Computations*, 37(1):93–119, July 2019.

[122] Jiří Vohánka, Martin Čermák, Daniel Franta, and Ivan Ohlídal. Efficient method to calculate the optical quantities of multi-layer systems with randomly rough boundaries using the Rayleigh–Rice theory. *Physica Scripta*, 94(4):045502, April 2019.

[123] Feng-ling HANG, Yang-yang ZHANG, Ai-bing ZHANG, Tao ZHANG, Jian-ke DU, and Ji WANG. An Analysis of Vibrations of Elastic Cuboids Covered with thin Films. In *2019 14th Symposium on Piezoelectrcity, Acoustic Waves and Device Applications (SPAWDA)*, pages 1–5, 2019.

[124] Muhammad Nawaz Naeem, Awais Gul Khan, Shahid Hussain Arshad, Abdul Ghafar Shah, and Madiha Gamkhar. Vibration of Three-Layered FGM Cylindrical Shells with Middle Layer of Isotropic Material for Various Boundary Conditions. *World Journal of Mechanics*, 04(11):315–331, 2014.

[125] Guoyong Jin, Chuanmeng Yang, and Zhigang Liu. Vibration and damping analysis of sandwich viscoelastic-core beam using Reddy's higher-order theory. *Composite Structures*, 140:390–409, 2016.

[126] Zinan Zhao, Zhenghua Qian, Bin Wang, and Jiashi Yang. Energy trapping of thickness-extensional modes in thin film bulk acoustic wave resonators. *Journal of Mechanical Science and Technology*, 29(7):2767–2773, July 2015.

[127] Zinan Zhao, Bin Wang, Zhenghua Qian, and Yook-Kong Yong. A novel approach to quantitative predictions of high-frequency coupled vibrations in layered piezoelectric plates. *International Journal of Engineering Science*, 157:103407, December 2020.

[128] Michele D'Ottavio, Lorenzo Dozio, Riccardo Vescovini, and Olivier Polit. The Ritz – Sublaminate Generalized Unified Formulation approach for piezoelectric composite plates. *International Journal of Smart and Nano Materials*, 9(1):34–55, January 2018.

[129] Yingli Li and Yiming Fu. Reliability Analysis for the Stability of Piezoelectric Delaminated Axisymmetric Laminated Cylindrical Shells. *Mechanics of Advanced Materials and Structures*, 21(4):284–292, April 2014.

[130] Roland L. Woodcock. Free vibration of advanced anisotropic multilayered composites with arbitrary boundary conditions. *Journal of Sound and Vibration*, 312(4):769–788, May 2008.

[131] D. Zhou, F.T.K. Au, Y.K. Cheung, and S.H. Lo. Effect of built-in edges on 3-D vibrational characteristics of thick circular plates. *International Journal of Solids and Structures*, 43(7-8):1960–1978, April 2006.

[132] R. Uhrig. The transfer matrix method seen as one method of structural analysis among others. *Journal of Sound and Vibration*, 4(2):136–148, September 1966.

[133] Andrew Melro and Kefu Liu. Determination of the modal parameters of a single lap adhesively bonded joint using the transfer matrix method plus model updating. *International Journal of Adhesion and Adhesives*, 101:102628, September 2020.

[134] W. T. Thomson. Matrix Solution for the Vibration of Nonuniform Beams. *Journal of Applied Mechanics*, 17(3):337–339, 1950.

[135] yuan Wang. *Application study on structural calculation method of bridge based on the transfer matrix method*. Doctor, Southwest Jiaotong University, 2019.

[136] Xiaoting Rui, Guoping Wang, Yuqi Lu, and Laifeng Yun. Transfer matrix method for linear multibody system. *Multibody System Dynamics*, 19(3):179–207, April 2008.

[137] K.B. Subrahmanyam and A.K. Garg. Uncoupled flexural vibrations of straight beams with all possible boundary conditions treated by a transfer matrix method. *Journal of Sound and Vibration*, 204(3):397–419, July 1997.

[138] Tianrong Zhan, Xi Shi, Yunyun Dai, Xiaohan Liu, and Jian Zi. Transfer matrix method for optics in graphene layers. *Journal of Physics: Condensed Matter*, 25(21):215301, April 2013. Publisher: IOP Publishing.

[139] Jung Woo Lee and Jung Youn Lee. Free vibration analysis using the transfer-matrix method on a tapered beam. *Computers & Structures*, 164:75–82, February 2016.

[140] Mostafa Attar. A transfer matrix method for free vibration analysis and crack identification of stepped beams with multiple edge cracks and different boundary conditions. *International Journal of Mechanical Sciences*, 57(1):19–33, April 2012.

[141] Wave propagation in magneto-electro-elastic multilayered plates. 44.

[142] Hui-dong Gao, Shu-yi Zhang, Xue Qi, K. Wasa, and Hao-dong Wu. Influence of material parameters on acoustic wave propagation modes in ZnO/Si bi-layered structures. *IEEE Transactions on Ultrasonics, Ferroelectrics, and Frequency Control*, 52(12):2361–2369, December 2005. Conference Name: IEEE Transactions on Ultrasonics, Ferroelectrics, and Frequency Control.

[143] P.-C. Xu and S. K. Datta. Guided waves in a bonded plate: A parametric study. *Journal of Applied Physics*, 67(11):6779–6786, June 1990.

[144] P. C. Vinh, V. T. N. Anh, and N. T. K. Linh. On a technique for deriving the explicit secular equation of Rayleigh waves in an orthotropic half-space coated by an orthotropic layer. *Waves in Random and Complex Media*, 26(2):176–188, April 2016.

[145] Wing Kam Liu, Shaofan Li, and Harold Park. Eighty Years of the Finite Element Method: Birth, Evolution, and Future. *Archives of Computational Methods in Engineering*, (29):4431–4453, 2022. Publisher: arXiv Version Number: 1.

[146] G. R. Liu and S. S. Quek Jerry. A non-reflecting boundary for analyzing wave propagation using the finite element method. *Finite Elements in Analysis and Design*, 39(5):403–417, March 2003.

[147] Yulin Huang, Jingfu Bao, Xinyi Li, Benfeng Zhang, Luyan Qiu, Tatsuya Omori, and Ken-Ya Hashimoto. Analysis of SAW Scattering at Discontinuity Between Periodic Gratings Using Travelling Wave Excitation and Hierarchical Cascading Technique. In *2018 IEEE International Ultrasonics Symposium (IUS)*, pages 1–9, Kobe, October 2018. IEEE.

[148] Isaac Harari and Thomas J. R. Hughes. Galerkin/least-squares finite element methods for the reduced wave equation with non-reflecting boundary conditions in unbounded domains. *Computer Methods in Applied Mechanics and Engineering*, 98(3):411–454, August 1992.

[149] Ding Wang and Yuan Zhang. Rayleigh waves propagation in an elastic medium with discrete subsurface fractures. *Journal of Sound and Vibration*, 509:116224, September 2021.

[150] Wenyi Hu, Aria Abubakar, and Tarek M. Habashy. Application of the nearly perfectly matched layer in acoustic wave modeling. *GEOPHYSICS*, 72(5):SM169–SM175, 2007.

[151] Marco Petrolo, Erasmo Carrera, Maria Cinefra, and Enrico Zappino. *Finite element analysis of structures through unified formulation*. John Wiley & Sons, 2014.

[152] Erasmo Carrera, Riccardo Augello, Alfonso Pagani, and Xiangyang Xu. Component-wise approach to reinforced concrete structures. *Mechanics of Advanced Materials and Structures*, 25(29):3871–3888, 2021. Publisher: Taylor & Francis.

[153] Marin Marin, Erasmo Carrera, and Dumitru Baleanu. On the boundary value problem in the nonlinear theory of dipolar elastic materials. *Mechanics of Advanced Materials and Structures*, 27(18):1619–1625, September 2020.

[154] A. Pagani and E. Carrera. Coupling three-dimensional peridynamics and high-order one-dimensional finite elements based on local elasticity for the linear static analysis of solid beams and thin-walled reinforced structures. *International Journal for Numerical Methods in Engineering*, 121(22):5066–5081, 2020. _eprint: https://onlinelibrary.wiley.com/doi/pdf/10.1002/nme.6510.

[155] E. Zappino, G. Li, A. Pagani, and E. Carrera. Global-local analysis of laminated plates by node-dependent kinematic finite elements with variable ESL/LW capabilities. *Composite Structures*, 172:1–14, July 2017.

[156] G. Li, M. Cinefra, and E. Carrera. Coupled thermo-mechanical finite element models with node-dependent kinematics for multi-layered shell structures. *International Journal of Mechanical Sciences*, 171:105379, April 2020.

[157] B. Wu, A. Pagani, M. Filippi, W. Q. Chen, and E. Carrera. Accurate stress fields of post-buckled laminated composite beams accounting for various kinematics. *International Journal of Non-Linear Mechanics*, 111:60–71, 2019. Publisher: Elsevier.

[158] E. Carrera, A. Pagani, and R. Augello. Effect of large displacements on the linearized vibration of composite beams. *International Journal of Non-Linear Mechanics*, 120:103390, April 2020.

[159] Ayoob Entezari, Matteo Filippi, Erasmo Carrera, and Mohammad Ali Kouchakzadeh. 3D-wave propagation in generalized thermoelastic functionally graded disks. *Composite Structures*, 206:941–951, December 2018.

Appendix A

List of publication

Journal articles

1. J. Wu, J. Wang, E. Carrera, R. Augello. An Analysis of the Propagation of Surface Acoustic Waves in a Substrate Covered by a Metal T-plate with the Carrera Unified Formulation. *Transactions of Nanjing University of Aeronautics & Astronautics* .

2. J. Wu, J. Wang, S. Zhao, L. Xie. Analysis of Vibration Frequencies of Piezoelectric Ceramic Rings as Ultrasonic Transducers in Welding of Facial Mask Production. *Transactions of Nanjing University of Aeronautics & Astronautics* , 38(1): 124, 2021. DOI:10.16356/j.1005-1120.2021.01.012.

3. J. Wu, J. Wang, L. Xie, S. Zhgoon, R. Wu, A. Zhang, T. Ma, J. Du. An analysis and experimental validation of natural frequencies of elastic ellipsoids with the Rayleigh–Ritz method. *Mechanics of Advanced Materials and Structures* , 1-11, 2022. DOI:10.1080/15376494.2022.2077486.

4. Y. Tian, L. Wang, Y. Wang, Y. Li, H. Wu, L. Qian, H. Li, J. Wu, J. Wang. Research in Nonlinearity of Surface Acoustic Wave Devices. *Micromachines*, 12(12): 1454, 2021. DOI:10.3390/mi12121454.

5. Z. Cao, S. Dai, S. Ding, J. Wu. Correlation between acousto-optic and structural properties of Ge–Sb–S chalcogenide glasses. *Ceramics International*, 46(8): 10385-10391,

2020. DOI:10.1016/j.ceramint.2020.01.036.

6. S. Ding, S. Dai, Z. Cao, J. Wu. Composition dependence of the physical and acousto-optic properties of transparent Ge–As–S chalcogenide glasses. *Optical Materials*, 108: 110175, 2020. DOI:10.1016/j.optmat.2020.110175.

7. J. Ding, J. Wu, D. Wu, T. Ma, J. Wang. The influence factors for measurements of elastic constants of isotropic steel cylinders by resonant ultrasound spectroscopy. *Journal of Ningbo University*, 33(06):53-58, 2020.

Conference Proceedings

1. J. Wang, J. Wu, E. Carrera, H. Li. An Analysis of Surface Acoustic Wave Modes of a Finite Solid Covered with Electrodes by Rayleigh-Ritz Method, In: *2021 IEEE International Ultrasonics Symposium (IUS)*. 1-3, 2021.

2. J. Wu, K. Hashimoto, Z. Wu, B. Huang, J. Wang. Higher-order Surface Acoustic Wave Modes of a Finite Elastic Solid, In: *2020 IEEE International Ultrasonics Symposium (IUS)*. Las Vegas, NV, USA. 1-3, 2020.

3. S. Ding, J. Wu, L. Xie, Y. Zhang, R. Wu, J. Wang. In-Plane Free Vibrations of Curved Beams by Rayleigh-Ritz Method, In: *2019 13th Symposium on Piezoelectrcity, Acoustic Waves and Device Applications (SPAWDA)*. Harbin, China. 1-4, 2019.

4. J. Wu, L. Xie, A. Zhang, J. Du, K. Hashimoto, J. Wang. The Analysis of Surface Acoustic Waves in a Finite Solid with Electrodes by the Rayleigh-Ritz Method, In: *2019 14th Symposium on Piezoelectrcity, Acoustic Waves and Device Applications (SPAWDA)*. Shijiazhuang, China. 1-4, 2019.

5. X. Gong, J. Wu, J. Du, J. Chen, J. Wang. An Analysis of Surface Acoustic Wave in Elastic Solids with Curved Boundary, In: *2019 14th Symposium on Piezoelectrcity, Acoustic Waves and Device Applications (SPAWDA)*. Shijiazhuang, China. 1-4, 2019.